Dana Barry
Hideyuki Kanematsu *Editors*

Studies to Combat COVID-19 using Science and Engineering

Springer

Studies to Combat COVID-19 using Science and Engineering

Dana Barry • Hideyuki Kanematsu
Editors

Studies to Combat COVID-19 using Science and Engineering

Springer

Editors
Dana Barry
Department of Electrical & Computer Engineering
Clarkson University
Potsdam, NY, USA

Hideyuki Kanematsu
National Institute of Technology,
Suzuka College
Shiroko-cho, Suzuka, Mie, Japan

ISBN 978-981-19-1355-6 ISBN 978-981-19-1356-3 (eBook)
https://doi.org/10.1007/978-981-19-1356-3

This Springer imprint is published by the registered company Springer Nature Singapore Pte Ltd.
The registered company address is: 152 Beach Road, #21-01/04 Gateway East, Singapore 189721, Singapore

Preface

We are proud to introduce our unique book *Studies to Combat COVID-19 Using Science and Engineering*. This exciting book provides excellent examples of ongoing, leading-edge research (being carried out by the chapter authors and others) that relates to viruses, especially COVID-19. It is written from the viewpoint of various scientific fields including materials science. The book is divided into four parts. Part I starts by introducing the topics of viruses and infections. It describes a virus as an infectious agent that replicates inside the living cells of an organism. Mutations and the replication process of viruses are discussed, along with details about several diseases including Shingles and Rabies. This part also compares viruses to bacteria and points out their differences. Part II describes the spread of infections through a material's surface (which serves as an interface between a material and a microbial/viral environment). This part contains leading-edge research about antiviral materials and coatings, etc. Also, an international standard is presented for evaluating the activity of a virus on a specified material. Part III focuses on the virus known as COVID-19. Background information is provided about this virus and its variants, along with potential vaccines and therapeutic drugs to help control them. This part also relates to other aspects of COVID-19: the spread of the virus through air, computational modeling of aerosol transmission of COVID-19, respiratory virus deposition and resuspension from indoor surfaces, wastewater surveillance for the virus, and the use of algorithms for hotspot detection of COVID-19. The last part (Part IV) discusses what has been learned during the pandemic, what more needs to be done, and tips for preparing for future pandemics. It also proposes reform in funeral services for properly and safely accommodating large numbers of bodies during a pandemic.

Our book (*Studies to Combat COVID-19 Using Science and Engineering*) provides fundamental information and leading-edge research about viruses and COVID-19 to challenge and captivate the interests of undergraduate and graduate students as well as professional engineers, scientists, and researchers. It describes research that relates to antiviral, antibacterial, and antibiofilm materials too. The book serves as an excellent textbook as well as a reference book (practical guide). It may also be of interest to individuals wanting to obtain information about

COVID-19 and pandemics. The many fields addressed in this book include biochemistry, chemistry, biology, microbiology, virology, pandemics, materials science and engineering, chemical engineering, mechanical engineering, civil engineering, environmental engineering, electrical and computer engineering, medical science, funeral services, and pharmaceutical sciences.

We invite you to join us on an exciting adventure (through this book) into the world of viruses, with a focus on COVID-19. You will find it to be a rewarding and educational experience.

Very Best Wishes for the Present and the Future.

Potsdam, NY, USA — Dana M. Barry
Shiroko-cho, Suzuka, Mie, Japan — Hideyuki Kanematsu

Acknowledgments

We thank the Japanese Government and the headquarters of KOSEN (National Institute of Technology, Japan) for supporting our research activities to develop anti-infective materials. Particularly, we thank Dr. Isao Taniguchi, the President of the National Institute of Technology (KOSEN) Japan, from the bottom of our hearts, for his encouragement and support. Under the GEAR 5.0 Project of KOSEN, we thank Professor Mitsuteru Inoue, The Senior Executive Directors of KOSEN, Professor Takaya Sato (Senior Executive Professor), and Professor Hitoshi Wake (Specially Appointed Professor for the GEAR 5.0 Project) who have also encouraged us to pursue our international projects in various ways. We greatly appreciate them. We are very thankful to Clarkson University, the Dean of Clarkson's Wallace H. Coulter School of Engineering Professor William Jemison, Clarkson's Department of Electrical & Computer Engineering, the Chair of this Department Professor Paul McGrath, and the former Chair Professor David Crouse. We also thank the State University of New York at Canton, Arizona State University, the National Institute of Technology, Suzuka College in Japan, and its President Professor Motomu Takeshige. Thanks are extended to Executive Vice President of Osaka University Professor Toshihiro Tanaka, Professor Eiji Arai of Osaka University, Osaka University in Japan, the American Chemical Society, Professor Dr. Roger Haw Boon Hong, and Ansted University, for their greatly appreciated support. We thank ISIJ (the Iron and Steel Institute of Japan), the Iron and Steel Society of Japan, ASM International, and SIAA (the Society of International Sustaining Growth for Antimicrobial Articles) and that Society's Biofilm Evaluation Committee.

We are grateful to the great materials science and surface finishing societies in the United States (ASM International, National Association for Surface Finishing, NASF), the United Kingdom (Institute of Materials Finishing, IMF), Japan's Institute of Metals and Materials (JIM), the Materials Research Society of Japan (MRS-J), and the Surface Finishing Society of Japan, SFSJ.

Some information contained in this book was obtained from work carried out for national funding projects in Japan. (Particularly, we appreciate JSPS Kakenhi 20K05185, 21K12739, 17K06826, 16K06819, etc. in Japan and enthusiastic colleagues all over the world related to these funding projects.) In addition, some

researchers received funding from the National Science Foundation. (In particular, we appreciate the NSF Award 2032114 to Arizona State University and the NSF Award 2032106 to Clarkson University.)

Special thanks are extended to the chapter authors for their excellent contributions to this book. Those from Clarkson University include Professor Andrea Ferro of the Department of Civil and Environmental Engineering, Mahender Singh Rawat, Professor Susan Bailey of Biology, Mahfuza Akter, Distinguished Professor of Mechanical & Aerospace Engineering Goodarz Ahmadi, and a group from the Department of Electrical & Computer Engineering including Chair Professor Paul McGrath, Stephanie Schuckers (the Paynter-Krigman Endowed Professor in Engineering Science), Professor Mahesh Banavar, Research Professor Dana Barry, and Monalisa Achalla. Three authors from Arizona State University are Professor Andreas Spanias (who is in the School of Electrical, Computer, and Energy Engineering and is also Director of the SenSIP Center), Professor of Electrical Engineering Cihan Tepedelenlioglu, and Gowtham Muniraju. The final two authors are Specially Appointed Professor/Professor Emeritus Hideyuki Kanematsu at the National Institute of Technology (KOSEN), Suzuka College, Japan, and Dr. David Penepent, CFSP, who is the Program Director of Funeral Services Administration at the State University of New York at Canton and the co-owner of Johnson and Penepent Consulting.

We also express our sincerest appreciation to Springer Nature Singapore and to the Editor Dr. Mei Hann Lee.

In addition, we would like to thank our families for their continued interest and support: Dr. Barry's parents (Daniel and Celia Malloy), her husband (James), and children (James, Brian, Daniel, and Eric) and Dr. Kanematsu's parents (Shoji and Michiko Kanematsu), his wife (Reiko), and children (Hitomi and Hiroyuki).

Dana M. Barry
Hideyuki Kanematsu

Contents

About the Editors

Dr. Dana Barry is a Research Professor in the Department of Electrical & Computer Engineering at Clarkson University in the USA. She is the Scientific Board President for Ansted University, works part time at SUNY Canton, and has frequently served as a visiting professor and keynote speaker overseas. Dr. Barry has 5 graduate degrees including a M.S. degree in Chemistry from Clarkson University and a Ph.D. in Engineering from Osaka University, Japan. Her name is on the Mars Rovers (Spirit, Opportunity, and Curiosity), the NASA spacecraft that landed on the asteroid Bennu in 2020, and on the Japanese spacecraft Hayabusa -2, the first one in the world to land on an asteroid. She has over 300 academic publications including four Springer textbooks. Her honors include 21 consecutive APEX Awards for Publication / Communication Excellence, a Marquis Who's Who Lifetime Achievement Award (2017), an Outstanding Volunteer Award (2017) and a National Chem-Luminary Award both from the American Chemical Society. In 2019, she received an Outstanding Achievement Award from the Materials Research Society of Japan (MRS-J) for outstanding work involving biofilms. She was nominated (2021) by the Academic Union of Oxford, UK, to receive the special title "The Name in Science," an award for the most respected personalities in the fields of science, technology, and innovations.

Dr. Hideyuki Kanematsu, FASM (a Fellow of ASM) and FIMF (a Fellow of IMF) is a Specially Appointed Professor and Professor Emeritus at the National Institute of Technology (NIT KOSEN), Suzuka College, as well as a visiting professor at Nagoya University, Japan. He was the Dean of the Dept. of MS and Eng., and the former Deputy President of NIT (KOSEN), Suzuka, Mie, Japan. Now he serves as the Unit Leader (Director) of the KOSEN Materials Science and Engineering Center under the GEAR 5.0 Project and is a specially appointed professor (Professor Emeritus). He has been an active researcher in the areas of Surface Science and Engineering of Materials for many years. He is particularly interested in R&D of antibacterial, antiviral, and antibiofilm materials. Dr. Kanematsu holds a B.Eng. (1981), a M. Eng. (1983) and a Ph.D. in Materials Science and Engineering (1989), all from Nagoya University. He is a NASF Scientific Achievement Award winner.

Also, he received Japan's Minister of Education, Culture, Sports, Science, and Technology Award in May 2021. This award is considered the number one prize from the Minister of Education in the Japanese government. In addition, he is an active member of many organizations like the ASM International, the National Association for Surface Finishing, etc.

Part I
Viruses and Infections

Chapter 1
General Information About Viruses

Dana Barry and Paul McGrath

Abstract This chapter includes background information about viruses. It starts by describing a virus as an infectious agent that is submicroscopic and replicates inside the living cells of an organism. These organisms include plants, animals, and humans. Viruses contain a nucleic acid (DNA or RNA) and proteins. They exist in a variety of forms such as spheres, cubes, rods, etc. Some (like the influenza virus) are surrounded by a membrane envelope that is covered with spikes that project outward from the surface. This chapter mentions mutations and discusses the replication process of viruses, including the retrovirus HIV (human immunodeficiency virus). Retro (backward) refers to a reverse direction of flow for the genetic information of these viruses. In addition, two types of viral infections (shingles and rabies) are introduced and described.

1.1 Introduction

A virus is an infectious agent that is submicroscopic and replicates inside the living cells of an organism. It infects various forms of life including plants, animals, and humans. The study of viruses is called virology. Viruses lack the cellular organization that characterizes life [1]. They have no nucleus or other organelles and no cytoplasm. Viruses must enter a living host to multiply. They contain a nucleic acid (DNA or RNA) and proteins. The nucleic acid occupies the core region of the virus. Some viruses contain DNA (deoxyribonucleic acid), while others have RNA (ribonucleic acid). True cells have both types. Viruses are extremely small. Some are

D. Barry (✉)
Department of Electrical and Computer Engineering, Clarkson University, Potsdam, NY, USA

State University of New York at Canton, Canton, NY, USA
e-mail: dmbarry@clarkson.edu

P. McGrath
Department of Electrical and Computer Engineering, Clarkson University, Potsdam, NY, USA
e-mail: pmcgrath@clarkson.edu

D. Barry, H. Kanematsu (eds.), *Studies to Combat COVID-19 using Science and Engineering*, https://doi.org/10.1007/978-981-19-1356-3_1

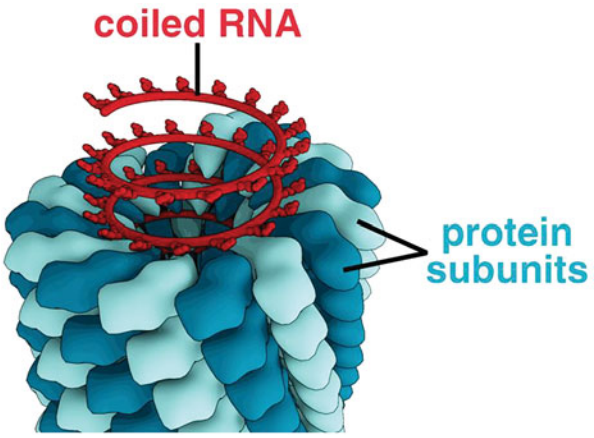

Fig. 1.1 The tobacco mosaic virus contains a strand of RNA coiled in a helix of protein subunits

only 20 nanometers in diameter. Knowledge about their structure became available by using the electron microscope [2–5]. Viruses exist in a variety of forms such as spheres, cubes, rods, etc. The nucleic acid of a virus is enclosed within a shell made of protein. This shell or jacket is called a capsid. It may be rod-shaped or a more complex form, depending upon the type of virus. Capsids are made of many protein subunits called capsomeres. For a simple example, tobacco mosaic virus is a plant virus that has RNA and a helical structure. See Fig. 1.1 [6]. This virus infects a wide variety of plants, especially tobacco [7]. It causes the plant's leaves to have patterns such as mosaic-like mottling and discoloration.

Some animal viruses and others have a complex structure in which their capsid is surrounded by a membrane envelope. This envelope is covered with spikes that project outward from the surface. The influenza virus has an outer envelope studded with glycoprotein spikes [8–10]. Its genome (set of genes) consists of eight single-stranded RNA segments (each of which is wrapped in a helical capsid). This virus generally has a spherical shape. Figure 1.2 shows the structure of a coronavirus with its harmful spikes [11]. It has the RNA genome too. The display is of the severe acute respiratory syndrome coronavirus 2 (SARS-CoV-2). This virus is contagious and can affect various parts of the human body [12–18]. It is primarily spread between people in close contact and by droplets from coughs, sneezes, etc. of individuals with the virus.

Viruses can't multiply on their own. They replicate in a living cell by using the energy and chemicals of their host cell [19–23]. Each type of virus can infect a limited range of host cells. A virus identifies a host cell. Then the virus matches and binds its outer proteins to specific receptor molecules on the surface of the cell. A viral infection starts when the genome of a virus enters a host cell. Consider the following simple viral replication cycle. A DNA virus, with a capsid containing a single type of protein, enters a host cell. After the virus enters the cell, the DNA is uncoated by enzymes to expose the genetic material. The viral DNA uses the host's

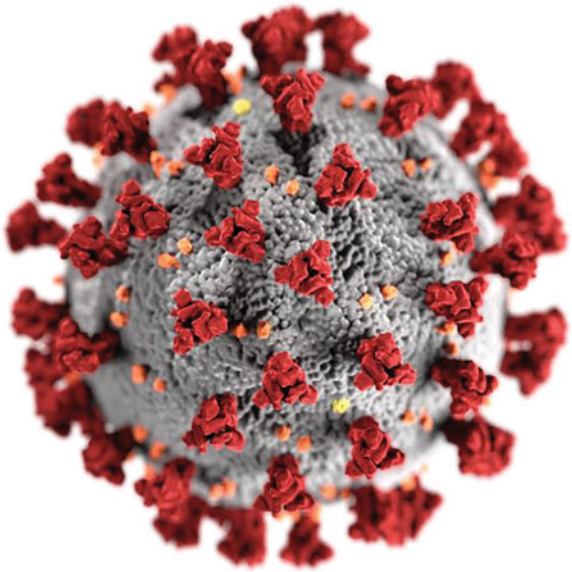

Fig. 1.2 This figure shows the structure of a coronavirus with its harmful spikes

nucleotides and enzymes to replicate itself. It uses other host materials to produce its capsid proteins. It should be mentioned that RNA is synthesized from DNA (by the process of transcription) and specifies the structure of the capsid proteins. The DNA and capsid proteins assemble into new viruses. This cycle ends when the new viruses exit the cell. They are now able to infect additional cells and spread the infection.

Most DNA viruses use the DNA polymerase of the host cell to synthesize new genomes for the templates made available by the viral DNA [24]. On the other hand, RNA viruses replicate their genomes by using special virus-encoded polymerases that use RNA as a template. In any case, the host provides the nucleotides for the nucleic acid synthesis and the enzymes, etc. for making viral proteins dictated by messenger RNA, mRNA (that is transcribed from viral genes). The RNA viruses with the most complicated replication cycles are the retroviruses [25]. Retro (backward) refers to a reverse direction of flow for the genetic information of these viruses. A retrovirus inserts a copy of its RNA into the DNA of a host cell. The virus uses its own reverse transcriptase enzyme to produce DNA from its RNA genome. Then the host cell uses the viral DNA as part of its own genome to produce the required proteins to assemble new copies of the virus. An example of a retrovirus is HIV (human immunodeficiency virus) [26–31]. This virus targets the immune system. It attacks CD4 cells (immune cells, types of T cell). They are white blood cells that circulate and detect infections within the body. HIV uses CD4 cells to create more copies of the virus while decreasing the body's ability to combat diseases, etc. An advanced stage of HIV infection is AIDS (acquired immunodeficiency syndrome). Treatments for HIV are called antiretroviral drugs. They can stop the progression of the infection and increase a

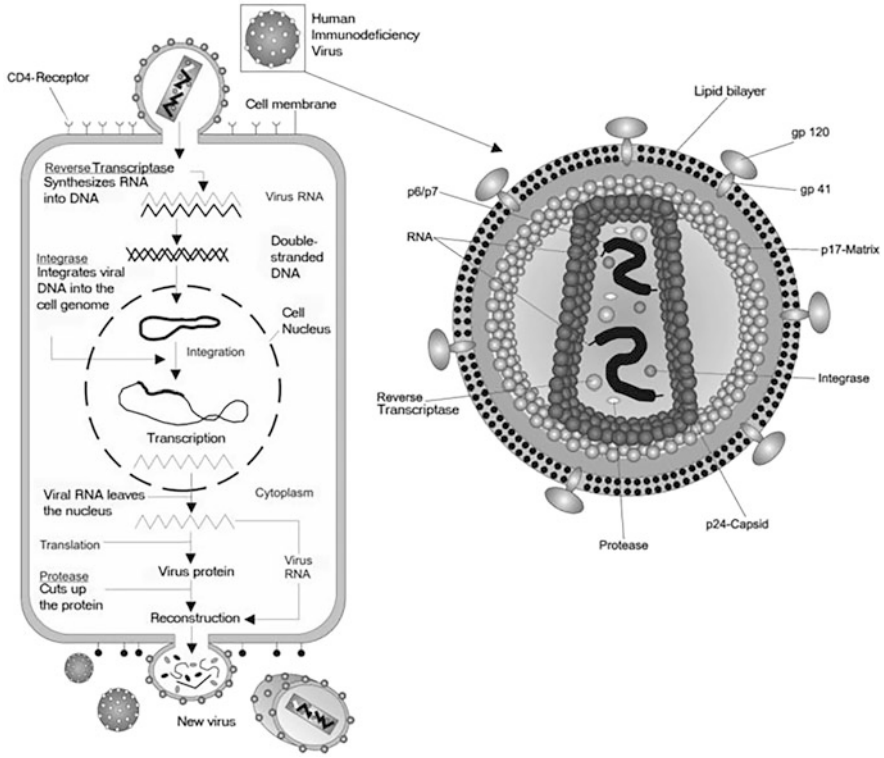

Fig. 1.3 This figure shows the replication cycle of HIV, a retrovirus

person's life expectancy. For protection against HIV, one should avoid the sharing of needles and exposure to body fluids. Figure 1.3 provides a diagram for the replication cycle of HIV [32].

1.2 Examples of Viral Infections

As previously mentioned, a virus is an infectious agent that is submicroscopic and replicates inside the living cells of an organism. It can also mutate. A mutation is a change in a virus's genome, a set of genetic instructions needed for the virus to function [33–38]. It happens when a virus has contact with a host and starts to replicate. When the virus replicates, there is a chance that its genetic code is not copied correctly. The errors result in variants of the virus. Some mutations die out, while others survive and spread. Public health organizations are concerned about variants that increase infectivity or allow a virus to escape the immune system. Viruses can change genetically by a method called antigenic shift. For example,

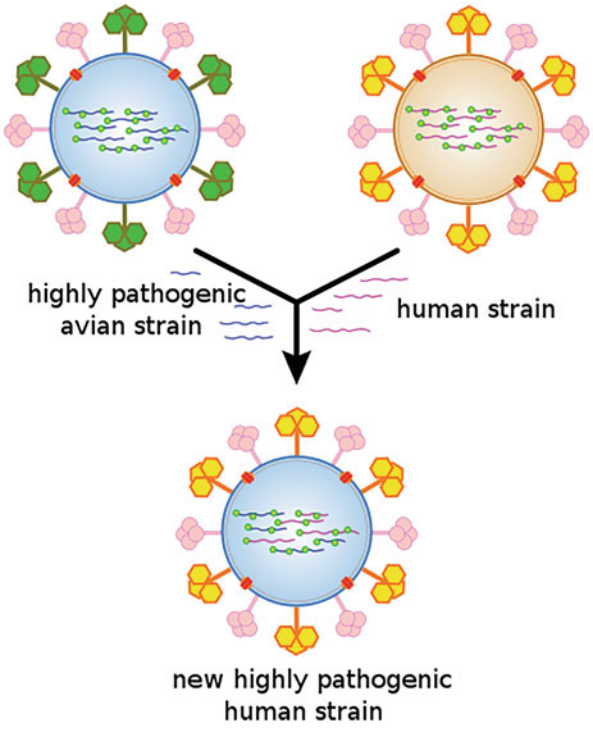

Fig. 1.4 This figure shows an antigenic shift that results in a new and highly pathogenic strain of the human flu

a nucleotide base is changed, inserted, or deleted from a DNA or RNA sequence of an organism's genome. Figure 1.4 displays an antigenic shift resulting in a new and highly pathogenic strain of the human flu [39].

Mutations can be detected through genome sequencing, which reveals the order of bases (adenine, cytosine, guanine, and thymine) present in the entire genome of an organism. This technique (which involves computer software, etc.) allows scientists to monitor small changes in the virus to understand how it works. A person with a particular virus provides a swab sample. Then the genetic code can be extracted before being read using a sequencer. Finally, the genomes and mutations are compared. Then the information is shared with scientists.

The genetic material inside a virus helps determine how fast a virus mutates. This impacts how the illness spreads in the population. Viruses that replicate through DNA use the same process that the host cell uses to create its DNA. Therefore, mutations occur slowly. Smallpox is an example of such a DNA virus. Smallpox (now considered eradicated by the WHO) was an infectious disease caused by the *Variola* virus. *Variola* is a large brick-shaped virus with a single linear double-stranded DNA genome. The two virus variants (for smallpox) include *Variola major* and *Variola minor* [40, 41].

Initial symptoms for smallpox included fever and vomiting. These symptoms were followed by ulcers forming in the mouth and a skin rash resulting in fluid-filled blisters with a dent in the center. These blisters eventually scabbed over and fell off. However, scars remained. The disease was spread by infected people (especially through sneezes, coughs, etc.) and by contaminated items and surfaces. Smallpox vaccine was used to prevent this disease, which is no longer a problem. Dr. Edward Jenner, an English physician and scientist, created the world's first smallpox vaccine.

RNA viruses, on the other hand, replicate using a more complex mechanism. Therefore, errors in genetic coding can occur in RNA viruses, like the influenza virus. These errors allow RNA viruses to quickly mutate from host cell to host cell. This makes it hard to keep up and prepare vaccines for new strains of the virus. A virus can be spread by insects, animals, and humans (especially through droplets from sneezes and coughs) [42]. The diagram of body infection sites (for viruses) is displayed in Fig. 1.5 [43]. Keep in mind that vaccines and antiviral drugs are used to help prevent and control the spread of viruses. The next section introduces and describes two types of viral infections: shingles and rabies.

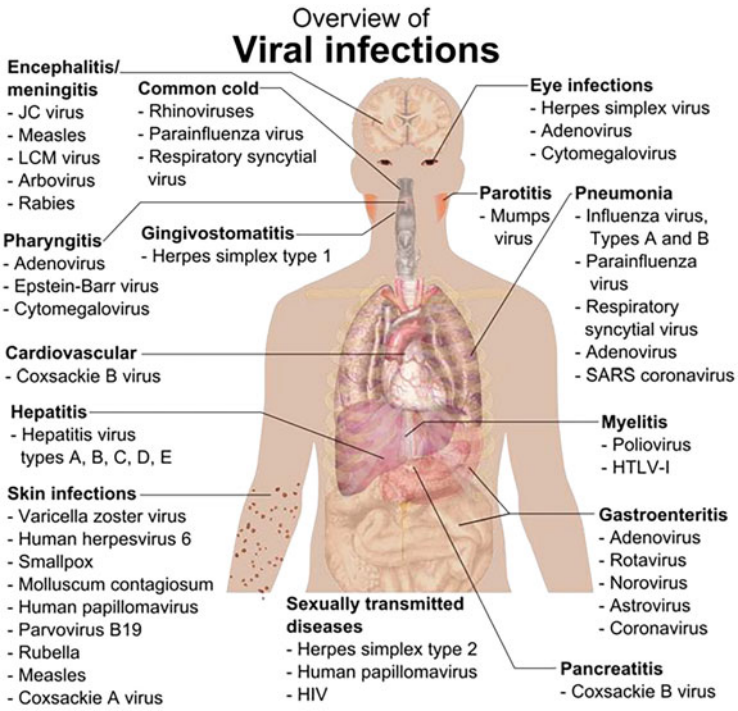

Fig. 1.5 This diagram shows infection sites in the human body

1.2.1 Shingles

Shingles is a viral infection that causes a painful rash with blisters [44–47]. The rash is generally in a localized area on the left or right side of the body. It usually heals within a few weeks, but some people develop nerve pain that can last for a long time. If the virus involves the eyes, then a loss of vision may occur. Shingles (herpes zoster) is caused by reactivation of the varicella zoster virus (a double-stranded DNA virus) which is responsible for chickenpox. See Fig. 1.6 [48]. After chickenpox infection, the virus remains dormant in the body's nerve tissues. However, later in life, the virus can be reactivated and cause shingles. Once reactivated, the virus travels from the nerve body to the skin where it produces blisters. Figure 1.7 shows the progression of shingles starting with the dormant virus and ending with a rash, etc. on the surface of the skin [49]. Number 1 in the diagram represents bumps. Number 2 shows the blisters which break open (number 3) and crust over (number 4). Then they disappear. These steps take about 4 weeks. A painful condition called postherpetic neuralgia occurs sometimes. It is thought to be caused by nerve damage (number 5) and can last weeks or much longer after the rash disappears. Shingles is more likely to occur in older people and those who have impaired immune systems. NOTE: It is rare for a person to have shingles more than three times. Antiviral drugs may reduce the amount of time one suffers with the shingles and its severity. However, they need to be started within 72 h after the rash appears. The standard treatment has been acyclovir. The newer and superior antiviral drugs include valaciclovir and famciclovir. Vaccines are available to prevent shingles. Zostavax was licensed by the FDA in 2006. It is given as one shot and can reduce

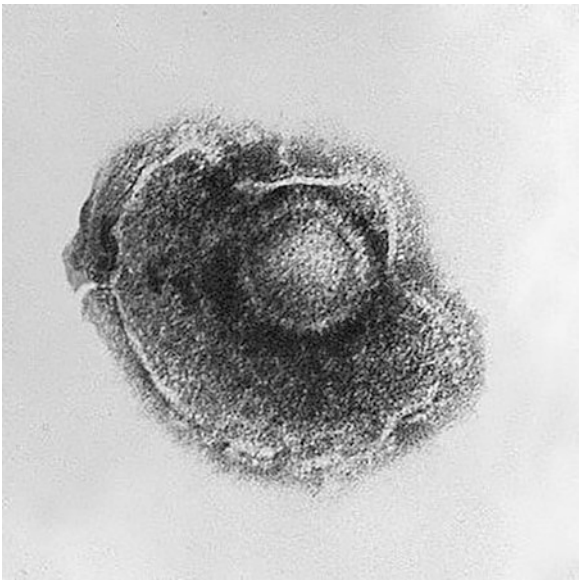

Fig. 1.6 This is an electron micrograph of varicella zoster virus magnified about 150,000×

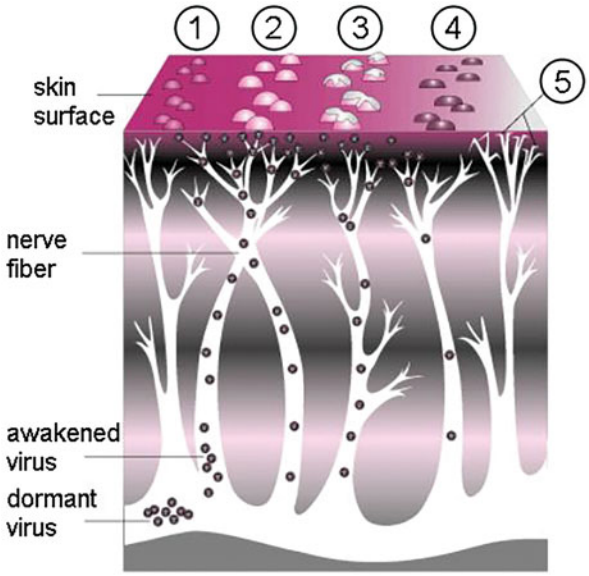

Fig. 1.7 This diagram shows the progression of shingles (from dormant virus to the skin surface)

the risk of developing shingles by about 50%. This vaccine contains a weakened chickenpox virus. Shingrix requires two shots and is recommended for individuals aged 50 years and older. It is about 90% effective and does not contain live virus [50].

1.2.2 Rabies

The rabies virus is a neurotropic virus, one that infects nerve cells [51–55]. It has the scientific name *Rabies lyssavirus*. This virus infects the central nervous system and causes inflammation of the brain in mammals and humans. It is mainly spread by bites and scratches from infected animals, which have the virus stored in their salivary glands. Also, transplants from donors who have died from rabies or unspecified encephalitis have transmitted rabies to humans. Most cases of rabies come from dogs, especially in developing and underdeveloped countries. According to the World Health Organization (WHO), India experienced a high death rate for humans (due to rabies) in 2004 [56]. Common sources of rabies in the United States include bats, raccoons, foxes, and skunks. Silver-haired bats and tricolored bats (formerly known as the eastern pipistrelle) are generally reported for causing cases of human rabies in the United States [57]. It should be mentioned that many tricolored bats previously died from the fungal disease known as the white-nose syndrome [58, 59]. Figure 1.8 shows the tricolored bat [60].

Fig. 1.8 A photo of the tricolored bat is provided

Initial symptoms for the rabies virus include a fever, a headache, and tingling at the site of exposure. As the disease progresses, a person might experience partial paralysis, confusion, abnormal behavior, a fear of water, and a coma. A sick individual usually dies 2–10 days after the onset of initial symptoms. The incubation period of this virus for humans is generally from 1–3 months. However, it may be as short as a few days or longer than a year.

The *Rabies lyssavirus* displays a cylindrical shape. It has a single-stranded RNA genome with negative sense. (A negative sense RNA virus consists of viral RNA that is complementary to the viral mRNA. On the other hand, positive sense RNA virus consists of viral mRNA that can be directly translated into proteins.) The rabies virus has a lipoprotein envelope with spikes composed of glycoprotein (G). Beneath the envelope is the membrane or matrix (M) protein layer. The core of the virus particle contains helically arranged ribonucleoprotein. Figure 1.9 displays a 3D structure of the rabies virus [61].

Rabies can be prevented. Since dogs are the main source of human deaths from rabies worldwide, they should get pre-exposure vaccinations to prevent rabies in people. Also, oral vaccinations in pellet form need to be distributed and made available to wildlife. Individuals with high-risk occupations should receive pre-exposure immunizations too. These people include veterinarians, laboratory

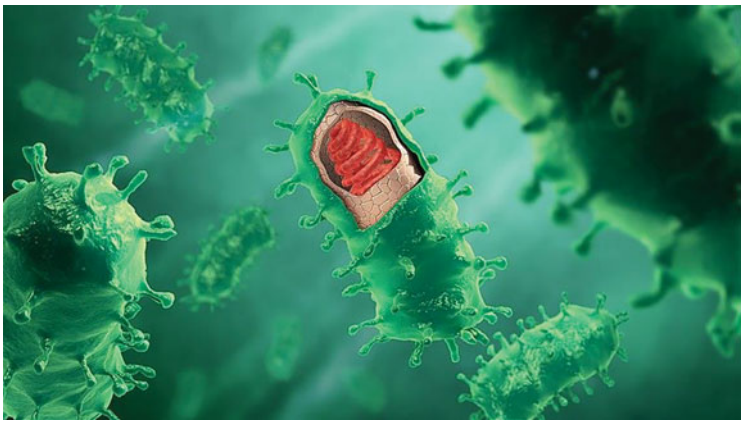

Fig. 1.9 This figure shows the structure of a rabies virus

workers who handle rabies viruses, animal disease control staff, wildlife rangers, and more.

Bite victims need immediate treatment after being exposed to rabies. This fast action helps prevent the virus from entering the central nervous system, which usually results in death. First, the wound should be thoroughly washed and flushed (for at least 15 min) using soap and water, detergents, etc. to remove and kill the rabies virus. Postexposure prophylaxis involves one dose of rabies immune globulin and five doses of rabies vaccine within a 28-day period. The rabies immune globulin has antibodies from blood donors, who were given the rabies vaccine. The rabies vaccine stimulates a person's immune system to make antibodies that neutralize the virus.

Animals can be diagnosed for rabies. Those displaying unusual behavior and other symptoms of the disease may have the virus. Postmortem diagnosis of rabies in animals is easier. Tests are carried out on parts of the affected brain. For example, one looks for virus antigens in brain tissue by using a fluorescent antibody technique. Other available methods include isolating the virus in a cell culture, etc.

1.3 Conclusions

This chapter includes background information about viruses. It describes a virus as an infectious agent that is submicroscopic and replicates inside the living cells of an organism. These organisms include plants, animals, and humans. Viruses contain a nucleic acid (DNA or RNA) and proteins. They exist in a variety of forms such as spheres, cubes, rods, etc. Some (like the influenza virus) are surrounded by a membrane envelope that is covered with spikes that project outward from the surface. The replication process of viruses, including the retrovirus HIV (human

immunodeficiency virus), is presented and described. (Retro, backward, refers to a reverse direction of flow for the genetic information of these viruses.) Viruses can mutate during the replication process. A mutation is a change in a virus's genome, a set of genetic instructions needed for the virus to function. It happens when a virus has contact with a host and starts to replicate. When the virus replicates, there is a chance that its genetic code is not copied correctly. Errors result in variants of the virus. Some mutations die out, while others survive and spread. Public health organizations are concerned about variants that increase infectivity or allow a virus to escape the immune system.

In addition, two types of viral infections (shingles and rabies) are introduced and described. Information is provided about their virus structure, cause of disease, transmission, symptoms, methods of prevention and treatment, etc.

References

1. Breitbart, M., & Rohwer, F. (2005, June). Here a virus, there a virus everywhere the same virus? *Trends in Microbiology, 13*(6), 278–284.
2. Councilman, M., Ellison, S., Rose, H., & Moore, D. (1954). Structure and development of viruses observed in the electron microscope: 11. Vaccinia and fowl pox viruses. *Journal of Experimental Medicine, 100*(3), 301–310.
3. Lawrence, C. M., Menon, S., Eilers, B. J., Bothner, B., Khayat, R., Douglas, T., & Young, M. J. (2009). Structural and functional studies of archaeal viruses. *The Journal of Biological Chemistry, 284*(19), 12599–12603.
4. Lodish, H., Berk, A., Zipursky, S. L., et al. (2000). *Molecular cell biology* (4th ed.). W. H. Freeman. Section 6.3, viruses: Structure, function, and uses. Retrieved from https://www.ncbi.nlm.nih.gov/books/NBK21523/
5. Rossmann, M. G. (2013, May). Structure of viruses: A short history. *Quarterly Reviews of Biophysics, 46*(2), 133–180. https://doi.org/10.1017/S0033583513000012
6. Splettsfoesser, T. (2012, July 20). File: TMV structure simple.png. License: Creative Commons Attribution—Share Alike 3.0. File:TMV structure simple.png - Wikimedia Commons
7. Donchenko, E., Pechnikova, E., Mishyna, M., et al. (2017, August 24). Structure and properties of virions and virus-like particles derived from the coat protein of Alternanthera mosaic virus. *PLoS One, 12*(8), e0183824.
8. Dadonaite, B., Gilbertson, B., Knight, M. L., Trifkovic, S., Rockman, S., Laederach, A., Brown, L. E., Fodor, E., & Bauer, D. L. V. (2019, November). The structure of the influenza A virus genome. *Nature Microbiology 4*(11), 1781–1789. https://doi.org/10.1038/s41564-019-0513-7. Epub 2019 Jul 22. PMID: 31332385; PMCID: PMC7191640.
9. Webster, R. G., Bean, W. J., Gorman, O. T., Chambers, T. M., & Kawaoka, Y. (1992). Evolution and ecology of influenza a viruses. *Microbiological Reviews, 56*, 152–179.
10. Vemula, S. V., Zhao, J., Liu, J., Wang, X., Biswas, S., & Hewlett, I. (2016). Current approaches for diagnosis of influenza virus infections in humans. *Viruses, 8*(4), 96. https://doi.org/10.3390/v8040096
11. Eckert, A., & Higgins, D. (2020, January 30). File: SARS-CoV-2 without background.png. License: This image is in the public domain. File:SARS-CoV-2 without background.png - Wikimedia Commons
12. Amanat, F., & Krammer, F. (2020). SARS-CoV-2 vaccines: status report. *Journal of Immunity, 52*(4), 583–589. https://doi.org/10.1016/j.immuni.2020.03.007

13. Boopathi, S., Poma, A. B., & Kolandaivel, P. (2021). Novel 2019 coronavirus structure, mechanism of action, antiviral drug promises and rule out against its treatment. *Journal of Biomolecular Structure and Dynamics, 39*(9), 3409–3418. https://doi.org/10.1080/07391102.2020.1758788
14. Mittal, A., Manjunath, K., Ranjan, R. K., Kaushik, S., Kumar, S., & Verma, V. (2020). COVID-19 pandemic: Insights into structure, function, and hACE2 receptor recognition by SARS-CoV-2. *PLoS Pathogens, 16*(8), e1008762. https://doi.org/10.1371/journal.ppat.1008762
15. Neuman, B. W., Adair, B. D., Yoshioka, C., et al. (2006). Supramolecular architecture of severe acute respiratory syndrome coronavirus revealed by electron cryomicroscopy. *Journal of Virology, 80*, 7918–7928.
16. Beniac, D. R., Andonov, A., Grudeski, E., et al. (2006). Architecture of the SARS coronavirus prefusion spike. *Nature Structural & Molecular Biology, 13*, 751–752.
17. Delmas, B., & Laude, H. (1990). Assembly of coronavirus spike protein into trimers and its role in epitope expression. *Journal of Virology, 64*, 5367–5375.
18. Bosch, B. J., van der Zee, R., de Haan, C. A., et al. (2003). The coronavirus spike protein is a class I virus fusion protein: Structural and functional characterization of the fusion core complex. *Journal of Virology, 77*, 8801–8811.
19. Ooi, E. E., Chew, J. S. W., Loh, J. P., et al. (2006). In vitro inhibition of human influenza a virus replication by chloroquine. *Virology Journal, 3*, 39. https://doi.org/10.1186/1743-422X-3-39
20. Denison, M. R. (2008). Seeking membranes: Positive-strand RNA virus replication complexes. *PLoS Biology, 6*(10), e270. https://doi.org/10.1371/journal.pbio.0060270
21. Mackenzie, J. (2005). Wrapping things up about virus RNA replication. *Traffic, 6*, 967–977.
22. Miller, S., & Krijnse-Locker, J. (2008). Modification of intracellular membrane structures for virus replication. *Nature Reviews. Microbiology, 6*, 363–374.
23. Novoa, R. R., Calderita, G., Arranz, R., Fontana, J., Granzow, H., et al. (2005). Virus factories: Associations of cell organelles for viral replication and morphogenesis. *Biology of the Cell, 97*, 147–172.
24. Van Etten, J. L., Lane, L. C., & Dunigan, D. D. (2010). DNA viruses: The really big ones (Giruses). *Annual Review of Microbiology, 64*, 83–99.
25. Reiss, C. S. (2008). Introduction: Retroviruses, DNA viruses, and prions. In *Neurotropic viral infections* (pp. 139–140). Cambridge University Press.
26. Mandsager, P., Marier, A., Cohen, S., Fanning, M., Hauck, H., & Cheever, L. W. (2018). Reducing HIV-related health disparities in the health resources and services administration's Ryan white HIV/AIDS program. *American Journal of Public Health, 108*(S4), S246–S250. https://doi.org/10.2105/AJPH.2018.304689. PMID: 30383416; PMCID: PMC6215373.
27. Chartier, M., Gylys-Cowell, I., Van Epps, P., Beste, L. A., Ohl, M., Lowy, E., & Maier, M. M. (2018). Accessibility and uptake of pre-exposure prophylaxis for HIV prevention in the veterans' health administration. *Federal Practitioner, 35*(Suppl 2), S42–S48.
28. Kunisaki, K. M., Nouraie, M., Jensen, R. L., Chang, D., D'Souza, G., Fitzpatrick, M. E., McCormack, M. C., Stosor, V., & Morris, A. (2020, July). Lung function in men with and without HIV. *AIDS, 34*(8), 1227–1235. https://doi.org/10.1097/QAD.0000000000002526
29. Barnett, P. G., Schmitt, S. K., Yu, W., Goetz, M. B., Ohl, M. E., & Asch, S. M. (2016, July). How will new guidelines affect CD4 testing in veterans with HIV? *Clinical Infectious Diseases, 63*(1), 96–100. https://doi.org/10.1093/cid/ciw194
30. Riddell, J. T., Amico, K. R., & Mayer, K. H. (2018). HIV preexposure prophylaxis: A review. *Journal of the American Medical Association, 319*, 1261–1268.
31. Giroir, B. P. (2020). The time is now to end the HIV epidemic. *American Journal of Public Health, 110*, 22–24.
32. Raul 654, translator (2004, December 24). File: Hiv gross.png. License: Creative Commons Attribution – Share Alike 3.0. File:Hiv gross.png - Wikimedia Commons
33. Růžička, M., Kulhánek, P., Radová, L., Čechová, A., Špačková, N., Fajkusová, L., et al. (2017). DNA mutation motifs in the genes associated with inherited diseases. *PLoS One, 12*(8), e0182377. https://doi.org/10.1371/journal.pone.0182377

34. Cooper, D. N., Bacolla, A., Ferec, C., Vasquez, K. M., Kehrer-Sawatzki, H., & Chen, J. M. (2011). On the sequence-directed nature of human gene mutation: The role of genomic architecture and the local DNA sequence environment in mediating gene mutations underlying human inherited disease. *Human Mutation, 32*, 1075–1099.
35. Brown, A.-L., Li, M., Goncearenco, A., & Panchenko, A. R. (2019). Finding driver mutations in cancer: Elucidating the role of background mutational processes. *PLoS Computational Biology, 15*(4), e1006981. https://doi.org/10.1371/journal.pcbi.1006981
36. Sanjuán, R., Nebot, M. R., Chirico, N., Mansky, L. M., & Belshaw, R. (2010). Viral mutation rates. *Journal of Virology, 84*, 9733–9748. https://doi.org/10.1128/JVI.00694-10
37. Duffy, S., Shackelton, L. A., & Holmes, E. C. (2008). Rates of evolutionary change in viruses: Patterns and determinants. *Nature Reviews. Genetics, 9*, 267–276. https://doi.org/10.1038/nrg2323
38. Sanjuan, R., & Doingo-Calap, P. (2016). Mechanisms of viral mutation. *Cellular and Molecular Life Sciences, 73*(23), 4433–4448.
39. Jiver (2012, August 18). File: Influenza geneticshift.svg. License: Creative Commons Attribution-Share Alike 3.0. File:Influenza geneticshift.svg - Wikimedia Commons
40. Belongia, E. A., & Naleway, A. L. (2003). Smallpox vaccine: The good, the bad, and the ugly. *Clinical Medicine & Research, 1*(2), 87–92. https://doi.org/10.3121/cmr.1.2.87
41. Breman, J., & Henderson, D. A. (2002). Diagnosis and management of smallpox. *The New England Journal of Medicine, 346*, 1300–1308.
42. Subbarao, K., & Mahanty, S. (2020). Respiratory virus infections: Understanding COVID-19. *Immunity, 52*(6), 905–909. https://doi.org/10.1016/j.immuni.2020.05.004
43. Haggstrom, M. (2009, April 4). File: Viral infections and involved species.png. License: This work is in the public domain. File:Viral infections and involved species.png - Wikimedia Commons
44. Nussbaum, R. (2014). Theories on varicella zoster virus reactivation based on shingles patterns. *The Science Journal of the Lander College of Arts and Sciences, 8*(1) Retrieved from https://touroscholar.touro.edu/sjlcas/vol8/iss1/10
45. Baird, N. L., Yu, X., Cohrs, R. J., & Gilden, D. (2013). Varicella zoster virus (VZV)-human neuron interaction. *Viruses, 5*(9), 2106–2115.
46. Gershon, A. A., Breuer, J., Cohen, J. I., Cohrs, R. J., Gershon, M. D., Gilden, D., Grose, C., Hambleton, S., Kennedy, P. G., Oxman, M. N., Seward, J. F., & Yamanishi, K. (2015). Varicella zoster virus infection. *Nature Reviews. Disease Primers, 2*(1), 15016. https://doi.org/10.1038/nrdp.2015.16
47. Sauerbrei, A. (2016). Diagnosis, antiviral therapy, and prophylaxis of varicella-zoster virus infections. *European Journal of Clinical Microbiology & Infectious Diseases, 35*(5), 723–734.
48. Palmer, E., & Patin, B. G. (1982). File: Varicella (Chickenpox) Virus PHIL 1878 lores. jpg. License: This image is in the public domain. File:Varicella (Chickenpox) Virus PHIL 1878 lores.jpg - Wikimedia Commons
49. Gordon, R. (2007, January 1). File: A Course of Shingles diagram.png. License: This diagram is in the public domain. File:A Course of Shingles diagram.png - Wikimedia Commons
50. Saguil, A., Kane, S., Mercado, M., & Lauters, R. (2017). Herpes zoster and postherpetic neuralgia: prevention and management. *American Family Physician, 96*(10), 656–663.
51. Warrell, M., & Warrell, D. (2015, February). Rabies: The clinical features, management, and prevention of the classic zoonosis. *Clinical Medicine Journal, 15*, 78–81. https://doi.org/10.7861/clinmedicine.14-6-78
52. El-Sayed, A. (2018). Advances in rabies prophylaxis and treatment with emphasis on immunoresponse mechanisms. *International Journal of Veterinary Science and Medicine, 6*(1), 8–15. https://doi.org/10.1016/j.ijvsm.2018.05.001
53. Deviatkin, A., & Lukashev, A. (2018). Recombination in the rabies virus and other lyssaviruses. *Infection, Genetics and Evolution, 60*, 97–102.
54. Fooks, A., Banyard, A., Horton, D., Johnson, N., McElhinney, L., & Jackson, A. (2014). Current status of rabies and prospects for elimination. *Lancet, 384*, 1389–1399.

55. Yousaf, M. Z., Qasim, M., Zia, S., et al. (2012). Rabies molecular virology, diagnosis, prevention, and treatment. *Virology Journal, 9*, 50. https://doi.org/10.1186/1743-422X-9-50
56. Plotkin, S. A. (2000, January). Rabies. *Clinical Infectious Diseases, 30*(1), 4–12. https://doi.org/10.1086/313632
57. Davis, A. D., Morgan, S. M., Dupuis, M., Poulliott, C. E., Jarvis, J. A., Franchini, R., Clobridge, A., & Rudd, R. J. (2016). Overwintering of rabies virus in silver haired bats (Lasionycteris noctivagans). *PLoS One, 11*(5), e0155542. https://doi.org/10.1371/journal.pone.0155542
58. Perry, R., & Jordan, P. (2020). Survival and persistence of tricolored bats hibernating in Arkansas mines. *Journal of Mammalogy, 101*(2), 535–543.
59. Hanttula, M. K., & Valdez, E. W. (2021). First record and diet of the tri-colored bat (*Perimyotis subflavus*) from Guadalupe Mountains National Park and Culberson County, Texas. *Western North American Naturalist, 81*(1), 11. Retrieved from https://scholarsarchive.byu.edu/wnan/vol81/iss1/11
60. Enweb. (2019, September 20). File: Perimyotis subflavus picture cropped.jpg. License: Creative Commons Attribution-Share Alike 4.0. File:Perimyotis subflavus picture cropped.jpg - Wikimedia Commons
61. Author. (2019, July 2). File: Rabies virus structure. License: Creative Commons Attribution—Share Alike 4.0. Rabies virus structure—Rabies virus—Wikipedia. Retrieved from https://www.scientificanimations.com/wiki-images/

Chapter 2
Infection

Hideyuki Kanematsu and Dana Barry

Abstract Infection is caused by pathogens outside of our bodies or by usual inhabitants within our bodies. It can be defined as the phenomenon that pathogens such as microbes, viruses, etc. enter organisms and grow there. Bacteria can grow by themselves under certain conditions. From this viewpoint, we can understand that bacteria are able to grow inside our bodies. On the other hand, viruses can't grow by themselves. They need host cells to grow. Therefore, viruses are not organisms but just tiny particles conveying nucleic acids. We should keep the differences in mind to combat COVID-19 and other viruses with researchers in various disciplines. In this chapter, we describe what infection is and how viruses differ from bacteria.

2.1 Introduction

At the end of 2019, we had chilling news from Mainland China. In Wuhan, an unknown viral disease prevailed. Also, the number of patients kept increasing according to the news. Before we could say boo, the situation turned into a pandemic. Since then, the worldwide battle with the COVID-19 virus began and has continued to this day [1–5].

The critical situation has redirected us to the original meaning of infection as well as those of viruses and bacteria again. The increasing concerns about the infection and the market for antibacterial, antiviral, and antifungal materials, along with anti-biofilm products, have increased tremendously. For example, the economic size of the total market in Japan was about 80 billion yen (around eight million dollars) at

H. Kanematsu (✉)
National Institute of Technology, Suzuka College, Shiroko-cho, Suzuka, Mie, Japan
e-mail: kanemats@mse.suzuka-ct.ac.jp

D. Barry
Department of Electrical and Computer Engineering, Clarkson University, Potsdam, NY, USA

State University of New York at Canton, Canton, NY, USA
e-mail: dmbarry@clarkson.edu

D. Barry, H. Kanematsu (eds.), *Studies to Combat COVID-19 using Science and Engineering*, https://doi.org/10.1007/978-981-19-1356-3_2

the end of 2019 before the pandemic. However, it increased drastically and reached the level of 150 billion yen (around 15 billion dollars) in the middle of 2020 [6]. Such a drastic expansion of the related markets could be attributed to the pandemic of COVID-19. As a result, the infection problems are now central topics from both the personal and industrial viewpoints.

In this chapter, we describe the original meaning of infection. Basically, infection occurs by the growth of pathogens. Therefore, we explain how pathogens grow inside of the human body. We also discuss the ways our bodies respond to infectious diseases. This chapter points out the differences between bacterial and viral infections. Next is a description of what would happen outside of our human body regarding bacteria and viruses. Finally, we are presented with a better way of picturing inanimate materials and products as they relate to viruses and their infections.

2.2 What Is Infection?

Infection can be defined as the phenomenon that pathogens such as microbes, viruses, etc. enter organisms and grow there. As shown in Fig. 2.1, infection is classified into two main categories, endogenous and exogenous infections. For the former, pathogens already exist within organisms. They are called normal inhabitants. As examples, we can mention periodontal diseases, aspiration pneumonitis, etc. The latter is caused by pathogenic bacteria and viruses such as influenza, noroviruses, COVID-19, dysentery, cholera, etc.

In both cases, growth is the key point for infection. As for bacteria, the cause for diseases is mainly the toxic substances derived from them. The growth process could be described as follows.

Generally, bacteria are classified into two categories from the viewpoint of outer structures: gram-positive and gram-negative bacteria. Concretely speaking, the former is stained well through the gram staining process, and the latter is not. This

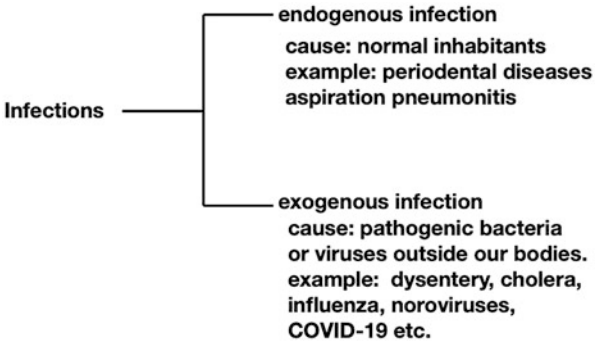

Fig. 2.1 Classification of infections—endogenous and exogenous infection

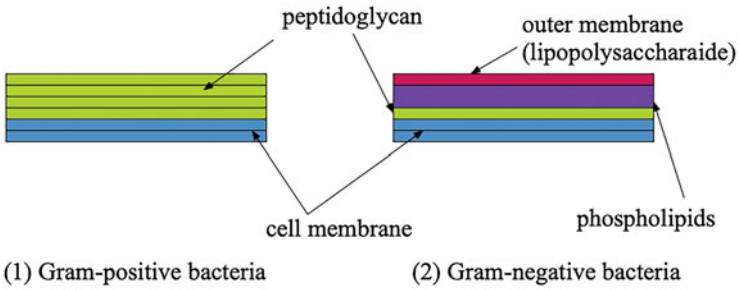

Fig. 2.2 The schematic illustration for the outer parts of bacteria. Part 1 (2.2**a**), part 2 (2.2**b**)

could be attributed to the structural differences at the outer parts of bacterial cells. Figure 2.2 shows the schematic figures for the outer part structures. Figure 2.2a, also indicated by the number 1 in the figure, shows that of gram-positive bacteria, and Fig. 2.2b, also indicated by a number 2 in the figure, shows that of gram-negative bacteria. Gram-positive bacteria have a thick peptidoglycan layer on the cell membranes, while gram-negative bacteria have lipid bilayers on thin peptidoglycan layers: lipopolysaccharide (LPS). The toxic substances causing bacterial infections can be classified into two categories: endotoxin and exotoxin. Endotoxin basically consists of lipopolysaccharides, and exotoxin is protein excreted from bacterial cells. Therefore, bacterial infections could happen, even when bacteria exist outside of our human bodies. This type of infection is closely related to bacterial growth. Therefore, it is very important for us to know how bacteria grow. They can continue to grow, even outside of our bodies, if the environmental conditions are favorable for them. They generally tend to attach to materials' (products') surfaces, since the nutrients that they need exist on materials (products). When the number of attached bacteria exceeds a certain value, the bacteria simultaneously excrete polysaccharides. As a result, the materials' surfaces are enclosed and surrounded by external polymeric substances (EPSs). These encasements are called biofilms. They are the source of infection for bacteria outside of our bodies.

On the other hand, viruses have simpler structures, as compared to those for bacteria. Figure 2.3 shows the schematic figures. In the light of structures, viruses are mainly classified into two types: envelope and non-envelope types. The former includes the influenza virus and the one for COVID-19. An example of the latter type is the norovirus. In both cases, the nucleic acid is the center of the structure. Some types of viruses contain RNA, while others have DNA. The protein sheath that surrounds the nucleic acid is called a capsid. In addition, a lipid layer surrounds other types of viruses such as influenza and COVID-19. The lipid cover is called an "envelope." Many glycoproteins protrude from the envelope. Therefore, both bacteria and viruses have somewhat similar outer structures from the viewpoint of engineers who investigate the interaction between products and pathogens. The interaction between products/materials and viruses will be discussed in other chapters.

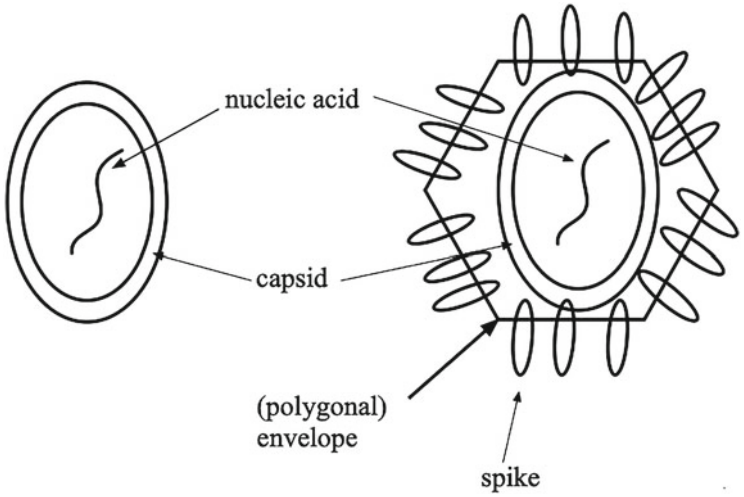

Fig. 2.3 Viral structures: (**a**) non-envelope type, (**b**) envelope type

Figure 2.4 shows bacterial growth schematically. Basically, bacteria grow by cell divisions. Cell divisions of bacteria are characteristic of bacterial growth.

Bacteria generally multiply by binary fission or budding. As for binary fission, bacterial cells copy the components to be divided. Bacterial cells produce copies of components faithfully through the production of walls to produce two daughter cells in the binary fission process. On the other hand, a new cell appears on the mother cell and detaches from it to grow.

Viral growth has a different process because viruses are not able to grow by themselves. They need host cells. Therefore, they enter organisms' bodies to begin their growth process, as shown in Fig. 2.5. The process basically involves the following five steps.

1. The virion (viral particle) attaches to the host cell.
2. The virion genome enters the host cell.
3. Proteins are synthesized to shut down that of the host cell, to regulate the expression of viral genes, and to synthesize viral nucleic acids.
4. The components assemble into the complete virion.
5. The newly assembled viruses are released.

The process provides information for devising countermeasures to their growth. Viruses are basically inanimate matters (virions) in the light of their growth form. For example, they can't grow by themselves. They contain nucleic acids and need host cells to grow.

Bacteria grow outside of our bodies, while viruses need host cells to grow. Therefore, the countermeasure for bacterial growth should include chemicals

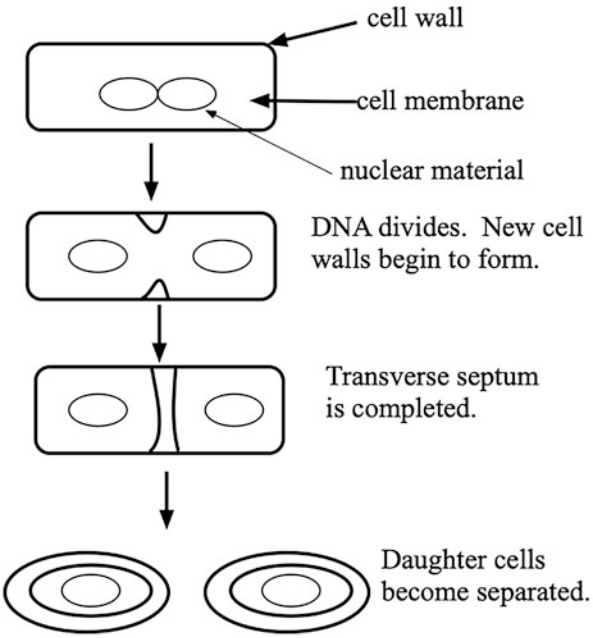

Fig. 2.4 General schematic illustration for bacterial growth

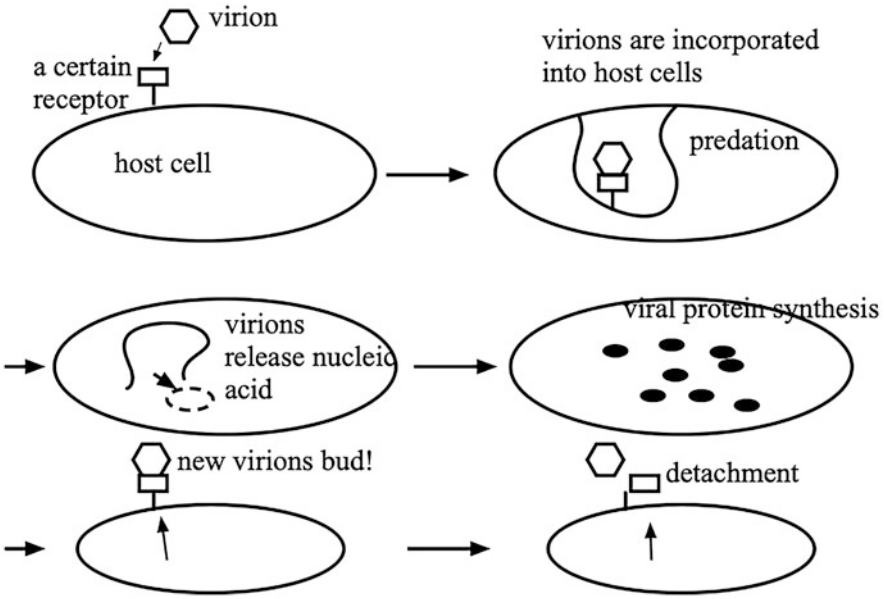

Fig. 2.5 Schematic illustration for viral growth

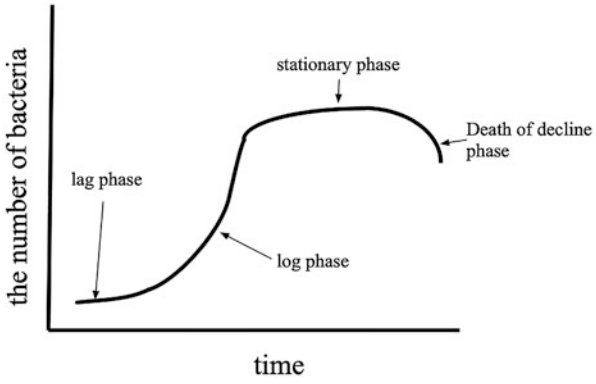

Fig. 2.6 Schematic bacterial growth curve

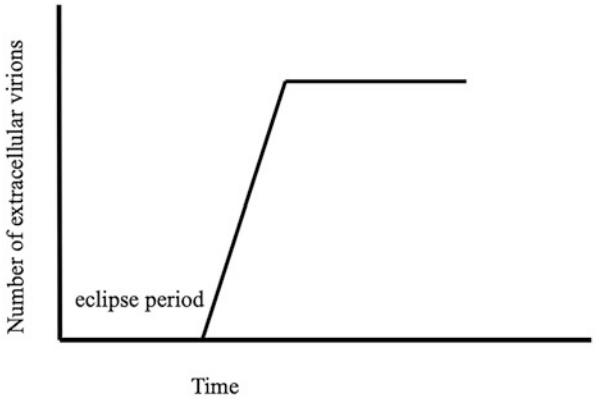

Fig. 2.7 Schematic illustration for general viral growth behavior

(biocides), antibiotics, etc. As for viruses, antiviral drugs are helpful. Inside of our bodies, our immune systems work to control the growth of both bacteria and viruses.

Figure 2.6 shows the general growth curve for bacteria schematically. At the beginning of their growth stage, they have lag phases where bacterial growth does not seem to happen, or it takes place very slowly. Then they begin to grow exponentially. This period is called the log growth phase. Next is the stationary phase where their growth reaches a saturation condition. Finally, the number of bacteria decreases, and the bacteria gradually die (death of decline phase).

On the other hand, Fig. 2.7 shows the general viral growth curve schematically. When viruses enter the host cells, they become undetectable for a certain amount of time. This period is called the "eclipse period" where no cells reproduce. Then the growth abruptly happens. This phenomenon is called "burst."

2.3 What Happens in Our Body When Pathogens Enter It?

When pathogens enter the human body, they activate the inherent defense systems. Our defense system is classified into two main types as shown in Fig. 2.8: innate immunity and adaptive immunity.

When pathogenic matter tries to enter our bodies, the skin, mucous membranes, etc. provide strong resistance to them. If our skin has scrapes, etc., then its outer layer composed of epithelial cells (epidermis) serves as a barrier to prevent bacteria from entering our bodies. This would serve as a first line of defense against pathogens. Saliva, sweat, and tears, along with nasal and vaginal secretions, etc., also break the cell walls of bacteria. These defense factors exist in mucous membrane secretions. However, it seems like the abovementioned first lines of defense do not work well against viruses.

Our second line of defense includes cytokines, phagocytes, peptides, neutrophils, and various proteins. They are not all discussed in this chapter. The second line of defense is composed of our inherent functions that mainly try to destroy bacteria. In most cases, the immune system recognizes pathogens and works to kill and eliminate them from our bodies. In the case of viruses, NK cells (natural killer cells) work to eliminate cells infected by viruses. Generally, the natural immune system does not work well against tiny pathogens in blood and cells like viruses. In such a case, we rely on the third line of defense.

The third line of defense corresponds to acquired immunity. Usually, B cells and helper T cells can be mentioned as representative cells for acquired immunity. B cells produce antibodies which recognize and eliminate antigens (foreign substances such as viruses). Helper T cells generally find the infected cells and command the immune cells. Killer T cells usually destroy the infected cells. Therefore, the acquired immune system works well for viruses.

Information about how to control bacteria and viruses in our human bodies would be very helpful to scientists and engineers who want to establish countermeasures for new viral infections.

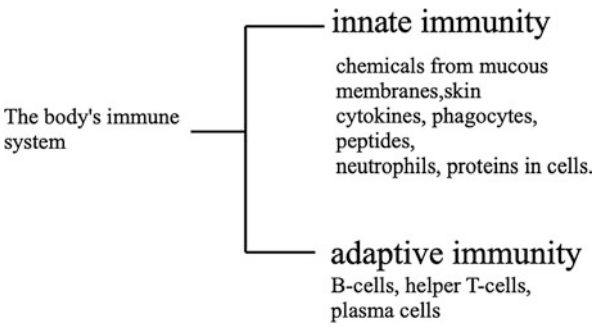

Fig. 2.8 The body's immune system

2.4 Thoughts for the Future

In this chapter, we introduced some basic information about both bacterial and viral infections and compared them. Their differences would be important to scientists and engineers who are trying to develop countermeasures for them. For example, let's take the production of materials. Nowadays (with the COVID-19 pandemic), people are very sensitive to infection, even by touching products like doorknobs, railings, cell phones, computer screens, and many other materials. As a result, the market for antibacterial and antiviral materials expanded very abruptly from the end of 2019 to the present. In Japan, the home country for one of the authors, the market size was around eight billion dollars at the end of 2019. However, it was about 15 billion dollars in the middle of 2020 (a big jump in just about 6 months). In such a situation, we need to know the type of antiviral actions required to protect various materials from virions and the differences that exist between antibacterial and antiviral actions. Then we could establish appropriate, correct, and effective countermeasures. This would also be true for other applications where scientists from many disciplines have combatted COVID-19.

References

1. Ciotti, M., Ciccozzi, M., Terrinoni, A., Jiang, W.-C., Wang, C.-B., & Bernardini, S. (2020). The COVID-19 pandemic. *Critical Reviews in Clinical Laboratory Sciences, 57*(6), 365–388.
2. Omer, S. B., Malani, P., & Del Rio, C. (2020). The COVID-19 pandemic in the US: A clinical update. *Journal of the American Medical Association, 323*(18), 1767–1768.
3. Lone, S. A., & Ahmad, A. (2020). COVID-19 pandemic—An African perspective. *Emerging Microbes & Infections, 9*(1), 1300–1308.
4. Kumar, A., Gupta, P. K., & Srivastava, A. (2020). A review of modern technologies for tackling COVID-19 pandemic. *Diabetes and Metabolic Syndrome: Clinical Research and Reviews, 14*(4), 569–573.
5. Chowell, G., & Mizumoto, K. (2020). The COVID-19 pandemic in the USA: What might we expect? *The Lancet, 395*(10230), 1093–1094.
6. KOSEN Headquarter. (2020). *The market trend of anti-bacterial and anti-viral technology*. The internal investigation document.

Part II
Infection Spread Through Materials

Chapter 3
Infection and Materials: The Role of Materials' Surfaces as Interfaces Between Materials and the Microbial/Virus Environments

Hideyuki Kanematsu and Dana Barry

Abstract This chapter deals with virions and materials. (A virion is an infective form of a virus outside of a host cell). The chapter clarifies the way virions infect humans (or organisms) and the factors that affect virions on materials. Firstly, we discuss the relationship between materials and viral infection and then point out the kinds of interactions that could take place between materials' surfaces and virions. Based on this knowledge, potential countermeasures are proposed. The infection of human beings through materials is not clearly understood. However, if it was, then this information would be helpful for eradicating viral infections. Further research on this topic is needed.

3.1 Introduction

In the previous chapter, we focused on the basic phenomenon of infection for viruses and compared it to bacteria. Basically, infections must occur within organisms, like our human bodies, etc. When viruses enter the human body, they fight our initial line of defense which includes the skin, various mucosal membranes, etc. [1]. When the first line of defense is broken by the pathogenic invaders, then the second line of defense immediately begins to operate. This second line is our bodies' innate function called innate immunity. Any foreign matter would induce this innate form of protection which includes phagocytes, the cells that ingest and digest foreign particles. Phagocytes might break down dead tissue cells and remove them from

H. Kanematsu (✉)
National Institute of Technology, Suzuka College, Shiroko-cho, Suzuka, Mie, Japan
e-mail: kanemats@mse.suzuka-ct.ac.jp

D. Barry
Department of Electrical and Computer Engineering, Clarkson University, Potsdam, NY, USA

State University of New York at Canton, Canton, NY, USA
e-mail: dmbarry@clarkson.edu

D. Barry, H. Kanematsu (eds.), *Studies to Combat COVID-19 using Science and Engineering*, https://doi.org/10.1007/978-981-19-1356-3_3

the tissues. Macrophages also belong to our second innate immunity. They are large cells derived from blood monocytes. The monocytes move within our bodies looking for foreign matter. When they find such a target, they gather around the site and become macrophages to engulf the foreign matter. When the second line of defense fails to completely remove foreign matter, then the third line of defense takes over. This final function is called adaptive immunity. In this case, antibodies play important roles to destroy bacteria and viruses entering our bodies. Antigens (foreign pathogenic matter) stimulate T lymphocytes and B lymphocytes, the main components of our final defense system. The antibodies react with parts of bacteria and viruses to inactivate their pathogenic activities. We already know a lot about our body's defense mechanisms. However, we still don't know how viruses and bacteria on materials (products) cause infections for humans and other organisms.

In this chapter, we deal with the virions on materials and discuss how they infect humans and other organisms.

3.2 The Meaning of Infection on Materials

We described the general meaning of infection in the previous chapter (Chap. 2). Viruses can be found on materials, which are completely inanimate. This leads to the following question. What do we mean by saying that infection is on materials? It refers to the length of time that a virus remains active (on a material) and could possibly infect humans, etc. when it enters their bodies. To make this possible, virions need to keep their structures free from damage.

Let's first survey the potential infection routes between human beings. Figure 3.1 shows the general potential routes for viral infections between human beings. From the viewpoint of risk management, experts often say that air droplets play an important role for the spread of infection. When patients cough or sneeze, their air droplets could contaminate the space of a circle with about a 2–5 m radius. When a droplet is expelled directly from a patient's mouth, it could travel about 2–5 m. If the person wears a mask, this distance could be reduced quite a bit. However, the droplet might deposit on materials (such as various products) and keep its infectious potential for a while. If another individual contacts these materials, then the infectious virion(s) could enter his or her body to grow and multiply by utilizing the person's host cells.

The information and knowledge, about virions' behavior on materials, are not completely understood. Therefore, the database is not sufficient for us to utilize internationally. Since the start of the COVID-19 pandemic, people's concern has been oriented toward viral behaviors on materials.

We have been wondering if people touching the surfaces of products contaminated by pathogenic viruses would be infected. The clear and precise answer has not been obtained. Contradictory results have been shown. However, the CDC (Centers for Disease Control and Prevention, the USA) [2] and WHO (World Health Organization) [3] have stressed repeatedly how very important and effective hand

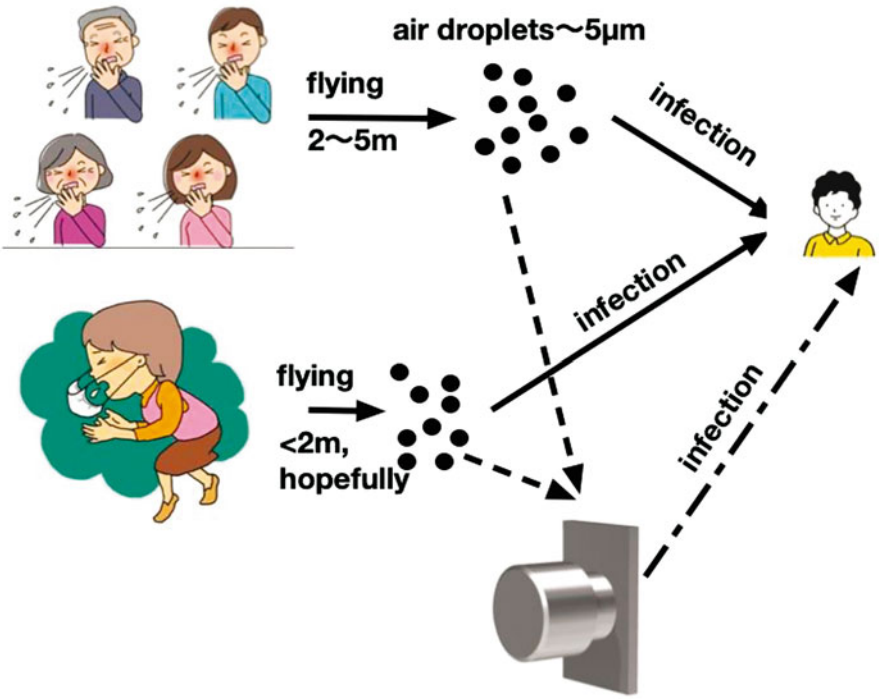

Fig. 3.1 Infection routes through materials (products) from human to human

washing is for us. On the other hand, we have confirmed that people could be infected by COVID-19 viruses through airborne droplets. When a person coughs, thousands of droplets are scattered in the atmosphere. These droplets would carry viruses and attach to products' surfaces such as doorknobs, stair railings, clothing, desks, etc. They could stay in the ambient air for an extended amount of time. Virions stay in feces too. Therefore, washing hands after using restrooms should be very important for protection from infection.

How long do viruses remain infectious? To tell the truth, this is a complex question, but such data would be very helpful for controlling viral infections. Many researchers are working to obtain this type of information. For example, coronaviruses inducing SARS (severe acute respiratory syndrome) or MERS (Middle East respiratory syndrome) could maintain their infectious activity for 9 days at the most, according to some research results [4–6]. Other investigators said that some viruses could remain active for about 28 days at low temperatures. Researchers in the USA investigated the activities of SARS-CoV-2 on various materials. They publicized their results and confirmed that the virus could keep active for about several hours in air droplets. Droplets with smaller diameters remain active longer in the air. Based on these fragmentary results, we could presume that viruses remain active much longer on materials' (products') surfaces than in air droplets. Nowadays, the

MATERIALS	active period
STAINLESS STEEL	7 days
WOOD	2 days
GENERAL TYPES OF PAPER	3 hours
TISSUE PAPER	3 hours
GLASS	4 days
PLASTIC	7 days
CLOTHES	2 days
MONEY (PAPER FORM)	4 days
INNER SURFACE OF MASKS	7 days
OUTER SURFACE OF MASKS	>14 days

Fig. 3.2 Life cycles of viruses on various materials

effect of viruses in air droplets has attracted people's concern much more. However, since viruses on materials (products) could remain active much longer, one should also focus on controlling materials containing viruses. The mechanism for virus longevity on materials and the correlation between viruses and materials need to be clarified. Figure 3.2 shows the longevities of infectious activities on various materials according to some investigators' results [7].

As for the infectious capabilities (longevities of viruses on materials), there are three main problems to solve. One of them is the results researchers have so far. Those shown in Fig. 3.2 for example, were obtained on unconditioned or uncontrolled materials' surfaces. An important point is humidity or water content on a material's surface. As presented in the following section of this chapter, viruses are affected by humidity in the environment. If viruses on materials' surfaces would be issued, they should be controlled in a certain way. Researchers obtained the data for the longevity of viruses on materials with completely or partially dried materials' surfaces. However, the data of viruses' longevities on real materials (those with some moisture) have been missing so far. This problem will be addressed in the following section where viruses and biofilms are described in terms of the humidity on materials' surfaces.

The second problem is how to properly evaluate viral activities on materials' surfaces. The next chapter (Chap. 4) will present a newly standardized evaluation method. However, it will still be difficult to get the correct evaluation results on practical wet materials' surfaces.

The third problem is related to the second one. When we are able to properly evaluate the viral activities on materials' surfaces, is that evaluation still available to evaluate the infectious potential within the human bodies of the new people who

would get the virus from the materials' surfaces? If not, what kinds of evaluation exist between virions on materials and that within human bodies? This problem is very difficult to answer at this point. However, we should keep this problem in mind and always be conscious about the differences.

3.3 Factors Affecting the Viral Activities on Materials

In the previous section, we surveyed the infectious route with the existence of air droplets carrying virions outside of the human body. We realized that virions on materials' surfaces could keep their infectious activities for a certain period, depending on the kinds of materials and viral species. When the virions lose their infectious activities, they are called inactivated ones. What happens to viruses on materials' surfaces and why do they lose their activity to become inactivated virions?

Generally, viruses become inactivated when their structures collapse. As we already know, viruses have genes (DNA or RNA) in the center of their structures. The genes are protected by a capsid, which contains protein subunits called capsomeres. Some viruses like influenza have double layers of lipids surrounding them. This virus has a layer of spikes on the outside. Viruses have spherical or polygonal structures. Usually, viruses become inactive when their original structures collapse. The breakdown process is caused by various factors. For example, the effect of materials' surfaces must begin the collapse of the virus's outer parts first. Then the effects change from the outer parts to the inner ones. The process is shown in Fig. 3.3 schematically.

Firstly, the double layers of lipid must be broken for the envelope type of viruses such as influenza. In this case, some property of the material's surface must interact with the lipids. A strong bond between them might result in the breakdown of the lipid layers. Then the proteinous membrane existing on the lipid layers would be denatured. This could be followed by denaturing of the proteinous capsid. Finally, a substance reacting with nucleic acids in the center of a virus could inactivate that virus (Fig. 3.4). Examples occur in our daily lives. Alcohol, ether, isopropanol, and many surfactants can breakdown lipid layers and inactivate viruses.

3.4 Biofilms and Viruses

Biofilms are inhomogeneous film-like substances formed on materials' surfaces by bacterial activities. As shown in Fig. 3.5, the local association of attached bacteria on materials' surfaces and the density growth would lead to quorum sensing, a signal transduction process where the relatively low molecular weight substances such as peptides and AHL (acyl homoserine lactone) would be produced from the cells in the local area and react with DNA to produce polysaccharides. As a result, the local surface area would be covered with sticky substances composed of polysaccharides,

proteins, lipids, and nucleic acids derived from bacterial cells. The noteworthy point is that biofilms must contain lots of water in them. Therefore, we could say that biofilms are sticky water films formed on materials' surfaces. Biofilms contain lots of bacteria too. Therefore, there must be lots of bacteriophages in them, and they might play an important role for the correlation between viruses and biofilms on materials' surfaces [8–17]. At this point, we want to consider the relationship between humidity (derived from biofilms) and general viruses. Since biofilms maintain water content to some extent, they must reflect the effect of humidity on viruses attached to materials. In fact, there are no real surfaces of materials that are completely dry because materials have biofilms on their surfaces. Keep in mind that the main component of biofilm is water. Therefore, this relationship must be important to clarify the longevity of viruses on real materials. The results shown in Fig. 3.2 might be different for the real cases described here.

A new project is introduced. In the next chapter, a different view of viral behavior on materials' surfaces is presented. It has been observed by using cellular cultures since viruses need host cells. Also, the cells broken by viruses are examples of viral activities. Therefore, animal cells are needed for such a study. The cellular operation must be very sensitive and delicate, because the culture needs to avoid contamination from bacteria, fungi, etc. On the other hand, biofilms are composed of lots of bacteria. Therefore, biofilms containing bacteria (in the real state) would not be used for the study. In this case, attention is paid to the water contents for this investigation. We are now preparing for the process mentioned in Fig. 3.6 schematically.

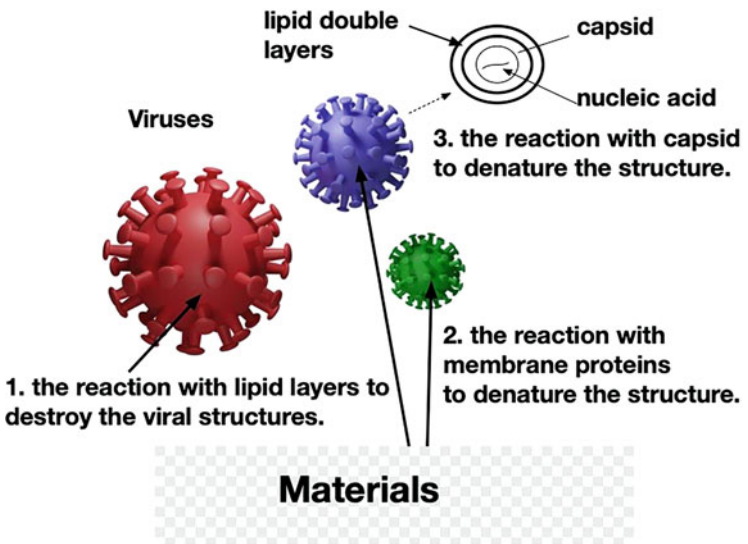

Fig. 3.3 The schematic illustration for interactions between viruses and materials' surfaces

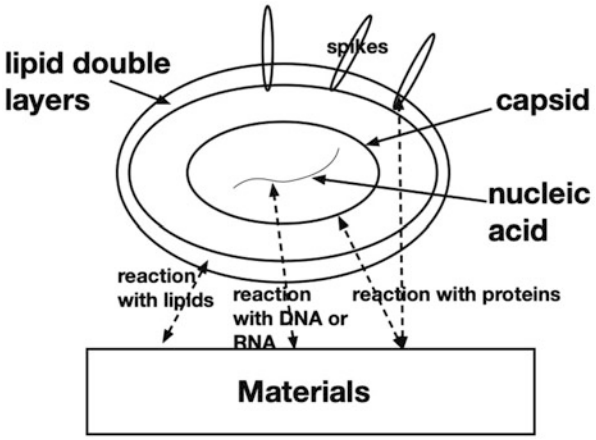

Fig. 3.4 Viral components and materials' surfaces

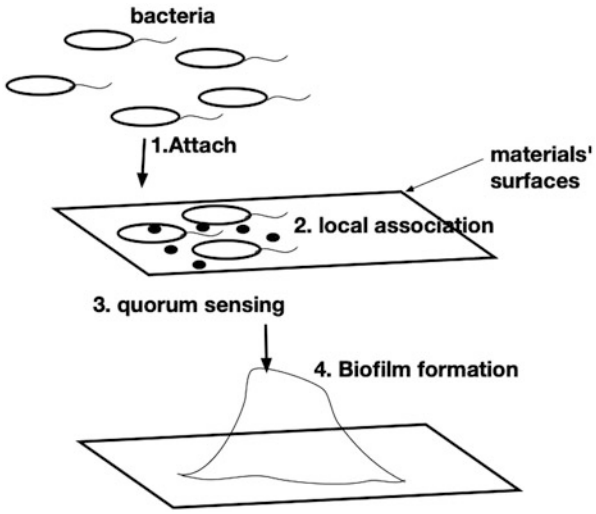

Fig. 3.5 Schematic illustration of biofilm formation

First, we could produce biofilms artificially on the laboratory scale. There are already many kinds of biofilm reactors where biofilms could be formed experimentally on materials' surfaces. We already described these methods for preparing biofilms in our other books [18, 19]. Next, the specimens should be sterilized somehow, so that the polymeric substances and water would remain. The surface products (biofilms) could be sterilized through tiny filters. Also, a process for returning the filtered, sterilized matter to the materials' surfaces might be needed. We have just begun this investigation. However, we are expecting to get results and knowledge about the longevity of activated viruses on real materials.

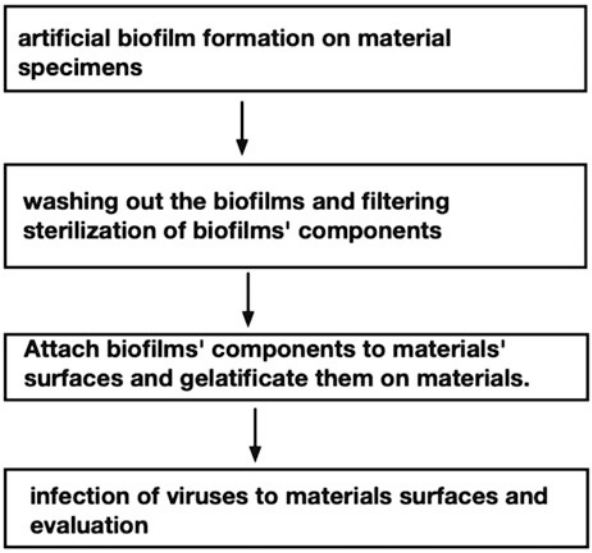

Fig. 3.6 Trial to investigate the effect of the coexistence of biofilms and viruses for viral behaviors on materials' surfaces

3.5 Possible Countermeasures to Control Viruses on Materials' Surfaces

As shown in Figs. 3.3 and 3.4, there are various interactions between materials' surfaces and viruses. Each of them can be a potential countermeasure to inactivate viruses.

At this point, the countermeasures for viruses are very similar to those for bacteria, when we come to think about the antiviral materials. The guidelines for antiviral materials are classified into two main types as shown in Fig. 3.7. One of them is the control of a viral attachment to materials. They are classified into three subcategories.

The attachment could be controlled by the state of surface energy. It could be realized by the control of hydrophobicity/hydrophilicity. Since the viral outer structure is composed of lipids or proteins, the interaction between those polymeric substances and materials' surfaces should be considered. To achieve this goal, surface coatings might be the best choice. Plating, coating, and mixing other second elements into the surface part of a material could change the contact angles between virions and materials' surfaces.

The second possibility to control viruses on materials' surfaces is the arrangement of the surface charges on the materials. This could be accomplished by surface finishing and coating. Also, the pH could be adjusted to properly change the surface charges. Since the viral outer parts are composed of polymeric substances, they

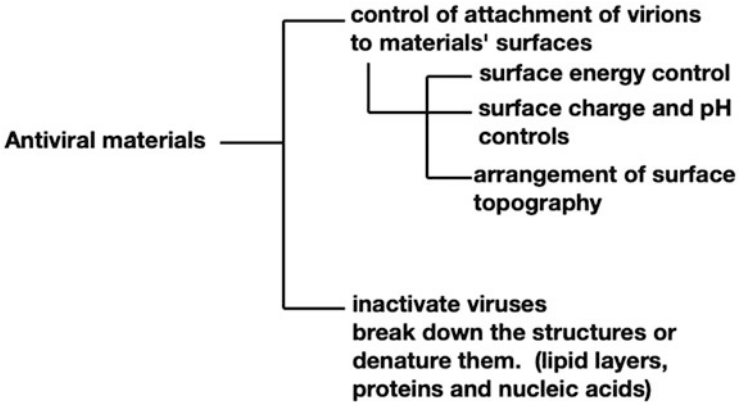

Fig. 3.7 Guidelines to develop antiviral materials

are locally charged, even though the total structure might be completely neutral. Changing surface charges could produce a proper repelling force if needed.

The third possibility is the arrangement of the surface topography. Generally, the rough surface might produce an anchor for the virions. A special pattern of surfaces such as polymer brushes could produce the lotus effect and repel the virions. The reverse effect could also happen. Anyway, the surface morphological arrangement could avoid viral attachments.

The other main category is the breakdown or denaturing of viral structures on materials' surfaces, as described in the previous section and shown in Figs. 3.3 and 3.4. As described in the previous section, we already know what kind of chemicals could break or denature the parts of virions. The problem is how to fix those substances on the surface of materials. To achieve this purpose, surface finishing and coating might play important roles again. For examples, chemicals, elements such as silver, and various organic substances could be fixed in the coating materials. In addition, titanium oxides produce active oxygen species (by using light) that could break the outer parts of virions. NOTE: There are already many antiviral coatings on the market.

3.6 For the Future

In this chapter, we surveyed the interactions between materials and virions (viruses) from the viewpoint of infection. Firstly, we fixed the kind of meanings that materials would have for a viral infection. We also provided an overview of the types of interactions to be considered between materials' surfaces and virions. Based on available information, we suggested potential countermeasures that could be devised.

At this point, some problems need to be solved. We should have a common, solid system to evaluate viral behaviors on materials' surfaces. The system must be available for lots of people, industries, etc., and it needs to be inexpensive, rapid, and user-friendly. Fortunately, we have one or two industrial standards, which will be discussed in the next chapter. However, we should always continue to improve and develop a much better system. This would lead us to establish a new standardized evaluation system and to new findings about mechanisms and countermeasures.

Secondly, the countermeasures for viruses on materials are very similar and overlap with those for bacteria. When we come to think about the similarity of outer structures for both, it may be very natural. However, bacteria and viruses must be different in many ways. Therefore, we must clarify and devise new countermeasures, especially for viruses.

Infection between human beings through materials is still not fully understood, so more research and development are needed and expected. The answers might be very useful for eradicating viral infections.

References

1. Lee, G., & Bishop, P. (2015). *Microbiology—and infection control for health professional* (6th ed.). Pearson.
2. CDC Web Page. Retrieved from https://www.cdc.gov/coronavirus/2019-ncov/index.html
3. WHO Web Page. Retrieved from https://www.who.int/emergencies/diseases/novel-coronavirus-2019
4. Kampf, G., Todt, D., Pfaender, S., & Steinmann, E. (2020). Persistence of coronaviruses on inanimate surfaces and their inactivation with biocidal agents. *Journal of Hospital Infection, 104*(3), 246–251.
5. Chin, A. W. H., et al. (2020). Stability of SARS-CoV-2 in different environmental conditions. *Lancet Microbe, 1*, e10. (Published online).
6. Isu, N. Surface analyses of attached microbes. In *Proceedings of 142nd annual meetings*. Surface Finishing Society of Japan. (in Japanese).
7. The society of risk analysis Japan: The special web page for COVID-19—The guidance for removal of viruses on environmental surfaces. Retrieved from https://drive.google.com/file/d/1G5q0Aj9_zNvlZEx4wFUgadE00qFz8JEt/view. (in Japanese).
8. Parasion, S., Kwiatek, M., Gryko, R., Mizak, L., & Malm, A. (2014). Bacteriophages as an alternative strategy for fighting biofilm development. *Polish Journal of Microbiology, 63*(2), 137.
9. Harper, D. R., Parracho, H. M., Walker, J., Sharp, R., Hughes, G., Werthén, M., Morales, S., et al. (2014). Bacteriophages and biofilms. *Antibiotics, 3*(3), 270–284.
10. Gutiérrez, D., Rodríguez-Rubio, L., Martínez, B., Rodríguez, A., & García, P. (2016). Bacteriophages as weapons against bacterial biofilms in the food industry. *Frontiers in Microbiology, 7*, 825.
11. Chan, B. K., & Abedon, S. T. (2015). Bacteriophages and their enzymes in biofilm control. *Current Pharmaceutical Design, 21*(1), 85–99.
12. Donlan, R. M. (2009). Preventing biofilms of clinically relevant organisms using bacteriophage. *Trends in Microbiology, 17*(2), 66–72.
13. Szafrański, S. P., Winkel, A., & Stiesch, M. (2017). The use of bacteriophages to biocontrol oral biofilms. *Journal of Biotechnology, 250*, 29–44.

14. Curtin, J. J., & Donlan, R. M. (2006). Using bacteriophages to reduce formation of catheter-associated biofilms by Staphylococcus epidermidis. *Antimicrobial Agents and Chemotherapy, 50*(4), 1268–1275.
15. Łusiak-Szelachowska, M., Weber-Dąbrowska, B., & Górski, A. (2020). Bacteriophages and lysins in biofilm control. *Virologica Sinica, 35*(2), 125–133.
16. Chibeu, A., Lingohr, E. J., Masson, L., Manges, A., Harel, J., Ackermann, H. W., Boerlin, P., et al. (2012). Bacteriophages with the ability to degrade uropathogenic Escherichia coli biofilms. *Viruses, 4*(4), 471–487.
17. Lu, T. K., & Collins, J. J. (2007). Dispersing biofilms with engineered enzymatic bacteriophage. *Proceedings of the National Academy of Sciences, 104*(27), 11197–11202.
18. Kanematsu, H., & Barry, D. M. (2020). *Formation and control of biofilm in various environments*. Springer.
19. Kanematsu, H., & Barry, D. M. (Eds.). (2015). *Biofilm and materials science*. Springer.

Chapter 4
Viral Behaviors on Materials and the International Standard Between Materials and Microbial/Viral Environments

Hideyuki Kanematsu and Dana Barry

Abstract In this chapter, we surveyed the differences of viral behaviors inside and outside of our bodies. Then, we introduced an international standard to evaluate the viral activity on various materials. This evaluation technique is the combination of a film covering method developed for antibacterial evaluation of materials by SIAA (Society of International Sustaining Growth of Antimicrobial Articles) in Japan and the conventional plaque assay. However, this evaluation process provides visualization to the researchers and engineers who use it. From this viewpoint, we would say the method is intuitive, rapid, relatively inexpensive, and user-friendly. It is used in industry to evaluate materials.

4.1 Introduction

As already shown in the previous chapter, viruses grow inside of organisms. When restricting the topic to human beings, then we would say that viruses grow inside of a human body. They must "borrow" human cells to replicate genes [1–3]. So, what kind of behavior would viruses exhibit outside of the human body? Viruses can't replicate genes on their own. They need to use cells and nucleic acids of other organisms. Since this self-multiplication is one of the important properties of organisms, they are not considered to be organisms. They are just inanimate tiny particles called virions. In the previous chapter, we surveyed how virions interact with materials' surfaces and discussed some factors that are involved. For this

H. Kanematsu (✉)
National Institute of Technology, Suzuka College, Shiroko-cho, Suzuka, Mie, Japan
e-mail: kanemats@mse.suzuka-ct.ac.jp

D. Barry
Department of Electrical and Computer Engineering, Clarkson University, Potsdam, NY, USA

State University of New York at Canton, Canton, NY, USA
e-mail: dmbarry@clarkson.edu

D. Barry, H. Kanematsu (eds.), *Studies to Combat COVID-19 using Science and Engineering*, https://doi.org/10.1007/978-981-19-1356-3_4

chapter, we describe how virions behave on materials and compare their activities to those that take place in human bodies. We also present ways to evaluate the viral activity. The international standard (ISO), established in 2019 for the evaluation of antiviral materials, is introduced and described [4–12]. Also, information is provided about the direction of research and development for the future.

4.2 The Meaning of Antiviral Materials (Products)

As previously stated, viruses cannot grow outside of an organism (host cell). Viruses outside of organisms are just particles called virions. Virions contain nucleic acids in their center part (DNA or RNA) which is surrounded by a protein capsid. However, for some viruses, these components are surrounded by lipid double layers. Therefore, the duration of viral activities outside of bodies depends on the interaction between virions and materials' surfaces (the interaction between lipids and materials in the case of envelope type viruses and the interaction between proteins and materials' surfaces in the case of non-envelope type viruses) [1, 3].

The situation within our bodies is quite different. When viruses enter our bodies as antigens, they are recognized by two processes in our host cells. One of them involves B cells and their surface antibodies (sig M), and the other one includes T-cell receptors on T cells. Both types of cells (B cells and T cells) react with the same antigens. However, the parts reacting on the foreign antigen (called "epitope") are different from each other. The antibodies existing on the surfaces of B cells could recognize entire foreign pathogens (antigens) as three-dimensional matter and could detect if the antigen would be harmful or not. B cells are a sort of leucocyte (lymphocyte) and made from blood-forming cells in our bone marrow. After the reaction with antigens, B cells become phagocytes to fight against antigens, while they produce memory B cells to be ready for the next invasion of the same type of antigen. Then the memory B cells could control the same antigens when they enter our bodies next time. The immune process is called humoral immunity or humoral-mediated immunity, since the antibodies produced by our immune cells could control viruses. The humoral immunity process is shown in Fig. 4.1 schematically [1].

On the other hand, there is an adaptive immune system called "cell immunity," which occurs inside infected cells and is mediated by T lymphocytes. The T cell plays an important role for the immunity. (For example, the memory T cell is trained to recognize specific antigens.) In any case, the T cell is one of the lymphocytes (a white blood cell) that is originally produced in bone marrow and matures in the thymus gland. Our immune system also includes macrophages that engulf and digest antigens which then appear as segments within them. Segments of the antigens react with proteins called MHC and are released to bind receptors on T cells. T cells will only respond to an antigen when it is bound to a particular MHC molecule. (Note: MHC is a group of genes that code for proteins.) Then the T cells are activated to be type 1 helper (Th1) cells which produce interferon gamma, a cytokine, IFN-γ. This

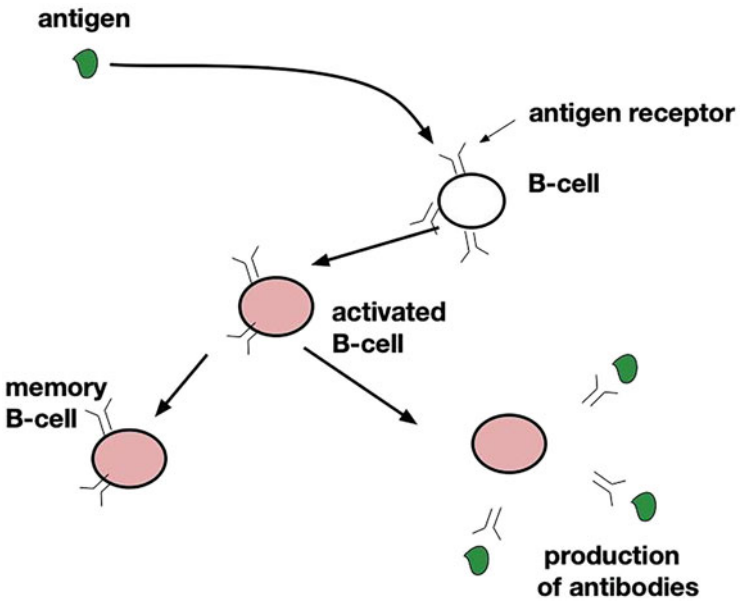

Fig. 4.1 Schematic illustration for humoral immunity

cytokine activates the macrophages and stimulates the natural killer cells. Perforin is a secreted protein synthesized by activated cytotoxic T lymphocytes and natural killer cells. It forms a pore, so the enzyme granzyme can enter and destroy targeted cells. This leads to apoptosis, death of the cell (Fig. 4.2). The cell immunity process is shown in Fig.4.3 schematically [1].

Outside of our bodies, there are no immune responses. Instead, materials' surfaces have a role to control virions. The interaction between materials' surfaces and the virions on them has not been clarified yet. However, as described in the previous chapter, some hypotheses have been proposed so far. Obtaining answers to these hypotheses might lead to the development of new antiviral materials.

In the previous chapter, we described two types of antiviral materials. One of them is to control the attachment of viruses on materials' surfaces. The other is the material groups where viruses react with materials' surfaces. This latter type is divided into two more categories.

The first category is the material group that releases chemicals from their surfaces to react with viruses and control them. This category contains lots of materials like metallic ions (such as silver, copper, etc.) iodine, organic materials, etc. that seem to destroy various parts of viruses. Photocatalytic materials belong to this category [13–21].

On the other hand, there are some materials that capture viruses and cause them to lose their original structures. These viruses become inactive. For example, polymer brushes and graphene belong to this category. The former group attracts viruses by

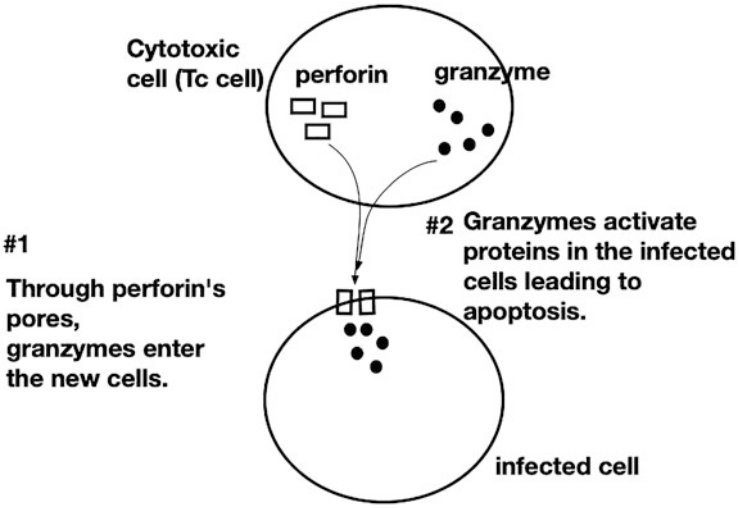

Fig. 4.2 The mechanism of apoptosis by viruses

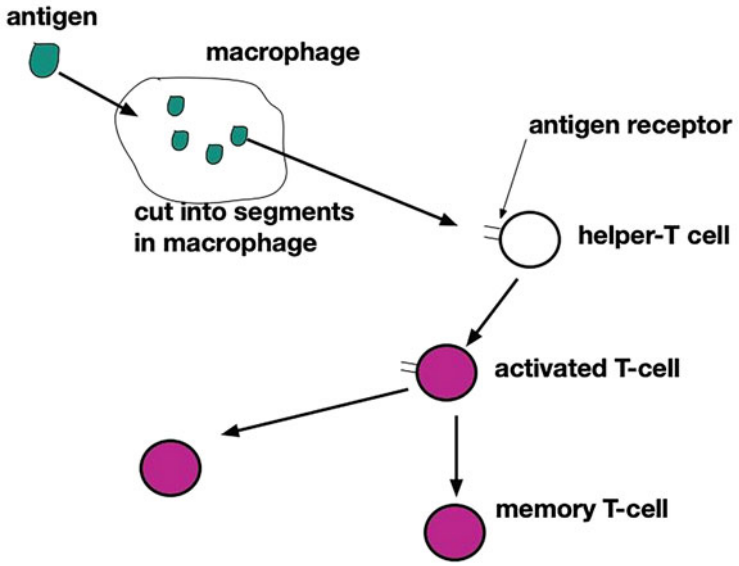

Fig. 4.3 Schematic illustration of cell immunity

electrostatic force, when cationic or anionic parts exist on materials' surfaces [22–29]. The latter type seems to attract viruses by their pi electron clouds protruding in the perpendicular direction on materials [30–39]. Figure 4.4 shows the schematic illustration of this mechanism schematically.

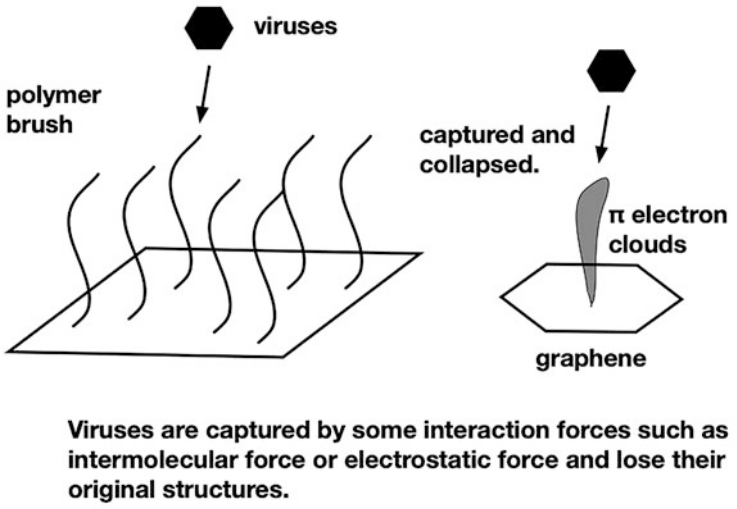

Fig. 4.4 Some examples for antiviral materials

As described above, materials' surfaces can't control viral activities found within our human bodies. However, we can add artificial elements or processes to control viral activities on materials' surfaces.

4.3 General Evaluation for Viral Activity

We can easily imagine how hard it is to properly visualize viruses. The size of viruses depends on the species. There are many kinds of viruses. For example, compare the poliovirus (20 nm) to the poxvirus (400 nm). Some viruses are more than 1 μm in diameter. Viruses are very small and belong to the nanoworld. We need electron microscopes to directly observe viruses and their effects. It is impossible for us to observe viruses by using our well- known and easy handling optical microscopes. Electron microscopes are mainly classified into two types: transmission and scanning types. To directly observe something of a nano-size, one usually utilizes transmission electron microscopes. However, if topographical information is needed about the viruses, then scanning microscopes should be used. To improve the operation of transmission-type microscopes, a scanning function has been successfully incorporated into transmission electron microscopes. The introduction of the field-emission electron gun allowed this innovation to be possible. The apparatus provides us with useful information. On the other hand, visualization methods using expensive high-tech apparatus might be restricted to quantitative analyses. However, the quantitative evaluation of viruses' activities is

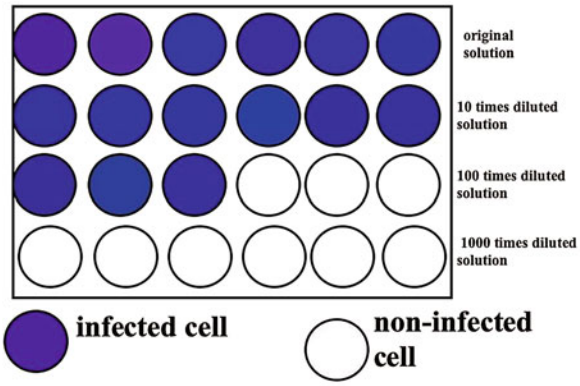

Fig. 4.5 Schematic illustration for $TCID_{50}$ assay

important and needed by industries. For example, the biological viral evaluations depend on these methods.

Conventional evaluation methods to evaluate viruses' activities are based on the measurement of virus titers and calculations. A virus titer refers to the concentration of infectious viral particles. The measurement of virus titer is usually carried out by $TCID_{50}$ assay or plaque assay.

For the $TCID_{50}$ assay [40, 41], a series of diluted virus solutions are made, as shown in Fig. 4.5. Those viral solutions, containing a certain concentration of infectious viral particles, are inoculated into cells prepared in plastic wells. According to the change of viral content, the inoculation extent changes too. At a certain threshold dilution value, infection could be observed. Usually, the dilution rates of original solutions prepared by ATCC, etc. are 10 times, 10^2 times, 10^3 times, 10^4 times, 10^5 times, 10^6 times, 10^7 times, and 10^8 times for the use of such an assay. When the solution of a certain dilution rate shows that half (50%) of the infected cells display the cytopathic effect, then the ratio of index of dilution rate to 1 mL is defined as viral infectivity. The cytopathic effect refers to changes in the structure of the host cell caused by viral infections. It can result in the death of host cells.

A good visualization method to use for determining the concentration of virus in a sample is the plaque assay [42–44]. In the same way (as previously described), viral solutions of various dilution rates are inoculated onto cells in plastic wells. Cells infected by viruses are altered or detached and might appear on the wall of a plastic well. When methylene blue stains the well, the well shows white circles, zones of infected cells called plaque. Dyes are used to stain the living cells for a contrast with the plaques. The number of plaques corresponds to the extent of infection. The amount of altered and detached cells depends on the dilution rate. If the number of altered and detached cells increases, then more plaques appear. Figure 4.6 shows an example of plaque.

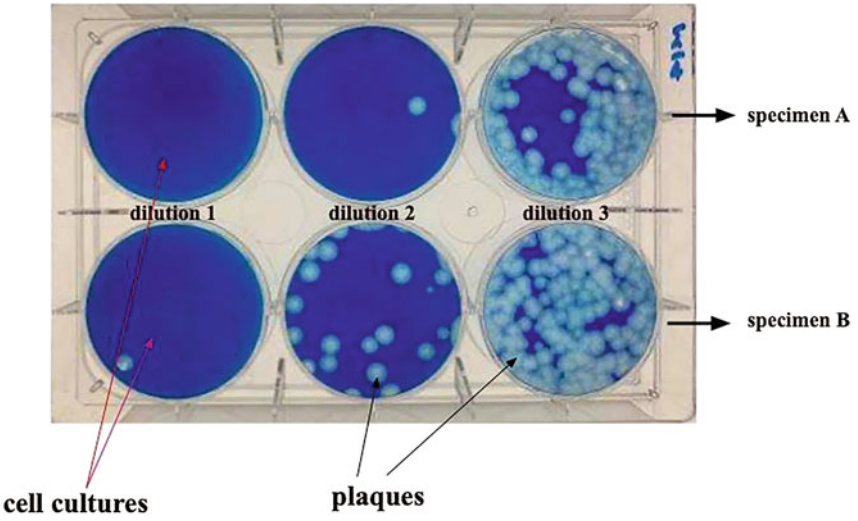

Fig. 4.6 Typical plaques observed in plaque assay

4.4 International Standard for Viral Activity on Materials (Products)

In the previous section, we described some viral evaluation methods. In particular, the plaque assay seemed to be favored from an industrial viewpoint because this method should be rapid, intuitive, not expensive, and quantitative. The plaque number could be treated just like the colony number in the case of bacteria. The SIAA (Society of International Sustaining Growth of Antimicrobial Articles) in Japan is an organization of manufacturers and antimicrobial testing institutions for antimicrobial agents, fungicides, viruses, etc. The organization set the rules governing the quality and safety of treated antimicrobial products. It certifies the security of products by labeling them with SIAA marks (which they devised as symbols for the security of products). This organization has been successful at setting the international standard for antibacterial (Kohkin) products (materials) and certifying high-quality antibacterial products by providing them with the certification mark (Fig. 4.7). This certification mark and the activity for antibacterial products are now very well known in Japan and other Asian countries. They are also known in the world because the standard (ISO 22196) has defined only one unique evaluation method [45, 46]. Then the organization decided to set the rule (international standard) for antiviral products and materials around 2010. The group organized the committee for the evaluation of antiviral products (materials) which resulted in the international standard (ISO 21702).

The procedure is as follows. Target viruses can be selected for this purpose. Usually in Japan, two viral infections historically take place each winter (influenza

Fig. 4.7 Certification for antibacterial and antiviral products in Japan

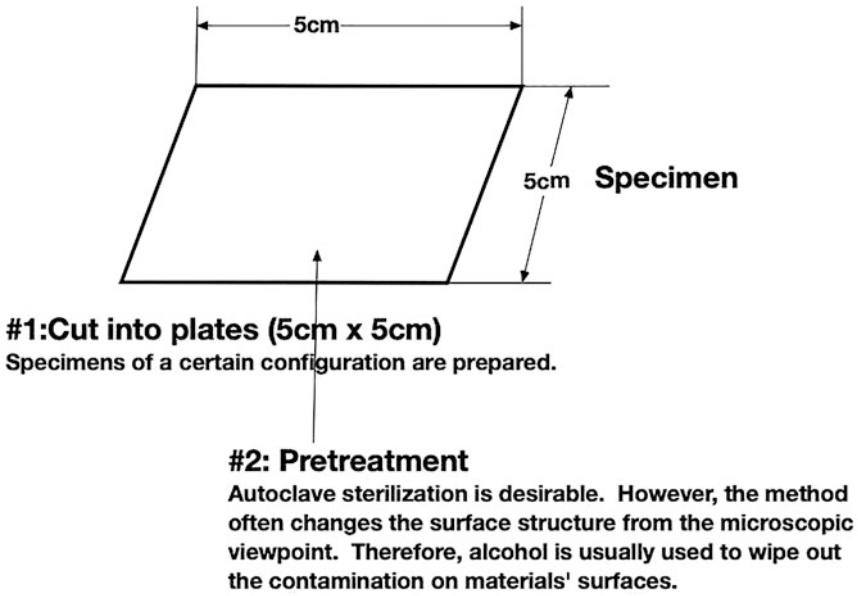

Fig. 4.8 This displays the size of the specimen needed for the antiviral test

and noroviruses). Therefore, for our purpose, the following two viruses are used: influenza A (H3N2, ATCC 1679) and *Feline calicivirus* (strain, F-9, ATCC VR-782). The former is a typical influenza virus and belongs to the envelope type. The latter is a non-envelope type and has a structure like a norovirus. The cell cultures are chosen, depending on the viruses used. As for H3N2 influenza, MDCK cells (ATCC CCL-34) are used, and for the *Feline calicivirus*, the CRFK cell (ATCC CCL-94) is used.

Sheets of materials are prepared as specimens. The size should be 5 cm × 5 cm, but the thickness doesn't need a fixed value (Fig. 4.8).

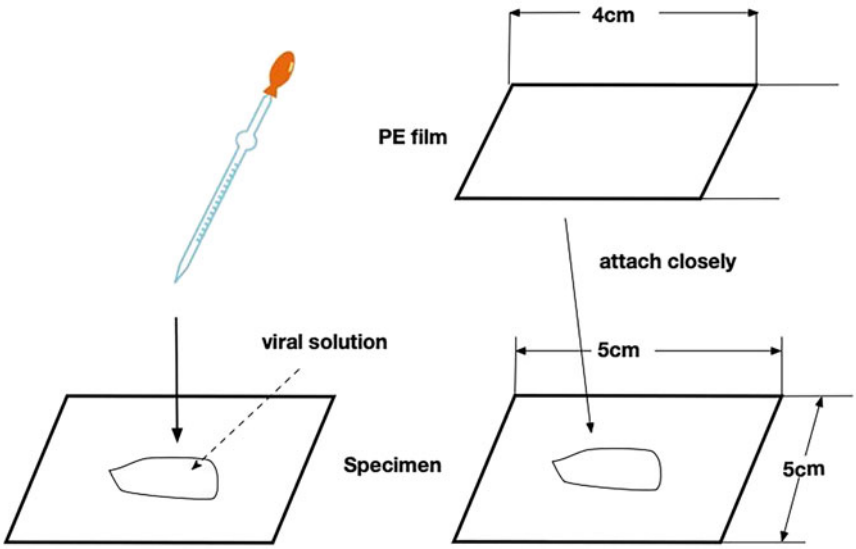

Fig. 4.9 This figure shows the film covering process and the viral solution

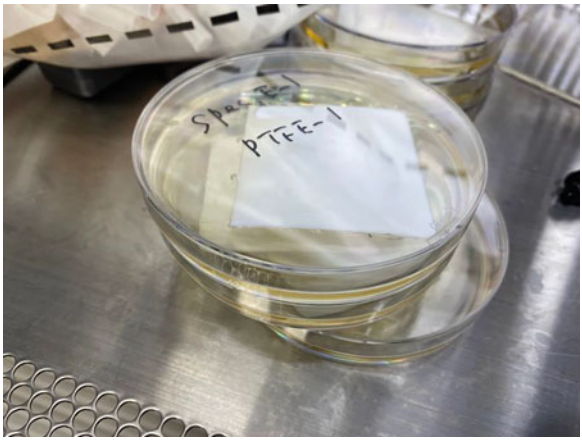

Fig. 4.10 Incubation at 25 °C after the film covering process takes place

A certain concentration of a viral solution is prepared and dropped on the sheet. Then a polymeric transparent film (usually polyethylene film) of 4 cm × 4 cm is closely attached to the surface of the specimen (Fig. 4.9). (These processes are usually carried out in a petri dish.) Then the specimens are incubated for 1 day (24 h) at 25 °C and 90% relative humidity.

As for a control specimen, any material sheets are available. However, the incubation process is omitted (Fig. 4.10).

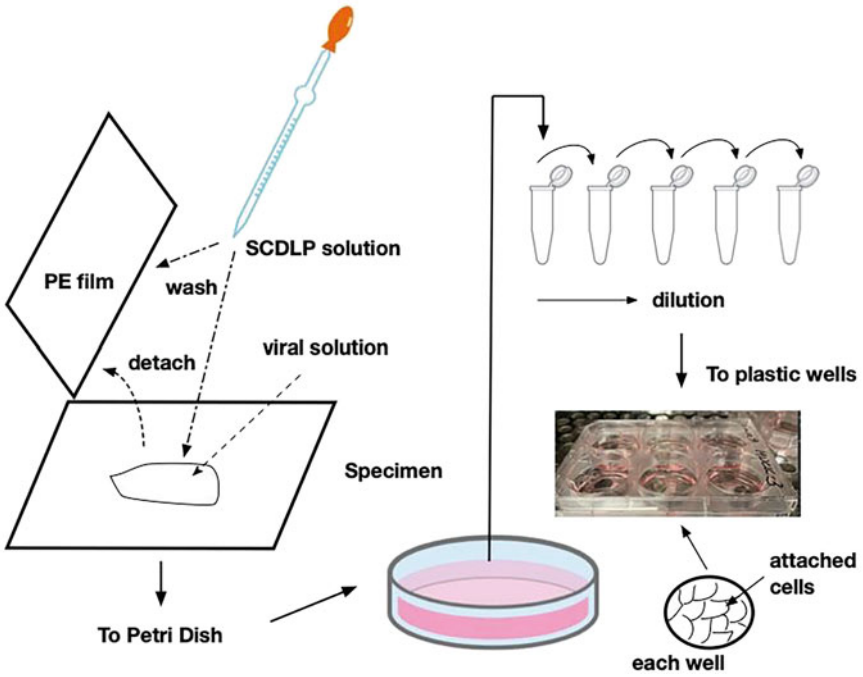

Fig. 4.11 Film covering process and the following infection process

After the incubation at 25 °C, the specimens' surfaces and attached films are washed down into a petri dish by SCDLP solution. The solution from each specimen's surface is diluted by a culture solution (e.g., MEME solutions for influenza viruses) to prepare a series of diluted solutions (e.g., 10^2, 10^3, 10^4, 10^5, 10^6, 10^7, and 10^8 solutions). The diluted viral solutions are inoculated in advance into the cells prepared in plastic wells. This process is shown schematically in Fig. 4.11. The infected cells in the wells are covered with agar that causes a gel to form. Then they are kept in a CO_2 incubator for 2 or 3 days, as shown in Fig. 4.12.

After the final incubation, the infected cells are solidified by glutaraldehyde and stained by methylene blue solutions. The cells infected by the viruses are detached and altered. They are not stained by methylene blue. Therefore, they look like white circles and can be counted by the naked eye (Fig. 4.13). As described in the figure, the number of plaques (called plaque formation unit, PFU) corresponds to the viral activities. When the PFU for the target specimen is P_i and the PFU of the control specimen is P_0, then the viral activity can be calculated as follows:

$$\text{Infectivity (viral titer)} = \log P_0 - \log P_i \tag{4.1}$$

The evaluation method is the combination of a film covering method developed for the antibacterial evaluation of materials by SIAA and the conventional plaque assay.

Fig. 4.12 Incubation of infected cells in plastic wells. The incubation is carried out in a CO_2 incubator

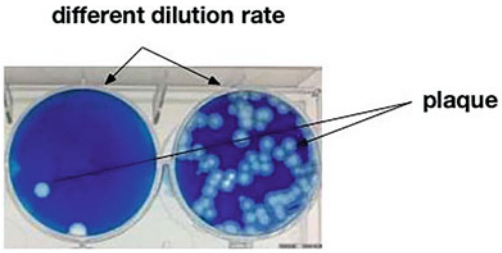

viral titer (infectivity) = log P0 - log Pi

P0: Plaque Formation Unit for control specimen
Pi: Plaque Formation Unit for target specimen

Fig. 4.13 Plaque and PFU followed by the calculation of viral titer

However, this evaluation technique can be used by researchers and engineers as a visualization method. It is intuitive, rapid, relatively inexpensive, and user-friendly. This is an industrial evaluation method for materials.

4.5 For the Future

In this chapter, we described viral behaviors on materials and pointed out the differences for viruses inside and outside of the human body. If they are inside our bodies, the physiological responses (immune systems) work properly. On the other hand, viruses outside of our bodies don't have such a control factor. However, materials' surfaces could negatively affect viruses. We could utilize those phenomena to control viruses and infections. This must lead to the development of new antiviral materials. To develop new antiviral materials, we must have proper evaluation methods. Fortunately, SIAA in Japan successfully developed an international standard for the evaluation process. This process (which benefits industry) is discussed in this chapter. On the other hand, almost 80% of the evaluation process is based on cell technology. Therefore, mastering the use of this method may take a relatively long time. From this viewpoint, easier and more acceptable evaluation methods are still needed. Sensors and monitoring systems are also welcomed. We must mention that a serious problem is that the relationship between the infectivity of materials and real infections is missing. Are materials that are evaluated to have low infectivity (by the ISO method) completely safe? If the answer is no, then the evaluation method might only provide a potential infectivity of each material. To address these concerns, further investigations are needed.

References

1. Lee, G., & Bishop, P. (2015). *Microbiology—and infection control for health professional* (6th ed.). Pearson.
2. Nelson, D. L., & Cox, M. M. (2008). *Lehninger principles of biochemistry* (5th ed.). W. H. Freeman.
3. Lostroh, P. (2019). *Molecular and cellular biology of viruses* (Vol. 523). Garland Science.
4. Djellabi, R., Basilico, N., Delbue, S., D'Alessandro, S., Parapini, S., Cerrato, G., Laurenti, E., Falletta, E., & Bianchi, C. L. (2021). Oxidative Inactivation of SARS-CoV-2 on Photoactive AgNPs@TiO2 Ceramic Tiles. *Int. J. Mol. Sci., 22*, 8836. https://doi.org/10.3390/ijms22168836.
5. Butot, S., Baert, L., & Zuber, S. (2021). Assessment of antiviral coatings for high-touch surfaces by using human coronaviruses HCoV-229E and SARS-CoV-2. *Applied and Environmental Microbiology, 87*(19), e01098–e01021.
6. Thraenhart, O., Jursch, C., & Buozzi, V. B. (2021). *Testing of the antiviral equipped product "Argentum 20 a-Base" against the Bovine Coronavirus (Bocv) at 25°C –Evaluation of the virucidal activity against the Bovine Coronavirus (S379 Riems) using the quantitative carrier test according to ISO 21702: 2019*. (Excerpt from the Test Report Ter_Eur-09_181220_Bocv). Eurofins Co.
7. Fu, H., & Gray, K. A. (2021). The key to maximizing the benefits of antimicrobial and self-cleaning coatings is to fully determine their risks. *Current Opinion in Chemical Engineering, 34*, 100761.
8. Tatsuma, T., Nakakido, M., Ichinohe, T., Kuroiwa, Y., Tomioka, K., Liu, C., Wakihara, T., et al. (2021). *Inactivation of novel coronavirus and alpha variant by photo-renewable CuxO/TiO2 nanocomposites*. Cambridge University Press.

9. Hong, S. G., Lee, Y. K., Yim, J. H., Chun, J., & Lee, H. K. (2008). Sanguibacter antarcticus sp. nov., isolated from Antarctic Sea sand. *International Journal of Systematic and Evolutionary Microbiology, 58*(1), 50–52.
10. Falcó, I., Randazzo, W., Sánchez, G., Vilarroig, J., Climent, J., Chiva, S., Navarro-Laboulais, J., et al. (2021). Experimental and CFD evaluation of ozone efficacy against coronavirus and enteric virus contamination on public transport surfaces. *Journal of Environmental Chemical Engineering, 9*(5), 106217.
11. Li, Z., Qiao, D., Xu, Y., Zhou, E., Yang, C., Yuan, X., Wang, F., et al. (2021). Cu-bearing high-entropy alloys with excellent antiviral properties. *Journal of Materials Science & Technology, 84*, 59–64.
12. Kanematsu, H., Kawai, R., & Barry, D. M. (2021). Measuring virus infectivity on material surfaces: Various methods are available to evaluate the behavior of viruses on material surfaces, an important area of research for determining how long a virus can live on an inanimate object, and learning how to design and develop advanced antiviral materials. *Advanced Materials & Processes, 179*(5), 28–31.
13. Govind, V., Bharadwaj, S., Sai Ganesh, M. R., Vishnu, J., Shankar, K. V., Shankar, B., & Rajesh, R. (2021). Antiviral properties of copper and its alloys to inactivate COVID-19 virus: A review. *Biometals, 34*(6), 1217–1235.
14. Botequim, D., Maia, J., Lino, M. M. F., Lopes, L. M. F., Simões, P. N., Ilharco, L. M., & Ferreira, L. (2012). Nanoparticles and surfaces presenting antifungal, antibacterial and antiviral properties. *Langmuir, 28*(20), 7646–7656.
15. Jung, S., Yang, J. Y., Byeon, E. Y., Kim, D. G., Lee, D. G., Ryoo, S., Lee, S., et al. (2021). Copper-coated polypropylene filter face mask with SARS-COV-2 antiviral ability. *Polymers, 13*(9), 1367.
16. Ordon, M., Nawrotek, P., Stachurska, X., & Mizielińska, M. (2021). Polyethylene films coated with antibacterial and antiviral layers based on CO2 extracts of raspberry seeds, of pomegranate seeds and of rosemary. *Coatings, 11*(10), 1179.
17. Seidi, F., Deng, C., Zhong, Y., Liu, Y., Huang, Y., Li, C., & Xiao, H. (2021). Functionalized masks: Powerful materials against COVID-19 and future pandemics. *Small, 17*(42), 2102453.
18. Idumah, C. I. (2021). Influence of nanotechnology in polymeric textiles, applications, and fight against COVID-19. *The Journal of the Textile Institute, 112*(12), 2056–2076.
19. Malmsten, M. (2011). Antimicrobial and antiviral hydrogels. *Soft Matter, 7*(19), 8725–8736.
20. Nowacek, A. S., Balkundi, S., McMillan, J., Roy, U., Martinez-Skinner, A., Mosley, R. L., Gendelman, H. E., et al. (2011). Analyses of nanoformulated antiretroviral drug charge, size, shape and content for uptake, drug release and antiviral activities in human monocyte-derived macrophages. *Journal of Controlled Release, 150*(2), 204–211.
21. Chen, L., & Liang, J. (2020). An overview of functional nanoparticles as novel emerging antiviral therapeutic agents. *Materials Science and Engineering: C, 112*, 110924.
22. Mallakpour, S., Azadi, E., & Hussain, C. M. (2021). Recent breakthroughs of antibacterial and antiviral protective polymeric materials during COVID-19 pandemic and post-pandemic: Coating, packaging, and textile applications. *Current Opinion in Colloid & Interface Science, 55*, 101480.
23. Tang, S., Puryear, W. B., Seifried, B. M., Dong, X., Runstadler, J. A., Ribbeck, K., & Olsen, B. D. (2016). Antiviral agents from multivalent presentation of sialyl oligosaccharides on brush polymers. *ACS Macro Letters, 5*(3), 413–418.
24. Erkoc, P., & Ulucan-Karnak, F. (2021). Nanotechnology-based antimicrobial and antiviral surface coating strategies. *PRO, 3*(1), 25–52.
25. Rosilo, H., McKee, J. R., Kontturi, E., Koho, T., Hytönen, V. P., Ikkala, O., & Kostiainen, M. A. (2014). Cationic polymer brush-modified cellulose nanocrystals for high-affinity virus binding. *Nanoscale, 6*(20), 11871–11881.
26. Koylu, D., & Carter, K. R. (2009). Stimuli-responsive surfaces utilizing cleavable polymer brush layers. *Macromolecules, 42*(22), 8655–8660.

27. Zan, T., Wu, F., Pei, X., Jia, S., Zhang, R., Wu, S., Zhang, Z., et al. (2016). Into the polymer brush regime through the "grafting-to" method: Densely polymer-grafted rodlike viruses with an unusual nematic liquid crystal behavior. *Soft Matter, 12*(3), 798–805.
28. Riedel, T., Rodriguez-Emmenegger, C., de los Santos Pereira, A., Bědajánková, A., Jinoch, P., Boltovets, P. M., & Brynda, E. (2014). Diagnosis of Epstein–Barr virus infection in clinical serum samples by an SPR biosensor assay. *Biosensors and Bioelectronics, 55*, 278–284.
29. Demirci, S., Kinali-Demirci, S., & Jiang, S. (2017). A switchable polymer brush system for antifouling and controlled detection. *Chemical Communications, 53*(26), 3713–3716.
30. Vermisoglou, E., Panáček, D., Jayaramulu, K., Pykal, M., Frébort, I., Kolář, M., Otyepka, M., et al. (2020). Human virus detection with graphene-based materials. *Biosensors and Bioelectronics, 166*, 112436.
31. Afsahi, S., Lerner, M. B., Goldstein, J. M., Lee, J., Tang, X., Bagarozzi, D. A., Jr., Goldsmith, B. R., et al. (2018). Novel graphene-based biosensor for early detection of Zika virus infection. *Biosensors and Bioelectronics, 100*, 85–88.
32. Liu, F., Choi, K. S., Park, T. J., Lee, S. Y., & Seo, T. S. (2011). Graphene-based electrochemical biosensor for pathogenic virus detection. *BioChip Journal, 5*(2), 123–128.
33. Joshi, S. R., Sharma, A., Kim, G. H., & Jang, J. (2020). Low cost synthesis of reduced graphene oxide using biopolymer for influenza virus sensor. *Materials Science and Engineering: C, 108*, 110465.
34. Deokar, A. R., Nagvenkar, A. P., Kalt, I., Shani, L., Yeshurun, Y., Gedanken, A., & Sarid, R. (2017). Graphene-based "hot plate" for the capture and destruction of the herpes simplex virus type 1. *Bioconjugate Chemistry, 28*(4), 1115–1122.
35. Jin, X., Zhang, H., Li, Y. T., Xiao, M. M., Zhang, Z. L., Pang, D. W., Zhang, G. J., et al. (2019). A field effect transistor modified with reduced graphene oxide for immunodetection of Ebola virus. *Microchimica Acta, 186*(4), 1–9.
36. Innocenzi, P., & Stagi, L. (2020). Carbon-based antiviral nanomaterials: Graphene, C-dots, and fullerenes. A perspective. *Chemical Science, 11*(26), 6606–6622.
37. Palmieri, V., & Papi, M. J. N. T. (2020). Can graphene take part in the fight against COVID-19? *Nano Today, 33*, 100883.
38. Ye, S., Shao, K., Li, Z., Guo, N., Zuo, Y., Li, Q., Han, H., et al. (2015). Antiviral activity of graphene oxide: How sharp edged structure and charge matter. *ACS Applied Materials & Interfaces, 7*(38), 21571–21579.
39. Du, T., Lu, J., Liu, L., Dong, N., Fang, L., Xiao, S., & Han, H. (2018). Antiviral activity of graphene oxide–silver nanocomposites by preventing viral entry and activation of the antiviral innate immune response. *ACS Applied Bio Materials, 1*(5), 1286–1293.
40. Darling, A. J., Boose, J. A., & Spaltro, J. (1998). Virus assay methods: Accuracy and validation. *Biologicals, 26*(2), 105–110.
41. Manceur, A. P., & Kamen, A. A. (2015). Critical review of current and emerging quantification methods for the development of influenza vaccine candidates. *Vaccine, 33*(44), 5913–5919.
42. Baer, A., & Kehn-Hall, K. (2014). Viral concentration determination through plaque assays: Using traditional and novel overlay systems. *Journal of Visualized Experiments*, (93), e52065.
43. Smither, S. J., Lear-Rooney, C., Biggins, J., Pettitt, J., Lever, M. S., & Olinger, G. G., Jr. (2013). Comparison of the plaque assay and 50% tissue culture infectious dose assay as methods for measuring filovirus infectivity. *Journal of Virological Methods, 193*(2), 565–571.
44. Tobita, K., Sugiura, A., Enomoto, C., & Furuyama, M. (1975). Plaque assay and primary isolation of influenza A viruses in an established line of canine kidney cells (MDCK) in the presence of trypsin. *Medical Microbiology and Immunology, 162*(1), 9–14.
45. Wiegand, C., Völpel, A., Ewald, A., Remesch, M., Kuever, J., Bauer, J., Bossert, J., et al. (2018). Critical physiological factors influencing the outcome of antimicrobial testing according to ISO 22196/JIS Z 2801. *PLoS One, 13*(3), e0194339.
46. Cunliffe, A. J., Askew, P. D., Stephan, I., Iredale, G., Cosemans, P., Simmons, L. M., Redfern, J., et al. (2021). How do we determine the efficacy of an antibacterial surface? A review of standardised antibacterial material testing methods. *Antibiotics, 10*(9), 1069.

Part III
Approaches for Studying Viruses and COVID-19 from Various Disciplines

Chapter 5
The Evolution of SARS-CoV-2

Susan F. Bailey and Mahfuza Akter

Abstract Species evolve over time and viruses are no exception. Extensive genome sequencing of SARS-CoV-2 throughout the global pandemic has allowed for highly detailed and invaluable characterization of the molecular evolution in a virus population, to an extent that has never been seen before. Tracking of the molecular evolutionary changes in SARS-CoV-2 allows for (1) inference of important local and global transmission routes by tracking the distribution of specific genotypes, (2) identification of adaptive evolutionary changes with potential human health implications, and (3) generation of expectations/predictions for future evolutionary changes to better tailor detection, mitigation, and treatment strategies. In this chapter, we begin by outlining the key processes driving evolution in viruses, namely, random genetic drift and natural selection. We summarize the evolutionary history of SARS-CoV-2 within the context of other coronavirus species. Then we explore how ongoing genomic and epidemiological patterns have been used to identify the extent to which natural selection has played a role in the evolution of SAR-CoV-2 throughout the global pandemic. Next, an outline is provided for the World Health Organization's criteria for identifying evolved Variants of Concern (VOC), along with a discussion about the impact of these evolved VOCs on human health. Finally, mechanisms are identified for extensive and rapid adaptive evolution in SARS-CoV-2 which suggest the need for closer monitoring. In addition, the possibilities for future evolution in SARS-CoV-2 are mentioned.

5.1 Evolution in Viruses

Viruses are parasites of cells, containing transmissible deoxyribonucleic acid (DNA) or ribonucleic acid (RNA) as their genetic material. They are a large, extremely diverse group, capable of rapid evolution as genetic variation is continually gen-

S. F. Bailey (✉) · M. Akter
Department of Biology, Clarkson University, Potsdam, NY, USA
e-mail: sbailey@clarkson.edu; akterm@clarkson.edu

D. Barry, H. Kanematsu (eds.), *Studies to Combat COVID-19 using Science and Engineering*, https://doi.org/10.1007/978-981-19-1356-3_5

erated through random mutations and continually removed from the population through the processes of natural selection and genetic drift. These are the processes that drive evolution—changes in the inherited characteristics of a population from one generation to the next. In viruses, new genetic variation arises rapidly due to high mutation rates, typically through errors in replication which are then passed on to subsequent generations. However, in some RNA viruses, recombination and reassortment can also play an important role. For example, reassortment is quite common among influenza virus strains and may occur when multiple strains infect the same host cell and exchange segments of their genomes to produce hybrid viral progeny [1]. RNA viruses typically have higher mutation rates than DNA viruses. This is because they lack the proofreading activity of RNA polymerases, so new genetic variants constantly arise, allowing for evolution in changing environments [2, 3].

The processes of genetic drift and natural selection impact evolving populations to different degrees, depending on population size. Genetic drift drives random fluctuations in the frequency of different genetic variants in populations simply due to chance events. Under genetic drift conditions, new mutations with a whole range of effects (good, bad, neutral) may rise in frequency in a population simply by chance [4]. Evolution by means of genetic drift occurs in small sized populations, for example, a population that has undergone a severe population "bottleneck." However, for large populations, evolution is typically driven by natural selection. Natural selection will drive a mutation to increase in frequency in a population if it confers a fitness benefit. On the other hand, it will drive a decrease in frequency if the mutation has a deleterious effect on fitness [5]. Evolutionary change driven by natural selection is referred to as "adaptive evolution."

Viral life cycles are characterized by massive fluctuations in population sizes across multiple scales (see Fig. 5.1), and these fluctuations result in shifts in the balance between natural selection and genetic drift in driving evolutionary dynamics. In some virus species, infection of a new host can be initiated with as little as a single viral particle or virion (e.g., HIV; [7]). The data are still preliminary, but the transmission bottleneck in SARS-CoV-2 appears to be very small as well [8]. Once a new host is infected, the viral population typically grows rapidly, reaching population sizes that are easily over a billion virions within a matter of days (e.g., SAR-CoV-2: 1–100 billion virions at peak infection; [9]). With some infections, there are additional population fluctuations within the host, for example, dengue viruses experience a large bottleneck in their mosquito hosts as they move into the mosquito salivary gland [10]. Once a viral population has reached sufficient size in its host, it may then be transmitted onto the next susceptible host. At this stage, the size of transmission bottleneck can also depend on the specific mode of transmission, for example, with influenza, fewer virions are passed on through aerosol transmission versus contact transmission [11].

At the inter-host level, viruses can also experience extreme population fluctuations as epidemics initiate, spread exponentially, decrease (e.g., due to the implementation of public health practices such as quarantining), and then repeat, potentially going through multiple epidemic waves. Finally, a virus spreading

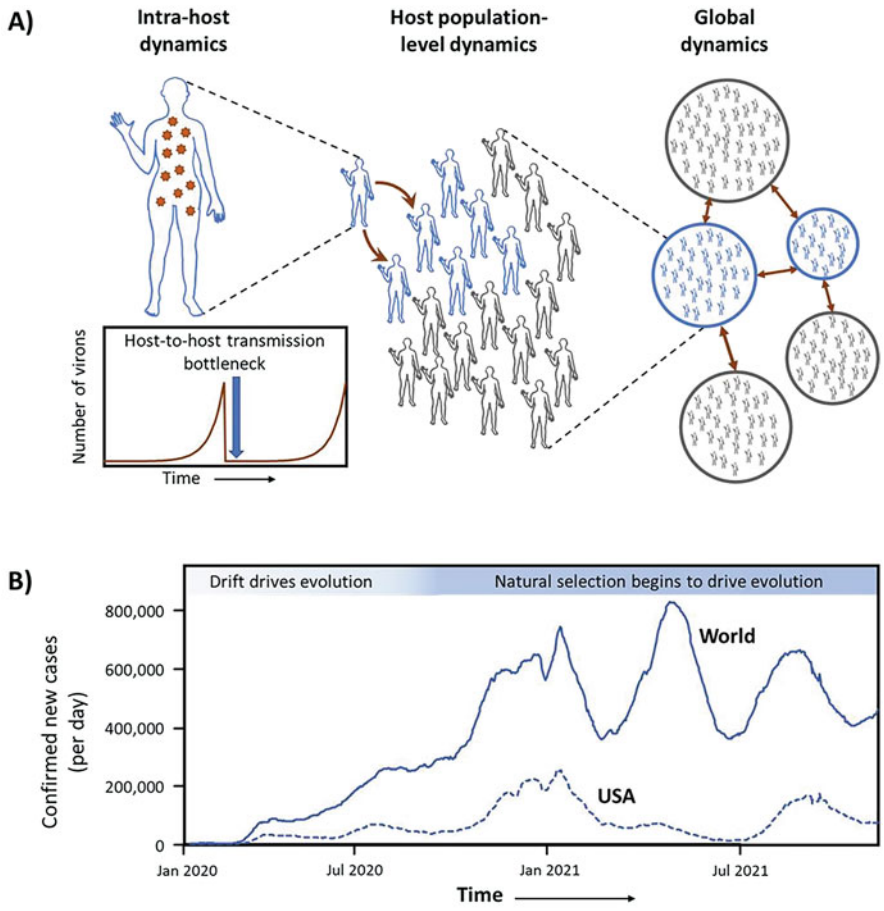

Fig. 5.1 (**a**) Overview of the different scales at which viral populations fluctuate in size from intra-host to local populations of hosts to global networks of populations. Different selection pressures may be important at each of these levels, and genetic drift will dominate evolutionary dynamics at small population sizes. (**b**) Fluctuating global population dynamics of SARS-CoV-2 showing the shifting importance of genetic drift versus natural selection in driving evolutionary dynamics in the viral population. Case count data was retrieved from the COVID-19 Content Portal https://systems.jhu.edu/research/public-health/ncov/ [6]

through a host population may infect another geographically distinct host population, usually via host migration, resulting in complex and even asynchronous viral population fluctuations across an interconnected network of host populations. Figure 5.1 gives an overview of these different scales at which population fluctuations are expected in a virus population, such as that of SARS-CoV-2 (case numbers shown in Fig. 5.1b). Thus, virus populations follow a complex pattern of extreme changes in size which can have important implications for the relative impacts of genetic drift versus natural selection over the course of a pandemic.

Two key characteristics or traits of viruses that can impact their fitness are *transmission rate* and *virulence*. Transmission rate is the rate at which a virus moves from one infected host to a new susceptible host, while virulence can be defined as the harm that a pathogen inflicts on its host and results from the pathogen using the host resources for replication [12]. Much theoretical and empirical work on pathogen evolution has centered on the hypothesis that a trade-off between virulence and transmission drives pathogen fitness [13]. The assumption is that while increasing virulence might initially increase transmission rates (because there are more virions to transmit), increasing virulence may eventually result in increased host mortality rates, which typically slows the transmission rate because the host's infectious period is cut short—deceased hosts don't transmit the virus. Thus, the transmission rate is expected to be highest at intermediate levels of virulence, balancing the costs of replication and infectious period length [13]. Although empirical evidence of this trade-off is not clear-cut, there are many pathogens that appear to have evolved to maintain intermediate virulence because of this trade-off. Some examples are the Zika virus [14], HIV-1 [15], dengue virus [16], and the influenza virus [17]. It remains to be seen whether SARS-CoV will also follow this pattern.

5.2 Evolutionary History of SARS-CoV-2 Within the Coronavirus Group

Coronaviruses (CoVs) are a widely distributed group of RNA viruses, typically highly specialized at infecting humans, birds, and a range of mammals, causing mild to severe disease with both respiratory and gastrointestinal symptoms, depending on the species. This group of viruses is considered one of the zoonotic viruses posing great challenges for the global health community [18, 19]. Coronaviruses belong to the subfamily *Coronaviridae* which is subdivided in four genera: *Alphacoronavirus*, *Betacoronavirus*, *Gammacoronavirus*, and *Deltacoronavirus* in family *Coronaviridae* (not to be confused with the Alpha, Beta, Gamma, and Delta SARS-CoV-2 variants), categorized in the order *Nidovirales* [20]. Among the four genera, alpha- and betacoronaviruses infect only mammals, while gamma- and delta-coronaviruses infect primarily avian species along with few mammals [21, 22]. Alpha- and beta-CoVs normally cause respiratory illness to humans and gastroenteritis to other animals; however, there are also reports of hepatic and neurologic syndromes due to infection [23]. Although bats are considered as the major natural host shaping the evolutionary dynamics of CoVs, these viruses also circulate among wildlife and domestic livestock. These secondary animal species can play important roles as intermediate hosts before infecting humans [21, 24]. There are already seven reported instances of CoVs being transmitted from animals to humans that have led to the emergence of human CoVs with a wide range of virulence and transmission rates [25]. There are also some CoVs circulating in bats that are reported to have the capability of infecting humans without an intermediate host [20]. Table 5.1 outlines

Table 5.1 Species of coronavirus reported in human hosts [19, 21, 26]

Species in human host	Year of isolation in humans	Possible reservoir	Intermediate host
HCoV-229E	1965	*Hipposideros caffer ruber* (Noack's leaf-nosed bat)	Alpacas
HCoV-OC43	1967	Unconfirmed rodent	Cattle
SARS-CoV	2003	Horseshoe bat	Civet cat
HCoV-HKU1	2004	Unconfirmed rodent	Unknown
HCoV-NL63	2004	*Triaenops afer* (African trident bat)	Unknown
MERS-CoV	2012	*Taphozous perforatus* (Egyptian tomb bat), *Pipistrellus* spp. (Common pipistrelle), *Neoromicia* spp. (Vesper bat)	Dromedary camels
SARS-CoV-2	2019	*Rhinolophus* spp. (Horseshoe bat)	Pangolin (unconfirmed)

the seven human coronaviruses (HCoVs), and their animal origins. Figure 5.2 shows the evolutionary relationships between those HCoVs and a few other animal hosted coronaviruses within the alpha and beta groups.

Among the seven reported human coronaviruses, four of them include HCoV-229E, HCoV-OC43, HCoV-NL63, and HCoV-HKU1 that represent endemic and low virulence HCoVs causing upper respiratory tract disease, responsible for up to 15–30% of the common cold symptoms in adults. The earliest, HCoV-229E, was isolated in 1965 using standard tissue culture from a volunteer. In 1967, HCoV-OC43 was recovered from a tracheal and nasal organ culture from the Common Cold Unit in Salisbury, United Kingdom. Only these two HCoVs were widely reported and under study until the twenty-first century. In 2004, HCoV-NL63 was isolated from a 7-month-old child in the Netherlands, while in 2005, HCoV-HKU1 was isolated from a Hong Kong patient with pneumonia. Later both strains were identified in adults and infants, indicating that these two HCoVs can be considered as new agents responsible for respiratory infections [29, 30]. These four HCoVs generally demonstrate winter seasonality between the months of December and April and typically cause mild upper respiratory infections in humans with some exception of severe lower respiratory infection, for example, in the cases of elderly or immunocompromised individuals [31].

Apart from these four mild HCoVs, over the last two decades, the world has witnessed three major outbreaks of coronaviruses with increased morbidity and transmission rates. In 2002–2003, the outbreak of severe acute respiratory syndrome (SARS-CoV) occurred in Guangdong Province of China and quickly spread to over 30 countries, infecting 8000 people with a mortality rate of approximately 10%. A decade later, in 2012, MERS-CoV caused a severe respiratory disease that emerged in the 27 countries in the Middle East, Europe, North Africa, and Asia. MERS-CoV virus is still posing a potential threat in the Middle East where it is still

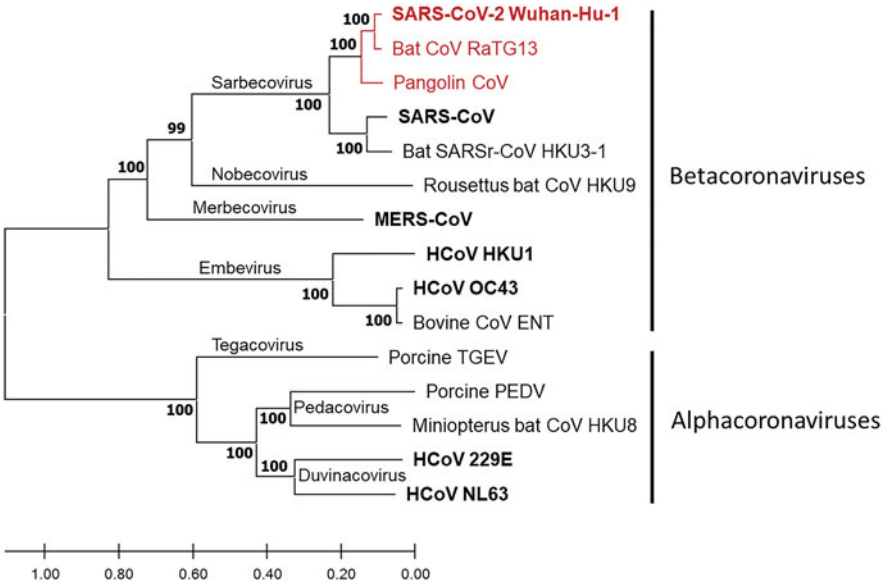

Fig. 5.2 Maximum likelihood phylogeny of a selection of alpha- and betacoronaviruses, including the seven coronaviruses known to infect humans (labeled in bold). This phylogeny was inferred using the GTR + G + I model [27] fit to ORF1ab nucleotide sequences and is drawn to scale with branch lengths measured in the number of substitutions per site (see scale bar). Evolutionary analyses were conducted in MEGA X [28], and bootstrap values were calculated from 500 replications. Red labels indicate coronaviruses in the SARS-CoV-2 group; bold text indicates species found in humans. Accession numbers for sequence data used in this figure include the following: NC_019843.3, MT797634.1, NC_006577.2, NC_006213.1, NC_004718.3, NC_045512.2, MN996532.2, MT121216.1, NC_003045.1, NC_003436.1, MG762674.1, DQ022305.2, NC_010438.1, NC_038861.1, and NC_005831.2

sporadically detected in the human population [32]. In December 2019, the novel coronavirus entitled severe acute respiratory syndrome coronavirus 2 (SARS-CoV-2) was reported in Wuhan, Hubei, China. On March 11, 2020, the World Health Organization declared a global COVID-19 (the disease caused by SARS-CoV-2) pandemic due to the emergence of different variants and global spread [33, 34].

Bats are considered the most probable zoonotic origin for all three of these major outbreaks of coronavirus. SARS-CoV and MERS-CoV appear to have passed through intermediate hosts: civets and camels, respectively, before transmitting to humans. However, the details of these transmission events are unclear [19, 35, 36]. As for SARS-CoV-2, the highest average genetic similarity with other sequenced virus genomes to date is with CoV RaTG13 sampled from a *Rhinolophus affinis* bat, estimated to have shared a common ancestor with SARS-CoV-2 decades prior to the emergence of SARS-CoV-2 in humans [37]. So far, no viruses with a closer genetic similarity to SARS-CoV-2 have been collected, and so there remains some ambiguity about the immediate source of the virus [18]. Pangolins were also initially

considered as the possible SARS-CoV-2 reservoir due to high genomic similarity of Pangolin CoV with SARS-CoV-2. However, infected pangolins also exhibit clinical and histopathological changes when infected with CoV [32], and natural CoV hosts are expected to be asymptomatic due to their long coevolutionary history.

5.3 Evolution of SARS-CoV-2 in Human Hosts

As the SARS-CoV-2 epidemic began to emerge globally in early 2020, one key part of the global effort to characterize the virus and understand how it was spreading was to acquire whole genome sequence data. These sequence data quickly began to reveal mutational changes. The rate of change of the SARS-CoV-2 genome has been estimated at between $1–5 \times 10^{-6}$ nucleotide substitutions per site per day [38], or across the whole SARS-CoV-2 genome, approximately 20 genetic changes per year within a lineage [39]. In the early days of the pandemic, the observed mutations all appeared to be random and effectively neutral, but they provided a way of tracking transmission routes of specific genotypes, as the virus began to spread around the globe. For example, early on there was much discussion about what the initial transmission routes were for SAR-CoV-2 into the USA. Through sequencing and tracking of specific mutations, researchers were able to conclude that SARS-CoV-2 entered the USA via multiple independent sources from both Asia and Europe [40].

5.4 SARS-CoV-2 Whole Genome Sequence Data

The SARS-CoV-2 genome consists of ~29,903 nucleotides and has a gene composition and structure similar to that of other betacoronaviruses: ~70% of the genome comprises replicase orf1ab, and the rest of the genome consists of S (encoding the structural spike glycoprotein), ORF3a (ORF3a protein), E (structural envelope protein), M (structural membrane glycoprotein), ORF6 (ORF6 protein), ORF7a (ORF7a protein), ORF7b (ORF7b protein), ORF8 (ORF8 protein), N (structural nucleocapsid phosphoprotein), and ORF10 (ORF10 protein). We know much about SARS-CoV-2 diversity and evolution throughout the global pandemic from ongoing analysis of the unprecedented quantity of publicly available SARS-CoV-2 whole genome sequence data. This continually growing collection of sequence data has given researchers the opportunity to observe viral molecular evolution, essentially in real time. For decades, the research field of bioinformatics has supported and promoted the practice of open data sharing [41], and the SARS-CoV-2 sequence data has been no different. Importantly, free access to SARS-CoV-2 sequence data for all researchers means more teams can work in parallel and hopefully allow for more rapid characterization of patterns and even solutions. Data has been made available through databases, including NCBI as well as GISAID, a database

originally developed to organize sharing of influenza sequence data but now the main repository for global SAR-CoV-2 genome sequence data. As of late 2021, there were close to six million publicly available whole SARS-CoV-2 genome sequences on GSAID. Data are from all over the globe, but unsurprisingly the origin of sequence data is unevenly distributed, with the USA and the United Kingdom contributing the highest total numbers. However, on a per-case basis, the USA is far behind many other countries, having sequenced samples from less than 1% of patients diagnosed with COVID-19 [42]. Iceland has the best per-case sequencing rate, at close to 100% of diagnosed infections [43]. Figure 5.3 shows the inferred evolutionary relationships between a subset of available SARS-CoV-2 genomes ($N = 3643$) to give an idea of how the virus population has evolved and diversified over the course of the pandemic.

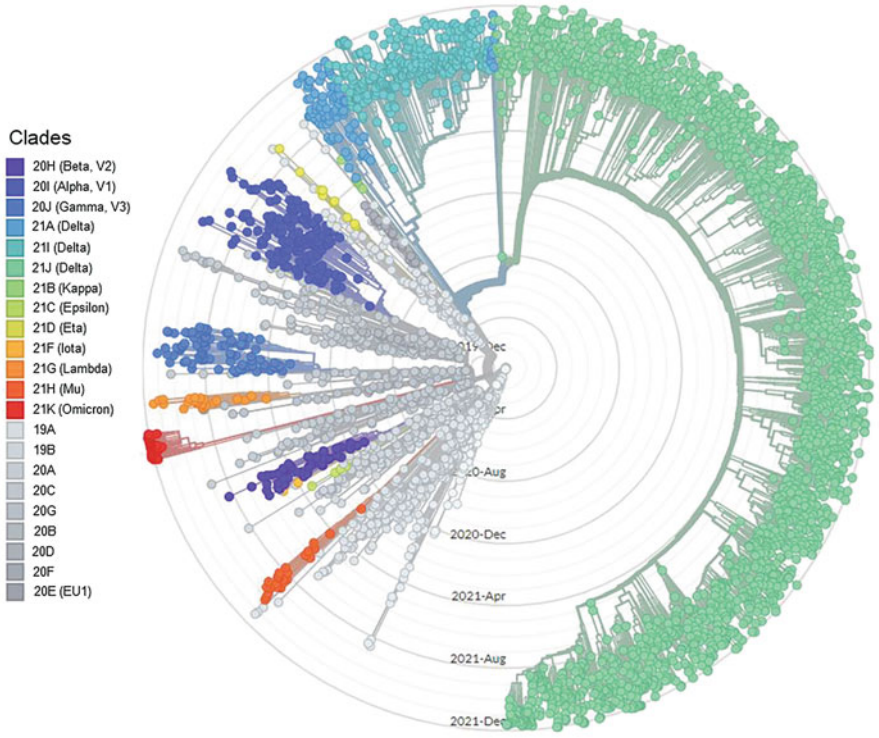

Fig. 5.3 Phylogenetic tree of 3643 genomes sampled globally between December 2019 and December 2021. Clades are named according to Nextstrain nomenclature, which distinguishes clades based on global frequency, year of emergence, and a unique letter. Visualization was performed by nextstrain.org [123] with data from GISAID

5.5 Natural Selection Begins to Drive Adaptive Evolution

By the fall of 2020, clear evidence was emerging to suggest that a few key mutations in the SARS-CoV-2 genome conferred adaptive impacts of human health concern, in particular increased transmission rates and virulence. These adaptations presented new challenges for governments and public health officials trying to reduce cases. Therefore, understanding and predicting the adaptive evolution of SARS-CoV-2 have become increasingly important. Here, we identify two broad categories of approaches that researchers have taken to identify regions in the SARS-CoV-2 genome where natural selection is driving evolution. The first type of approach aims to infer how specific mutations are likely to impact *protein structure and function at the molecular level* and so lead to impacts on virus fitness. The second type of approach analyzes variation in genome sequences collected during the SARS-CoV-2 pandemic to identify *epidemiological and phylogenetic patterns* that are unlikely to have occurred simply due to chance and are likely driven by natural selection. We discuss what we can learn from both types of approaches, as well as their drawbacks. Typically, multiple lines of evidence are required before a specific mutation is identified by consensus as adaptive.

5.6 Evidence of Selection from Models and Experimental Tests of Protein Function

At the molecular and functional level, predictive protein models and a range of in vitro experimental tests have allowed researchers to identify genes and even specific sites within genes on the SARS-CoV-2 genome where mutations are under selection and likely to have impacts on human health. The focus here is on exploring protein function and interactions with the human immune system and host cell. Using this kind of approach, earlier studies examining other coronaviruses had already identified the spike protein as one of crucial importance [44]. Soon after SARS-CoV-2 emerged, the spike protein was identified as important in this novel coronavirus as well [45]. The spike protein interacts with the angiotensin-converting enzyme 2 (ACE2) receptor on the surface of the human host cell. If this interaction is successful, then the coronavirus has access into the human host cell. Predictive models and experimental studies have identified specific regions and amino acid positions that are likely to be most important in impacting how the spike protein interfaces with ACE2 receptors. Of particular importance is the receptor-binding domain (RBD) of the spike protein [46]. This region varies between a closed/down position and an open/up position. To successfully bind with the human ACE2 receptor, it must be in the up position [47–49]. This is also the region where many neutralizing antibodies bind to prevent interaction with ACE2, effectively neutralizing the virus. Many in vitro experiments have been performed looking at the impacts of specific mutations in this region (e.g., [50, 51]). Other regions of

interest in the spike protein that have been identified using this approach include the furin cleavage site (e.g., [52]) and the N-terminal domain (e.g., [53]). There is also evidence that mutations in other genes of the SARS-CoV-2 genome may impact virus fitness (e.g., [54, 55]). However, the spike gene appears to have the largest predicted impact.

While studies exploring the impact of mutations on the structure and function of key proteins are useful for identifying genes and regions of potential importance, sometimes they give us only a hint at the true impacts of these mutations when in vivo. Furthermore, for logistical reasons, these studies typically examine the impacts of a single mutational change at a time. However, the impact of a mutation often depends on which other mutations are also present in a genome, a phenomenon known as epistasis [56]. There is now growing evidence of epistatic effects of mutations in SARS-CoV-2 [57]. Therefore, the impacts of multiple mutation combinations will often remain unclear until they play out in real human hosts.

5.7 Evidence of Selection from Phylogenetic and Epidemiological Data

This second type of approach uses observed SARS-CoV-2 sequence data to identify patterns that are unlikely to have occurred simply due to chance and so must be driven by natural selection. One way to do this is by tracking variant frequencies over time and looking for rapid increases in the frequency of virus variants. The assumption is that the genomes of those variants rapidly increasing in frequency must contain one or more mutations that increase viral fitness as compared to other variants circulating at that time. It is usually unclear from this type of data which mutation or mutations are the ones that are impacting fitness. Another drawback of this approach is that sometimes an observed rapid increase in variant frequency may occur simply due to random loss of other variants when a small number of viruses establish in a new host population. These are the potential results of evolution by means of genetic drift in a small population. Because of this potential for genetic drift to result in evolutionary patterns that are difficult to distinguish from the results of natural selection, the evidence for adaptive evolution is significantly strengthened when the same pattern of a rapidly rising variant frequency is observed in multiple independent host populations. This is the type of evidence that allowed for the identification of the spike protein amino acid change D614G as one that increases virus fitness and therefore is a potential human health concern. SARS-CoV-2 variants with this mutation were observed to rapidly increase in frequency across the globe and at multiple geographic levels: national, regional, and municipal, beginning in the spring of 2020 [58].

Another way that researchers have used observed SARS-CoV-2 sequence data to look for evidence of selection is by using phylogenetic techniques to fit models of molecular evolution and identify mutations that have evolved multiple times

across different independently evolving lineages of SARS-CoV-2. This pattern of repeated evolution is called "convergent evolution" and provides strong evidence for adaptive evolution, suggesting that the convergently evolved mutation must provide a fitness benefit of some kind to the virus. For example, Hodcroft et al. [59] showed evidence of convergent evolution at amino acid 677 in the spike protein. Their phylogenetic analyses of SARS-CoV-2 genome sequences from the USA (Sept.–Nov. 2020) revealed the independent evolution of spike mutations at position 677 in seven distinct lineages. The independent rise and spread of the mutation this many times is highly unlikely to have occurred by chance alone. It strongly suggests a fitness advantage in viruses that have it.

5.8 Adaptively Evolved Variants of Human Health Concern

In response to evidence that natural selection was driving the evolution of SARS-CoV-2 variants with important impacts on global human health, the Virus Evolution Working Group of the World Health Organization (WHO) established a name scheme for the variants to simplify and standardize communication about SARS-CoV-2 [60]. This naming scheme also has the added benefit of encouraging the media and the public to move away from location-based names such as the "UK variant" or the "South African variant" which can be stigmatizing to countries and their residents. Other nomenclature systems for naming and tracking SARS-CoV-2 genetic lineages have also been used [61–63]. However, the WHO naming scheme is specifically focused on identifying variants of potential interest for public health. In particular, as is outlined in detail on their website (www.who.int/en/activities/tracking-SARS-CoV-2-variants; [64]), they provide working definitions of what they have named variants under monitoring (VUMs), variants of interest (VOIs), and variants of concern (VOCs). Variants classified into these categories are more closely monitored and assessed through coordinated field and laboratory investigations by WHO member states and partners. Variants are placed on these lists if they seem to have increased transmissibility, virulence, immune escape, or undergone any other evolutionary changes with the potential to impact global public health. VOCs are those variants for which these evolutionary changes with global health impacts have been clearly demonstrated through the types of approaches described in the previous section of this chapter. Variants may be removed from these lists if "they have been conclusively demonstrated to no longer pose a major added risk to global public health compared to other circulating SARS-CoV-2 variants" [64]. Figure 5.4 shows the frequencies of five identified VOCs over time in four different representative countries.

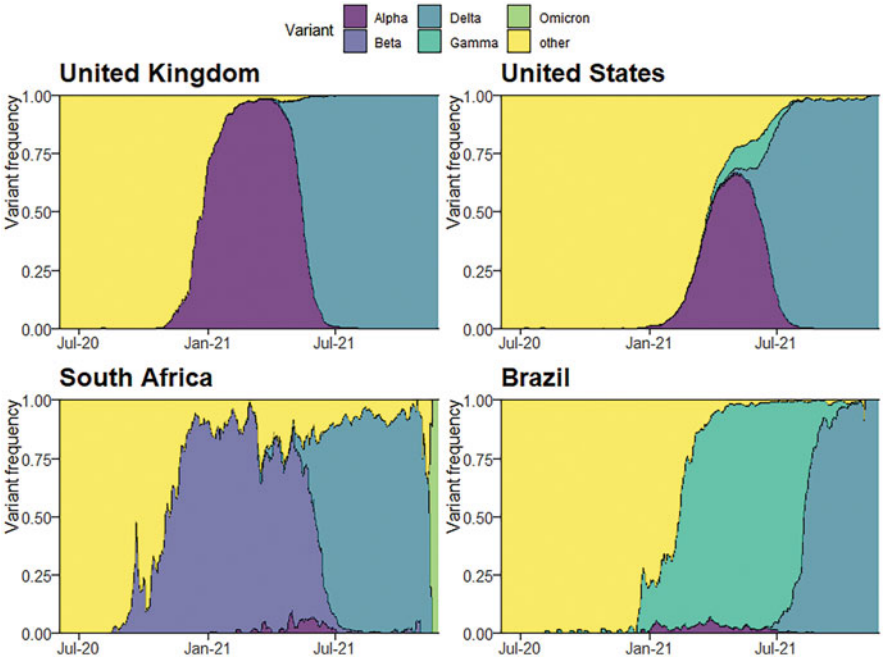

Fig. 5.4 Frequency of five SARS-CoV-2 variants of concern (VOCs) and pre-VOC variants over time, from June 2020 to Nov 2021, in the United Kingdom, the USA, South Africa, and Brazil. Variant frequency data retrieved from https://cov-spectrum.ethz.ch

5.8.1 The First Clearly Identified Adaptively Evolved Variant: Alpha

The Alpha variant (also known as B.1.1.7, or colloquially the UK variant) was the first SARS-CoV-2 variant for which there was clear evidence suggesting it had evolved impacts on human health. First detected in the United Kingdom in September 2020, it was officially designated as a VOC on December 18, 2020. The genome of the Alpha variant has 23 mutations compared to the Wuhan ancestor strain, but mutations of potential concern for human health all lie in the gene that codes for the spike protein [65]. A few lines of evidence confirmed that this variant evolved by means of natural selection and so has increased fitness compared to the other variants circulating at that time. The first line of evidence was its rapid increase in frequency, starting in Kent and Greater London in September 2020. It rapidly moved across the United Kingdom [65, 66], despite a country-wide lockdown, and was widespread across the United Kingdom by early December [67]. The Alpha variant also quickly rose in frequency in other countries as it began to spread globally. It accounted for most of the infections in the USA and many European countries by the second quarter of 2021 [38, 68, 69]. Epidemiological

models fit to case counts estimated from community-based COVID-19 testing, and secondary contact data suggested that the Alpha variant had a significant transmission advantage of 59–74% over other lineages circulating at that time [70–72]. Further evidence of adaptively evolved changes came from structural modeling of the amino acid changes in the spike protein. Modeling of the evolved amino acid changes predicted that the Alpha variant could bind more easily to host cells in the human respiratory tract [73]. Viral load (the number of viral particles in a host), measured in both hospitalized and walk-in test center patients, showed that patients with the Alpha variant had viral loads that were higher by a factor of 10 relative to non-Alpha variant patients [74, 75]. This suggested that high viral load might be driving the observed increase in transmission rates.

Adaptive evolution of higher transmission rates in SARS-CoV-2 variants is not surprising given that transmission is an important component of viral fitness [76]. Unfortunately, and less clearly linked to viral fitness, higher virulence has also evolved in the Alpha variant. Statistical models examining community test data and deaths found a significant increase in the mortality rate (64% higher; 95% CI: 32–104%) for patients testing positive for the Alpha variant compared to patients with other variants [77–79]. The Alpha variant does not appear to be associated with increased risk of reinfection [80] nor a significant decrease in vaccine efficacy [81–83]. Therefore, these initial adaptively evolved changes did not impact reinfection rates.

5.8.2 Other Adaptively Evolved Variants Identified: Beta, Gamma, and Delta

The Beta and Gamma variants emerged around roughly the same time as the Alpha variant but in different regions of the world. The Beta variant (also known as B.1.351) was first detected in South Africa in October 2020. However, subsequent phylogenetic analysis suggests that the variant first evolved in July or August 2020 [84]. The Gamma variant (also known as P.1) was first detected in Brazil in November/December 2020 [85].

Preliminary data suggested that the *Beta variant* had evolved to be more transmissible [84, 86] and resulted in higher rates of reinfection compared with earlier SARS-CoV-2 lineages [87, 88]. In South Africa, the second wave of the SARS-CoV-2 epidemic was larger than the first and was characterized by a more rapid increase in admissions to hospitals, along with increased in-hospital mortality. Some of the increased mortality in the second wave likely arose from higher numbers of cases in older individuals and increased pressure on the health system. However, some of the increased mortality may have also been due to higher virulence of the Beta variant compared to the variants that dominated the first epidemic wave in South Africa [89].

The *Gamma variant* spread rapidly through Brazil and other parts of South America, and its rate of spread suggested that it also had an increased transmission rate. Analysis of samples from SARS-CoV-2 patients in the Manaus region of Brazil showed that Gamma variant samples were significantly associated with higher viral loads. Epidemiological models for variant counts of cases in Manaus, Brazil, also suggest that the Gamma variant was between 1.7 and 2.4 times more transmissible that other non-Gamma variants as it emerged in Brazil [85]. The model further showed that SARS-CoV-2 infections were 1.2–1.9 times more likely to result in mortality after the emergence of Gamma in Brazil. However, this effect may have also been driven by increased stresses on the healthcare system at that time [85].

The *Delta variant* (also known as B.1.617.2) began to emerge a little later. It was first documented in India in October of 2020 and declared a VOC in May 2021. This variant has shown increased transmissibility compared to previous variants, spreading across much of the globe and rapidly replacing the Alpha variant in the United Kingdom [90, 91] and the USA [92]. Studies are ongoing to characterize this variant, but increased transmission is likely driven by higher viral loads, a shorter time to peak viral load, and a shorter incubation period [93–95], along with the ability to effectively resist antibodies [96].

5.8.3 Emerging Variants of Concern: Omicron

The first documented case of Omicron was in early November 2021. Since then, it has quickly swept through South Africa and was declared a VOC on November 26, 2021 [97]. Omicron is unusual as compared to other variants sequenced previously. It has more unique mutations than expected and so is quite distantly related to other sequenced SARS-CoV-2 variants. At the time of this writing, the impacts of these unique mutations are still emerging. However, the number and location of mutations on the gene that codes for the spike protein are a concern and suggest that transmission rate is likely to be further increased in this variant. Impacts of these mutations on virulence and vaccine efficacy are unclear.

5.8.4 Evolved Impacts on Immunity and Vaccine Effectiveness

Individuals who are infected with SARS-CoV-2 retain some level of immunity after recovery and so are less likely to become infected again. If they are reinfected, they tend to have milder symptoms. Similarly, individuals who have been fully vaccinated with one of the multiple available COVID-19 vaccines are also much less likely to become reinfected. No vaccine is 100% effective but at a roughly 80–95% effectiveness for preventing symptomatic pre-VOC SARS-CoV-2 infections, vaccines have made a significant impact [98]. One concern is that the virus is evolving to better evade human immune defenses, both those generated by past

Table 5.2 Estimates of vaccine efficacy at preventing symptomatic SARS-CoV-2 infection with pre-variant and evolved variants Alpha, Beta, and Delta

	Vaccine type		
Variant	Pfizer/BioNTech BNT162b	Moderna mRNA-1273	Janssen AD26.CoV2b
Pre-variant	95%[99]	93%[100]	72%[101]
Alpha	92%[102]	90%[100]	–
Beta	75%[81, 100]	88%[100]	64%[101]
Delta	83%[102]	73%[103]	–

Numbers shown are for people who are fully vaccinated following recommendations for that vaccine type. "–" indicates that no peer-reviewed estimates were available

infection and those generated through vaccination. There certainly have been significant shifts in vaccine efficacy due to some of the evolved VOCs, and these evolved shifts in vaccine efficacy differ between specific vaccine types. Table 5.2 summarizes some of these evolved shifts in vaccine efficacy for three of the available vaccines. The potential for future adaptive evolution of SARS-CoV-2 in response to vaccines remains to be seen.

5.9 Immunocompromised Patients as Hotspots for SARS-CoV-2 Adaptive Evolution

Typically, individuals infected with SAR-CoV-2 remain infectious for no longer than 10 days, while patients with severe-to-critical illness remain infectious for up to 20 days [104, 105]. However, in immunocompromised patients, SARS-CoV-2 can sometimes successfully evade the immune system and persist for much longer [106–109], such as for over 6 months in one documented case [110]. Over the course of a long-term infection, the virus population can evolve extensively within the patient ("intra-host evolution") and accumulate an unusually high number of mutations. Immunocompromised patients are often treated over the course of their SARS-CoV-2 infection with the antiviral drug remdesivir or convalescent plasma (blood plasma derived from patients who have recovered from COVID-19), which may drive adaptive evolution in SARS-CoV-2 to better evade these treatments. For example, in Kemp et al. [109], the authors report on a long-term SARS-CoV-2 infection in an immunosuppressed patient treated with convalescent plasma. In this patient, the viral population evolved to better escape neutralizing antibodies, and eventually this infection was fatal. Thus, rapid evolution driven by selection in immunocompromised patients may have driven the adaptive evolution of some (if not all) of the VOCs [84, 106, 108].

The key piece of evidence suggesting that long-term intra-host evolution (due to chronic infections) has driven the adaptive evolution of many of the VOCs is that these variants all have more unique mutations than expected as compared to other co-circulating variants. For example, each of the first three identified VOCs had

about twice as many mutations in their genomes compared to other co-circulating lineages at the time they first emerged. The Alpha variant had 23 mutations compared to the Wuhan-Hu-1 reference sequence [65]. The Beta variant had 21 mutations [85], and the Gamma variant had 23 mutations [84]. These mutations are spread across the whole genome but tend to be biased toward non-synonymous mutations (those mutations that can affect protein structure) and focused on the S1 gene (the gene that codes for the spike protein) [38].

5.10 Potential Impacts of Cross-Species Spillback on Adaptive Evolution

Since SARS-CoV-2 is originally derived from a nonhuman animal host, we know it is certainly capable of cross-species transmission. Thus, reports of "spillback infections"—transmission of SARS-CoV-2 from humans to nonhuman animals—are not unexpected. Indeed, there have been quite a few species of nonhuman animals reported to have been infected with SARS-CoV-2 including pets and domesticated animals (e.g., cats, dogs, hamsters, rabbits, ferrets, and cows) and those commonly found in zoos (e.g., cougars, tigers, lions, gorillas), along with wildlife (e.g., white-tailed deer and skunks) [29, 111, 112]. Along with being a potential threat to the health of these nonhuman animals, repeated human to animal transmission increases the risk of adaptive evolution of SARS-CoV-2 occurring in a new animal host, followed by retransmission back to humans. The main concern with a high number of spillover cases is that new animal hosts may act as reservoirs, maintaining high numbers of infections and driving novel adaptive evolution of the virus. In 2020, this risk was realized in Denmark [113] and the Netherlands, where SARS-CoV-2 was transmitted from humans to farmed mink and then back to humans again [114, 115]. During its time in the mink population, the virus accumulated some new mutations including up to five in the spike protein, one of which was later found to confer partial escape from human antibodies [116]. In response to these events, the Danish government ordered the culling of all farmed mink in the country, estimated at approximately 17 million animals, and in the Netherlands, more than 2.7 million minks were culled [117]. At this time, it is not clear how big a risk mink farms are of becoming dangerous reservoirs of SARS-CoV-2, but at least for now, proactive measures have been taken to reduce this potential risk.

Other clear examples of transmission to other nonhuman animal hosts and then back to humans again have not been documented, but the potential for this occurring in the future is certainly there. Wild animal species of particular concern as SARS-CoV-2 reservoirs are those that are both abundant and live in close association with humans [111], for example, North American white-tailed deer. A study screening serum samples from wild deer in four US states in 2021 detected SARS-CoV-2 antibodies in 40% of the samples [118]. The high prevalence of antibodies in deer

sampled in this study across multiple states suggests a high likelihood of within-herd spread. A second study tested samples from free-living and captive deer in Iowa in 2020 for the presence of SAR-CoV-2 RNA—evidence of a current or recent infection. These researchers found that one-third of those deer sampled tested positive for SARS-CoV-2 [119]. These studies highlight the need for increased surveillance of deer and potentially other wildlife populations to better determine whether nonhuman animal populations are on their way to becoming long-term reservoirs for SARS-CoV-2, generating novel evolved variants that will spill back over into humans or even other animal hosts.

5.11 Future Evolution of SARS-CoV-2

What will the future evolution of SARS-CoV-2 look like? The evolutionary outcomes depend crucially on population size and spread. The larger the virus population, the greater the chance for rapid and continued adaptive evolution of SARS-CoV-2, with further implications for human health. The more we can work to reduce infection numbers through a range of public health practices including mask-wearing and vaccinations, the better the chance that random genetic drift will dominate the evolutionary dynamics of SARS-CoV-2 instead of natural selection. Without dramatic reductions in case numbers, natural selection will likely continue to drive adaptive evolution in SARS-CoV-2 in ways that are possible. It could be that the virulence-transmission trade-off hypothesis [13] will play out, and we will see a reduction in SARS-CoV-2 virulence moving forward, eventually shifting the disease to one that resembles the common cold. We may also see SARS-CoV-2 evolve in response to some of the biomedical interventions currently in use – either treatments or vaccinations or both. Certainly, we have already started to see SARS-CoV-2 evolve to better evade human host immune defenses generated by the current vaccines. It is very possible that the COVID-19 vaccines need periodic updates to counter ongoing evolutionary changes, much like the annually updated flu vaccine. The best way to prepare for these possibilities is through continued and globally coordinated surveillance, analysis, and modeling of the evolving SARS-CoV-2 genome (e.g., [120–122]).

References

1. McDonald, S. M., Nelson, M. I., Turner, P. E., & Patton, J. T. (2016). Reassortment in segmented RNA viruses: Mechanisms and outcomes. *Nature Reviews. Microbiology, 14*, 448–460.
2. Abbasi, J. (2021). Researchers tie severe immunosuppression to chronic COVID-19 and virus variants. *JAMA, 325*, 2033–2035.
3. Elena, S. F., & Sanjuán, R. (2005). Adaptive value of high mutation rates of RNA viruses: Separating causes from consequences. *Journal of Virology, 79*, 11555–11558.

4. Chao, L. (1990). Fitness of RNA virus decreased by Muller's ratchet. *Nature, 348*, 454–455.
5. Sanjuán, R., & Domingo-Calap, P. (2021). Genetic diversity and evolution of viral populations. In *Encyclopedia of virology* (pp. 53–61). Elsevier.
6. Dong, E., Du, H., & Gardner, L. (2020). An interactive web-based dashboard to track COVID-19 in real time. *The Lancet Infectious Diseases, 20*, 533–534.
7. Zanini, F., Brodin, J., Thebo, L., Lanz, C., Bratt, G., Albert, J., et al. (2015). Population genomics of intrapatient HIV-1 evolution. *eLife, 4*, e11282.
8. Braun, K. M., Moreno, G. K., Wagner, C., Accola, M. A., Rehrauer, W. M., Baker, D. A., et al. (2021). Acute SARS-CoV-2 infections harbor limited within-host diversity and transmit via tight transmission bottlenecks. *PLoS Pathogens, 17*, e1009849.
9. Sender, R., Bar-On, Y. M., Gleizer, S., Bernshtein, B., Flamholz, A., Phillips, R., et al. (2021). The total number and mass of SARS-CoV-2 virions. *Proceedings of the National Academy of Sciences of the United States of America, 118*, e2024815118.
10. Sim, S., Aw, P. P. K., Wilm, A., Teoh, G., Hue, K. D. T., Nguyen, N. M., et al. (2015). Tracking dengue virus intra-host genetic diversity during human-to-mosquito transmission. *PLoS Neglected Tropical Diseases, 9*, e0004052.
11. Varble, A., Albrecht, R. A., Backes, S., Crumiller, M., Bouvier, N. M., Sachs, D., et al. (2014). Influenza A virus transmission bottlenecks are defined by infection route and recipient host. *Cell Host & Microbe, 16*, 691–700.
12. Bull, J. J. (1994). Virulence. *Evolution, 48*, 1423–1437.
13. Anderson, R. M., & May, R. M. (1992). *Infectious diseases of humans: Dynamics and control* (Revised ed.). Oxford University Press.
14. Hanley, K. A., Azar, S. R., Campos, R. K., Vasilakis, N., & Rossi, S. L. (2019). Support for the transmission-clearance trade-off hypothesis from a study of Zika virus delivered by mosquito bite to mice. *Viruses, 11*, 1072.
15. Blanquart, F., Grabowski, M. K., Herbeck, J., Nalugoda, F., Serwadda, D., Eller, M. A., et al. (2016). A transmission-virulence evolutionary trade-off explains attenuation of HIV-1 in Uganda. *eLife, 5*, e20492.
16. Ben-Shachar, R., & Koelle, K. (2018). Transmission-clearance trade-offs indicate that dengue virulence evolution depends on epidemiological context. *Nature Communications, 9*, 2355.
17. McKay, B., Ebell, M., Dale, A. P., Shen, Y., & Handel, A. (2020). Virulence-mediated infectiousness and activity trade-offs and their impact on transmission potential of influenza patients. *Proceedings of the Royal Society B: Biological Sciences, 287*, 20200496.
18. Holmes, E. C., Goldstein, S. A., Rasmussen, A. L., Robertson, D. L., Crits-Christoph, A., Wertheim, J. O., et al. (2021). The origins of SARS-CoV-2: A critical review. *Cell, 184*, 4848–4856.
19. Singh, D., & Yi, S. V. (2021). On the origin and evolution of SARS-CoV-2. *Experimental & Molecular Medicine, 53*, 537–547.
20. Rehman, S., Shafique, L., Ihsan, A., & Liu, Q. (2020). Evolutionary trajectory for the emergence of novel coronavirus SARS-CoV-2. *Pathogens, 9*, 240.
21. Cui, J., Li, F., & Shi, Z.-L. (2019). Origin and evolution of pathogenic coronaviruses. *Nature Reviews. Microbiology, 17*, 181–192.
22. Woo, P. C. Y., Lau, S. K. P., Lam, C. S. F., Lau, C. C. Y., Tsang, A. K. L., Lau, J. H. N., et al. (2012). Discovery of seven novel mammalian and avian coronaviruses in the genus Deltacoronavirus supports bat coronaviruses as the gene source of Alphacoronavirus and Betacoronavirus and avian coronaviruses as the gene source of Gammacoronavirus and Deltacoronavirus. *Journal of Virology, 86*, 3995–4008.
23. Weiss, S. R., & Leibowitz, J. L. (2011). Coronavirus pathogenesis. In *Advances in virus research* (pp. 85–164). Elsevier.
24. Tang, X., Wu, C., Li, X., Song, Y., Yao, X., Wu, X., et al. (2020). On the origin and continuing evolution of SARS-CoV-2. *National Science Review, 7*, 1012–1023.
25. Chen, B., Tian, E.-K., He, B., Tian, L., Han, R., Wang, S., et al. (2020). Overview of lethal human coronaviruses. *Signal Transduction and Targeted Therapy, 5*, 89.

26. de Wit, E., van Doremalen, N., Falzarano, D., & Munster, V. J. (2016). SARS and MERS: Recent insights into emerging coronaviruses. *Nature Reviews. Microbiology, 14*, 523–534.
27. Nei, M., & Kumar, S. (2000). *Molecular evolution and phylogenetics*. Oxford University Press.
28. Kumar, S., Stecher, G., Li, M., Knyaz, C., & Tamura, K. (2018). MEGA X: Molecular evolutionary genetics analysis across computing platforms. *Molecular Biology and Evolution, 35*, 1547–1549.
29. Liu, Y., Hu, G., Wang, Y., Ren, W., Zhao, X., Ji, F., et al. (2021). Functional and genetic analysis of viral receptor ACE2 orthologs reveals a broad potential host range of SARS-CoV-2. *Proceedings of the National Academy of Sciences, 118*, 2025373118.
30. Vijgen, L., Keyaerts, E., Moës, E., Thoelen, I., Wollants, E., Lemey, P., et al. (2005). Complete genomic sequence of human coronavirus OC43: Molecular clock analysis suggests a relatively recent zoonotic coronavirus transmission event. *Journal of Virology, 79*, 1595–1604.
31. Li, X., Luk, H. K. H., Lau, S. K. P., & Woo, P. C. Y. (2019). Human coronaviruses: General features. In *Reference module in biomedical sciences* (p. B9780128012383957000). Elsevier.
32. Schoeman, D., Gordon, B., & Fielding, B. C. (2021). Pathogenic human coronaviruses. In *Reference module in biomedical sciences* (p. B9780128187319001000). Elsevier.
33. Sharma, A., Ahmad Farouk, I., & Lal, S. K. (2021). COVID-19: A review on the novel coronavirus disease evolution, transmission, detection, control and prevention. *Viruses, 13*, 202.
34. WHO. (2020b). *WHO Director-General's opening remarks at the media briefing on COVID-19—11 March 2020*. WHO.
35. Guan, Y., Zheng, B. J., He, Y. Q., Liu, X. L., Zhuang, Z. X., Cheung, C. L., et al. (2003). Isolation and characterization of viruses related to the SARS coronavirus from animals in southern China. *Science, 302*, 276–278.
36. Kahn, J. S., & McIntosh, K. (2005). History and recent advances in coronavirus discovery. *The Pediatric Infectious Disease Journal, 24*, S223–S227.
37. Boni, M. F., Lemey, P., Jiang, X., Lam, T. T.-Y., Perry, B. W., Castoe, T. A., et al. (2020). Evolutionary origins of the SARS-CoV-2 sarbecovirus lineage responsible for the COVID-19 pandemic. *Nature Microbiology, 5*, 1408–1417.
38. Tao, K., Tzou, P. L., Nouhin, J., Gupta, R. K., de Oliveira, T., Kosakovsky Pond, S. L., et al. (2021). The biological and clinical significance of emerging SARS-CoV-2 variants. *Nature Reviews. Genetics, 22*, 757–773.
39. Otto, S. P., Day, T., Arino, J., Colijn, C., Dushoff, J., Li, M., et al. (2021). The origins and potential future of SARS-CoV-2 variants of concern in the evolving COVID-19 pandemic. *Current Biology, 31*, R918–R929. https://doi.org/10.1016/j.cub.2021.06.049
40. Zhang, W., Govindavari, J. P., Davis, B. D., Chen, S. S., Kim, J. T., Song, J., et al. (2020). Analysis of genomic characteristics and transmission routes of patients with confirmed SARS-CoV-2 in Southern California during the early Stage of the US COVID-19 pandemic. *JAMA Network Open, 3*, e2024191.
41. EMBL-EBI. (2021). *Data sharing collaborations*. EMBL-EBI.
42. Maxmen, A. (2021). Why US coronavirus tracking can't keep up with concerning variants. *Nature, 592*, 336–337.
43. Furuse, Y. (2021). Genomic sequencing effort for SARS-CoV-2 by country during the pandemic. *International Journal of Infectious Diseases, 103*, 305–307.
44. Li, W., Moore, M. J., Vasilieva, N., Sui, J., Wong, S. K., Berne, M. A., et al. (2003). Angiotensin-converting enzyme 2 is a functional receptor for the SARS coronavirus. *Nature, 426*, 450–454.
45. Zhou, P., Yang, X.-L., Wang, X.-G., Hu, B., Zhang, L., Zhang, W., et al. (2020). A pneumonia outbreak associated with a new coronavirus of probable bat origin. *Nature, 579*, 270–273.
46. Wrapp, D., Wang, N., Corbett, K. S., Goldsmith, J. A., Hsieh, C.-L., Abiona, O., et al. (2020). Cryo-EM structure of the 2019-nCoV spike in the prefusion conformation. *Science, 367*, 1260–1263.

47. Carvalho, T., Krammer, F., & Iwasaki, A. (2021). The first 12 months of COVID-19: A timeline of immunological insights. *Nature Reviews. Immunology, 21*, 245–256.
48. Lan, J., Ge, J., Yu, J., Shan, S., Zhou, H., Fan, S., et al. (2020). Structure of the SARS-CoV-2 spike receptor-binding domain bound to the ACE2 receptor. *Nature, 581*, 215–220.
49. Shang, J., Ye, G., Shi, K., Wan, Y., Luo, C., Aihara, H., et al. (2020). Structural basis of receptor recognition by SARS-CoV-2. *Nature, 581*, 221–224.
50. Baum, A., Fulton, B. O., Wloga, E., Copin, R., Pascal, K. E., Russo, V., et al. (2020). Antibody cocktail to SARS-CoV-2 spike protein prevents rapid mutational escape seen with individual antibodies. *Science, 369*, 1014–1018.
51. Schmidt, F., Weisblum, Y., Muecksch, F., Hoffmann, H.-H., Michailidis, E., Lorenzi, J. C. C., et al. (2020). Measuring SARS-CoV-2 neutralizing antibody activity using pseudotyped and chimeric virusesSARS-CoV-2 neutralizing antibody activity. *The Journal of Experimental Medicine, 217*, e20201181.
52. Johnson, B. A., Xie, X., Bailey, A. L., Kalveram, B., Lokugamage, K. G., Muruato, A., et al. (2021). Loss of furin cleavage site attenuates SARS-CoV-2 pathogenesis. *Nature, 591*, 293–299.
53. McCallum, M., De Marco, A., Lempp, F. A., Tortorici, M. A., Pinto, D., Walls, A. C., et al. (2021). N-terminal domain antigenic mapping reveals a site of vulnerability for SARS-CoV-2. *Cell, 184*, 2332–2347.e16.
54. Jiang, H., Zhang, H., Meng, Q., Xie, J., Li, Y., Chen, H., et al. (2020). SARS-CoV-2 Orf9b suppresses type I interferon responses by targeting TOM70. *Cellular & Molecular Immunology, 17*, 998–1000.
55. Xia, H., Cao, Z., Xie, X., Zhang, X., Chen, J. Y.-C., Wang, H., et al. (2020). Evasion of type I interferon by SARS-CoV-2. *Cell Reports, 33*, 108234.
56. Phillips, P. C. (2008). Epistasis—The essential role of gene interactions in the structure and evolution of genetic systems. *Nature Reviews. Genetics, 9*, 855–867.
57. Rochman, N. D., Faure, G., Wolf, Y. I., Freddolino, P. L., Zhang, F. & Koonin, E. V. (2021). Epistasis at the SARS-CoV-2 RBD Interface and the propitiously boring implications for vaccine escape. In *bioRxiv* 2021.08.30.458225.
58. Korber, B., Fischer, W. M., Gnanakaran, S., Yoon, H., Theiler, J., Abfalterer, W., et al. (2020). Tracking changes in SARS-CoV-2 spike: Evidence that D614G increases infectivity of the COVID-19 virus. *Cell, 182*, 812–827.e19.
59. Hodcroft, E. B., Domman, D. B., Snyder, D. J., Oguntuyo, K. Y., Van Diest, M., Densmore, K. H., et al. (2021). Emergence in late 2020 of multiple lineages of SARS-CoV-2 spike protein variants affecting amino acid position 677. In *medRxiv* 2021.02.12.21251658.
60. Konings, F., Perkins, M. D., Kuhn, J. H., Pallen, M. J., Alm, E. J., Archer, B. N., et al. (2021). SARS-CoV-2 variants of interest and concern naming scheme conducive for global discourse. *Nature Microbiology, 6*, 821–823.
61. Bedford, T., Hodcroft, E. B. & Neher, R. A. (2021). *Updated Nextstrain SARS-CoV-2 clade naming strategy*. https://nextstrain.org/blog/2021-01-06-updated-SARS-CoV-2-clade-naming
62. GISAID. (2021). *Clade and lineage nomenclature aids in genomic epidemiology studies of active hCoV-19 viruses*. GISAID.
63. Rambaut, A., Holmes, E. C., O'Toole, Á., Hill, V., McCrone, J. T., Ruis, C., et al. (2020). A dynamic nomenclature proposal for SARS-CoV-2 lineages to assist genomic epidemiology. *Nature Microbiology, 5*, 1403–1407.
64. WHO. (2021). *Tracking SARS-CoV-2 variants*. WHO.
65. Rambout, A., Loman, N., Pybus, O., Barclay, W., Barrett, J., Carabelli, A., et al. (2020). *Preliminary genomic characterisation of an emergent SARS-CoV-2 lineage in the UK defined by a novel*. https://virological.org/t/preliminary-genomic-characterisation-of-an-emergent-sars-cov-2-lineage-in-the-uk-defined-by-a-novel-set-of-spike-mutations/563
66. Chand, M., Hopkins, S., Achison, C., Anderson, C., Allen, H., Blomquist, P., et al. (2020). Investigation of novel SARS-CoV-2 variant: Variant of concern 202012/01. Public Health England Technical Briefing 2. https://assets.publishing.service.gov.uk/government/

uploads/system/uploads/attachment_data/file/959361/Technical_Briefing_VOC202012-2_Briefing_2.pdf

67. Kraemer, M. U. G., Hill, V., Ruis, C., Dellicour, S., Bajaj, S., McCrone, J. T., et al. (2021). Spatiotemporal invasion dynamics of SARS-CoV-2 lineage B.1.1.7 emergence. *Science, 373*, 889–895.
68. Alpert, T., Brito, A. F., Lasek-Nesselquist, E., Rothman, J., Valesano, A. L., MacKay, M. J., et al. (2021). Early introductions and transmission of SARS-CoV-2 variant B.1.1.7 in the United States. *Cell, 184*, 2595–2604.e13.
69. O'Toole, Á., Hill, V., Pybus, O. G., Watts, A., Bogoch, I. I., Khan, K., et al. (2021). *Tracking the international spread of SARS-CoV-2 lineages B.1.1.7 and B.1.351/501Y-V2 with grinch*. Wellcome Open Research.
70. Davies, N. G., Abbott, S., Barnard, R. C., Jarvis, C. I., Kucharski, A. J., Munday, J. D., et al. (2021a). Estimated transmissibility and impact of SARS-CoV-2 lineage B.1.1.7 in England. *Science, 372*, eabg3055.
71. Leung, K., Shum, M. H., Leung, G. M., Lam, T. T., & Wu, J. T. (2021). Early transmissibility assessment of the N501Y mutant strains of SARS-CoV-2 in the United Kingdom, October to November 2020. *Eurosurveillance, 26*, 2002106.
72. Volz, E., Mishra, S., Chand, M., Barrett, J. C., Johnson, R., Geidelberg, L., et al. (2021). Assessing transmissibility of SARS-CoV-2 lineage B.1.1.7 in England. *Nature, 593*, 266–269.
73. Teruel, N., Mailhot, O., & Najmanovich, R. J. (2021). Modelling conformational state dynamics and its role on infection for SARS-CoV-2 spike protein variants. *PLoS Computational Biology, 17*, e1009286.
74. Jones, T. C., Biele, G., Mühlemann, B., Veith, T., Schneider, J., Beheim-Schwarzbach, J., et al. (2021). Estimating infectiousness throughout SARS-CoV-2 infection course. *Science, 373*, eabi5273.
75. Kidd, M., Richter, A., Best, A., Cumley, N., Mirza, J., Percival, B., et al. (2021). S-variant SARS-CoV-2 lineage B1.1.7 is associated with significantly higher viral load in samples tested by TaqPath polymerase chain reaction. *The Journal of Infectious Diseases, 223*, 1666–1670.
76. Wargo, A. R., & Kurath, G. (2012). Viral fitness: Definitions, measurement, and current insights. *Current Opinion in Virology, 2*, 538–545.
77. Challen, R., Brooks-Pollock, E., Read, J. M., Dyson, L., Tsaneva-Atanasova, K., & Danon, L. (2021a). Risk of mortality in patients infected with SARS-CoV-2 variant of concern 202012/1: Matched cohort study. *British Medical Journal, 372*, n579.
78. Davies, N. G., Jarvis, C. I., Edmunds, W. J., Jewell, N. P., Diaz-Ordaz, K., & Keogh, R. H. (2021b). Increased mortality in community-tested cases of SARS-CoV-2 lineage B.1.1.7. *Nature, 593*, 270–274.
79. Grint, D. J., Wing, K., Williamson, E., McDonald, H. I., Bhaskaran, K., Evans, D., et al. (2021). Case fatality risk of the SARS-CoV-2 variant of concern B.1.1.7 in England, 16 November to 5 February. *Eurosurveillance, 26*, 2100256.
80. Graham, M. S., Sudre, C. H., May, A., Antonelli, M., Murray, B., Varsavsky, T., et al. (2021). Changes in symptomatology, reinfection, and transmissibility associated with the SARS-CoV-2 variant B.1.1.7: An ecological study. *The Lancet Public Health, 6*, e335–e345.
81. Abu-Raddad, L. J., Chemaitelly, H., & Butt, A. A. (2021). Effectiveness of the BNT162b2 Covid-19 vaccine against the B.1.1.7 and B.1.351 variants. *The New England Journal of Medicine, 385*, 187–189.
82. Emary, K. R. W., Golubchik, T., Aley, P. K., Ariani, C. V., Angus, B., Bibi, S., et al. (2021). Efficacy of ChAdOx1 nCoV-19 (AZD1222) vaccine against SARS-CoV-2 variant of concern 202012/01 (B.1.1.7): An exploratory analysis of a randomised controlled trial. *The Lancet, 397*, 1351–1362.
83. Heath, P. T., Galiza, E. P., Baxter, D. N., Boffito, M., Browne, D., Burns, F., et al. (2021). Safety and efficacy of NVX-CoV2373 Covid-19 vaccine. *The New England Journal of Medicine, 385*, 1172–1183.

84. Tegally, H., Wilkinson, E., Giovanetti, M., Iranzadeh, A., Fonseca, V., Giandhari, J., et al. (2021). Detection of a SARS-CoV-2 variant of concern in South Africa. *Nature, 592*, 438–443.
85. Faria, N. R., Mellan, T. A., Whittaker, C., Claro, I. M., Candido, D., Mishra, S., et al. (2021). Genomics and epidemiology of the P.1 SARS-CoV-2 lineage in Manaus, Brazil. *Science, 372*, 815–821.
86. Pearson, C. A., Russell, T. W., Davies, N. G., Kucharski, A. J., CMMID COVID-19 Working Group, Edmunds, W. J., et al. (2021). *Estimates of severity and transmissibility of novel SARS-CoV-2 variant 501Y.V2 in South Africa*. UpToDate.
87. Cele, S., Gazy, I., Jackson, L., Hwa, S.-H., Tegally, H., Lustig, G., et al. (2021). Escape of SARS-CoV-2 501Y.V2 from neutralization by convalescent plasma. *Nature, 593*, 142–146.
88. Wibmer, C. K., Ayres, F., Hermanus, T., Madzivhandila, M., Kgagudi, P., Oosthuysen, B., et al. (2021). SARS-CoV-2 501Y.V2 escapes neutralization by south African COVID-19 donor plasma. *Nature Medicine, 27*, 622–625.
89. Jassat, W., Mudara, C., Ozougwu, L., Tempia, S., Blumberg, L., Davies, M.-A., et al. (2021). Difference in mortality among individuals admitted to hospital with COVID-19 during the first and second waves in South Africa: A cohort study. *The Lancet Global Health, 9*, e1216–e1225.
90. Challen, R., Dyson, L., Overton, C. E., Guzman-Rincon, L. M., Hill, E. M., Stage, H. B., et al. (2021b). Early epidemiological signatures of novel SARS-CoV-2 variants: Establishme.06.05.21258365.
91. Riley, S., Wang, H., Eales, O., Haw, D., Walters, C. E., Ainslie, K. E. C., et al. (2021). REACT-1 round 12 report: Resurgence of SARS-CoV-2 infections in England associated with increased frequency of the Delta variant. In *MedRxiv* 2021.06.17.21259103.
92. Bolze, A., Cirulli, E. T., Luo, S., White, S., Wyman, D., Rossi, A. D., et al. (2021). SARS-CoV-2 variant Delta rapidly displaced variant alpha in the United States and led to higher viral loads. In *MedRxiv* 2021.06.20.21259195.
93. Grant, R., Charmet, T., Schaeffer, L., Galmiche, S., Madec, Y., Platen, C. V., et al. (2021). Impact of SARS-CoV-2 Delta variant on incubation, transmission settings and vaccine effectiveness: Results from a nationwide case-control study in France. *Lancet Regional Health—Europe, 13*, 100278.
94. Li, B., Deng, A., Li, K., Hu, Y., Li, Z., Xiong, Q., et al. (2021). *Viral infection and transmission in a large well-traced outbreak caused by the Delta SARS-CoV-2 variant—SARS-CoV-2 coronavirus/nCoV-2019 genomic epidemiology*. Virological.
95. Ong, S. W. X., Chiew, C. J., Ang, L. W., Mak, T.-M., Cui, L., Toh, M. P. H., et al. (2021). *Clinical and virological features of SARS-CoV-2 variants of concern: A retrospective cohort study comparing B.1.1.7 (alpha), B.1.315 (Beta), and B.1.617.2 (Delta)*. Social Science Research Network.
96. Planas, D., Veyer, D., Baidaliuk, A., Staropoli, I., Guivel-Benhassine, F., Rajah, M. M., et al. (2021). Reduced sensitivity of SARS-CoV-2 variant Delta to antibody neutralization. *Nature, 596*, 276–280.
97. TAG-VE. (2021). *Classification of Omicron (B.1.1.529): SARS-CoV-2 Variant of Concern*.
98. Shah, A. S. V., Gribben, C., Bishop, J., Hanlon, P., Caldwell, D., Wood, R., et al. (2021). Effect of vaccination on transmission of SARS-CoV-2. *The New England Journal of Medicine, 385*, 1718–1720.
99. Polack, F. P., Thomas, S. J., Kitchin, N., Absalon, J., Gurtman, A., Lockhart, S., et al. (2020). Safety and efficacy of the BNT162b2 mRNA Covid-19 vaccine. *The New England Journal of Medicine, 383*, 2603–2615.
100. Chung, H., He, S., Nasreen, S., Sundaram, M. E., Buchan, S. A., Wilson, S. E., et al. (2021). Effectiveness of BNT162b2 and mRNA-1273 covid-19 vaccines against symptomatic SARS-CoV-2 infection and severe covid-19 outcomes in Ontario, Canada: Test negative design study. *BMJ, 374*, n1943.

101. Sadoff, J., Gray, G., Vandebosch, A., Cárdenas, V., Shukarev, G., Grinsztejn, B., et al. (2021). Safety and efficacy of single-dose Ad26.COV2.S vaccine against Covid-19. *The New England Journal of Medicine, 384*, 2187–2201.
102. Sheikh, A., McMenamin, J., Taylor, B., & Robertson, C. (2021). SARS-CoV-2 Delta VOC in Scotland: Demographics, risk of hospital admission, and vaccine effectiveness. *The Lancet, 397*, 2461–2462.
103. Tang, P., Hasan, M. R., Chemaitelly, H., Yassine, H. M., Benslimane, F. M., Al Khatib, H. A., et al. (2021). BNT162b2 and mRNA-1273 COVID-19 vaccine effectiveness against the SARS-CoV-2 Delta variant in Qatar. *Nature Medicine*, 1–8.
104. Liu, W.-D., Chang, S.-Y., Wang, J.-T., Tsai, M.-J., Hung, C.-C., Hsu, C.-L., et al. (2020). Prolonged virus shedding even after seroconversion in a patient with COVID-19. *The Journal of Infection, 81*, 318–356.
105. Wölfel, R., Corman, V. M., Guggemos, W., Seilmaier, M., Zange, S., Müller, M. A., et al. (2020). Virological assessment of hospitalized patients with COVID-2019. *Nature, 581*, 465–469.
106. Avanzato, V. A., Matson, M. J., Seifert, S. N., Pryce, R., Williamson, B. N., Anzick, S. L., et al. (2020). Case study: Prolonged infectious SARS-CoV-2 shedding from an asymptomatic immunocompromised individual with cancer. *Cell, 183*, 1901–1912.e9.
107. Bazykin, G. A., Stanevich, O., Danilenko, D., Fadeev, A., Komissarova, K., Ivanova, A., et al. (2021). *Emergence of Y453F and Δ69-70HV mutations in a lymphoma patient with long-term COVID-19—SARS-CoV-2 coronavirus/nCoV-2019 genomic epidemiology*. Virological.
108. Choi, B., Choudhary, M. C., Regan, J., Sparks, J. A., Padera, R. F., Qiu, X., et al. (2020). Persistence and evolution of SARS-CoV-2 in an immunocompromised host. *The New England Journal of Medicine, 383*, 2291–2293. https://doi.org/10.1056/NEJMc2031364
109. Kemp, S. A., Collier, D. A., Datir, R. P., Ferreira, I. A. T. M., Gayed, S., Jahun, A., et al. (2021). SARS-CoV-2 evolution during treatment of chronic infection. *Nature, 592*, 277–282.
110. Borges, V., Isidro, J., Cunha, M., Cochicho, D., Martins, L., Banha, L., et al. (2021). Long-term evolution of SARS-CoV-2 in an immunocompromised patient with non-Hodgkin Lymphoma. *mSphere, 6*, e0024421.
111. Bosco-Lauth, A. M., Root, J. J., Porter, S. M., Walker, A. E., Guilbert, L., Hawvermale, D., et al. (2021). Peridomestic mammal susceptibility to severe acute respiratory syndrome coronavirus 2 infection. *Emerging Infectious Diseases, 27*, 2073–2080.
112. Fischhoff, I. R., Castellanos, A. A., Rodrigues, J. P. G. L. M., Varsani, A., & Han, B. A. (2021). Predicting the zoonotic capacity of mammals to transmit SARS-CoV-2. *Proceedings of the Royal Society B: Biological Sciences, 288*, 20211651.
113. WHO. (2020a). *SARS-CoV-2 mink-associated variant strain—Denmark*. WHO.
114. Bas, B., Munnink, O., Sikkema, R. S., Nieuwenhuijse, D. F., Molenaar, R. J., Munger, E., et al. (2021). Transmission of SARS-CoV-2 on mink farms between humans and mink and back to humans. *Science, 371*, 172–177.
115. Larsen, H. D., Fonager, J., Lomholt, F. K., Dalby, T., Benedetti, G., Kristensen, B., et al. (2021). Preliminary report of an outbreak of SARS-CoV-2 in mink and mink farmers associated with community spread, Denmark, June to November 2020. *Eurosurveillance, 26*, 2100009.
116. Hoffmann, M., Zhang, L., Krüger, N., Graichen, L., Kleine-Weber, H., Hofmann-Winkler, H., et al. (2021). SARS-CoV-2 mutations acquired in mink reduce antibody-mediated neutralization. *Cell Reports, 35*, 109017.
117. Koopmans, M. (2021). SARS-CoV-2 and the human-animal interface: Outbreaks on mink farms. *The Lancet Infectious Diseases, 21*, 18–19.
118. Chandler, J. C., Bevins, S. N., Ellis, J. W., Linder, T. J., Tell, R. M., Jenkins-Moore, M., et al. (2021). SARS-CoV-2 exposure in wild white-tailed deer (Odocoileus virginianus). *Proceedings of the National Academy of Sciences, 118*, e2114828118.
119. Kuchipudi, S. V., Surendran-Nair, M., Ruden, R. M., Yon, M., Nissly, R. H., Nelli, R. K., et al. (2021). Multiple spillovers and onward transmission of SARS-CoV-2 in free-living and captive white-tailed deer. *Proceedings of the National Academy of Sciences of the United States of America, 119*, e2121644119.

120. Egeren, D. V., Novokhodko, A., Stoddard, M., Tran, U., Zetter, B., Rogers, M., et al. (2021). Risk of rapid evolutionary escape from biomedical interventions targeting SARS-CoV-2 spike protein. *PLoS One, 16*, e0250780.
121. Rella, S. A., Kulikova, Y. A., Dermitzakis, E. T., & Kondrashov, F. A. (2021). Rates of SARS-CoV-2 transmission and vaccination impact the fate of vaccine-resistant strains. *Scientific Reports, 11*, 15729.
122. Starr, T. N., Greaney, A. J., Addetia, A., Hannon, W. W., Choudhary, M. C., Dingens, A. S., et al. (2021). Prospective mapping of viral mutations that escape antibodies used to treat COVID-19. *Science, 371*, 850–854.
123. Hadfield, J., Megill, C., Bell, S. M., Huddleston, J., Potter, B., Callender, C., Sagulenko, P., Bedford, T., Neher, R. A., (2018).*Nextstrain: real-time tracking of pathogen evolution, Bioinformatics, 34*, 4121–4123, https://doi.org/10.1093/bioinformatics/bty407.

Chapter 6
Computational Modeling of Aerosol Transmission of COVID-19

Goodarz Ahmadi

Abstract In this chapter, recent advances in computational modeling of respiratory droplets in indoor environments in connection with the aerosol transmission of COVID-19 are presented. In addition, the available literature on respiratory droplet emission by speaking, coughing, and sneezing are reviewed. The computational modeling approach for simulation of airflows and droplet and particle motions in a ventilated environment is described in layman's terms. Examples of dispersion and transport of respiratory droplets emitted due to coughing and speaking in a classroom, in a subway train compartment, and in small and large ventilated office spaces are presented. Finally, the filtration effects of wearing masks and their influence on reducing our chances of exposure are described.

6.1 Introduction

On March 11, 2020, the World Health Organization (WHO) declared the global outbreak of severe acute respiratory syndrome coronavirus 2 (SARS-CoV-2), the pathogen that incites infectious pneumonia COVID-19, a pandemic. Since then, there has been a severe worldwide economic disruption, as well as numerous loss of life. According to WHO, as of November 25, 2021, there were 258.8 million confirmed infection cases and 5.2 million deaths by the COVID-19 disease worldwide [1]. The total number of infections reached 47.9 million in the US, with 774,000 deaths [2].

According to the Centers for Disease Control and Prevention [2], the primary transmission mode is the exposure to respiratory droplets emitted by an infected person during breathing, speaking, coughing, or sneezing. The other modes of transmission are deposition of virus-carrying respiratory droplets on mucous membranes in the mouth, nose, or eye, by direct splashes and sprays, or by touching with hands

G. Ahmadi (✉)
Department of Mechanical and Aerospace Engineering, Clarkson University, Potsdam, NY, USA
e-mail: gahmadi@clarkson.edu

D. Barry, H. Kanematsu (eds.), *Studies to Combat COVID-19 using Science and Engineering*, https://doi.org/10.1007/978-981-19-1356-3_6

virus-containing respiratory fluids deposited on surfaces (fomites). The transmission of airborne diseases has been studied by numerous researchers [3–6]. Airborne transmission of SARS-CoV-2 viruses was studied by Buonanno et al. [7, 8], Asadi et al. [9], Morawska and Cao [10], Allen and Marr [11], Zhang et al. [12], Ahmed et al. [13], and Bazant and Bush [14], among others.

Respiratory droplets have various size distributions and are emitted from the mouth at different speeds during breathing, speaking, coughing, and sneezing [10, 15–23]. When a respiratory droplet expels from the mouth with an initial velocity, it is subject to the hydrodynamic and gravitational forces, as well as evaporation [3, 24–27]. As a result, large droplets settle quickly and fall to the ground, while the smaller droplets evaporate. Wells [28, 29] was the first to study the fate of an evaporating droplet under gravity. He concluded that a droplet would evaporate or fall to the floor within (a distance of) 2 m (6 ft). His estimate is the basis for the public health agencies' (WHO, CDC) guidelines for social distancing. However, this estimate does account for the role of the ventilation systems and the turbulence dispersion. In addition, the respiratory droplets evaporate to nuclei containing viruses and other nonvolatile compounds. However, the resulting small nuclei that contain all the viruses in the original droplet are aerosolized and remain suspended in the air for a long time. Xie et al. [23] reported recent estimates for safe social distancing.

Studies of transport, dispersion, and deposition of small particles in fluid flows have a long history due to their many important industrial, environmental, and biological applications. Reviews of the earlier experimental and modeling studies on aerosols and particle transport and deposition processes were provided by Levich [30], Fuchs [31], Mercer [32], Twomey [33], Hinds [34], Spurny [35], Seinfeld [36], Vincent [37], and Tu et al. [38], among others.

Computer simulation of transport and dispersion of small, suspended particles in turbulent flows was reported by Ahmadi and Goldschmidt [39], Riley and Patterson [40], Reeks [41], Reeks and Mckee [42], Rizk and Elghobashi [43], Maxey [44], Wang and Stock [45, 46], Crowe [47], and Li and Ahmadi [48, 49]. Li and Ahmadi [50] generalized the method to cover particle deposition rates on rough surfaces. He and Ahmadi [51] reported the results of their computer simulations of particle deposition with thermophoresis and electrophoresis.

Friedlander and Johnstone [52] developed a model for particle deposition in turbulent flows. Davies [53], Sehmel [54], Wood [55], and Fernandez de la Mora and Friedlander [56] extended their approach. Cleaver and Yates [57] proposed an inertial deposition mechanism during the "turbulent burst." Fichman et al. [58] and Fan and Ahmadi [59–61] reported the extension of this approach.

Wood [55] and Papavergos and Hedley [62] reported several collections of available data on wall deposition rates. They also reviewed the available methods for evaluating the deposition velocity in turbulent duct flows. Finally, Kvasnak and Ahmadi [63] and Kvasnak et al. [64] reported their experimental data for the deposition rate of glass beads and various dust components in a horizontal duct flow.

Transport and deposition of particles in the human respiratory tract were studied by many researchers [34, 38]. For example, Inthavong et al. [65], Li et al. [66], Naseri et al. [67], and Azhdari et al. [68] studied the effect of the human thermal plume on the aspiration efficiency of microparticles. Furthermore, Bahmanzadeh et al. [69] reported microparticle deposition in the human nasal cavity under cyclic inspiratory flows. In addition, Ghahramani et al. [70] investigated turbulent airflow and microparticle deposition in a realistic human upper airway model using LES. Finally, Tavakol et al. [71] analyzed ellipsoidal fibers' deposition in a human nasal cavity for laminar and turbulent flows.

In this chapter, recent advances in computational modeling of respiratory droplets in indoor environments in connection with the aerosol transmission of COVID-19 are presented. In addition, the available literature on respiratory droplet emission by speaking, coughing, and sneezing are reviewed. The computational modeling approach for simulation of airflows and droplet and particle motions in a ventilated environment is described in layman's terms. Examples of dispersion and transport of respiratory droplets emitted due to coughing and speaking in a classroom, in a subway train compartment, and in small and large ventilated office spaces are presented. Finally, the filtration effects of wearing masks and their influence on reducing exposure chances are described.

6.2 Computational Modeling of Airflow Dynamics and Droplet Transport and Dispersion

There have been significant advances in computational fluid dynamics (CFD), with commercial software (such as [72]) becoming available in the last two decades. The CFD model solves the Navier-Stokes equations for laminar airflows and the Reynolds-averaged Navier-Stokes (RANS) and large eddy simulation (LES) for turbulent airflows. The RANS model, which is computationally efficient, requires modeling the turbulence effects. There are several two-equation models such as the k-ε and the k-ω models, and their various variants have been used extensively for numerous practical applications. The Reynolds stress transport model (RSTM) solves for the components of the turbulence stress tensor and involves seven additional equations. The RSTM has been used on many occasions when the effect of anisotropy of turbulence is significant [51, 73–76]. The LES model accounts for the time variations of turbulence larger than the grid size. However, the subgrade scale effect of turbulence needs to be modeled [77–80]. The LES model is computationally more expensive than RANS by an order of magnitude. Direct numerical simulation (DNS) is the most accurate approach for simulating turbulent flows. This method solves the Navier-Stokes equations with no modeling [81–85]. The DNS resolves all the scales of turbulence down to the Kolmogorov scale (the smallest scale of turbulence). Therefore, it requires a highly refined grid that makes

it computationally costly for practical applications. However, it is an important and powerful research tool for simplified configurations.

Thatcher et al. [86], Chen et al. [87], Inthavong et al. [88], Zhao and Guan [89], Gao Niu [90], and Ahmadzadeh et al. [91], among others, studied particle transport, dispersion, and deposition in indoor environments. They reported the influences of airflow speed, the ventilation system, particle size, and surface conditions on the transport and deposition of particles in buildings. Liu et al. [92] estimated the COVID-19 infection risk for different ventilation rates and emission velocity of droplets in a restaurant. Abuhegazy et al. [93] and Mirzaie et al. [94] reported the dispersion and transport of cough droplets in a classroom generated by one infected person. They assessed the effects of droplet size, distance from the source, ventilation flow rates, glass barriers on droplet concentration, and deposition on different surfaces in the classroom. Satheesan et al. [95] and Borro et al. [96] studied the ventilation effect on the dispersion of infected droplets in hospital rooms. Finally, Cui et al. [97] simulated the transport of virus-laden respiratory droplets in a supermarket. In these studies, the computational fluid dynamics (CFD) coupled with the Lagrangian particle tracking were used to assess the fate of emitted respiratory droplets. These studies showed that the ventilation system with high air exchange rates dilutes the virus-infected droplet concentration and reduces the infection risk.

There is a wide range of Reynolds number conditions from transitional to fully turbulent flows in the airflows in indoor environments. Therefore, care should be given to selecting turbulence models for the RANS and the LES simulations. To quantify the dispersion of particles into the indoor environment, droplet size distributions representative of those found during speaking, coughing, and sneezing, as reported by Asadi et al. [15], Duguid [17], Bourouiba et al. [3], Memarzadeh [19], and Balachandar et al. [98], would be introduced into the airflow at the mouth of the emitter. Their subsequent motion would be tracked using a Lagrangian trajectory analysis and a diffusion model approach [76, 84, 99]. Fabian et al. [100] reported respiratory droplet concentrations of the order of 8500 particles/L, which is considered a dilute suspension.

The presented review of the literature shows that CFD simulations could identify the fate of the respiratory droplets that are expelled into the air during the talking, coughing, and sneezing of an infected person and the time evolution of their concentration in indoor environments. The accurate modeling of the respiratory generated droplet transport could help mitigate the risks for human-to-human transmission of infectious respiratory diseases.

Figure 6.1 compares the nondimensional deposition velocities of 10 nm to 30 μm particles with $0.0001 < \tau^+ < 200$ in ducts as predicted by different models with the experimental data collected by Papavergos and Hedley [62]. Here, u_d^+ is the nondimensional deposition velocity, and τ^+ is the nondimensional particle relaxation time. In this figure, the earlier simulation results [48, 51, 76], the DNS results [82, 101–103], and the predictions of the empirical models [55, 59, 104] are shown. Figure 6.1 indicates that the conventional CRW and the non-normalized CRW models significantly overestimate the deposition velocities for particles with nondimensional relaxation time less than 10. Earlier, Tian and Ahmadi [76] showed

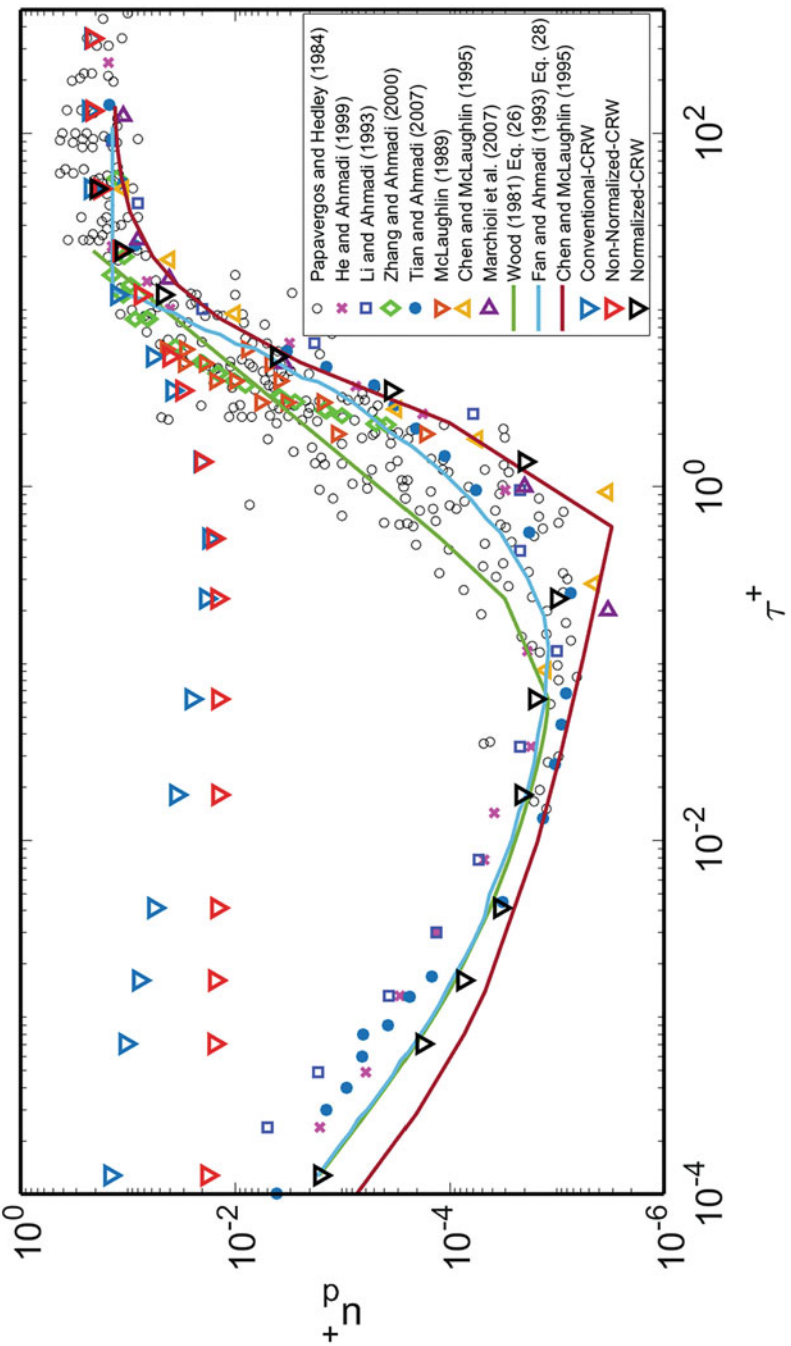

Fig. 6.1 Comparison of the nondimensional deposition velocities of different size particles as predicted by various models with the experimental data and empirical equations

that the conventional DRW model also overpredicts the deposition velocity by orders of magnitude. Mofakham and Ahmadi [105–107] showed that using the normalized CRW model with the proper drift correction improves the particle deposition velocity predictions significantly. Figure 6.1 shows that the predictions of the normalized CRW model are in good agreement with the experimental data, the DNS data, and the empirical models.

Earlier, Tian and Ahmadi [76] pointed out the need to include the accurate near-wall quadratic variation of RMS normal fluctuations to evaluate the particle deposition velocity. Mofakham and Ahmadi [106, 107] simulated the cases with and without quadratic variation of the normal RMS fluid velocities. They reported that ignoring the normal RMS fluid velocity fluctuations' near-wall corrections leads to significant error in the deposition velocities.

6.3 Respiratory Droplet Size Distributions

This section reviews the properties of droplets emitted during speaking, coughing, and sneezing. Sneezing generates several hundred thousand to a million respiratory droplets with several thousand larger saliva droplets, while a single cough generates about 3000–5000 droplets [3, 4, 17, 21, 23, 108]. While the number of droplets emitting during talking is smaller than coughing, speaking for about 5 min can generate about 3000 droplets, the same number of droplets as a single cough. The respiratory droplet size distributions depend on the exhaled air velocity, the viscosity of the salvia or mucosa, and the droplets' formation location.

Duguid [17] measured respiratory droplet size distributions emitted during speaking and coughing. More recently, Asadi et al. [15] performed a series of experimental studies on the droplet size distribution during soft, intermediate, and loud speaking. Their results are reproduced in Fig. 6.2. It is seen that the droplet sizes are smaller than 20 μm, with the distribution peak at about 0.7–1 μm for soft as well as loud speaking. However, as the loudness increase, the number of expelled respiratory droplets increases.

The data of Duguid [17] for the size distribution of droplets' nuclei emitted during a typical cough is reproduced in Fig. 6.3. This figure shows that the cough-generated droplets have a wide range of sizes from 1 to 100 μm. However, most cough droplets' nuclei are in the range of 8–16 μm, with the peak at about 12 μm. In addition, many respiratory droplets (5000) are generated during a cough. While the duration and the flow rate of cough vary, Yang et al. [109] and Feng et al. [110] reported a duration of 0.5 s with a peak flow rate of about 4 L/s at about 0.1 s after the initiation of the cough, as shown in Fig. 6.4. This figure shows that the cough flow rate increases sharply for about 0.1 s to its peak value and then decreases gradually for the rest of the cough duration.

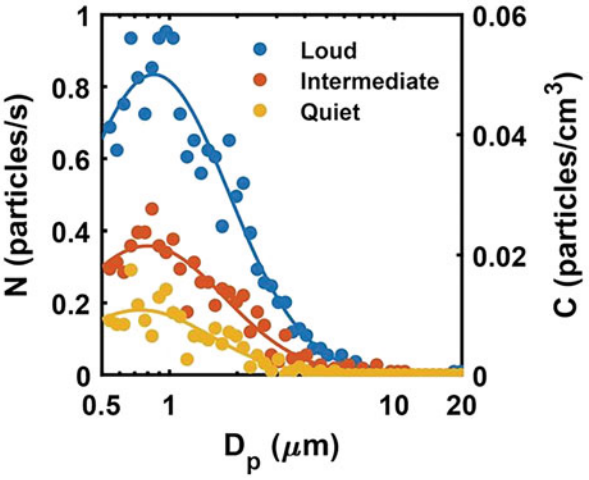

Fig. 6.2 Respiratory droplet size distribution during speaking as reported by Asadi et al. [15]

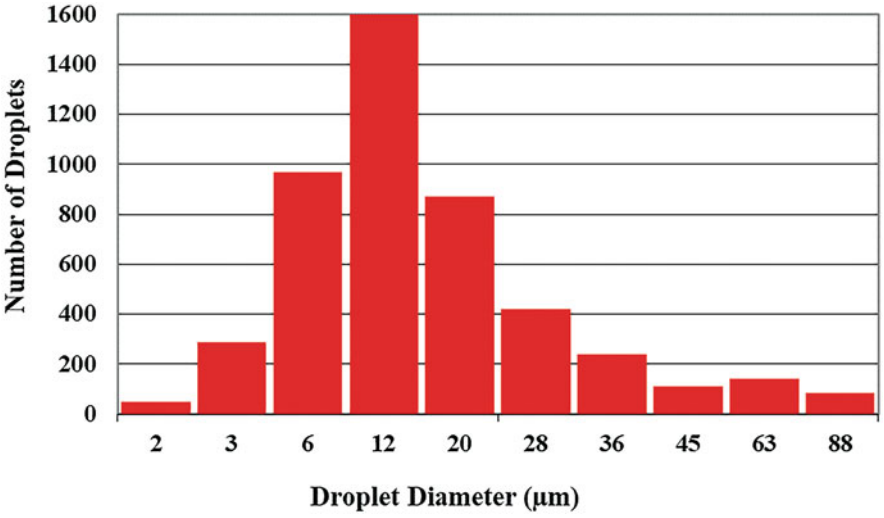

Fig. 6.3 Respiratory droplet nuclei size distribution during coughing based on the data of Duguid [17]

Han et al. [18] reported the experimental data for the size distribution of droplets emitted during sneezing. They also provided the unimodal and bimodal Gaussian fits to their experimental data. Accordingly, the sneeze generates large droplets in the range of 50 μm to more than 1 mm. Their unimodal distribution shows a dominant peak at about 500–700 μm. Their bimodal distribution shows a secondary peak at 80–100 μm.

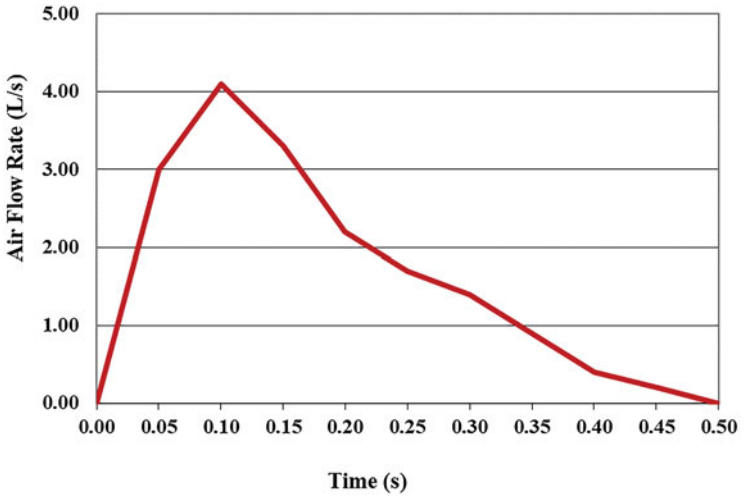

Fig. 6.4 Time variation of the volumetric flow rate of a cough. (Adapted from [109, 110])

6.4 Simplified Airborne Transmission Models

Wells [28] was the first to develop a model for airborne transmission of respiratory diseases. He analyzed the evaporation of droplets as they fall under gravity. He evaluated the time that a droplet falls (a distance of) 2 m to the ground and the time for the droplet to evaporate completely. Wells had results that were reported by Xie et al. [23]. Accordingly, water droplets smaller than 160 μm would completely evaporate before settling on the ground. On the other hand, droplets larger than 160 μm would rapidly fall to the ground within a short distance from the emitter. According to Wells [28], the maximum horizontal distance that a cough droplet travels before either falling to the ground or completely evaporating is about 2 m (6 ft). This estimate has been the basis for social distancing during the COVID pandemic. However, the evaporating droplets reduce to small nuclei containing viruses and nonvolatile compounds that remain suspended in the air and could be carried long distances by the ventilation airflow [23].

Xie et al. [23] have re-examined Wells' approach using a circular jet model with diameter d_o. They performed a series of analyses for a range of velocities $U_o = 1$, 5, 10, 20, and 50 m/s. They also included the effect of evaporation and accounted for the RH variation, exhalation temperature T_{p0}, and room temperature T_∞. The group evaluated the time duration for the respiratory droplet to evaporate or fall to the ground for different mouth airflow velocities for $T_{p0} = 33$ °C, $T_\infty = 20$ °C, and RH = 50%. For a mouth opening with a diameter of $d_o = 0.04$ m, they estimated the maximum horizontal distances the droplet would travel. As expected, they found

that the time for complete evaporation and/or the time to fall to the ground is a function of the initial droplet size and exhalation airflow velocity. Their simulation results show that the maximum horizontal penetration distance for a droplet expelled with a velocity of 1 m/s (speaking) is about 0.4 m and occurs for 25 μm droplets. For coughing with velocities of 5–10 m/s, the maximum horizontal distances are about 1.2–2.2 m for droplets with initial diameters of 30–35 μm. For sneezing with expelling velocities of 20–50 m/s, the horizontal penetration distances are much larger and reach about 3.5–6.5 m.

6.5 Respiratory Air Flows

The human tracheobronchial tree comprises 23 generations from the trachea (generation 0) to the terminal bronchioles (generation 23). No gas exchange occurs from generation 0 (trachea) to generation 15, and the airway behaves as conducting tubes. From generation 16, the terminal bronchioles bifurcate into respiratory bronchioles, where the primary gas exchange occurs. The respiratory airway model shown in Fig. 6.5 shows the nasal and mouth cavities down to distal bronchial airways in generation 15, as reported by Tu et al. [111] and Dong et al. [112]. Dong et al. [113] used 2.9 million polyhedral elements to simulate the airflow velocity in the

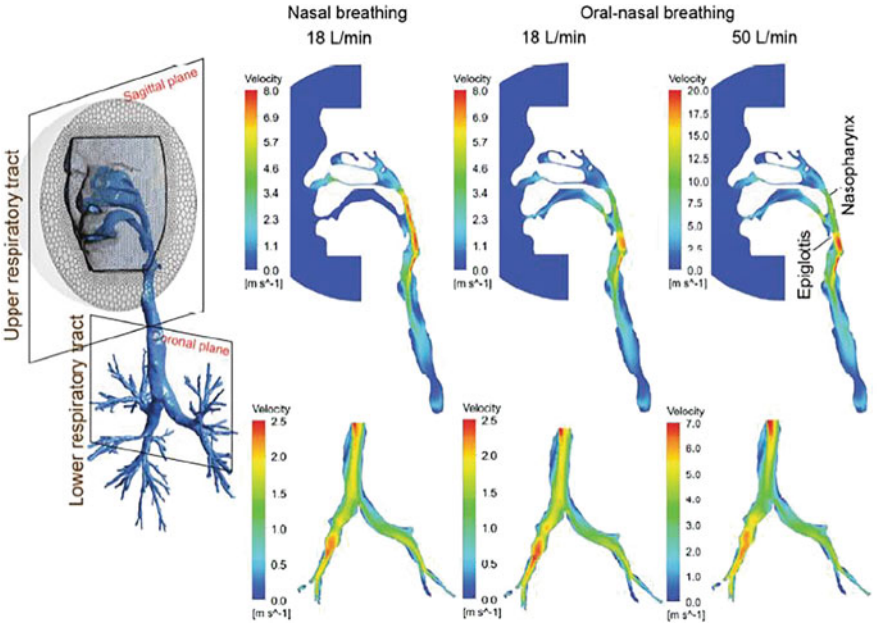

Fig. 6.5 Variations of velocity magnitude contours in the respiratory tract for different inhalation scenarios

entire airway for different breathing rates for the mouth and nasal breathing. The simulation was performed using the Ansys-Fluent Code. Sample airflow velocity contours under different inhalation modes, as reported by Dong et al. [113], are shown in Fig. 6.5. Different contour plot scaling was used for the upper and lower respiratory tracts for better visualization. It is seen that airflow accelerates as the airway narrows. For the nasal breathing of 18 L/min, a high-speed jet flow of 8 m/s forms along the nasopharynx and larynx. The airflow velocity reduces in the trachea due to the larger cross section.

The airflow enters from the nostril for nasal breathing and oral and nasal openings for the oral-nasal breathing of 18 L/min. The peak airflow velocity for both cases is 8.0 m/s near the epiglottis. However, for oral-nasal breathing, the airflow velocity reduces to about 4 m/s in the nasopharynx region due to the lower airflow rate through the nasal passage. The airflow velocity contours in the rest of the airways are similar to those for the nasal inhalation case at 18 L/min. For the oral-nasal breathing of 50 L/min, Fig. 6.5 shows that the airflow velocity increases proportionally with a peak of 20.0 m/s near the epiglottis. The other flow features are quite similar, with increased velocity magnitude.

The airflow contours in the lower respiratory tracts, shown in the lower part of Fig. 6.5 for nasal and oral-nasal breathing, show roughly similar patterns except for the increased velocity for the breathing rate of 50 L/min. The peak velocities occur at the trachea entrance and the right main bronchus.

6.6 Cough Droplet Distribution in a Classroom

Mirzaie et al. [94] recently reported a series of simulations on airflow and respiratory droplets emitted by an infected person's coughing in a ventilated classroom. The airflow conditions in the room were simulated using a 3D CFD model for different ventilation airflow rates. The k-ε model was used to account for the airflow turbulence in the classroom. The Lagrangian particle trajectory analysis was used to track the droplet motions. In addition, they studied the effect of installing transparent partitions around the seats in the classroom. Their simulation results showed that an increase in the ventilation air velocity reduces the cough droplet residence time in the classroom and, therefore, the chance for infection. In addition, the closest seats to the infected person are exposed to the highest droplet concentration in the absence of partitions. In addition, they showed that using the seat partitions could reduce the exposure to an extent.

Sample time variations of predicted distributions of cough droplets with different diameters emitted from the infected person's mouth in the front of a classroom are extracted from the study of Mirzaie et al. [94] that are shown in Fig. 6.6. These results are for the case with the ventilation airflow velocity of 5 m/s for a classroom without partitions. This figure shows the distributions of emitted particles at different times (0.5, 1, 5, 10, 20, and 50 s). Figure 6.6 shows that the emitted cough droplets stay near the face of the emitter for the time duration of 0.5–1 s. Then the

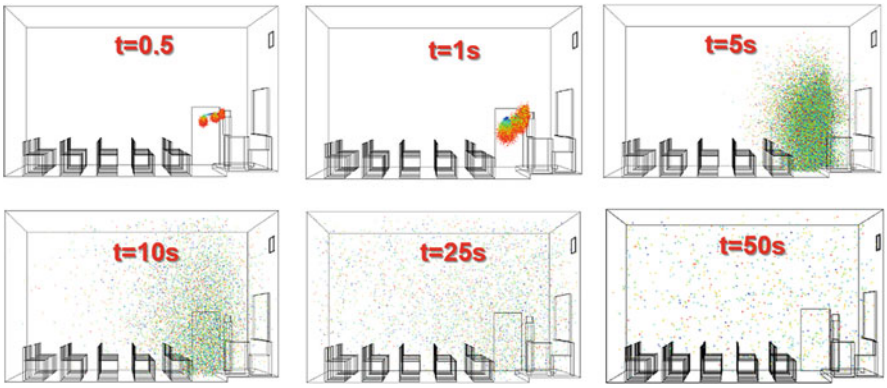

Fig. 6.6 Time variations of cough droplet distribution in a classroom [94]

ventilation airflow and flow turbulence disperse the droplets more. However, up to about 5 s, the cough droplets seem to stay in the front region of the classroom. At this point, the front row seats are exposed to the infected cough droplets. In contrast, the droplet concentrations near the back seats are negligible. However, the emitted droplets are dispersed throughout the classroom at about 10–25 s after the cough. At 25–50 s after the cough, all seats are exposed to the infected droplets but at lower concentrations. The concentration of the droplets decreases with time and approaches to a negligible level after about 100 s (not shown in Fig. 6.6), as most droplets leave the room through the ventilation outlet or deposit on various surfaces.

Mirzaie et al. [94] also reported their simulation results for the ventilation airflow speeds of 3 and 7 m/s. For the ventilation speed of 3 m/s, they found a uniform droplet concentration in the classroom at $t = 100$. However, for the ventilation speed of 7 m/s, the particle concentration in the classroom becomes negligible 50 s after the cough. Their results showed that the higher air change rate effectively removes the virus-laden cough droplets from the classroom.

Mirzaie et al. [94] also studied the cough droplet distribution in the classroom with partitions. They showed that the presence of relatively tall partitions could reduce the change of exposure in the front row seat immediately after the cough. Overall, they found that the partitions could reduce the exposure to an extent.

6.7 Dispersion of Respiratory Droplets in a Small Ventilated Room During Speaking

Masoomi et al. [114] studied the airflow and the droplet transport and dispersion in a room with two mannequins sitting across a table using a CFD model. They used the Eulerian approach, including the k-ε turbulence model, for the airflow simulation. The Lagrangian particle tracking approach was used to analyze the

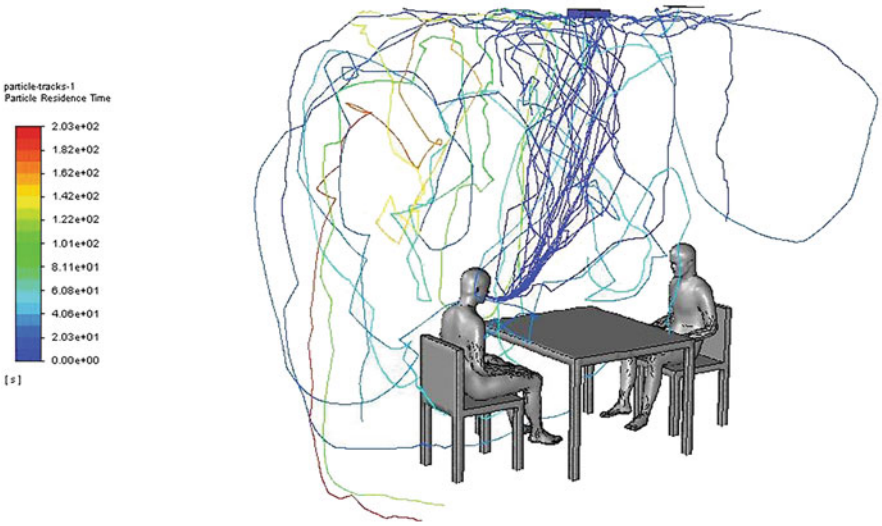

Fig. 6.7 Particle tracking in a room with a mixing ventilation system [114]

respiratory droplet trajectories omitted by one mannequin speaking. They include the evaporation of the droplets and the thermal plume effect due to the body temperature being higher than the room temperature. Attention was also given to the ventilation effects on the transport and dispersion of speaking droplets emitted in the room. Simulations were performed for both mixing and displacement ventilation systems. Their sample results for the respiratory droplet motions emitted by the mannequin on the left in a room with a mixing ventilation system are shown in Fig. 6.7. Their simulation results showed that the large particles are quickly deposited on various surfaces. However, the respiratory droplets of moderate sizes evaporate rapidly and reduce to small nuclei. The smaller droplets and small nuclei remained suspended in the room for a relatively long time. In addition, a significant fraction of small droplets is removed through the ventilation outlet. As expected, the concentration of droplets in the room is roughly uniform for the mixing ventilation system. Masoomi et al. [114] concluded that the displacement ventilation system removes a larger fraction of small droplets faster and decreases the chance for infection.

6.8 Dispersion of Cough Droplets in a Subway Train

Ahmadzadeh and Shams [115] and Hejazi et al. [116] studied the transport and dispersion of cough droplets in a subway train. A module of the train compartment was simulated with four mannequins seated across from each other at a table. Different ventilation systems were studied for different cough directions. They

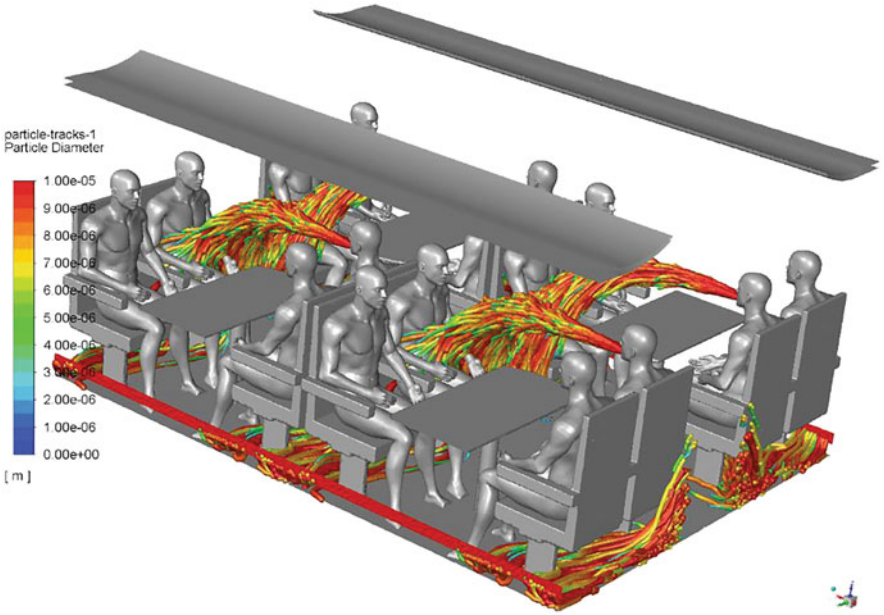

Fig. 6.8 Horizontal cough droplets' trajectories in a subway train [116]

showed that when a cough is directed horizontally toward the person across the table, the probability of exposure is much higher than when the cough is directed downward. Figure 6.8 shows sample cough droplet trajectories emitted horizontally in the subway train.

6.9 Airflow and Dispersion of Respiratory Droplets in a two-Person Office

Figure 6.9 shows the schematics of a two-person office with partitions. The room has a mixing ventilation system with a linear supply diffuser, a rectangular supply diffuser, and one rectangular outlet on the ceiling [99, 117].

It is assumed that the mannequin on the right in Fig. 6.9 is speaking and emitting respiratory droplets of different sizes. The airflow and droplet concentration in the room, particularly in the breathing zone of the receptor mannequin on the left, are studied. Figure 6.10 shows sample airflow velocity contours at a vertical plane crossing the two mannequins and another vertical plane across the inlet air supplies, as well as a horizontal one. Here, the air change rate per hour is ACH = 2.4, meaning the entire air on the room is changed 2.4 times an hour. In addition, the pick velocity magnitude is cut at 0.15 m/s so that the details of the airflow velocity can be more

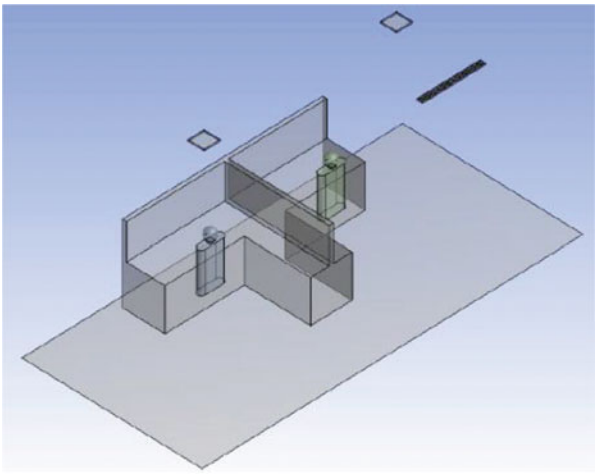

Fig. 6.9 Schematics of a two-person office geometry with partitions [99, 117]

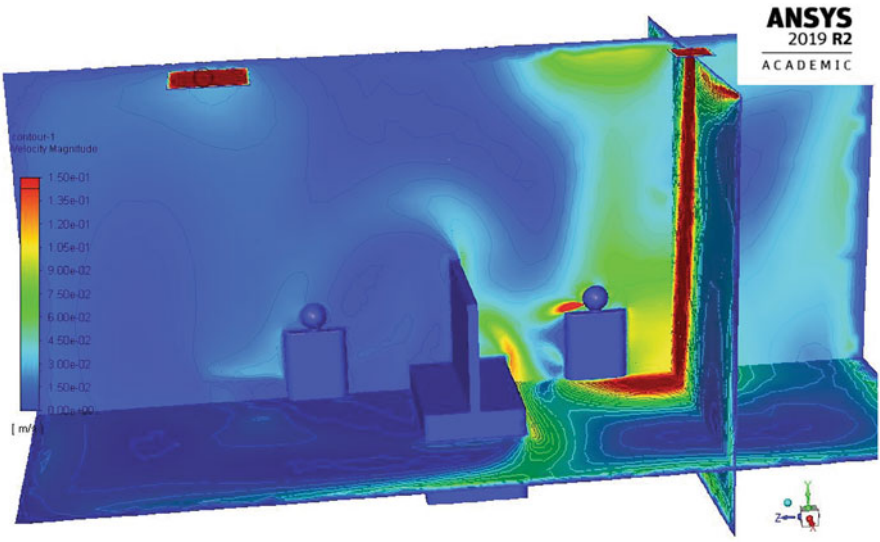

Fig. 6.10 Variations of velocity magnitude contours in the two-person office for ACH of 2.4 [99]

clearly seen. This figure shows the high-speed air jets from the ventilation supply registers on the right side of the room near the emitter mannequin. The airflow jet from the mouth of the emitter mannequin is also seen from this figure. This figure shows that the partition between the two mannequins diverts the airflow upward. Nevertheless, the airflow near the breathing zone of the receptor mannequin increases slightly.

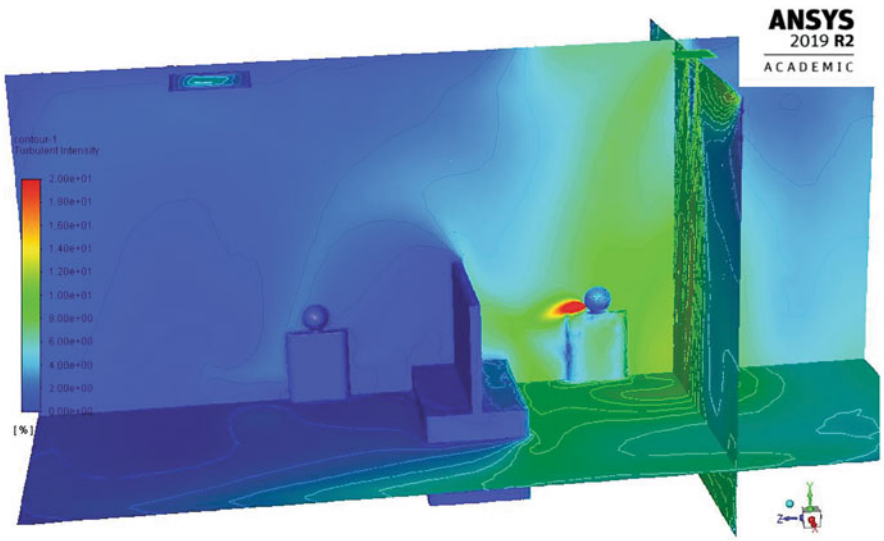

Fig. 6.11 Variations of turbulence intensity contours in the two-person office for ACH of 2.4 [99]

Figure 6.11 shows sample airflow turbulence intensity contours in the two-person office. Turbulence intensity is the ratio of the root-mean-square fluctuation velocity to the mean airflow velocity. This figure shows that turbulence intensity in the room is relatively low. The peak turbulence intensity is seen near the mouth of the speaking mannequin and the inlet registers.

Figure 6.12 shows the concentration contours of 1 μm droplets emitted by the continuous speaking in the two-person office space. Here it is assumed that the concentration at the mouth of the speaking mannequin is 1. Therefore, the concentrations shown are fractions of the concentration that leaves the speaker's mouth. The contours are also cut at 0.005 for better visualization of the low concentrations in the room. Here the air change rate per hour is ACH = 2.4. As expected, the concentration near the speaker mannequin is high, but it is less than 0.005 in most of the room. Figure 6.12 shows that the concentration near the receptor mannequin is about 0.0035.

6.10 Airflow and Dispersion of Respiratory Droplets in a Nine-Person Office

Obeid et al. [99] performed a series of simulations for different ACHs and various respiratory droplet sizes. In addition, they evaluated the concentrations in the breathing zone of the receptor mannequin under various ventilation rates and different partition sizes. They found that an increase in the ventilation rates (high

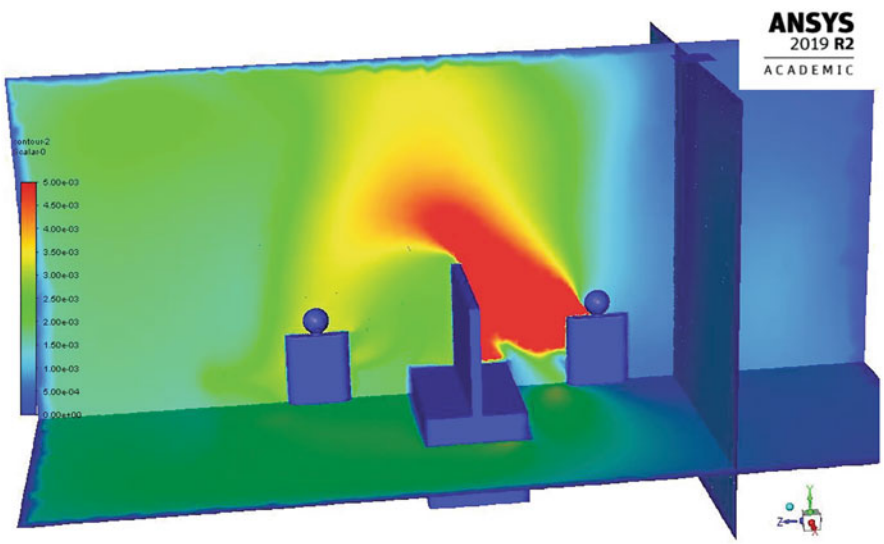

Fig. 6.12 Concentration contours of 1 μm droplets in the two-person office for ACH of 2.4 [99]

ACHs) would reduce the concentration near the receptor mannequin's breathing zone and, therefore, the chance for exposure. However, a slight increase in the height of the partition has a negligible effect on the concentration near the receptor mannequin.

Sample trajectories for 100 μm droplets expelled by the emitter mannequin during speaking are shown in Fig. 6.13. It is seen that all emitted 100 μm particles fall to the ground ballistically due to their large gravitational sedimentation velocity.

Figure 6.14 shows the schematics of a large nine-person office with partitions. This room has a mixing ventilation system with two linear supply diffusers, a rectangular supply diffuser, and one rectangular outlet on the ceiling [99]. The mannequins are identified from 1 to 9 from the front of the room in three rows. Thus, mannequin 4 is the one on the left in the second row.

Obeid et al. [99] studied the airflow and droplet concentration in the nine-person office space shown in Fig. 6.14 for the cases that one of the nine mannequins in the room is continuously speaking. They presented the simulation results for airflow and concentrations of respiratory droplets of various sizes for different ventilation ACHs. Particular attention was given to the concentrations of droplets of different sizes in the breathing zone of the other eight receptor mannequins in the room. Some sample simulation results for the airflow velocity contours and droplet concentrations are reproduced in this section.

For the case that the mannequin 4 is continuously speaking and emitting 1 μm respiratory droplets, the airflow velocity contours for ACH of 3 are shown in Fig. 6.15. The contours are shown at a vertical plane crossing the three mannequins on the left side of the room and a horizontal plane at the chest level of the mannequins.

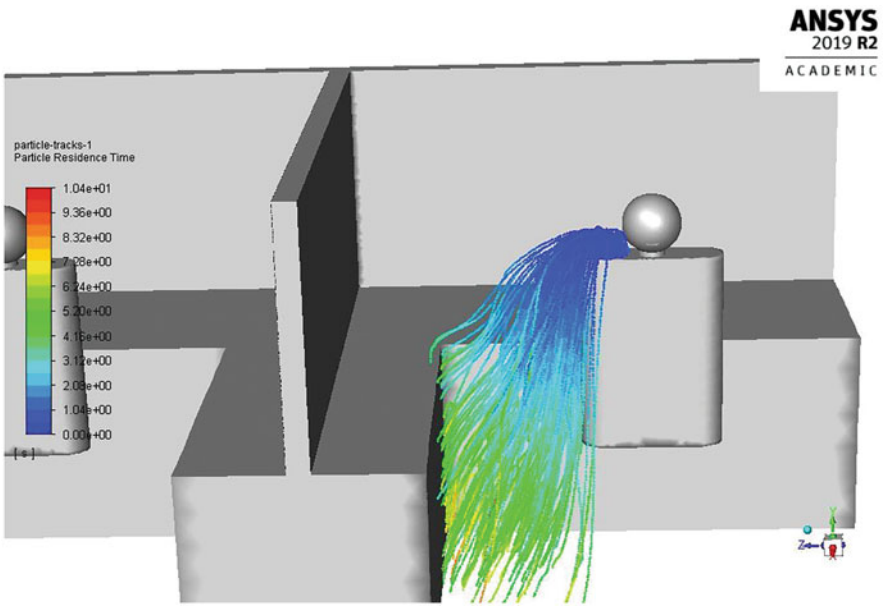

Fig. 6.13 Sample 100 μm droplets' trajectories emitted by the emitter mannequin in the two-person office for ACH of 2.4 [99]

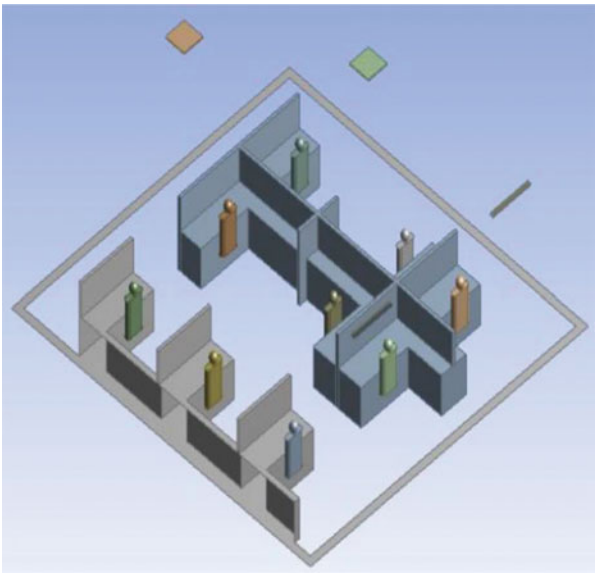

Fig. 6.14 Schematics of a nine-person office geometry with partitions [99]

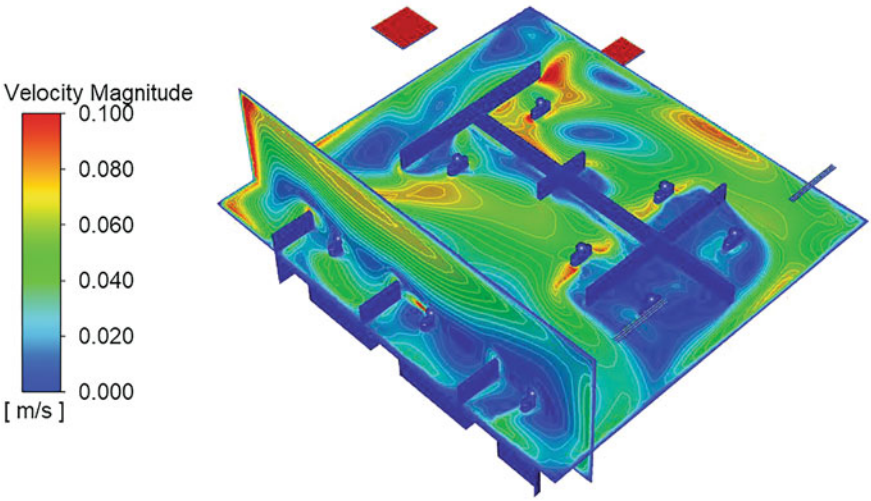

Fig. 6.15 Variations of velocity magnitude contours in the nine-person office for ACH of 3 for mannequin 4 speaking [99]

For better visualization of the velocity contours, the peak velocity magnitude is cut at 0.1 m/s. This figure shows that the airflow velocity magnitude varies significantly in the room and is controlled by the ventilation system. The speaking jet flow from the emitter mannequin 4 is also seen in this figure. Figure 6.15 indicates that the airflow velocities near mannequins 4, 7, 8, and 9 are low.

Figure 6.16 shows the concentration contours of 1 μm droplets emitted by the continuously speaking mannequin 4 in the nine-person office space for the ventilation rate of ACH = 3. As mentioned before, the concentration is normalized by the concentration at the mouth of the speaking mannequin. The contours are also cut at 0.01 for better visualization of the low concentrations in the room. This figure shows that the concentration in the area near mannequin 4 is high but decreases sharply with the distance from the speaker. The concentration is very low on the right side of the room. Figure 6.16 shows that the concentration near mannequin 7, behind the speaker, is relatively high. The next highest exposure is seen by mannequin 1, in front of the speaker mannequin 4. This is followed by mannequin 5 and then 2 and 8. Finally, mannequins 3, 6, and 9 are exposed to very low concentrations.

Figure 6.17 shows the concentration contours of 1 μm droplets emitted by the continuously speaking mannequin 5 in the nine-person office space for the ventilation rate of ACH = 4. Here the concentration contours are cut at 0.0035 for better visualization of the low concentrations in the room. It is seen that the concentration near mannequin 5 is high, and the high concentration region is extended toward mannequin 8 behind the emitter due to the circulating ventilation

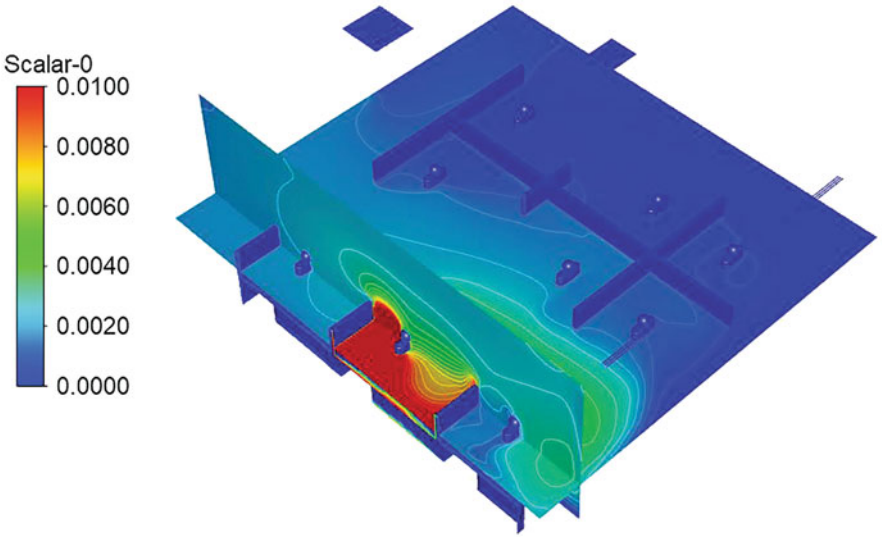

Fig. 6.16 Concentration contours of 1 μm droplets in the nine-person office for ACH of 3 for mannequin 4 speaking [99]

airflow in the room. As a result, mannequin 8 is exposed to a concentration of about 0.002. However, the concentration is very low in the rest of the room.

6.11 Respiratory Face Masks

According to the CDC, wearing a respiratory face mask protects against exposure to airborne viruses. Among the available face masks, N95 and surgical masks are highly effective [118, 119]. In the absence of face leakage, the filtration efficiency of N95 and KN95 masks is about 95% for submicron particles and much higher for larger particles (National Institute for Occupational Safety and Health (NIOSH) [120, 121]. Surgical masks are commonly used in hospitals [122]. The filtration efficiencies of different masks under normal breathing conditions, as reported by Zhang et al. [123] and Feng et al. [110], are shown in Fig. 6.18. It is seen that the efficiency of most masks is relatively high for particles larger than 10 μm. However, for submicron particles, the filtration efficiency of most cloth masks drops significantly.

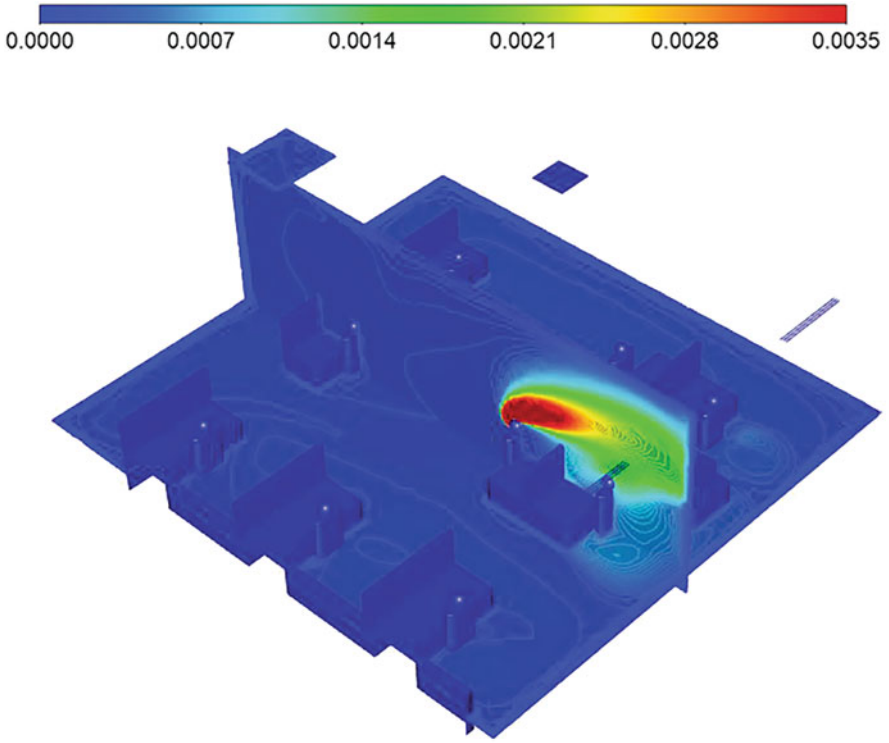

Fig. 6.17 Concentration contours of 1 μm droplets in the nine-person office for ACH of 4 for mannequin 5 speaking [99]

6.12 Simple Model for Exposure to Respiratory Puff

Balachandar et al. [98] developed a simple model for the evolution of droplet concentration in a puff generated by speaking, coughing, or sneezing. The model accounts for the evaporation of emitted droplets and larger droplets leaving the puff due to gravitational sedimentation. They assumed log-normal and Pareto initial droplet size distributions. Their results for the time variations of droplets/nuclei concentration as a function of droplet size for the initial log-normal distribution are reproduced in Fig. 6.19a. This figure shows that at times of $t = 0.025$ and 0.2 s, larger droplets fall off the puff. The droplets smaller than a specific size are fully evaporated. The distribution of intermediate-size airborne droplets indicates that they are continuing to evaporate. At $t = 0.68$ s, the number and size of droplets in the puff reach their limiting values. However, their concentration continues to decrease as the puff volume increases in time.

The exposure to respiratory droplet concentration is markedly affected when the receptor is wearing a mask. Balachandar et al. [98] included the filtration effect of

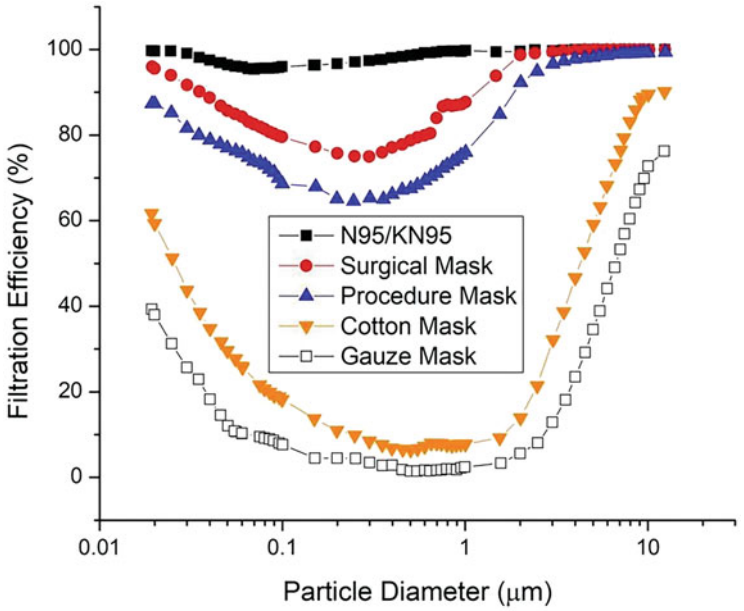

Fig. 6.18 Filtration efficiency of different masks for different particle sizes [98, 110, 123]

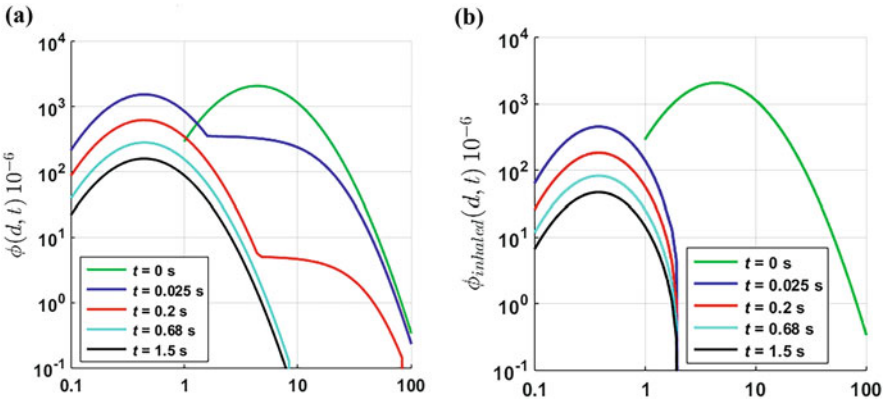

Fig. 6.19 Time evolution of an initially log-normal airborne droplet concentration in a puff. (**a**) A receptor without a mask. (**b**) A receptor with a surgical mask

wearing a mask on the concentration of airborne droplets. They assumed that the receptor is wearing a surgical mask, whose efficiency is given in Fig. 6.18, and included the aspiration efficiency of different size particles in their model. Their results for an initially log-normal droplet size distribution are reproduced in Fig. 6.19b. This figure shows that the surgical mask filters all droplets larger than 2 μm. In addition, the inhaled concentration of smaller droplets is substantially lower than

the receptor without a mask. As expected, the inhaled concentration would be higher for cotton or Gauze masks, while exposure would be much lower for the N95/KN95 masks.

6.13 Conclusions

In this chapter, the application of computational fluid dynamics for modeling the aerosol transmission of COVID-19 is described. The features of respiratory droplet generation by speaking, coughing, and sneezing are discussed. Several examples of simulations of airflows and droplet trajectories and concentrations in indoor environments are presented. The CFD results showed that the emitted aerosolized infected droplets spread in the entire indoor environment, so there is no completely safe distance. In addition, the concentration of respiratory droplets is highly nonuniform and generally decreases with the distance from the source. Furthermore, ventilation significantly affects droplet dilution in indoor environments. A high air change rate would reduce the chance for infection, while poor ventilation increases the risk. Finally, wearing a mask (K95 or surgical) would reduce exposure to the suspended respiratory droplets.

References

1. WHO. (2021). Retrieved from https://www.who.int/
2. CDC. (2021). Retrieved from https://www.cdc.gov/
3. Bourouiba, L., Dehandschoewercker, E., & Bush, J. W. M. (2014). Violent expiratory events: On coughing and sneezing. *Journal of Fluid Mechanics, 745*, 537–563.
4. Nicas, M., Nazaroff, W. W., & Hubbard, A. (2005). Toward understanding the risk of secondary airborne infection: Emission of respirable pathogens. *Journal of Occupational and Environmental Hygiene, 2*, 143–154.
5. Noakes, C. J., Beggs, C. B., Sleigh, P. A., & Kerr, K. G. (2006). Modelling the transmission of airborne infections in enclosed spaces. *Epidemiology and Infection, 134*, 1082–1091.
6. Stilianakis, N. I., & Drossinos, Y. (2010). Dynamics of infectious disease transmission by inhalable respiratory droplets. *Journal of the Royal Society Interface, 7*, 1355–1366.
7. Buonanno, G., Stabile, L., & Morawska, L. (2020a). Estimation of airborne viral emission: Quanta emission rate of SARS-CoV-2 for infection risk assessment. *Environment International, 141*, 105794.
8. Buonanno, G., Morawska, L., & Stabile, L. (2020b). Quantitative assessment of the risk of airborne transmission of SARS-CoV-2 infection. *Environment International, 145*, 106112.
9. Asadi, S., Bouvier, N., Wexler, A. S., & Ristenpart, W. D. (2020). The coronavirus pandemic and aerosols: Does COVID-19 transmit via expiratory particles? *Aerosol Science and Technology, 54*, 635–638.
10. Morawska, L., & Cao, J. (2020). Airborne transmission of SARS-CoV-2: The world should face the reality. *Environment International, 139*, 105730.
11. Allen, J. G., & Marr, L. C. (2020). Recognizing and controlling airborne transmission of SARS-CoV-2 in indoor environments. *Indoor Air, 30*(4), 557.

12. Zhang, R., Li, Y., Zhang, A. L., Wang, Y., & Molina, M. J. (2020). Identifying airborne transmission as the dominant route for the spread of COVID-19. *Proceedings. National Academy of Sciences. United States of America, 117*, 14857–14863.
13. Ahmed, T., Wendling, H. E., Mofakham, A. A., Ahmadi, G., Helenbrook, B. T., Ferro, A. R., Brown, D. M., & Erath, B. D. (2021). Variability in expiratory trajectory angles during consonant production by one human subject and from a physical mouth model: application to respiratory droplet emission. *Indoor Air, 31*, 1896–1912. Retrieved from https://onlinelibrary.wiley.com/doi/epdf/10.1111/ina.12908
14. Bazant, M. Z., & Bush, J. W. M. (2021). A guideline to limit indoor airborne transmission of COVID-19. *PNAS, 118*(17), 1–12.
15. Asadi, S., Wexler, A. S., Cappa, C. D., Barreda, S., Bouvier, N. M., & Ristenpart, W. D. (2019). Aerosol emission and superemission during human speech increase with voice loudness. *Scientific Reports, 9*(1), 1–10.
16. Chong, K. L., Ng, C. S., Hori, N., Yang, R., Verzicco, R., & Lohse, D. (2021). Extended lifetime of respiratory droplets in a turbulent vapour puff and its implications on airborne disease transmission. *Physical Review Letters, 126*, 034502.
17. Duguid, J. P. (1946). The size and the duration of air-carriage of respiratory droplets and droplet-nuclei. *Epidemiology and Infection, 44*(6), 471–479.
18. Han, Z. Y., Weng, W. G., & Huang, Q. Y. (2013). Characterizations of particle size distribution of the droplets exhaled by sneeze. *Journal of the Royal Society Interface, 10*, 20130560.
19. Memarzadeh, F. (2011). Improved strategy to control aerosol-transmitted infections in a hospital suite. In *Proceedings of IAQ Conference 2012, Freiburg, Germany, February 2011*.
20. Morawska, L., & Milton, D. K. (2020). It is time to address airborne transmission of COVID-19. *Clinical Infectious Diseases, 6*, ciaa939.
21. Papineni, R. S., & Rosenthal, F. S. (1997). The size distribution of droplets in the exhaled breath of healthy human subjects. *Journal of Aerosol Medicine, 10*, 105–116.
22. Scheuch, G. (2020). Breathing is enough: For the spread of influenza virus and SARS–CoV-2 by breathing only. *Journal of Aerosol Medicine and Pulmonary Drug Delivery, 33*(4), 230–234.
23. Xie, X., Li, Y., Chwang, A. T., Ho, P., & Seto, W. (2007). How far droplets can move in indoor environments–revisiting the Wells evaporation-falling curve. *Indoor Air, 17*(3), 211–225. https://doi.org/10.1111/j.1600-0668.2007.00469.x
24. Bradley, R. S., Evans, M. G., & Whytlaw-Gray, R. W. (1946). The rate of evaporation of droplets. Evaporation and diffusion coefficients, and vapour pressures of dibutyl phthalate and butyl stearate. *Proceedings of the Royal Society A: Mathematical, Physical and Engineering Sciences, 186*, 368–390. https://doi.org/10.1098/rspa.1946.0050
25. Langmuir, I. (1918). The evaporation of small spheres. *Physics Review, 12*, 368–370.
26. Pirhadi, M., Sajadi, B., Ahmadi, G., & Malekian, D. (2018). Phase change and deposition of inhaled droplets in the human nasal cavity under cyclic inspiratory airflow. *Journal of Aerosol Science, 118*, 64–81.
27. Sazhin, S. S. (2006). Advanced models of fuel droplet heating and evaporation. *Progress in Energy and Combustion Science, 32*(2), 162–214.
28. Wells, W. F. (1934). On air-borne infection: Study II. Droplets and droplet nuclei. *American Journal of Epidemiology, 20*(3), 611–618.
29. Wells, W. F. (1955). Airborne contagion and air hygiene. an ecological study of droplet infections. In *Airborne contagion and air hygiene. An ecological study of droplet infections*. Harvard University Press.
30. Levich, V. (1962). *Physicochemical hydrodynamics*. Prentice-Hall.
31. Fuchs, N. A. (1964). *The mechanics of aerosols*. Pergamon Press.
32. Mercer, T. T. (1973). *Aerosol technology in hazard evaluation of airborne particles*. Academic Press.
33. Twomey, S. (1976). *Atmospheric aerosols*. Elsevier.
34. Hinds, W. C. (1982). *Aerosol technology, properties, behavior, and measurement of airborne particles*. John Wiley and Sons.

35. Spurny, K. R. (1986). *Physical and chemical characterization of individual airborne particles*. John Wiley and Sons.
36. Seinfeld, J. H. (1986). *Atmospheric chemistry and physics of air pollution*. John Wiley and Sons.
37. Vincent, J. H. (1995). *Aerosol science for industrial hygienists*. Pergamon Press.
38. Tu, J., Inthavong, K., & Ahmadi, G. (2013). *Computational fluid and particle dynamics in the human respiratory system*. Springer. https://doi.org/10.1007/978-94-007-4488-2
39. Ahmadi, G., & Goldschmidt, V. W. (1971). Motion of particle in a turbulent fluid-the basset history term. *Journal of Applied Mechanics, Transactions ASME, 38*, 561–563.
40. Riley, J. J., & Patterson, G. S., Jr. (1974). Diffusion experiments with numerically integrated isotropic turbulence. *Physics of Fluids, 17*, 292–297.
41. Reeks, M. W. (1977). On the dispersion of small particles suspended in an isotropic turbulent flow. *Journal of Fluid Mechanics, 83*, 529–546.
42. Reeks, M. W., & Mckee, S. (1984). The dispersive effect of basset history forces on particle motion in a turbulent flow. *Physics of Fluids, 27*, 1573–1582.
43. Rizk, M. A., & Elghobashi, S. E. (1985). The motion of a spherical particle suspended in a turbulent flow near a plane wall. *Physics of Fluids, 20*, 806–817.
44. Maxey, M. R. (1987). The Gravitational settling of aerosol particles in homogeneous turbulence and random flow fields. *Journal of Fluid Mechanics, 174*, 441–445.
45. Wang, L.-P., & Stock, D. E. (1992). Stochastic trajectory models for turbulent diffusion: Monte-Carlo process versus Markov chains. *Atmospheric Environment, 26*, 1599–1607.
46. Wang, L.-P., & Stock, D. E. (1993). Dispersion of heavy particles by turbulent motion. *Journal of the Atmospheric Sciences, 50*, 1897–1913.
47. Crowe, C. T. (1982). Review - Numerical models for dilute gas-particle flows. *Journal of Fluids Engineering, Transactions of the ASME, 104*, 297–303.
48. Li, A., & Ahmadi, G. (1992). Dispersion and deposition of spherical particles from point sources in a turbulent channel flow. *Aerosol Science and Technology, 16*(4), 209–226.
49. Li, A., & Ahmadi, G. (1993a). Deposition of aerosols on surfaces in a turbulent channel flow. *International Journal of Engineering Science, 31*(3), 435–451.
50. Li, A., & Ahmadi, G. (1993b). Computer simulation of deposition of aerosols in a turbulent channel flow with rough wall. *Aerosol Science and Technology, 18*, 11–24.
51. He, C., & Ahmadi, G. (1999). Particle deposition in a nearly developed turbulent duct flow with electrophoresis. *Journal of Aerosol Science, 30*, 739–758.
52. Friedlander, S. K., & Johnstone, H. F. (1957). Deposition of suspended particles from turbulent gas streams. *Industrial and Engineering Chemistry, 49*, 1151.
53. Davies, C. N. (1966). *Aerosol science*. Academic Press.
54. Sehmel, G. A. (1973). Particle eddy diffusities and deposition velocities for isothermal flow and smooth surfaces. *Journal of Aerosol Science, 4*, 125–138.
55. Wood, N. B. (1981). A simple method for calculation of turbulent deposition to smooth and rough surfaces. *Journal of Aerosol Science, 12*, 275–290.
56. Fernandez de la Mora, J., & Friedlander, S. K. (1982). Aerosol and gas deposition to fully rough surfaces: Filtration model for blade-shaped elements. *International Journal of Heat and Mass Transfer, 25*, 1725–1735.
57. Cleaver, J. W., & Yates, B. (1975). A sub layer model for the deposition of particles from a turbulent flow. *Chemical Engineering Science, 30*, 983–992.
58. Fichman, M., Gutfinger, C., & Pnueli, D. (1988). A model for turbulent deposition of aerosols. *Journal of Aerosol Science, 19*, 123–136.
59. Fan, F. G., & Ahmadi, G. (1993). A sublayer model for turbulent deposition of particles in vertical ducts with smooth and rough surfaces. *Journal of Aerosol Science, 24*, 45–64.
60. Fan, F. G., & Ahmadi, G. (1994). On the sublayer model for turbulent deposition of aerosol particles in the presence of gravity and electric fields. *Aerosol Science and Technology, 21*, 49–71.
61. Fan, F., & Ahmadi, G. (1995). A sublayer model for wall deposition of ellipsoidal particles in turbulent stream. *Journal of Aerosol Science, 25*, 813–840.

62. Papavergos, P. G., & Hedley, A. B. (1984). Particle deposition behavior from turbulent flow. *Chemical Engineering Research and Design, 62*, 275–295.
63. Kvasnak, W., & Ahmadi, G. (1996). Deposition of ellipsoidal particles in turbulent duct flows. *Chemical Engineering Science, 51*, 5137–5148.
64. Kvasnak, W., Ahmadi, G., Bayer, R., & Gaynes, M. A. (1993). Experimental investigation of dust particle deposition in a turbulent channel flow. *Journal of Aerosol Science, 24*, 795–815.
65. Inthavong, K., Ge, Q. J., Li, X. D., & Tu, J. Y. (2012). Detailed predictions of particle aspiration affected by respiratory inhalation and airflow. *Atmospheric Environment, 62*, 107–117. https://doi.org/10.1016/j.atmosenv.2012.07.071
66. Li, X. D., Inthavong, K., Ge, Q. J., & Tu, J. Y. (2013). Numerical investigation of particle transport and inhalation using standing thermal manikins. *Building and Environment, 60*(2013), 116–125. https://doi.org/10.1016/j.buildenv.2012.11.014
67. Naseri, A., Abouali, O., & Ahmadi, G. (2017). Effect of turbulent thermal plume on aspiration efficiency of microparticles. *Building and Environment, 118*, 159–172.
68. Azhdari, M., Tavakol, M. M., & Ahmadi, G. (2021). Particle inhalability of a standing mannequin with large airways in a ventilated room. *Computers in Biology and Medicine, 138*(104858), 1–25. https://doi.org/10.1016/j.compbiomed.2021.104858
69. Bahmanzadeh, H., Abouali, O., & Ahmadi, G. (2016). Unsteady particle tracking of microparticle deposition in the human nasal cavity under cyclic inspiratory flow. *Journal of Aerosol Science, 101*, 86–103.
70. Ghahramani, E., Abouali, O., Emdad, H., & Ahmadi, G. (2017). Numerical investigation of turbulent airflow and microparticle deposition in a realistic model of human upper airway using LES. *Computers and Fluids, 157*, 43–54.
71. Tavakol, M. M., Ghahramani, E., Abouali, O., Yaghoubi, M., & Ahmadi, G. (2017). Deposition fraction of ellipsoidal fibers in a model of human nasal cavity for laminar and turbulent flows. *Journal of Aerosol Science, 113*, 52–70.
72. ANSYS. (2017). *ANSYS-fluent theory guide 18.0*. Ansys Inc.
73. Durbin, P. (1993). A Reynolds stress model for near-wall turbulence. *Journal of Fluid Mechanics, 249*, 465–498.
74. Hanjalić, K., & Launder, B. (1972). A Reynolds stress model of turbulence and its application to thin shear flows. *Journal of Fluid Mechanics, 52*(4), 609–638.
75. Pope, S. B. (2000). *Turbulent flows*. Cambridge University Press.
76. Tian, L., & Ahmadi, G. (2007). Particle deposition in turbulent duct flows - Comparisons of different model predictions. *Journal of Aerosol Science, 38*, 377–397.
77. Lesieur, M., Métais, O., & Comte, P. (2005). *Large-eddy simulations of turbulence*. Cambridge University Press.
78. Rogallo, R. S., & Moin, P. (1984). Numerical simulation of turbulent flows. *Annual Review of Fluid Mechanics, 16*(1), 99–137.
79. Sagaut, P. (2006). *Large eddy simulation for incompressible flows: An introduction*. Springer Science & Business Media.
80. Salmanzadeh, M., Rahnama, M., & Ahmadi, G. (2010). Effect of sub-grid scales on large eddy simulation of particle deposition in a turbulent channel flow. *Aerosol Science and Technology, 44*, 796–806.
81. Kim, J., Moin, P., & Moser, R. (1987). Turbulence statistics in fully developed channel flow at low Reynolds number. *Journal of Fluid Mechanics, 177*, 133–166.
82. McLaughlin, J. B. (1989). Aerosol particle deposition in numerically simulated channel flow. *Physics of Fluids A: Fluid Dynamics (1989–1993), 1*(7), 1211–1224.
83. Moser, R. D., Kim, J., & Mansour, N. N. (1999). Direct numerical simulation of turbulent channel flow up to Re τ= 590. *Physics of Fluids, 11*(4), 943–945.
84. Nasr, H., Ahmadi, G., & McLaughlin, J. B. (2009). A DNS study of effects of particle–particle collisions and two-way coupling on particle deposition and phasic fluctuations. *Journal of Fluid Mechanics, 640*, 507–536.
85. Ounis, H., Ahmadi, G., & McLaughlin, J. B. (1993). Brownian particle deposition in a directly simulated turbulent channel flow. *Physics of Fluids A: Fluid Dynamics, 5*(6), 1427–1432.

86. Thatcher, T. L., Lai, A. C., Moreno-Jackson, R., Sextro, R. G., & Nazaroff, W. W. (2002). Effects of room furnishings and air speed on particle deposition rates indoors. *Atmospheric Environment, 36*(11), 1811–1819. https://doi.org/10.1016/S1352-2310(02)00157-7
87. Chen, F., Simon, C. M., & Lai, A. C. (2006). Modeling particle distribution and deposition in indoor environments with a new drift–flux model. *Atmospheric Environment, 40*(2), 357–367. https://doi.org/10.1016/j.atmosenv.2005.09.044
88. Inthavong, K., Tian, Z. F., & Tu, J. Y. (2009). Effect of ventilation design on removal of particles in woodturning workstations. *Building and Environment, 44*(1), 125–136. https://doi.org/10.1016/j.buildenv.2008.02.002
89. Zhao, B., & Guan, P. (2007). Modeling particle dispersion in personalized ventilated room. *Building and Environment, 42*(3), 1099–1109. https://doi.org/10.1016/j.buildenv.2005.11.009
90. Gao, N. P., & Niu, J. L. (2007). Modeling particle dispersion and deposition in indoor environments. *Atmospheric Environment, 41*(18), 3862–3876. https://doi.org/10.1016/j.atmosenv.2007.01.016
91. Ahmadzadeh, M., Farokhi, E., & Shams, M. (2021). Investigating the effect of air conditioning on the distribution and transmission of COVID-19 virus particles. *Journal of Cleaner Production, 316*(128147), 1–23.
92. Liu, H., He, S., Shen, L., & Hong, J. (2021). Simulation-based study of COVID-19 outbreak associated with air-conditioning in a restaurant. *Physics of Fluids, 33*(2), 023301. https://doi.org/10.1063/5.0040188
93. Abuhegazy, M., Talaat, K., Anderoglu, O., & Poroseva, S. V. (2020). Numerical investigation of aerosol transport in a classroom with relevance to COVID-19. *Physics of Fluids, 32*(10), 103311. https://doi.org/10.1063/5.0029118
94. Mirzaie, M., Lakzian, S., Khan, A., Ebrahimi Warkiani, M., Mahian, O., & Ahmadi, G. (2021). COVID-19 spread in a classroom equipped with partition – A CFD approach. *Journal of Hazardous Materials, 420*(126587), 1–18. https://doi.org/10.1016/j.jhazmat.2021.126587
95. Satheesan, M. K., Mui, K. W., & Wong, L. T. (2020). A numerical study of ventilation strategies for infection risk mitigation in general inpatient wards. In *Building simulation* (pp. 1–10). Tsinghua University Press. https://doi.org/10.1007/s12273-020-0623-4
96. Borro, L., Mazzei, L., Raponi, M., Piscitelli, P., Miani, A., & Secinaro, A. (2021). The role of air conditioning in the diffusion of Sars-CoV-2 in indoor environments: A first computational fluid dynamic model, based on investigations performed at the Vatican State Children's hospital. *Environmental Research, 193*, 110343. https://doi.org/10.1016/j.envres.2020.110343
97. Cui, F., Geng, X., Zervaki, O., Dionysiou, D. D., Katz, J., Haig, S. J., & Boufadel, M. (2021). Transport and fate of virus-laden particles in a supermarket: recommendations for risk reduction of COVID-19 spreading. *Journal of Environmental Engineering, 147*(4), 04021007. https://doi.org/10.1061/(ASCE)EE.1943-7870.0001870
98. Balachandar, S., Zaleski, S., Soldati, A., Ahmadi, G., & Bourouiba, L. (2020). Host-to-host airborne transmission as a multiphase flow problem for science-based social distance guidelines. *International Journal of Multiphase Flow, 132*(103439), 1–20. https://doi.org/10.1016/j.ijmultiphaseflow.2020.103439
99. Obeid, O., Rawat, M. S., White, P., Rosati Rowe, J., Ferro, A., & Ahmadi, G. (2021). Respiratory droplet emissions and transport estimates using CFD for a nine-person, cubicle-style office. In *American Association for Aerosol Research, AAAR 39th Annual Conference, Virtual Conference, October 18–22*. Retrieved from https://www.aaar.org/2021/program/
100. Fabian, P., McDevitt, J. J., DeHaan, W. H., Fung, R. O. P., Cowling, B. J., Chan, K. H., Leung, G. M., & Milton, D. K. (2008). Influenza virus in human exhaled breath: an observational study. *PLoS One, 3*, 1–6. https://doi.org/10.1371/journal.pone.0002691
101. Marchioli, C., & Soldati, A. (2002). Mechanisms for particle transfer and segregation in a turbulent boundary layer. *Journal of Fluid Mechanics, 468*, 283–315.
102. Marchioli, C., Picciotto, M., & Soldati, A. (2007). Influence of gravity and lift on particle velocity statistics and transfer rates in turbulent vertical channel flow. *International Journal of Multiphase Flow, 33*(3), 227–251.

103. Zhang, H., & Ahmadi, G. (2000). Aerosol particle transport and deposition in vertical and horizontal turbulent duct flows. *Journal of Fluid Mechanics, 406*, 55–80.
104. Chen, M., & McLaughlin, J. B. (1995). A new correlation for the aerosol deposition rate in vertical ducts. *Journal of Colloid and Interface Science, 169*(2), 437–455.
105. Mofakham, A. A., & Ahmadi, G. (2019). Particles dispersion and deposition in inhomogeneous turbulent flows using continuous random walk models. *Physics of Fluids, 31*(8), 083301. 1–13.
106. Mofakham, A. A., & Ahmadi, G. (2020a). On random walk models for simulation of particle-laden turbulent flows. *International Journal of Multiphase Flow, 122*(103157), 1–21. https://doi.org/10.1016/j.ijmultiphaseflow.2019.103157
107. Mofakham, A. A., & Ahmadi, G. (2020b). Improved discrete random walk stochastic model for simulating particle dispersion and deposition in inhomogeneous turbulent flows. *Journal of Fluids Engineering, 142*, 101401-1–101401-14. https://doi.org/10.1115/1.4047538
108. Morawska, L. (2006). Droplet fate in indoor environments, or can we prevent the spread of infection? *Indoor Air, 16*, 335–347.
109. Yang, L., Li, X., Yan, Y., & Tu, J. (2018). Effects of cough-jet on airflow and contaminant transport in an airliner cabin section. *The Journal of Computational Multiphase Flows, 10*(2), 72–82. https://doi.org/10.1177/1757482X17746920
110. Feng, Y., Marchal, T., Sperry, T., & Yi, H. (2020). Influence of wind and relative humidity on the social distancing effectiveness to prevent COVID-19 airborne transmission: A numerical study. *Journal of Aerosol Science, 147*(105585), 1–19.
111. Tu, J., Inthavong, K., & Wong, K. K. L. (2015). Geometric model reconstruction. In *Computational hemodynamics—Theory, modelling and applications*. Springer.
112. Dong, J., Inthavong, K., & Tu, J. (2017). Multiphase flows in biomedical applications. In G. H. Yeoh (Ed.), *Handbook of multiphase flow science and technology*. Springer.
113. Dong, J., Tian, L., & Ahmadi, G. (2019). Numerical assessment of respiratory airway exposure risks to diesel exhaust particles. *Experimental and Computational Multiphase Flow, 1*, 51–59. Retrieved from https://link.springer.com/article/10.1007/s42757-019-0005-2
114. Masoomi, M. A., Salmanzadeh, M., & Ahmadi, G. (2021). Dispersion of droplets emitted during speaking in a ventilated indoor environment. In *FEDSM2021-65837, V003T08A017, Proceedings of the ASME 2021 Fluids Engineering Division Summer Meeting, FEDSM2021 Virtual Conference, Online, August 10–12, 2021*. https://doi.org/10.1115/FEDSM2021-65837. Retrieved from https://event.asme.org/FEDSM-2021
115. Ahmadzadeh, M., & Shams, M. (2021). Passenger exposure to respiratory aerosols in a train cabin: Effects of window, injection source, output flow location. *Sustainable Cities and Society, 75*(103280), 1–16.
116. Hejazi, M., Sadrizadeh, S., Ahmadi, G., & Abouali, O. (2021). Numerical simulation of the COVID-19 airborne transmission in trains. In *Proceedings of the ASME 2021 Fluids Engineering Division Summer Meeting, FEDSM2021 Virtual Conference, Online, August 10–12, 2021*.
117. Rawat, M. S., Obeid, O., White, P., Rosati Rowe, J., Ahmadi, G., & Ferro, A. (2021). Comparison of CFD model and one-compartment materials balance model for predicting 8-Hr exposure to pathogen-laden expiratory droplets in a two-person office. In *American Association for Aerosol Research, AAAR 39th Annual Conference, Virtual Conference. October 18–22*. Retrieved from https://www.aaar.org/2021/program/
118. Grinshpun, S. A., Haruta, H., Eninger, R. M., Reponen, T., McKay, R. T., & Lee, S. A. (2009). Performance of an N95 filtering facepiece particulate respirator and a surgical mask during human breathing: Two pathways for particle penetration. *Journal of Occupational and Environmental Hygiene, 6*(10), 593–603.
119. Loeb, M., Dafoe, N., Mahony, J., John, M., Sarabia, A., Glavin, V., Webby, R., Smieja, M., Earn, D. J., Chong, S., Webb, A., & Walter, S. D. (2009). Surgical mask vs. N95 respirator for preventing influenza among health care workers: A randomized trial. *Journal of the American Medical Association, 302*(17), 1865–1871.

120. National Institute for Occupational Safety and Health (NIOSH). (1997). *42 CFR 84 Respiratory Protective Devices: Final Rules and Notice. 60. Federal Register: 110.*
121. Qian, Y., Willeke, K., Grinshpun, S. A., Donnelly, J., & Coffey, C. C. (1998). Performance of N95 respirators: Filtration efficiency for airborne microbial and inert particles. *American Industrial Hygiene Association, 59*(2), 128–132.
122. Lipp, A., & Edwards, P. (2012). Disposable surgical face masks for preventing surgical wound infection in clean surgery. *Sao Paulo Medical Journal, 130*(4), 269. https://doi.org/10.1002/14651858.CD002929
123. Zhang, X., Li, H., Shen, S., & Cai, M. (2016). Investigation of the flow-field in the upper respiratory system when wearing n95 filtering facepiece respirator. *Journal of Occupational and Environmental Hygiene, 13*(5), 372–382.

Chapter 7
Respiratory Virus Deposition and Resuspension from Indoor Surfaces

Mahender Singh Rawat and Andrea R. Ferro

Abstract Virus-laden respiratory aerosols and droplets that are emitted during breathing, talking, coughing, and sneezing are removed from the indoor air via ventilation; filtration; deposition directly onto surfaces, such as clothing, furnishings, and floorings; and deposition onto dust present on these surfaces. The settled virus particles can be resuspended when they are disturbed via human activity or other external forces, such as strong air currents. The importance of resuspension as a transmission route for COVID-19 is unknown but was identified as a major research question during the 2020 US National Academies of Science, Engineering, and Medicine (NASEM) Airborne Transmission of SARS-CoV-2: A Virtual Workshop and remains an open question. Resuspended particles from human walking and other activities have been well characterized in the scientific literature and are known to play a large role in human inhalation exposure to many indoor pollutants. Based on preliminary estimates, the contribution of airborne SARS-CoV-2 virus is approximately 1/100 that of the direct emissions. Resuspension from clothing may play a more important role in exposure to viruses due to the closer proximity to the breathing zone. Further study is needed to confirm these preliminary results and better characterize resuspension of viruses in the indoor environment. Recommended mitigation measures to reduce exposure to resuspended particles indoors include reducing the initial viral particle emission into the indoor air via masks, reducing the concentration of airborne viral particles via ventilation and filtration, and reducing the loading of settled viral particles by maintaining clean surfaces.

M. S. Rawat · A. R. Ferro (✉)
Department of Civil & Environmental Engineering, Clarkson University, Potsdam, NY, USA
e-mail: rawatm@clarkson.edu; aferro@clarkson.edu

D. Barry, H. Kanematsu (eds.), *Studies to Combat COVID-19 using Science and Engineering*, https://doi.org/10.1007/978-981-19-1356-3_7

7.1 Introduction

It has been over 2 years since the first case of COVID-19 was reported. Health officials initially assumed and communicated that the disease was not airborne but transmitted via contact of large virus-laden respiratory droplet projectiles onto the eyes, nose, and mouth, as well as transference of SARS-CoV-2 virus from fomites (objects) and hands to the eyes, nose, and mouth. However, several studies demonstrated that respiratory aerosols emitted and breathed indoors have been responsible for COVID-19 transmission events, especially in poorly ventilated rooms [1–3]. The evidence for airborne transmission became overwhelming and eventually altered the public health communication and response to the disease. According to the US Centers for Disease Control and Prevention (CDC), the main mode of transmission of COVID-19 is via breathing respiratory (breathing, speaking, coughing, or sneezing) aerosols generated by an infected person [4].

Respiratory aerosols and droplets that are emitted during breathing, talking, coughing, and sneezing are removed from the indoor air three ways: (1) ventilation; (2) filtration; and (3) deposition onto surfaces, such as clothing, furnishings, and floorings. The deposited aerosol may adhere directly to the surface or to dust on the surface. The deposited aerosols and droplets can then be resuspended when they are disturbed via human activity or other external forces, such as strong air currents.

The importance of resuspension as a transmission route for COVID-19 is unknown but was identified as a major research question during the 2020 US National Academies of Science, Engineering, and Medicine (NASEM) Airborne Transmission of SARS-CoV-2: A Virtual Workshop. Committee member and session chair Dr. Kimberly Prather stated: "the role of resuspended virus-contaminated dust and particulates is an open question" and "studies are needed to determine the importance of transmission by viruses that are suspended into the air from surfaces" [5]. Thus far, little work has been conducted in this area, and the role of resuspension remains an open research question. This chapter provides some background information and describes the current understanding of resuspension of the respiratory particles as a potential source of airborne virus-carrying particles.

7.2 Indoor Aerosols and Bioaerosols

People in the United States spend approximately 87% of their time in indoor environments, such as homes, offices, and schools, 6% of their time is in an enclosed vehicle, and only 7% of their time is outdoors on average [6]. In addition, indoor air concentrations of many chemical pollutants and biological particles are higher than outdoor air concentrations [7, 8]. Thus, much of the human exposure to airborne pollutants and biological particles occurs indoors. Exposure to SARS-CoV-2 and other airborne respiratory pathogens is likewise transmitted primarily indoors due to the higher airborne concentrations and amount of time spent in occupied indoor

environments. Human health effects associated with inhalation exposure to indoor particles vary widely and depend on the type and duration of exposure, a person's age, gender, susceptibility, and other stressors [9].

An "aerosol" is defined as a suspension of liquid and/or solid particles in a gas. Indoor bioaerosols are suspensions of biological particles in air and are a component of the indoor aerosol. Bioaerosols contain viable and nonviable airborne particles consisting of living organisms such as bacteria, algae, fungi, and viruses as well as fragments and released molecules like bacterial endotoxin, mycotoxins, high molecular weight (HMW) allergens, 1–3 β-glucans, pollen, and spores [10]. Exposure to bioaerosols can lead to acute and chronic diseases in humans [11]. The size range of bioaerosols is approximately 0.001–100 μm in diameter, and biological components can be incorporated into a larger liquid (e.g., respiratory fluid) or solid (e.g., dust or soil) particle [12]. Major sources of indoor bioaerosols include humans, pets, pests, mold and other fungi, and pollen from plants. For humans and pets, biological and nonbiological particles are emitted via direct respiratory emissions as well as via shedding from skin/fur and clothing. Major sources of nonbiological particles in indoor aerosol include combustion from cooking, heating, candles, incense, and emissions from building materials, furnishings, and consumer products. Indoor aerosols may also come from outdoor aerosols that are transported indoors via mechanical and/or natural airflow and infiltration through the building envelope. Outdoor bioaerosols are primarily from direct natural emissions from water bodies, soil, and plants and anthropogenic sources, for example, from farms, landfills, and wastewater treatment plants [13].

Over the last few decades, numerous studies have resulted in a better understanding of bioaerosol emissions, transport, and exposure (e.g., [14–17]). The indoor air acts as a temporary residence as the air does not provide nutrients or substrate for microbial growth. However, processes such as condensation, evaporation, and surface chemistry can alter the size and composition of the biological particles while they are airborne. The loss of viability for environmentally sensitive organisms, such as viruses, is also impacted by indoor conditions, including temperature, relative humidity, and ultraviolet radiation [12]. Once they are emitted or transported into the indoor air, the particles that are not removed via ventilation and filtration eventually deposit on the floor, walls, and furnishings and can subsequently be resuspended back into the air via human activities such as walking, sitting on furniture, and cleaning [18]. Resuspension of particles from human activity accounts for a substantial portion of human particulate matter (PM) intake [19], and resuspension has been identified as the major source of bioaerosol in classrooms [20]. Figure 7.1 depicts the primary sources of indoor aerosols.

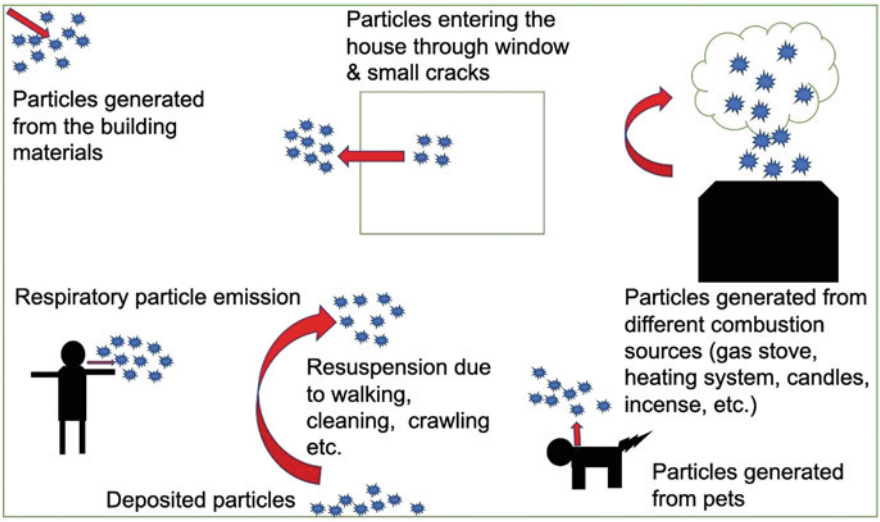

Fig. 7.1 Major sources of indoor aerosols

7.3 Material Balance Approach for Modeling Indoor Air Concentrations of Aerosols

A material balance approach is commonly used to predict indoor concentrations of aerosols and bioaerosols, including those containing SARS-CoV-2 (e.g., [21]). The material balance model for indoor air assumes that the particle emissions are instantaneously and uniformly mixed throughout the volume (i.e., the concentration is the same everywhere in the indoor compartment) and the air is noncompressible. Accordingly, the applicability of the material balance approach must be evaluated for the specific conditions and research questions being addressed. The material balance equation calculates the rate of change of particle mass in the indoor air by summing the mass entering the compartment from outside the compartment or via source emissions inside the compartment and subtracting the mass leaving the compartment and the sinks (e.g., deposition loss) in the compartment (Fig. 7.2). Note that for pathogens, the inactivation rate is included as a sink. For the example shown in Fig. 7.2, resuspension is included as one of the sources.

To calculate the concentration in the indoor air for which the volume and ventilation rate is known, the source emissions, particle deposition, and resuspension must be estimated. The following sections address these three terms, respectively. Note that for most SARS-CoV-2, it is usually reasonable to assume that the outdoor concentration is negligible and can be ignored. If the compartment being modeled has airflow from another compartment with a non-negligible concentration, the "mass entering" [the compartment] term would remain in the model. For resuspension mass balance models, a second compartment for the mass loading to

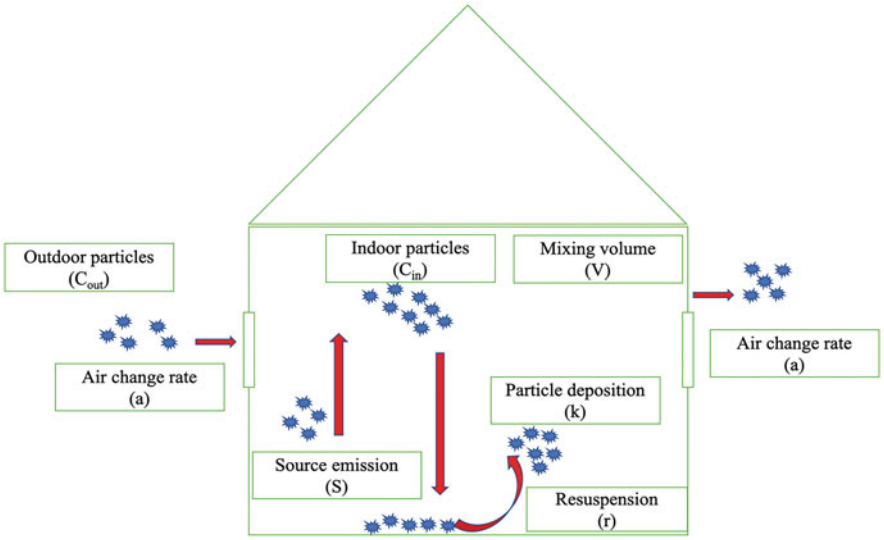

Fig. 7.2 Schematic for mass balance model with resuspension source

the floor or other surfaces is included. For the surface compartment, deposition is a source, and resuspension is a sink (i.e., mass is lost from the surface compartment as the particles are removed via resuspension).

7.4 Respiratory Aerosol Emissions

Respiratory emissions such as breathing, talking, coughing, singing, and sneezing are responsible for the airborne transmission of the infectious respiratory diseases caused by the microorganisms present in aerosols and droplets. Characterization of the respiratory emissions by using particle characterization techniques includes emission rate (particles per event or per time), emission concentration (particles per volume of air), and size distribution characterization (e.g., geometric mean diameter; particle size range; normalized number or mass concentration per size bin). Different studies have produced relatively consistent results for the particle number size distribution, with most of the particles emitted being less than 5 μm in diameter. Peaks (modes) in the particle size distribution are associated with the different aerosol generation sites in the respiratory tract [12].

Emission rate and emission concentration estimates vary widely between studies and individuals depending on the respiratory activity, measurement techniques, and other factors [22–24]. A study conducted by Morawska and colleagues reported that saying “aah” for 30 s released twice as many particles as continual coughing for 30 s. Counting using voiced speech every other 10 s for 2 min resulted in

half the emissions of continual coughing for 30 s. Voiced speech, with vocal folds vibrating, resulted in more particles released than whispering [25]. Chao et al. [26] measured the size distribution of particles emitted while coughing and while counting aloud from 1 to 100. They found that for coughing, the geometric mean diameter of droplets was 13.5 μm. The number of droplets expelled was 947–2085 per cough, and the concentration was 2.4–5.2 droplets/cm^3 per cough. Counting 1–100 resulted in a geometric mean diameter of 16.0 μm, along with 112–6720 total expelled droplets and 0.004–0.223 droplets/cm^3 [26]. Asadi et al. [46] and Alsved et al. [27] reported that both activity and loudness affected the generated respiratory particle emission rate. Alsved et al. [27] reported that breathing generated 85–691 particles/s, normal talking generated 120–1380 particles/s, and loud talking generated 180–1760 particles/s; normal singing generated 320–2870 particles/s, loud singing generated 390–2870 particles/s, and loud singing with exaggerated diction generated 500–2820 particles/s. Gregson et al. [24] reported that breathing generates much less aerosol than for speaking and singing. Like Alsved et al. [27], Gregson et al. [24] found the number for the concentration and emission rate to increase with an increase in loudness during speaking and singing. Ahmed et al. [22] found that more particles are also generated at higher vocalization frequency (i.e., pitch). Lindsley et al. [28] reported that more infectious particles are generated during coughing as compared to normal breathing, although the difference was not substantial. Since people breathe more than they cough, more infectious particles would be generated by breathing over time [28].

7.5 Particle Deposition in a Room

After expiratory emission, airborne respiratory particles undergo deposition onto surfaces via various mechanisms including gravitational settling, thermophoresis, electrophoresis, and Brownian motion. Aerosols remain suspended in the air for minutes to hours and therefore can be transported throughout the room via their initial emission velocity and via the air currents in the room. The particle transport processes are described by Dr. Ahmadi in Chap. 6 of this book. For particles with diameters of approximately 1 μm and larger, gravitational settling is the primary deposition mechanism. The gravitational settling velocity can be calculated via Stokes' law for spheres falling in quiescent fluid using standard correction factors. Terminal settling velocity is reached when the drag force resisting the fall of a spherical particle through a fluid medium is equal to the gravitational force. The gravitational force can be assumed to be constant for normal indoor applications, and the drag force acts opposite to the relative motion of the particle in the air, increasing as the velocity increases. Because the terminal settling velocity increases with the square of the particle diameter, larger particles settle much quicker than smaller particles. For example, Thatcher et al. [29] reported deposition rates of 0.28/h, 1.46/h, and 4.5/h, for 1 μm, 3 μm, and 7 μm diameter particles, respectively, in a furnished room with mean air velocity of 5.4 cm/s.

Studies have compared observed particle deposition rates in indoor environments with those predicted by the Stokes' settling velocity. For example, Thatcher and Layton [30] conducted experiments measuring the deposition of resuspended dust particles ranging from 1 to 10 μm in diameter in a residence. They found that the calculated settling velocity matched well with the experimentally determined settling velocity for particles smaller than 5 μm [30]. However, for the particles 5–10 μm, the experimentally determined settling velocities were smaller than the calculated settling velocities, possibly due to an increase in drag force caused by non-sphericity of the larger particles [30]. Thatcher et al. [29] found that increasing the furnishings and the airspeed in a room increases the particle deposition loss rates. The particle deposition rate for the fully furnished room was a factor of 2.6 larger than the particle deposition rate for the bare room. Also, by increasing the fan speed from <5 to 19 cm/s resulted in a deposition rate affected by a factor of up to 2.4. Thus, airspeed and furnishings should be considered when estimating the bulk deposition rate for respiratory particles.

7.6 Particle Resuspension from Human Activity

Resuspension is the detachment and re-entrainment of settled particles from the surfaces into the surrounding fluid (in this case, air). Resuspension of particles from human activities such as walking, crawling, and sitting on furniture is a major source of indoor airborne particles of both biological and nonbiological origin, with increased contributions to indoor air when settled dust concentrations and/or human activities are elevated [31, 32]. Factors affecting particle resuspension from human walking include the particle type, flooring type, shoe type, surface dust loading, relative humidity, and individual walking style [32].

One of the earliest indoor particle resuspension studies was conducted by Thatcher and Layton [30], who reported that the concentration of particles greater than 1 μm was increased by 100% by walking in the room. Later, researchers found that particles smaller than 1 μm were also easily resuspended via human activity [32]. The resuspension rate increases with increasing particle size due to the relative magnitudes of the adhesive and removal forces. Particle adhesion forces, including van der Waals and electrostatic and capillary forces, are proportional to the particle diameter, but the external forces acting on a particle from air currents, such as those from air squeezed beneath a foot during walking, are proportional to the square of the particle diameter [33]. Thus, larger particles are easier to resuspend. Reported resuspension emission rates range widely from 10^{-6} mg/m^3 for 0.01 μm particles [34] to 10^2 mg/min for 10 μm particles [35]. Flooring type is one of the most important resuspension factors, with higher resuspension fractions associated with carpet than hard flooring when the particle loading on the floor is the same [36, 37]. In addition, the loading of dust is typically higher for carpet as compared to hard flooring because hard flooring is easier to clean, which contributes to the observed

increased resuspension rate for walking on carpeted flooring in real environments [38].

For indoor air studies, resuspension has been quantified in multiple ways, including the following: (1) the increase in airborne particle concentration following a resuspension event; (2) the resuspension emission rate in mass (or particle number) per time; (3) the resuspension fraction, which is the fraction of particles on a surface resuspended from one contact; (4) the resuspension rate coefficient (also called the resuspension rate), which is a first-order rate coefficient; (5) the resuspension flux, which is the mass resuspended per area per time; (6) the resuspension emission factor, which is the ratio of the airborne particle concentration in the volume and settled dust loading on the surface during a resuspension event; and (7) the dust-to-breathing zone transport efficiency, which is the probability that a particle will be resuspended into the breathing zone [30, 35–37, 39–42].

The two most commonly used terms for resuspension are the resuspension rate coefficient and the resuspension fraction. The resuspension rate coefficient R_j for species or size fraction j (units, 1/time) can be expressed as:

$$R_j = S_j / A_r L_j \tag{7.1}$$

where S_j is the emission rate (mass/time) and L_j is the surface loading (mass per area) of the species or size fraction j and A_r is the resuspension area. The resuspension fraction r_j for species or size fraction j (dimensionless) per contact can be expressed as:

$$r_j = S_j / f\ A_s L_j \tag{7.2}$$

where f is the frequency of contact (e.g., per step) and A_s is the contact area. Thus, the source S_j can be calculated with either R_j or r_j as follows:

$$S_j = R_j A_r L_j = r_j f A_s L_j \tag{7.3}$$

The resuspension flux $F_{R,j}$ for species or size fraction j (units, mass per area-time) can also be calculated with either R_j or r_j as follows:

$$F_{R,j} = R_j L_j = r_j f A_s / A_r \tag{7.4}$$

With human activity, the settled viral particles can be resuspended back into the air stream and possibly infect the healthy individual in the room. However, the magnitude of the resuspension source for virus-laden respiratory particles is unknown. Ferro et al. [43] conducted a preliminary study to estimate the size-resolved settling flux, resuspension flux, and airborne concentration of viral particles from direct respiratory emissions versus those from resuspension using a material balance approach and available data from SARS-CoV-2 monitoring campaigns in hospital rooms containing COVID-19 patients. They estimated that the contribution

of resuspension to the airborne SARS-CoV-2 virus concentration would be approximately 1/100 that of the direct emissions. However, many assumptions were made for the calculations, and validation of the results is needed. Specifically, assumptions for the calculations included:

- Instantaneously mixed volume for mass balance approach.
- All particles deposit evenly on the floor (deposition onto other surfaces ignored).
- Deposited particles remain in same size bin for resuspension (incorporation of expiratory droplets onto settled dust particles ignored).
- Resuspension fraction is consistent with previous dust resuspension studies (capillary force for particle adhesion to surface not considered).
- Personal cloud effect ignored (personal cloud would increase exposure of person walking ~2–3×).
- Shedding from skin and clothing ignored (shedding source ~0.3× resuspension from walking source, but with larger intake fraction).
- Resuspension from other surfaces (e.g., furniture) is ignored.
- Hospital ventilation rates; a residential environment with an infected individual would have ~10× the concentration due to reduced ventilation.

Resuspension from clothing may be a more important pathway of exposure than resuspension from flooring due to the closer proximity to the breathing zone both for the emitter and the receptor as well as the differences in fluid flow around the person when the person is stationary versus walking. For example, the intake fraction, or the fraction of particles emitted that are inhaled, for particles resuspended from the clothing of a seated person was estimated to be five times higher than the intake fraction of particles resuspended for a person walking [44]. A study conducted by Ren et al. [45] demonstrated that clothing can act as a vector to transport the bioaerosols that deposit on the surface of clothing. From their study using fluorescent particles as tracers, approximately 46.8% deposited on the clothes were resuspended in a room over the period of 1 h of walking (60 steps/min speed) by the volunteer [45]. More study is required to better understand this exposure pathway for viruses like SARS-CoV-2.

7.7 Conclusions

This chapter includes a characterization of indoor aerosols and bioaerosols, the material balance model for the prediction of concentrations of indoor aerosols, the deposition of particles indoors, and the resuspension of particles from human activities. Resuspended particles from human walking have been well characterized in the scientific literature and are known to play a large role in human inhalation exposure to many indoor pollutants. However, based on preliminary estimates from applying a material balance approach, resuspension from floorings does not appear to be an important source of exposure to airborne viruses. Resuspension from clothing may play a more important role in exposure to viruses. Further study is

needed to confirm these preliminary results and better characterize resuspension of viruses in the indoor environment. Recommended mitigation measures to reduce exposure to resuspended particles indoors include reducing the initial viral particle emission into the indoor air via masks, reducing the concentration of airborne viral particles via ventilation and filtration, and reducing the loading of settled viral particles by maintaining clean surfaces.

References

1. Azimi, P., et al. (2021). Mechanistic transmission modeling of COVID-19 on the Diamond Princess cruise ship demonstrates the importance of aerosol transmission. *Proceedings of the National Academy of Sciences, 118*(8), e2015482118.
2. Li, Y., et al. (2020). Evidence for probable aerosol transmission of SARS-CoV-2 in a poorly ventilated restaurant. *MedRxiv*.
3. Miller, S. L., et al. (2021). Transmission of SARS-CoV-2 by inhalation of respiratory aerosol in the Skagit Valley Chorale superspreading event. *Indoor Air, 31*(2), 314–323.
4. CDC. (2021). *How COVID-19 spreads. COVID-19*. Author. Retrieved December 15, 2021, from https://www.cdc.gov/coronavirus/2019-ncov/
5. NASEM. (2020). *Airborne Transmission of SARS-CoV-2: A Virtual Workshop, Summary statements by Kimberly Prather, Session Chair for "What size particles are generated by people and how do they spread in air?" August 26–27, virtual*.
6. Klepeis, N. E., et al. (2001). The National Human Activity Pattern Survey (NHAPS): A resource for assessing exposure to environmental pollutants. *Journal of Exposure Science & Environmental Epidemiology, 11*(3), 231–252.
7. Bräuner, E., et al. (2014). Typical benign indoor aerosol concentrations in public spaces and designing biosensors for pathogen detection: A review. *Building and Environment, 82*, 190–202.
8. Ruthann, R. A., & Laura, J. P. (2009). Endocrine disrupting chemicals in indoor and outdoor air. *Atmospheric Environment, 43*(1), 170–181.
9. Morawska, L., et al. (2013). Indoor aerosols: From personal exposure to risk assessment. *Indoor Air, 23*(6), 462–487.
10. Douwes, J., et al. (2003). Bioaerosol health effects and exposure assessment: Progress and prospects. *The Annals of Occupational Hygiene, 47*(3), 187–200.
11. Kim, K. H., et al. (2018). Airborne bioaerosols and their impact on human health. *Journal of Environmental Sciences, 67*, 23–35.
12. Wang, C. C., et al. (2021). Airborne transmission of respiratory viruses. *Science, 373*(6558), eabd9149.
13. Xie, W., et al. (2021). The source and transport of bioaerosols in the air: A review. *Frontiers of Environmental Science & Engineering, 15*(3), 1–19.
14. Bourouiba, L., et al. (2014). Violent expiratory events: On coughing and sneezing. *Journal of Fluid Mechanics, 745*, 537–563.
15. Nicas, M., et al. (2005). Toward understanding the risk of secondary airborne infection: Emission of respirable pathogens. *Journal of Occupational and Environmental Hygiene, 2*(3), 143–154.
16. Noakes, C. J., et al. (2006). Modelling the transmission of airborne infections in enclosed spaces. *Epidemiology and Infection, 134*(5), 1082–1091.
17. Stilianakis, N. I., & Drossinos, Y. (2010). Dynamics of infectious disease transmission by inhalable respiratory droplets. *Journal of the Royal Society Interface, 7*(50), 1355–1366.
18. Qian, J., et al. (2008). Estimating the resuspension rate and residence time of indoor particles. *Journal of the Air & Waste Management Association, 58*(4), 502–516.

19. Kopperud, R. J., et al. (2004). Outdoor versus indoor contributions to indoor particulate matter (PM) determined by mass balance methods. *Journal of the Air & Waste Management Association, 54*, 1188–1196.
20. Yamamoto, N., et al. (2015). Indoor emissions as a primary source of airborne allergenic fungal particles in classrooms. *Environmental Science & Technology, 49*, 5098–5106.
21. Jimenez, J. L., & Peng, Z. (2021). *COVID-19 aerosol transmission estimator*. Retrieved December 15, 2021, from https://tinyurl.com/covid-estimator
22. Ahmed, T., et al. (2022). Characterizing respiratory aerosol emissions during sustained phonation. *Journal of Exposure Science & Environmental Epidemiology, 29*, 1–8. doi:10.1038/s41370-022-00430-z. Epub ahead of print. PMID: 35351959; PMCID: PMC8963400.
23. Asadi, S., et al. (2020). Efficacy of masks and face coverings in controlling outward aerosol particle emission from expiratory activities. *Scientific Reports, 10*(1), 1–13.
24. Gregson, F. K., et al. (2021). Comparing aerosol concentrations and particle size distributions generated by singing, speaking and breathing. *Aerosol Science and Technology, 55*(6), 681–691.
25. Morawska, L., et al. (2009). Size distribution and sites of origin of droplets expelled from the human respiratory tract during expiratory activities. *Journal of Aerosol Science, 40*, 256–269.
26. Chao, C. Y. H., et al. (2009). Characterization of expiration air jets and droplet size distributions immediately at the mouth opening. *Journal of Aerosol Science, 40*, 122–133.
27. Alsved, M., et al. (2020). Exhaled respiratory particles during singing and talking. *Aerosol Science and Technology, 54*(11), 1245–1248.
28. Lindsley, W. G., et al. (2016). Viable *influenza A* virus in airborne particles expelled during coughs versus exhalations. *Influenza and Other Respiratory Viruses, 10*(5), 404–413.
29. Thatcher, T. L., et al. (2002). Effects of room furnishings and air speed on particle deposition rates indoors. *Atmospheric Environment, 36*(11), 1811–1819.
30. Thatcher, T. L., & Layton, D. W. (1995). Deposition, resuspension, and penetration of particles within a residence. *Atmospheric Environment, 29*(13), 1487–1497.
31. Nicholson, K. W. (1988). A review of particle resuspension. *Atmospheric Environment (1967), 22*(12), 2639–2651.
32. Qian, J., et al. (2014). Walking-induced particle resuspension in indoor environments. *Atmospheric Environment, 89*, 464–481.
33. Hinds, W. C. (1999). *Aerosol technology: properties, behavior, and measurement of airborne particles* (2nd ed.). Wiley.
34. Benabed, A., et al. (2020). Experimental study of the human walking-induced fine and ultrafine particle resuspension in a test chamber. *Building and Environment, 171*, 106655.
35. Rosati, J. A., et al. (2008). Resuspension of particulate matter from carpet due to human activity. *Aerosol Science and Technology, 42*, 472–482.
36. Qian, J., & Ferro, A. R. (2008). Resuspension of dust particles in a chamber and associated environmental factors. *Aerosol Science & Technology, 42*, 566–578.
37. Tian, Y., et al. (2014). A comparative study of walking-induced dust resuspension using a consistent test mechanism. *Indoor Air, 24*, 592–603.
38. Bramwell, L., et al. (2015). An evaluation of the impact of flooring types on exposures to fine and coarse particles within the residential micro-environment using CONTAM. *Journal of Exposure Science & Environmental Epidemiology, 26*, 86–94.
39. Ferro, A. R., et al. (2004). Source strengths for indoor human activities that resuspend particulate matter. *Environmental Science & Technology, 38*, 1759–1764.
40. Serfozo, N., et al. (2014). The effect of particle resuspension during walking activity to PM10 mass and number concentrations in an indoor microenvironment. *Building and Environment, 82*, 180–189.
41. Wu, T., et al. (2021). Particle resuspension dynamics in the infant near-floor microenvironment. *Environmental Science & Technology, 55*, 1864–1875.
42. You, S., & Wan, M. (2014). Experimental investigation and modelling of human-walking-induced particle resuspension. *Indoor and Built Environment, 24*, 564–576.

43. Ferro, A. R., et al. (2020). *Resuspension exposure assessment for the SARS-CoV-2 virus*. Presented at the International Society of Indoor Air Quality and Climate biannual Indoor Air conference, Virtual, November.
44. Licina, D., et al. (2017). Emission rates and the personal cloud effect associated with particle release from the perihuman environment. *Indoor Air. 27*(4), 791–802. https://doi.org/10.1111/ina.12365
45. Ren, J., et al. (2022). Experimental study to quantify airborne particle deposition onto and resuspension from clothing using a fluorescent-tracking method. *Building and Environment, 209*, 108580.
46. Asadi, S., et al. (2019). Aerosol emission and superemission during human speech increase with voice loudness. *Scientific Reports, 9*(1), 1–10.

Chapter 8
Surveillance of Wastewater for COVID-19

Dana Barry and Hideyuki Kanematsu

Abstract This chapter starts by introducing the topic of wastewater (water that requires cleaning after it is used). It mentions water pollutants and various types of wastewater (sewage) like domestic and industrial sewage. Three main levels of wastewater treatment are presented and described. Also, a section is included that discusses the detection, identification, and disinfection of COVID-19 in municipal wastewater. Since this virus is found in human feces, wastewater surveillance seems to be ideal, noninvasive, cost-effective, and a very useful early warning approach for detecting this disease.

8.1 Introduction

Simply stated, wastewater is any water that requires cleaning after it is used. Examples include water used for toilets, bathing, dishwashing, industrial purposes, etc. Figure 8.1 is a display of raw sewage and industrial waste in the New River as it passes from Mexico to California [1]. Wastewater contains pollutants, unwanted chemicals, or materials that contaminate air, soil, and water. Common water pollutants are complex organic materials, nitrogen- and phosphorous-rich compounds, microplastics, pathogenic organisms (such as bacteria and viruses), and other types of pollutants like sediments, oil, etc. Water pollutants may come from point sources or from dispersed sources. A point source pollutant is from a single pipeline or channel such as a sewage discharge. An example of a dispersed source is surface runoff from farms carrying animal wastes, etc. into nearby streams.

D. Barry (✉)
Department of Electrical & Computer Engineering, Clarkson University, Potsdam, NY, USA

State University of New York at Canton, Canton, NY, USA
e-mail: dmbarry@clarkson.edu

H. Kanematsu
National Institute of Technology, Suzuka College, Shiroko-cho, Suzuka, Mie, Japan
e-mail: kanemats@mse.suzuka-ct.ac.jp

D. Barry, H. Kanematsu (eds.), *Studies to Combat COVID-19 using Science and Engineering*, https://doi.org/10.1007/978-981-19-1356-3_8

Fig. 8.1 This figure shows raw sewage and industrial waste in the New River

The three types of wastewater (sewage) are domestic, industrial, and storm sewage. Domestic sewage carries used water from houses, apartments, college buildings, etc. Industrial sewage contains used water from chemical, manufacturing, and other processes. As for storm sewage, it is runoff water from precipitation that is collected in a system of pipes or open channels. In any case, wastewater requires cleaning. Goals of wastewater management are to clean and protect water. The water should be acceptable for release into rivers, lakes, etc. It should also be clean enough so that it can be used by people for drinking and washing.

8.2 Sewage (Domestic Wastewater) Treatment

Domestic wastewater is produced by a community of people and is generally transported through a sewer system. It usually travels from a building's plumbing into a sewer or into an onsite sewage facility. Domestic sewage is about 99.9% water by weight [2]. The important impurities to mention are putrescible organic materials, plant nutrients, and disease-causing microbes. The amount of putrescible organic material in sewage is indicated by the biochemical oxygen demand (BOD). BOD is the amount of oxygen required by microorganisms to decompose the organic substances in sewage. The higher the concentration of dissolved oxygen, the better the water quality.

Suspended solids in sewage are important because the volume of sludge produced in a treatment plant is directly related to the total suspended solids in the sewage.

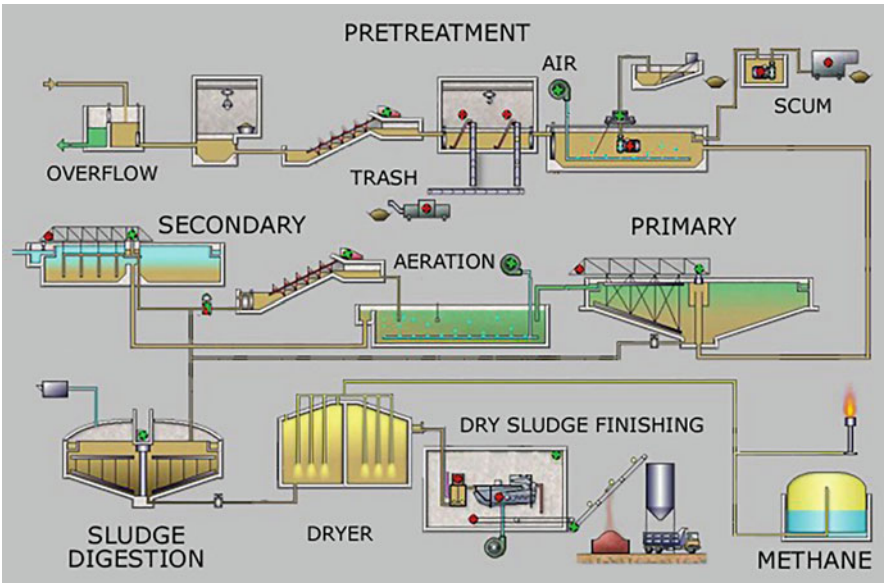

Fig. 8.2 This diagram shows the sewage treatment process

Domestic sewage contains plant nutrients. Excessive amounts of nitrates and phosphates in lakes can result in quick growths of algae. Domestic sewage also contains microorganisms like coliform bacteria and other microbes. A coliform bacterium (a rod-shaped bacterium, especially *E. coli*, that lives in the intestines of healthy people and animals) is found in fecal matter.

A sewage system (wastewater collection) includes a network of pipes, pumping stations, etc. that convey sewage from its starting location to a point of treatment and disposal. Sewage treatment facilities use physical, chemical, and biological processes to purify water. There are three main levels for wastewater treatment [3]. These include primary, secondary, and advanced (tertiary) treatments. Disinfection is the final step which is needed to destroy the remaining pathogens. A simple and general description of these treatment processes is provided. Figure 8.2 is a display of methods used for sewage treatment [4].

PRIMARY TREATMENT: Primary treatment is physical removal of material that floats or readily settles out by gravity. It involves the use of screens and sedimentation tanks, etc. The settled solids are known as raw or primary sludge. This sludge is moved along the bottom of a tank by mechanical scrapers. Then, it is collected in a hopper where the sludge is pumped out for removal. (Note: Sludge waste generated during treatment is stabilized separately. After being dewatered, it is sent to landfills, etc.) Grease and other floating materials are removed by surface-skimming devices.

SECONDARY TREATMENT: Secondary treatment removes more suspended solids and soluble organic matter remaining after the primary treatment. The

removal usually depends on biological processes where microbes consume the organic impurities as food. The microbes convert the organic materials into carbon dioxide, water, and energy for their own growth and reproduction. One main biological process is the trickling filter. This is a fixed bed of rocks over which sewage (wastewater) flows downward and causes microbial slime to grow and consume the organic material. Another process is called activated sludge, which is aerated sewage containing aerobic microorganisms which help to break it down. A third process is the oxidation pond. This is a lagoon that treats wastewater through the interaction of sunlight, bacteria, and algae. The algae grow within the pond and use sunlight to produce oxygen during photosynthesis. Aerobic bacteria use this oxygen to breakdown the organic waste in wastewater.

TERTIARY TREATMENT: Tertiary treatment is used to further treat secondary effluent to remove harmful microbiological contaminants from wastewater. It involves various types of filters and disinfectants (such as chlorine, ultraviolet light, and ozone treatments). Once it has been disinfected, the wastewater is ready to be discharged into the environment.

8.3 Detection, Identification, and Disinfection of COVID-19 in Wastewater

COVID-19 has created a major pandemic with adverse impact on public health and economic activities. Since this virus is found in human feces, wastewater surveillance seems to be ideal, noninvasive, cost-effective, and a very useful early warning approach for detecting COVID-19 [5–11]. This approach is known as wastewater-based epidemiology (WBE).

A wastewater surveillance program for monitoring COVID-19 was developed in 2020 at Clarkson University with the help of Professor Shane Rogers (of Clarkson's Department of Civil and Environmental Engineering) along with his students and colleagues [12]. They prepared seven aboveground wastewater sampler stations located on the campus. Wastewater is pumped through plastic tubing into a 2.5 gallon container at each station. It is collected every 15 min for a 24-h period twice a week. Internal controls maintain a temperature of 4 °C (about 39 °F). The samples are chilled to slow down the decay of the virus.

At the end of the 24-h cycle, the sampler container is detached from the tubing and brought to a lab for testing. To detect the virus in fecal matter diluted by other fluid, the wastewater samples must be re-concentrated using a centrifuge at 300,000 times the force of the Earth's gravity [13]. Once the fecal matter has been concentrated and buffered in new fluid, then the RNA from the virus can be extracted. The viral RNA is a single-stranded nucleic acid that is essential for genetic coding and regulation. Reference number [13] mentions, that the RNA extraction, amplification, and reading processes are basically the same as those used to test nasal swabs but with equipment calibrated for virus RNA detection in sewage

instead of people. The following is a more detailed statement. After the ribonucleic acid is concentrated, it is identified by reverse transcriptase amplification, nucleic acid sequence-based amplification, etc. along with high throughput screening and biosensor assays. Disinfectants are used to control viral spread. They include ultraviolet radiation, ozone, chlorine dioxides, and hypochlorite [14–18].

Measuring COVID-19 in wastewater has proved to be a reliable way of monitoring outbreaks for the virus [19–21]. Wastewater data represents a specified community, while the results of individual tests (like nasal swabs or saliva samples) represent a single person. Wastewater analyses find infections, but it is harder for them to spot emerging variants. In sewage, mostly damaged and degraded viruses are detected. Also, people infected with different variants shed the virus at different rates. However, researchers are figuring out how to monitor variants in wastewater. A team (including a computational biologist at the Swiss Federal Institute of Technology, Zurich) performs DNA sequencing to detect genomic variants in wastewater by using the same protocols as those for clinical samples but also uses a computational method called V-pipe to determine if variants are present [22]. It should be mentioned that in 2020 when the Centers for Disease Control and Prevention (CDC) realized that testing was not available everywhere, it established the National Wastewater Surveillance System (NWSS), a partnership with state health departments.

8.4 Conclusions

This chapter starts by introducing the topic of wastewater (water that requires cleaning after it is used). It mentions water pollutants and various types of wastewater (sewage) like domestic and industrial sewage. Three main levels of wastewater treatment are presented and described. Also, a section is included that discusses the detection, identification, and disinfection of COVID-19 in municipal wastewater. Since this virus is found in human feces, wastewater surveillance seems to be ideal, noninvasive, cost-effective, and a very useful early warning approach for detecting this disease.

References

1. Calexico New River Committee. (2005). *File: Nrborderborderentrythreecolorsmay05-1-.JPG*. License: This image is in the public domain. File: Nrborderborderentrythreecolorsmay05-1-.JPG - Wikimedia Commons.
2. Britannica. (n.d.). *Wastewater treatment. Process, history, importance, systems, & technologies*. Author.
3. Aghalari, Z., Dahms, H. U., Sillanpää, M., Sosa-Hernandez, J. E., & Parra-Saldívar, R. (2020). Effectiveness of wastewater treatment systems in removing microbial agents: A systematic review. *Globalization and Health, 16*(1), 13. https://doi.org/10.1186/s12992-020-0546-y

4. Leonard, G. (2006). *File: ESQUEMPEQUE-EN.jpg*. License: Creative Commons Attribution-Share Alike 2.5. File: ESQUEMPEQUE-EN.jpg - Wikimedia Commons.
5. ASTHO. (n.d.). *Detection of COVID-19 in wastewater*. Author. Retrieved from astho.org
6. Venugopal, A., Ganesan, H., Sudalaimuthu Raja, S. S., Govindasamy, V., Arunachalam, M., Narayanasamy, A., Sivaprakash, P., Rahman, P., Gopalakrishnan, A. V., Siama, Z., & Vellingiri, B. (2020). Novel wastewater surveillance strategy for early detection of coronavirus disease 2019 hotspots. *Current Opinion in Environmental Science & Health, 17*, 8–13. https://doi.org/10.1016/j.coesh.2020.05.003
7. Randazzo, W., Cuevas-Ferrando, E., Sanjuán, R., Domingo-Calap, P., & Sánchez, G. (2020). Metropolitan wastewater analysis for COVID-19 epidemiological surveillance. *International Journal of Hygiene and Environmental Health, 230*, 113621. https://doi.org/10.1016/j.ijheh.2020.113621
8. Mandal, P., Gupta, A. K., & Dubey, B. K. (2020). A review on presence, survival, disinfection/removal methods of coronavirus in wastewater and progress of wastewater-based epidemiology. *Journal of Environmental Chemical Engineering, 8*(5), 104317. https://doi.org/10.1016/j.jece.2020.104317
9. Stawicki, S. P., Jeanmonod, R., Miller, A. C., Paladino, L., Gaieski, D. F., Yaffee, A. Q., De Wulf, A., Grover, J., Papadimos, T. J., Bloem, C., Galwankar, S. C., Chauhan, V., Firstenberg, M. S., Di Somma, S., Jeanmonod, D., Garg, S. M., Tucci, V., Anderson, H. L., Fatimah, L., Worlton, T. J., Garg, M. (2020). The 2019-2020 Novel Coronavirus (Severe Acute Respiratory Syndrome Coronavirus 2) Pandemic: A Joint American College of Academic International Medicine-World Academic Council of Emergency Medicine Multidisciplinary COVID-19 Working Group Consensus Paper. *Journal of Global Infectious Diseases, 12*(2), 47–93. https://doi.org/10.4103/jgid.jgid_86_20
10. de Jong, F. C., GeurtsvanKessel, C. H., Molenkamp, R., Bangma, C. H., & Zuiverloon, T. (2020). Sewage surveillance system using urological wastewater: Key to COVID-19 monitoring? *Urologic Oncology, S1078-1439*(20), 30480–30484. https://doi.org/10.1016/j.urolonc.2020.10.008
11. Majid, S., Farooq, R., Khan, M. S., Rashid, S., Bhat, S. A., Wani, H. A., & Qureshi, W. (2020). Managing the COVID-19 pandemic: Research strategies based on the evolutionary and molecular characteristics of coronaviruses. *SN Comprehensive Clinical Medicine, 2*, 1–10. https://doi.org/10.1007/s42399-020-00457-z
12. Yahoo. (n.d.). *Detecting COVID-19 on campus: Can wastewater provide early warning signs?* Author. Retrieved from yahoo.com
13. Giacomelli, E. (2020). Wastewater tested for virus. *Watertown Daily Times*, A9–A10.
14. Singh, S., Kumar, V., Kapoor, D., Dhanjal, D. S., Bhatia, D., Jan, S., Singh, N., Romero, R., Ramamurthy, P. C., & Singh, J. (2021). Detection and disinfection of COVID-19 virus in wastewater. *Environmental Chemistry Letters, 19*, 1–17. https://doi.org/10.1007/s10311-021-01202-1
15. Sangkham, S. (2021). A review on detection of SARS-CoV-2 RNA in wastewater in light of the current knowledge of treatment process for removal of viral fragments. *Journal of Environmental Management, 299*, 113563. https://doi.org/10.1016/j.jenvman.2021.113563
16. Mohan, S. V., Hemalatha, M., Kopperi, H., Ranjith, I., & Kumar, A. K. (2021). SARS-CoV-2 in environmental perspective: Occurrence, persistence, surveillance, inactivation, and challenges. *Chemical Engineering Journal (Lausanne, Switzerland: 1996), 405*, 126893. https://doi.org/10.1016/j.cej.2020.126893
17. Deckert, A., Anders, S., de Allegri, M., Nguyen, H. T., Souares, A., McMahon, S., Boerner, K., Meurer, M., Herbst, K., Sand, M., Koeppel, L., Siems, T., Brugnara, L., Brenner, S., Burk, R., Lou, D., Kirrmaier, D., Duan, Y., Ovchinnikova, S., Marx, M., Denkinger, C. (2021). Effectiveness and cost-effectiveness of four different strategies for SARS-CoV-2 surveillance in the general population (CoV-Surv Study): A structured summary of a study protocol for a cluster-randomized, two-factorial controlled trial. *Trials, 22*(1), 39. https://doi.org/10.1186/s13063-020-04982-z

18. Ahmed, W., Tscharke, B., Bertsch, P. M., Bibby, K., Bivins, A., Choi, P., Clarke, L., Dwyer, J., Edson, J., Nguyen, T., O'Brien, J. W., Simpson, S. L., Sherman, P., Thomas, K. V., Verhagen, R., Zaugg, J., & Mueller, J. F. (2021). SARS-CoV-2 RNA monitoring in wastewater as a potential early warning system for COVID-19 transmission in the community: A temporal case study. *The Science of the Total Environment, 761*, 144216. https://doi.org/10.1016/j.scitotenv.2020.144216
19. Larsen, D. A., & Wigginton, K. R. (2020). Tracking COVID-19 with wastewater. *Nature Biotechnology, 38*, 1151–1153. https://doi.org/10.1038/s41587-020-0690-1
20. Vaselli, N. M., Setiabudi, W., Subramaniam, K., et al. (2021). Investigation of SARS-CoV-2 fecal shedding in the community: A prospective household cohort study (COVID-LIV) in the UK. *BMC Infectious Diseases, 21*, 784. https://doi.org/10.1186/s12879-021-06443-7
21. Randazzo, W., Truchado, P., et al. (2020). SARS – CoV-2 RNA in Wastewater anticipated COVID-19 occurrence in a low prevalence area. *Water Research, 181*, 115942.
22. Arnaud, C. H. (2021). Weighing wastewater's worth. *Chemical & Engineering News, 99*, 25–27.

Chapter 9
Distributed Consensus-Based COVID-19 Hotspot Density Estimation

Monalisa Achalla, Gowtham Muniraju, Mahesh K. Banavar, Cihan Tepedelenlioglu, Andreas Spanias, and Stephanie Schuckers

Abstract The primary focus of this work is an application of consensus and distributed algorithms to detect COVID-19 transmission hotspots and to assess the risks for infection. More specifically, we design consensus-based distributed strategies to estimate the size and density of COVID-19 hotspots. We assume every person has a mobile device and rely on data collected from the user devices, such as Bluetooth and Wi-Fi, to detect transmission hotspots. To estimate the number of people in a specific outdoor geographic location and their proximity to each other, we first perform consensus-based distributed clustering to group people into sub-clusters and then estimate the number of users in a cluster. Our algorithm has been configured to work for indoor settings where we consider the signal attenuation due to walls and other obstructions, which are detected by using the Canny edge detection and Hough transforms on the floor maps of the indoor space. Our results on indoor and outdoor hotspot simulations consistently show an accurate estimate of the number of people in a region.

M. Achalla · M. K. Banavar (✉) · S. Schuckers
Department of Electrical & Computer Engineering, Clarkson University, Potsdam, NY, USA
e-mail: achalls@clarkson.edu; mbanavar@clarkson.edu; sschucke@clarkson.edu

G. Muniraju · C. Tepedelenlioglu
Department of Engineering, Arizona State University, Tempe, AZ, USA
e-mail: gmuniraj@asu.edu; cihan@asu.edu

A. Spanias
Department of Engineering and the SenSIP Center, Arizona State University, Tempe, AZ, USA
e-mail: spanias@asu.edu

D. Barry, H. Kanematsu (eds.), *Studies to Combat COVID-19 using Science and Engineering*, https://doi.org/10.1007/978-981-19-1356-3_9

9.1 Introduction

The alarming rise of a COVID-19 pandemic brought the whole world to a halt in early 2020. The pandemic affected world economies and tremendously impacted the livelihood of people. The development and distribution of vaccinations helped in combating the virus to an extent, but there is always a risk from new variants and future pandemics. According to WHO, the Delta variant (B.167.2) [1] has been the "fastest and fittest" variant yet and 50–60% more transmissible than the original COVID-19 strain. The spread of Delta variant became a troubling statistic for countries around the globe. However, on 26 November 2021, WHO designated the variant B.1.1.529 a variant of concern, named Omicron. The WHO has called [2] Omicron a "variant of concern" and warned that the global risks posed by it were "very high," despite what officials described as a multitude of uncertainties. Cases have been identified in dozens of countries on every continent except Antarctica.

The adversities caused by this pandemic emphasize the need for extensive and ongoing research in the development of solutions that can help minimize the spread of any pandemic. Therefore, the development of stronger disease surveillance systems is essential—not only for detecting new variants as they emerge but also to monitor the impacts of those new variants on the effectiveness of our efforts against them—efforts including but not limited to distancing measures, masking, and vaccines. To help control the spread of the pandemic and be ready for the future ones, numerous solutions have been developed. There have been solutions with different approaches like machine learning/AI techniques [3–6], proximity detection with Bluetooth Low Energy signals [7, 8], epidemiological models [9, 10], etc. This work focuses primarily on transmission hotspots that are defined as a collection of "individuals in space and time where the density of contact between infected and uninfected persons is higher than average, increasing the risk for disease transmission" [11]. We focus on the estimation of potential transmission hotspots, using network size estimation and counting of mobile network nodes. This approach together with location mapping techniques can provide real-time risk information to mobile phone users about the areas that they plan to visit.

We use consensus-based strategies for estimating network size [12–15], node locations [16], and node counts [17] in a network created based on minimal transmit–receive data. In order to estimate the number of devices in a specific geographic location and their proximity to each other, we first perform consensus-based distributed clustering to group people into sub-clusters and then estimate the number of users in each sub-cluster. In indoor settings, we consider signal attenuation due to walls and other obstructions and identify walls and other obstructions using Canny edge detection and Hough transforms. Since consensus methods allow us to use a decentralized architecture and distributed processing, our approach will show improvements in terms of accuracy and power consumption.

We will also present our graphical user interface (GUI) that performs network size estimation and node counting over a specific area, only using local communications. The GUI has controls to perform clustering using the density-based spatial clustering of applications with noise (DBSCAN) algorithm and then selects a cluster to run distributed algorithms to obtain network size and node count. Our results on indoor and outdoor hotspot simulations consistently show an accurate estimate of the number of devices in a region and their proximity.

9.2 Background

A wireless sensor network (WSN) is a group of specialized distributed sensors used to monitor various conditions such as temperature, pressure, sound vibration, and pollutant levels [18–21]. Wireless sensor networks are also widely used in industrial and commercial applications. Applications include indoor/outdoor sensing [22], environmental monitoring [23], power monitoring [24], tracking a target or predicting the dynamics of a target [25], network security [26], localization [27, 28], Internet of things (IoT) [29], and detection and estimation [30, 31]. All WSNs are broadly classified into two types as centralized WSNs and distributed WSNs. In a centralized WSN, there is a central node (fusion center) controlling the entire network, and the fusion center has all the data from the sensor nodes (Fig. 9.1).

A distributed wireless sensor network, does not have a fusion center. The sensor nodes exchange data only with their neighbors (Fig. 9.2).

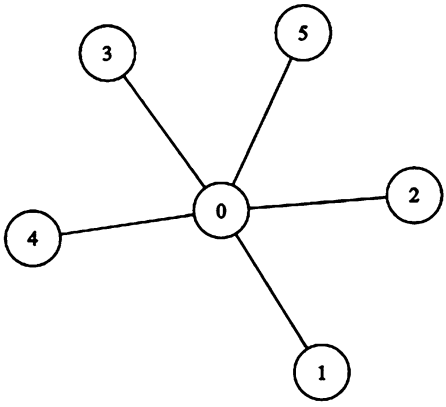

Fig. 9.1 A centralized WSN with the node marked '0' node acting as the fusion center

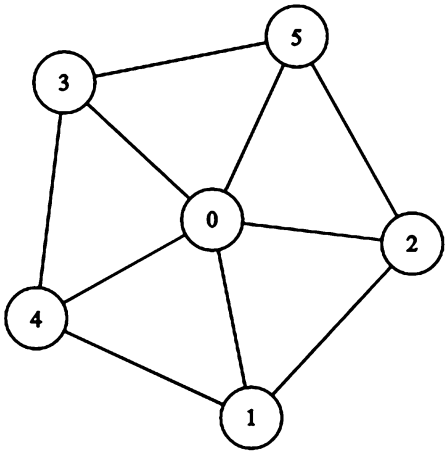

Fig. 9.2 A distributed WSN

The consensus problem, in a WSN has a long history of research in the fields of computer and network science. It requires an agreement among a number of agents to derive a single data value [32]. In WSN consensus, algorithms converge to a global agreement relying on local communications [33, 34]. The most widely used consensus algorithm is the average consensus [35]. In average consensus problems, the states of nodes are designed to converge to the average or the sample mean of the initial measurements or states.

The networks in a specific region with users are modelled as graphs where the user devices represent nodes and possible connections between the user devices represent edges of the network. Given a network of N nodes, we model the communication among the nodes as a connected undirected graph $\mathcal{G} = (\mathcal{V}, \mathcal{E})$, where $\mathcal{V} = \{1, \cdots, N\}$ is the set of nodes and $\mathcal{E}$ is the set of edges connecting the nodes. In case of an indoor setting, we consider the signal attenuation due to walls and other obstructions and then decide the existence of an edge between the nodes. The set of neighbors of node i is denoted by $\mathbb{N}_i = \{j | \{i, j\} \in \mathcal{E}\}$. The degree of the i-th node, denoted by $d_i = |\mathbb{N}_i|$, is the number of neighbors of the i-th node. The degree matrix $\mathbf{D}$ is a diagonal matrix that contains the degrees of the nodes. The connectivity structure of the graph is characterized by the adjacency matrix $\mathbf{A}$ defined by $a_{ij} = 1$ if $\{i, j\} \in \mathcal{E}$ and $a_{ij} = 0$ otherwise.

We consider a potential cluster as a network of devices (nodes), wherein a node i can communicate with other nodes that are within the communication radius, which depends on the transmission power of the node. Each node maintains a real-valued state and can generate a random vector, which is used to propagate cluster labels. At

each iteration, nodes broadcast their state values to their neighbors in a synchronized fashion. Every node is capable of locally estimating their own location [16, 36] and degree by exchanging information with their neighboring nodes. We develop algorithms to form sub-networks and reach consensus on the total number of active nodes and edges of a network, using only local communications.

The network creation and estimation using consensus algorithms heavily relies on the environment in which we are operating in. Hence detection of obstacles/walls in an environment becomes a crucial step. We have employed certain steps for wall detection using floor maps and the algorithms have been detailed in Sect. 9.3.1. The consensus algorithms for distributed node counting and distributed network size estimation have been detailed in Sects. 9.3.3 and 9.3.4.

9.3 Algorithms

9.3.1 Wall Detection Algorithm

In indoor environments, the signal attenuation [37] between the devices needs to be taken into account before network creation. The floor map of an environment is taken and position of walls and various obstacles are detected using various image processing algorithms. Figure 9.3 shows the flow chart of all steps involved in detection of walls.

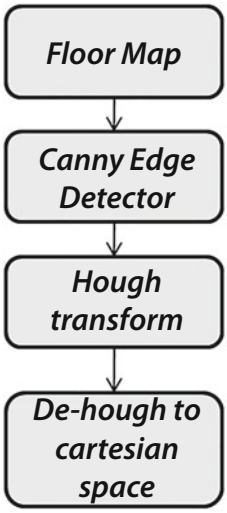

Fig. 9.3 Image processing methods for wall detection

To detect walls or obstacles in an indoor setting, we take floor maps of indoor spaces and transform the floor map into Hough space [38]. De-Houghing the transformed images provides us with information about the locations of walls. The Hough transform is implemented by quantizing the Hough parameter space into finite intervals or accumulator cells [39]. As the algorithm runs, each edge pixel (p_i, q_i) is transformed into a discretized (r, θ) curve and the accumulator cells which lie along this curve are incremented. Resulting peaks in the accumulator array represent strong evidence that a corresponding straight line exists in the image. Mapping back from Hough transform space into Cartesian space yields a set of line descriptions (walls) of the image subject. It has been reported in the literature [40] that the presence of a solid obstacle between nodes increases the attenuation of the signal and reduces the proximity by about twice the actual proximity.

Once walls are detected, we create network in the given indoor space using only local communication between nodes. For N nodes present in a location, networks are created based on two factors: the radius r and the presence of walls/obstacles in between two nodes. Two nodes i and j are considered neighbors if the distance is smaller than the specified radius. An adjacency matrix of size (i, j) describes the network. Let $W(i, j)$ be the wall descriptor matrix; if wall is present between two nodes i and j, $W(i, j) = 1$, else $W(i, j) = 0$.

The following is the algorithm for network creation:

Algorithm 1: Algorithm for network creation

```
if W(i,j)=0 then
    if Distance(i, j) < r then
        A(i,j)=1;
        else
            A(i,j)=0;
        end
    end
end
if W(i,j)=1 then
    if Distance(i, j) < r/2 then
        A(i,j)=1;
        else
            A(i,j)=0;
        end
    end
end
```

9.3.2 DBSCAN Clustering

Networks are clustered into sub-networks using distributed DBSCAN algorithm [41]. Clustering [42] is a technique that involves the grouping of data points. Given a set of data points, clustering algorithms are used to classify each data point into a specific group. The data points that are in the same group should have similar properties and/or features, while data points in different groups should have highly dissimilar properties and/or features. Distributed DBSCAN algorithm [41] is a clustering algorithm to group the network of nodes into sub-networks in a distributed way. The algorithm mainly depends on 2 parameters, i.e., the minimum number of points η within the radius of ϵ of that node. The first step of DBSCAN [43, 44] is to classify all the points into core points, reachable points, and outliers. Node a is a core point if at least η nodes are within its ϵ radius. Node b is directly reachable from a if node b is within ϵ radius from node a. Node b is reachable from node a if there is a path with all nodes being core points. All other not reachable nodes from any other nodes are considered as outliers. If node a is a core point, then it forms a cluster together with all nodes (core or non-core) that are reachable from it. In the sub-networks formed by DBSCAN, all nodes within the cluster are mutually connected, and if a node is density-reachable from another node within the sub-network, it is part of the same sub-network as well.

9.3.3 Distributed Average Consensus for Node Counting

In an average consensus problem, the nodes reach consensus on the global average of all sensed data based on only local communications [45]. It is assumed that nodes can communicate only with their neighbors and there is no communication noise between nodes (Fig. 9.4).

Consider $\mathbf{x}(0)$ to be the initial state values of the nodes in the network. The distributed node counting algorithm [12, 17] is formulated by relating the network size N of a graph with average consensus as

$$N \approx \frac{\frac{1}{N}\sum_{i=1}^{N} x_i^2(0)}{\mathbb{E}\left[\left(\frac{1}{N}\sum_{i=1}^{N} n_i x_i(0)\right)^2\right]}, \tag{9.1}$$

where $n_i \sim \mathcal{N}(0,1)$ is an i.i.d. Gaussian random variable. The node counting algorithm involves 3 steps: first, estimate the value of the numerator in Eq. (9.1), using the average consensus on the node state values. Assuming consensus is reached in t^* iterations,

$$z_i(t^*) \approx \lim_{t\to\infty} z_i(t) = \frac{1}{N}\sum_{i=1}^{N} x_i^2(0) = \frac{1}{N}||\mathbf{x}(0)||_2^2. \tag{9.2}$$

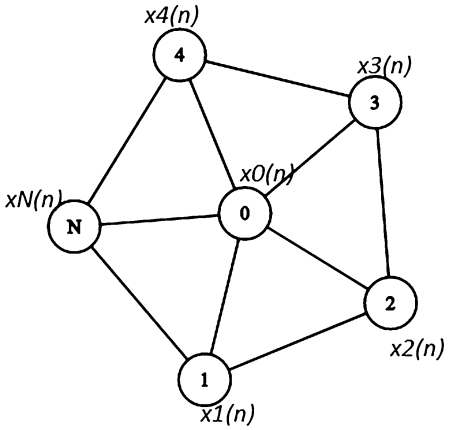

Fig. 9.4 Network model for average consensus

Next, in order to compute the denominator in Eq. (9.1), each node i generates a $K \times 1$ initial state vector, $\mathbf{y}_i(0) = [y_i^{(1)}(0), \cdots, y_i^{(K)}(0)]$, where the k-th element $y_i^{(k)}(0) = n_i^{(k)} x_i(0)$ and $n_i^{(k)}$ is a random variable drawn from any continuous distribution with mean 0 and variance 1. The average consensus is performed in parallel on each k-th element of $\mathbf{y}_i(0)$ using distributed average consensus. Assuming average consensus is reached at after t^* iterations $\mathbf{y}_i(t^*) \approx \lim_{t\to\infty} \mathbf{y}_i(t) = \frac{1}{N}\sum_{i=1}^{N} \mathbf{y}_i(0)$. Next, a post-processing function $g(\cdot)$ is applied at each node by squaring each element in the $K \times 1$ state vector $\mathbf{y}_i(t^*)$ and computing the average. For node i, the post-processing is performed as $g(\mathbf{y}_i(t^*)) = \frac{1}{K}\sum_{k=1}^{K} \left(y_i^{(k)}(t^*)\right)^2$. The post-processed result $g(\mathbf{y}_i(t^*))$ can be related to the l_2 norm of the initial measurements $\mathbf{x}(0)$ as

$$g(\mathbf{y}_i(t^*)) \approx \frac{1}{N^2}||\mathbf{x}(0)||_2^2. \tag{9.3}$$

The estimate of network size $\hat{N}$ is computed by taking the ratio of node state values computed in previous steps, i.e., Eqs. (9.2) and (9.3), as follows:

$$\hat{N}_i(t^*) = \frac{z_i(t^*)}{g(\mathbf{y}_i(t^*))}. \tag{9.4}$$

Note that computation of $z_i(t^*)$ and $g(\mathbf{y}_i(t^*))$ can be performed simultaneously, reducing the computation time.

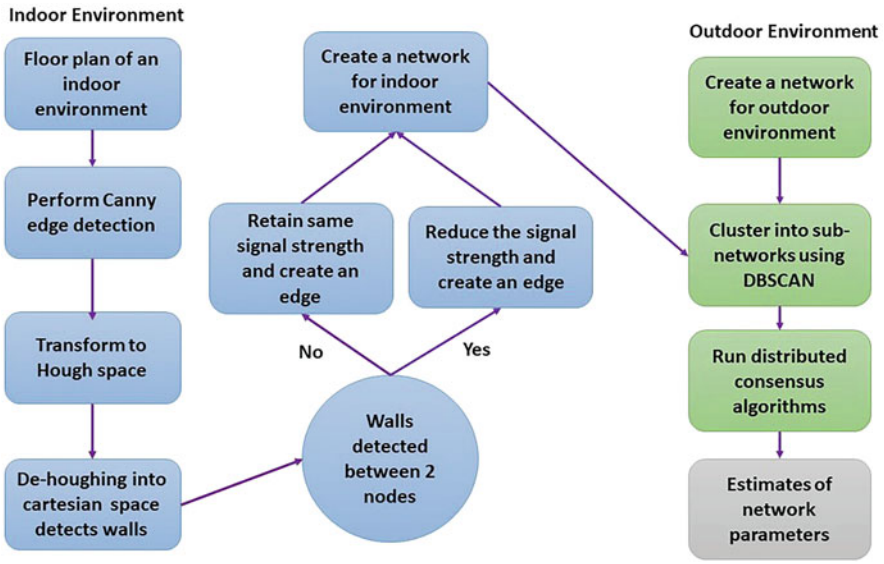

Fig. 9.5 Flowchart showing the steps involved in the creation of networks, clustering of nodes/users, and estimation of network characteristics

9.3.4 Distributed Network Size Estimation

In this section, we discuss the approach to estimate the number of nodes and edges in the COVID-19 hotspots. The flowchart of our proposed algorithm is shown in Fig. 9.5. The global characteristics of a network can be inferred using the consensus-based distributed algorithms on the larger network. However, in order to find the local characteristics, clustering algorithms are run on a larger network, to form the sub-networks, over which distributed algorithms are run to obtain local characteristics.

We use a wall detection algorithm, as discussed in Sect. 9.3.1, to detect the walls in the indoor setting and then establish an edge between two nodes which contains a wall between only if the signal strength between them is above a threshold τ. Alternatively, in case of outdoor setting, an edge is formed between two nodes if they are within the communication radius ϵ within each other.

The DBSCAN algorithm (Sect. 9.3.2) forms clusters by sharing the label to the neighboring nodes (label propagation), if there are at least η number of nodes within the communication radius of ϵ. Finally, after the sub-networks are formed, we run the distributed node counting (Sect. 9.3.3) and distributed edge counting algorithms (Sect. 9.3.4), to reach consensus on the number of nodes and edges in each sub-network. Our solutions thus allow a user to accurately estimate the number of devices and the size of the network within a certain radius.

9.4 Methodology

In a given geographical location, we create networks only based on local communications between the devices in a distributed fashion. We rely on the signal strength between the nodes for proximity calculation. However, in indoor environments, the proximity calculation often becomes tricky as the signal between nodes is attenuated due to the presence of walls and obstructions between the nodes. Hence, wall detection becomes a crucial step in network creation and estimation for indoor spaces, and various methods have been discussed in the literature for wall detection. Estimation of the presence of line of sight between nodes [46] using RSSI signal quality and using floor maps are among the commonly used wall detection methods. In this chapter, we take floor maps of each environment and use image processing techniques like Canny edge detection and Hough transform for wall detection as described in Sect. 9.3.1.

Once environment-appropriate networks have been created, we create clusters of users in close proximity. It has been observed that clustering users and using these clusters to estimate local hotspot density, where the spread of disease would be higher than in the network as a whole, is advantageous. Among the existing distributed clustering algorithms such as k-means, spectral clustering [47], and expectation maximization algorithms, DBSCAN (density-based spatial clustering of applications with noise) is optimal for distributed implementation as it is robust to communication noise and quantization and requires lower computational complexity to implement.

DBSCAN is then followed by density estimation in each cluster. This is performed using distributed note counting as detailed in Sect. 9.3.3. DBSCAN and the other distributed algorithms we use do not store any information about individual nodes and run only using local communications between nodes. This ensures that the privacy of all users/nodes is preserved. On every clustered hotspot, distributed consensus algorithms detailed in Sect. 9.3.1 have been run. The algorithms estimate hotspot characteristics like the number of nodes and edges present. Figure 9.5 summarizes the steps starting form network creation to using distributed consensus algorithms for approximating characteristics of clustered hotspots.

9.5 Simulation Results

In this section, we discuss the graphical user interfaces (GUIs) that have been developed for network size estimation in both indoor and outdoor settings. The GUIs are designed to give the estimates of the number of devices (nodes) and the number of edges (connections between the nodes) in any given network. Our algorithm can be actively tuned to provide the risk assessment based on the most recent public health guidelines.

To demonstrate our results for an indoor setting, we have used the floor map of Science Center, Clarkson University, shown in Fig. 9.6, and detect the presence of walls. The first step in wall detection is performing Canny edge detection to detect the edges in an image. Once the edges are detected through a Canny edge detector, the next step is to apply the Hough transform for exactly detecting the wall locations (Figs. 9.7, and 9.8). The image in Hough space is De-Houghed and the walls and obstacles in the floor map are reconstructed and detected as shown in Fig. 9.9.

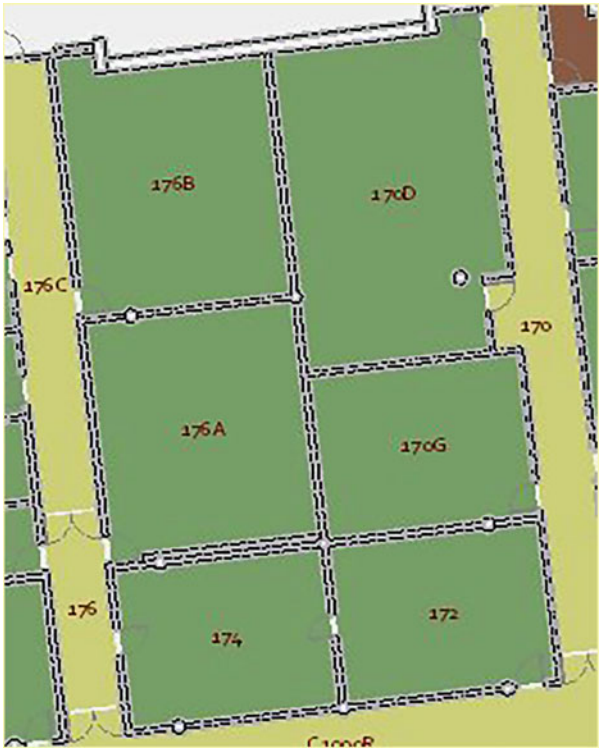

Fig. 9.6 Floor map of Science Center, Clarkson University

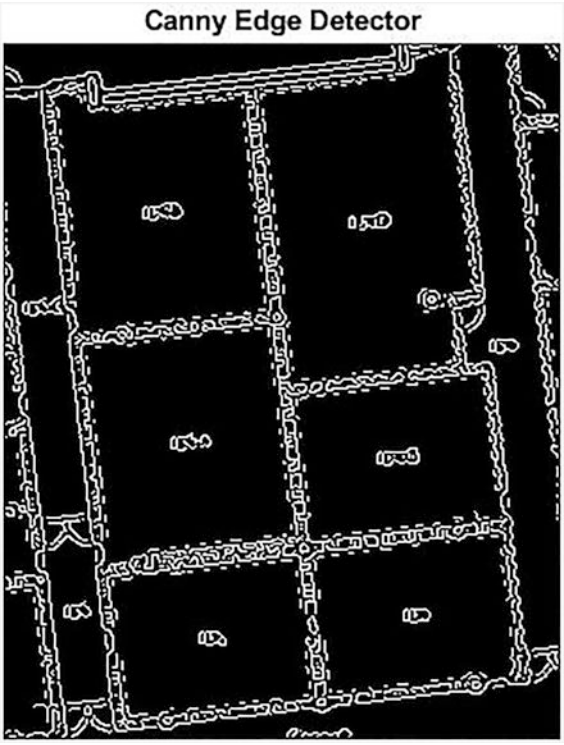

Fig. 9.7 Floor map of Science Center after passing through the Canny edge detector

We create a network with 160 nodes and run the distributed DBSCAN algorithm, with communication range ϵ as six feet. The DBSCAN clustered the nodes into 4 major clusters with nearly 6 nodes as outliers. The resulting clusters are shown in Fig. 9.10.

Consensus-based distributed algorithms as discussed above are used on clustered hotspots of Fig. 9.10.

The distributed average consensus algorithms as discussed in Sect. 9.3.3 are used on each cluster to estimate the number of nodes each cluster. The results of node and edge count estimates are in Figs. 9.11 and 9.12. In Table 9.1, we summarize the node and edge count estimates for each hotspot/cluster.

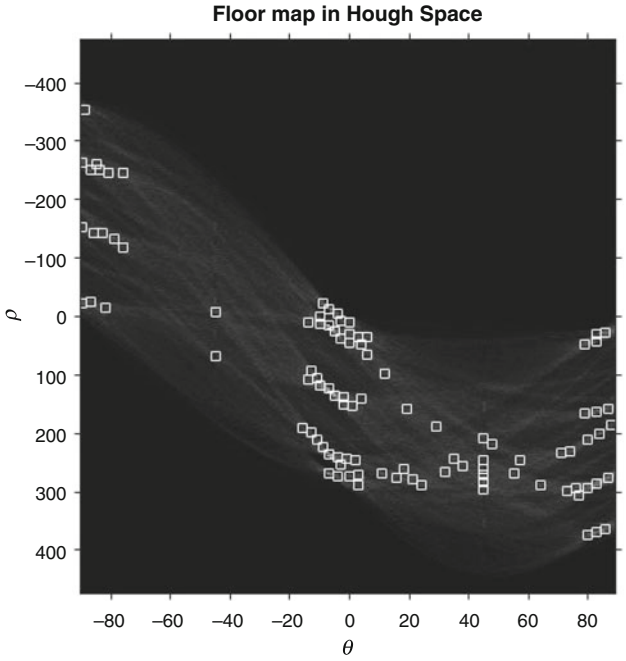

Fig. 9.8 Floor map of Science Center transformed into Hough space

9.5.1 GUI Demonstration

We developed a GUI in which a user can create networks in an environment of their choice and fine-tune the parameters like network range and number of nodes. The GUI shows the clusters formed on the right side and also gives details about each cluster and the estimated number of nodes (Fig. 9.13).

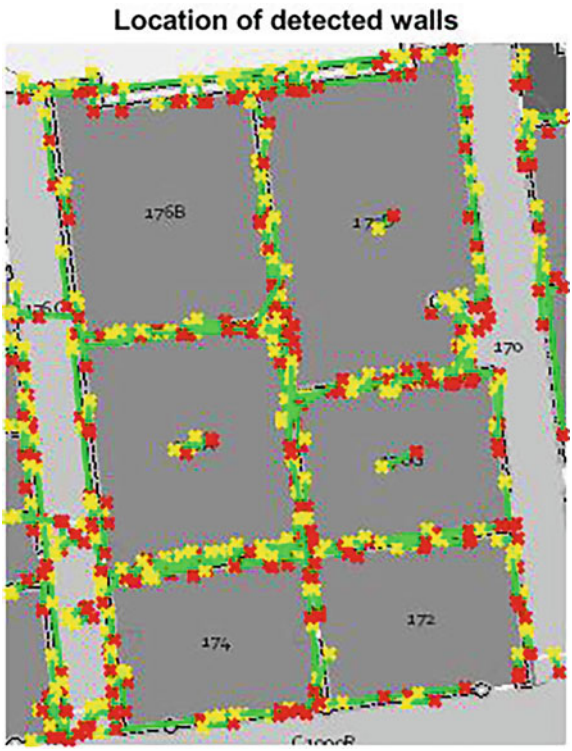

Fig. 9.9 Walls detected and reconstructed in Science Center, Clarkson University

For an outdoor setting, we verify our proposed algorithm by conducting experiments on synthetic data. We generate the hotspots using uniformly distributed nodes as shown in Fig. 9.14, which has 5 clusters with a total node count of $N = 250$. We tune the parameters η and ϵ and run the clustering algorithm by setting $\eta = 10$

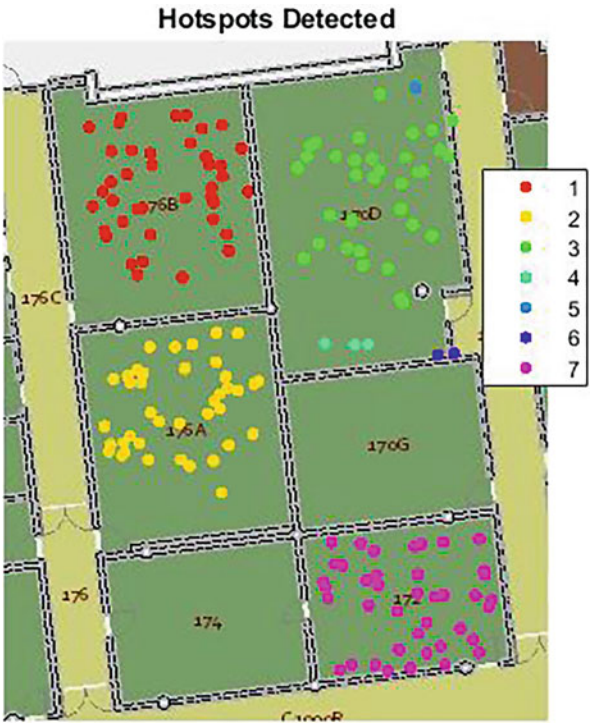

Fig. 9.10 Clustering the network using the DBSCAN algorithm helps in identifying COVID hotspots where the risk of disease spread is higher. The image shows hotspots across classrooms in Science Center, Clarkson University

and $\epsilon = 4$. As seen from Fig. 9.14, DBSCAN finds 5 clusters each forming a sub-network, along with 7 outliers (in red). Next, distributed node and edge counting is performed on each cluster and the result of the convergence of the consensus algorithm is also displayed.

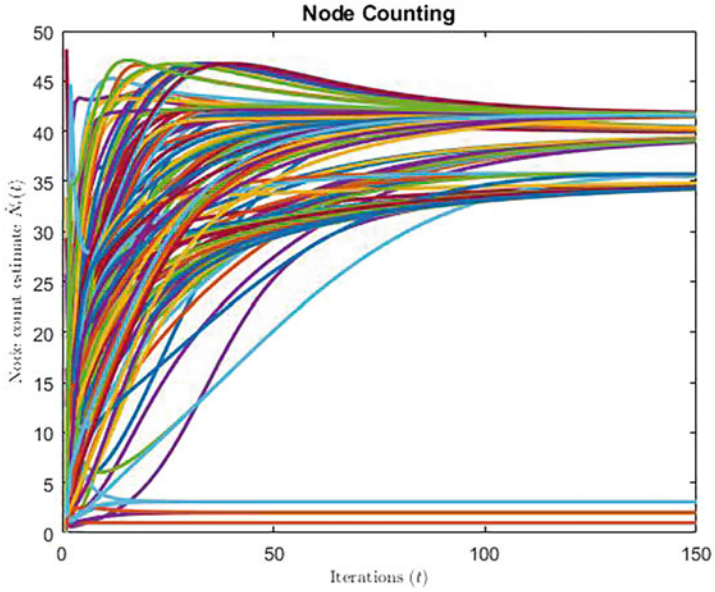

Fig. 9.11 The consensus algorithm is run for 150 iterations and it converges at a count of 40 nodes for three clusters and 34 for one cluster, and the node count below five as shown in the image above corresponds to the outliers

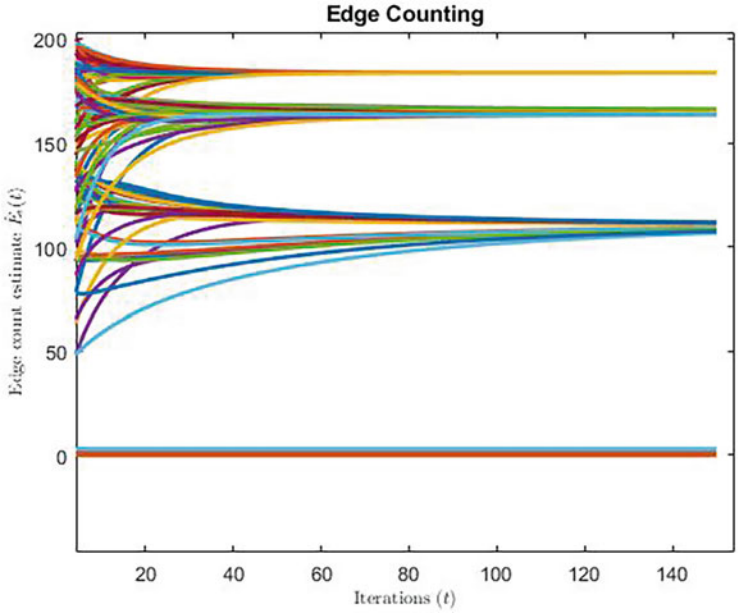

Fig. 9.12 Estimated edge count averaged over 150 iterations using consensus algorithms

Table 9.1 Number of nodes and edges estimated in each hotspot using consensus algorithms

Hotspot or cluster	Number of nodes estimated	Number of edges estimated
Cluster 1	40	183
Cluster 2	40	167
Cluster 3	34	112
Cluster 4	40	164
Outliers	6	–

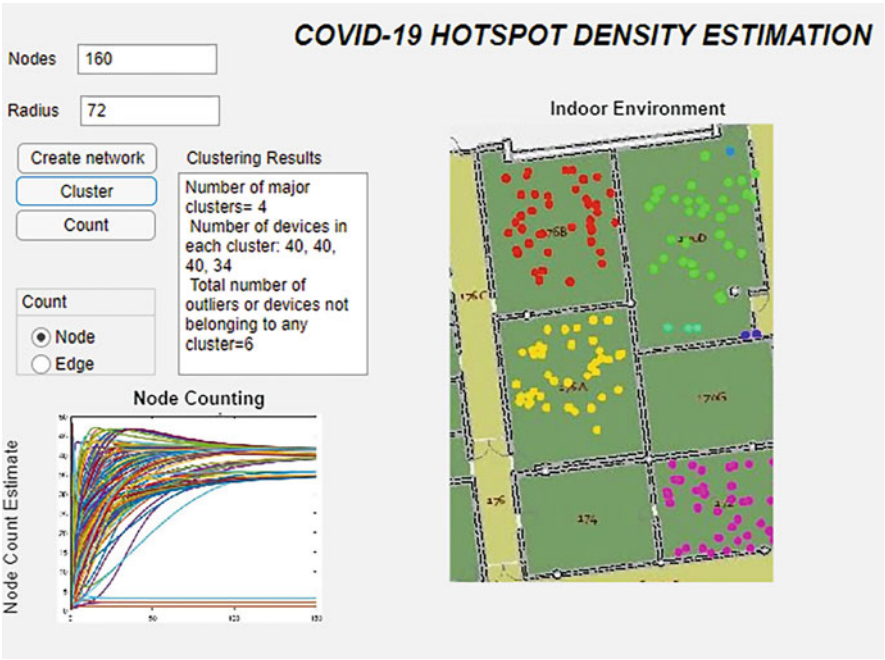

Fig. 9.13 GUI developed for hotspot detection application in an indoor setting. Wall detection algorithm is run on the floor map to detect the walls and the communication network was formed with 160 nodes and a communication range of six feet. On clustering the network using DBSCAN algorithm, the algorithm primarily identified four major clusters. Six nodes were identified as outliers

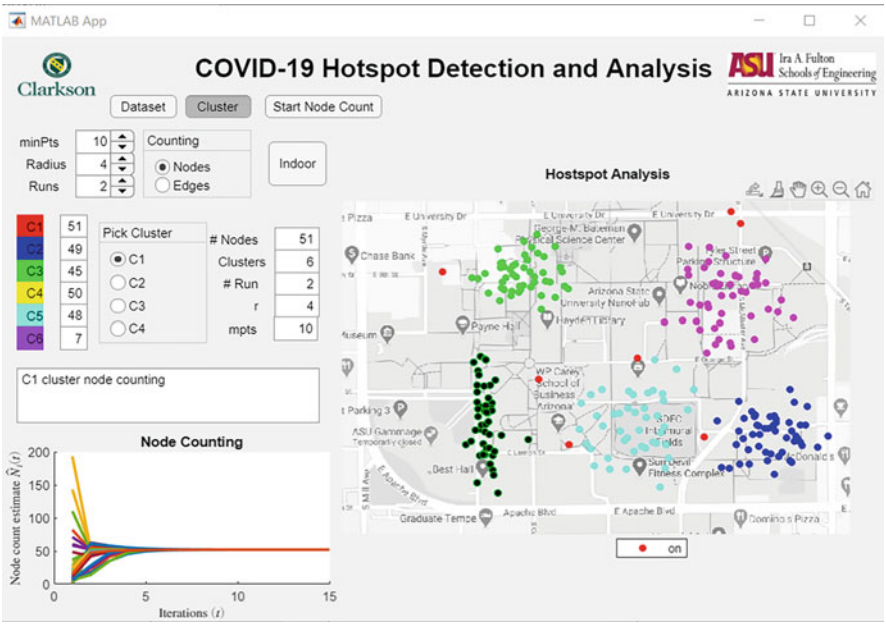

Fig. 9.14 GUI developed for hotspot detection in an outdoor setting. The DBSCAN algorithm grouped the nodes into 5 clusters and 7 outliers (in red). As shown in the left corner, distributed node and edge counting algorithms converge to the true values

9.6 Conclusions

In this chapter, we presented a suite of distributed algorithms to estimate the network size of clusters of devices and identify potential hotspots. We illustrated the working of our algorithm via simulation results and presented our GUIs that illustrate our work. Our algorithms will enable users to estimate the density of users in a region, leading to the identification of the seriousness of risk.

In future work, we will include localization algorithms in our proposed approach, which will not only enable us to calculate the proximity among the users but also help us identify absolute locations of concern. Our approach together with location mapping techniques can provide real-time risk information to mobile phone users about the areas that they plan to visit. Our research has applicability to other fields such as 5G+ communications, increasing the accuracy of location information and indoor user tracking. It can also be applied to robotics, location-aware patient care, and other mobile health applications.

Acknowledgments The authors from Arizona State University and Clarkson University are funded by NSF Awards 2032114 and 2032106, respectively.

References

1. https://www.yalemedicine.org/news/5-things-to-know-delta-variant-covid
2. https://www.nytimes.com/article/omicron-coronavirus-variant.html
3. Kwekha-Rashid, A. S., Abduljabbar, H. N., & Alhayani, B. (2021). Coronavirus disease (covid-19) cases analysis using machine-learning applications. *Applied Nanoscience* 1–13. https://pubmed.ncbi.nlm.nih.gov/34036034/
4. Banoei, M. M., Dinparastisaleh, R., Zadeh, A. V., & Mirsaeidi, M. (2021). Machine-learning-based covid-19 mortality prediction model and identification of patients at low and high risk of dying. *Critical Care, 25*(1), 1–14. https://link.springer.com/article/10.1007/s13204-021-01868-7#citeas
5. Mbunge, E., Akinnuwesi, B., Fashoto, S. G., Metfula, A. S., & Mashwama, P. (2021). A critical review of emerging technologies for tackling covid-19 pandemic. *Human Behavior and Emerging Technologies, 3*(1), 25–39.
6. Abd-Alrazaq, A., Schneider, J., Mifsud, B., Alam, T., Househ, M., Hamdi, M., & Shah, Z. (2021). A comprehensive overview of the covid-19 literature: Machine learning–based bibliometric analysis. *Journal of Medical Internet Research, 23*(3), e23703.
7. Su, Z., Pahlavan, K., & Agu, E. (2021). Performance evaluation of COVID-19 proximity detection using Bluetooth LE signal. *IEEE Access, 9*, 38891–38906.
8. Bahle, G., Fortes Rey, V., Bian, S., Bello, H., & Lukowicz, P. (2021). Using privacy respecting sound analysis to improve Bluetooth based proximity detection for covid-19 exposure tracing and social distancing. *Sensors, 21*(16), 5604.
9. Saldaña, F., & Velasco-Hernández, J. X. (2021). Modeling the covid-19 pandemic: A primer and overview of mathematical epidemiology. arXiv preprint arXiv:2104.08118.
10. Ledder, G., & Homp, M. (2021). Using a covid-19 model in various classroom settings to assess effects of interventions. *PRIMUS* 1–20. https://www.tandfonline.com/doi/full/10.1080/10511970.2020.1861143
11. de Jong, B. C., Gaye, B. M., Luyten, J., van Buitenen, B., André, E., Meehan, C. J., O'iochain, C., Tomsu, K., Urbain, J., Grietens, K. P., et al. (2019). Ethical considerations for movement mapping to identify disease transmission hotspots. *Emerging Infectious Diseases, 25*(7), e181421. https://www.tandfonline.com/doi/full/10.1080/10511970.2020.1861143
12. Zhang, S., Tepedelenlioglu, C., & Spanias, A. (2019). Distributed network center area estimation. US Patent 10,440,553.
13. Schizas, I. D., Mateos, G., & Giannakis, G. B. (2009). Distributed LMS for consensus-based in-network adaptive processing. *IEEE Transactions on Signal Processing, 57*(6), 2365–2382.
14. Zhu, S., Chen, C., Ma, X., Yang, B., & Guan, X. (2014). Consensus based estimation over relay assisted sensor networks for situation monitoring. *IEEE Journal of Selected Topics in Signal Processing, 9*(2), 278–291.
15. Spanos, D. P., Olfati-Saber, R., & Murray, R. M. (2005). Dynamic consensus on mobile networks. In *IFAC World Congress* (pp. 1–6).
16. Zhang, S., Tepedelenlioglu, C., Spanias, A., Banavar, M. (2018). Distributed network structure estimation using consensus methods. *Synthesis Lectures on Communications, Morgan & Claypool, 10*(1), 1–88.
17. Zhang, S., Tepedelenlioğlu, C., Banavar, M. K., & Spanias, A. (2016). Distributed node counting in wireless sensor networks in the presence of communication noise. *IEEE Sensors Journal, 17*(4), 1175–1186.
18. Stankovic, J. A. (2008). Wireless sensor networks. *Computer, 41*(10), 92–95.
19. Akyildiz, I. F., Su, W., Sankarasubramaniam, Y., & Cayirci, E. (2002). A survey on sensor networks. *IEEE Communications Magazine, 40*(8), 102–114.
20. Chong, C.-Y., & Kumar, S. P. (2003). Sensor networks: evolution, opportunities, and challenges. *Proceedings of the IEEE, 91*(8), 1247–1256.
21. Culler, D., Estrin, D., & Srivastava, M. (2004). Guest editors' introduction: Overview of sensor networks. *Computer, 37*(8), 41–49.

22. Banavar, M. K., Zhang, J. J., Chakraborty, B., Kwon, H., Li, Y., Jiang, H., Spanias, A., Tepedelenlioglu, C., Chakrabarti, C., & Papandreou-Suppappola, A. (2015). An overview of recent advances on distributed and agile sensing algorithms and implementation. *Digital Signal Processing, 39*, 1–14.
23. Castillo-Effer, M., Quintela, D. H., Moreno, W., Jordan, R., & Westhoff, W. (2004). Wireless sensor networks for flash-flood alerting. In *Proceedings of the Fifth IEEE International Caracas Conference on Devices, Circuits and Systems, 2004* (Vol. 1, pp. 142–146). IEEE.
24. Banavar, M. K., Tepedelenlioglu, C., & Spanias, A. (2012). Distributed SNR estimation with power constrained signaling over Gaussian multiple-access channels. *IEEE Transactions on Signal Processing, 60*(6), 3289–3294.
25. Zhou, Y., & Maskell, S. (2017). RB2—PF: A novel filter-based monocular visual odometry algorithm. In *2017 20th International Conference on Information Fusion (Fusion)* (pp. 1–8). IEEE.
26. Usman, M., Muthukkumarasamy, V., Wu, X.-W., & Khanum, S. (2012). Securing mobile agent based wireless sensor network applications on middleware. In *2012 International Symposium on Communications and Information Technologies (ISCIT)* (pp. 707–712). IEEE.
27. Zhang, X., Tepedelenlioglu, C., Banavar, M., & Spanias, A. (2016). Node localization in wireless sensor networks. *Synthesis Lectures on Communications, 9*(1), 1–62.
28. Simonetto, A., Keviczky, T., & Dimarogonas, D. V. (2012). Distributed solution for a maximum variance unfolding problem with sensor and robotic network applications. In *2012 50th Annual Allerton Conference on Communication, Control, and Computing (Allerton)* (pp. 63–70). IEEE.
29. Lee, J., Stanley, M., Spanias, A., & Tepedelenlioglu, C. (2016). Integrating machine learning in embedded sensor systems for internet-of-things applications. In *2016 IEEE International Symposium on Signal Processing and Information Technology (ISSPIT)* (pp. 290–294). IEEE.
30. Tepedelenlioglu, C., Banavar, M. K., & Spanias, A. (2011). On the asymptotic efficiency of distributed estimation systems with constant modulus signals over multiple-access channels. *IEEE Transactions on Information Theory, 57*(10), 7125–7130.
31. Zhang, X., Tepedelenlioglu, C., Banavar, M. K., & Spanias, A. (2018). Distributed location detection in wireless sensor networks. US Patent 10,028,085.
32. Hou, W., Fu, M., Zhang, H., & Wu, Z. (2017). Consensus conditions for general second-order multi-agent systems with communication delay. *Automatica, 75*, 293–298.
33. Ren, W., Beard, R. W., & Atkins, E. M. (2005). A survey of consensus problems in multi-agent coordination. In *Proceedings of the 2005, American Control Conference, 2005* (pp. 1859–1864). IEEE.
34. Kar, S., & Moura, J. M. (2008). Distributed consensus algorithms in sensor networks with imperfect communication: Link failures and channel noise. *IEEE Transactions on Signal Processing, 57*(1), 355–369.
35. Xiao, L., Boyd, S. (2004). Fast linear iterations for distributed averaging. *Systems & Control Letters, 53*(1), 65–78.
36. Zhang, X., Tepedelenlioğlu, C., Banavar, M. K., Spanias, A., & Muniraju, G. (2019). Location estimation and detection in wireless sensor networks in the presence of fading. *Physical Communication, 32*, 62–74.
37. Ali-Rantala, P., Ukkonen, L., Sydanheimo, L., Keskilammi, M., Kivikoski, M. (2003). Different kinds of walls and their effect on the attenuation of radiowaves indoors. In *IEEE Antennas and Propagation Society International Symposium. Digest. Held in conjunction with: USNC/CNC/URSI North American Radio Sci. Meeting (Cat. No. 03CH37450)* (Vol. 3, pp. 1020–1023). IEEE.
38. Furukawa, Y., Shinagawa, Y. (2003). Accurate and robust line segment extraction by analyzing distribution around peaks in Hough space. *Computer Vision and Image Understanding, 92*(1), 1–25.
39. Kamat-Sadekar, V., Ganesan, S. (1998). Complete description of multiple line segments using the Hough transform. *Image and Vision Computing, 16*(9–10), 597–613.

40. Banavar, M. K., Wickramasinghe, S., Achalla, M., & Sun, J. (2021). Ordinal UNLOC: Target localization with noisy and incomplete distance measures. *IEEE Internet of Things Journal, 8*(23), 17111–17119.
41. Liu, J., Huang, J. Z., Luo, J., & Xiong, L. (2012). Privacy preserving distributed dbscan clustering. In *Proceedings of the 2012 Joint EDBT/ICDT Workshops* (pp. 177–185)
42. https://towardsdatascience.com/the-5-clustering-algorithms-data-scientists-need-to-know
43. Ester, M., Kriegel, H.-P., Sander, J., Xu, X., et al. (1996). A density-based algorithm for discovering clusters in large spatial databases with noise. *Kdd, 96*(34), 226–231.
44. Schubert, E., Sander, J., Ester, M., Kriegel, H. P., & Xu, X. (2017). Dbscan revisited, revisited: Why and how you should (still) use dbscan. *ACM Transactions on Database Systems (TODS), 42*(3), 1–21.
45. Nedic, A., Ozdaglar, A., & Parrilo, P. A. (2010). Constrained consensus and optimization in multi-agent networks. *IEEE Transactions on Automatic Control, 55*(4), 922–938.
46. Achalla, M., Mack, K., Banavar, M. K., Vanitha, M., & Krishnamoorthi, H. (2020). Statistical methods for fast los detection for ranging and localization. In *2020 International Conference on Emerging Trends in Information Technology and Engineering (ic-ETITE)* (pp. 1–5). IEEE.
47. Muniraju, G., Zhang, S., Tepedelenlioglu, C., Banavar, M. K., Spanias, A., Vargas-Rosales, C., &Villalpando-Hernandez, R. (2017). Location based distributed spectral clustering for wireless sensor networks. In *2017 Sensor Signal Processing for Defence Conference (SSPD)* (pp. 1–5). London: IEEE.

Chapter 10
Antiviral Drugs, Antibodies, and Vaccines for COVID-19

Dana Barry and Hideyuki Kanematsu

Abstract This chapter starts by introducing COVID-19 and its variants. Then it gives brief descriptions of the human immune system and COVID-19 testing methods for antigens and antibodies. Information is also provided about COVID-19 treatments with antiviral drugs and antibodies. Finally, there is a discussion about vaccines including Pfizer, Moderna, and Johnson & Johnson.

10.1 Introduction

COVID-19 is a respiratory disease caused by SARS-CoV-2 (severe acute respiratory syndrome coronavirus 2). It is contagious and can affect many parts of the human body. Some general symptoms include a cough, digestive problems, a fever, trouble breathing, and the loss of taste and smell. It is mainly spread between people in close contact and by droplets from sneezes and coughs of those with the virus. To help prevent and slow down the spread of the virus, individuals should wear masks (especially inside buildings), keep a social distance of at least 6 ft, and frequently wash their hands with soap and water. Vaccines and antiviral drugs have been developed to provide protection from this disease. Figure 10.1 shows the structure of a coronavirus with its harmful spikes that can attack the lungs [1].

Variants of the coronavirus are emerging and spreading worldwide. Therefore, vaccines and treatments are needed to protect us from COVID-19, the novel coronavirus. Mutations occur in life. Each time a virus replicates, it is possible that the genetic code won't be copied correctly. The errors are inside the new virus

D. Barry (✉)
Department of Electrical & Computer Engineering, Clarkson University, Potsdam, NY, USA

State University of New York at Canton, Canton, NY, USA
e-mail: dmbarry@clarkson.edu

H. Kanematsu
National Institute of Technology, Suzuka College, Shiroko-cho, Suzuka, Mie, Japan
e-mail: kanemats@mse.suzuka-ct.ac.jp

D. Barry, H. Kanematsu (eds.), *Studies to Combat COVID-19 using Science and Engineering*, https://doi.org/10.1007/978-981-19-1356-3_10

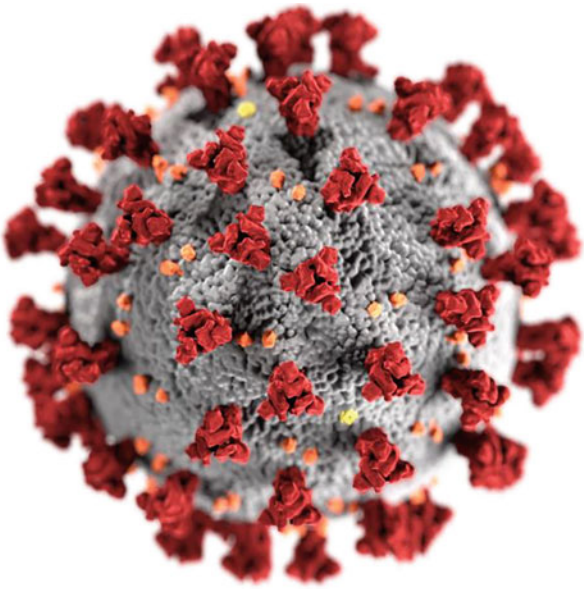

Fig. 10.1 This figure shows the structure of a coronavirus with its harmful spikes

particles that leave one person and move on to infect others. Some mutations die out, while others survive and spread. It should be mentioned that deletions or changes of single amino acids (in viruses) can change the shapes of different proteins which in turn may alter a virus's properties. Mutations on the spike protein (of SARS-CoV-2) are a problem because this protein is the target of antibody treatments and is mimicked by the COVID-19 vaccines. Researchers are especially concerned by changes (errors) in two parts of the spike protein. One part is the beginning of the protein (N-terminal domain) which is targeted by some antibodies. The other is the receptor-binding domain that attaches to ACE2 receptors on human cells and starts the infection.

Mutations that increase infectivity or allow a virus to better escape our immune systems are variants of concern by public health organizations [2]. Some variants of concern to the World Health Organization (as of September 2021) include Alpha, Beta, and Delta. Alpha was first identified in the UK in September 2020 and drove the second wave of the coronavirus in the UK. It is the first new strain of the originally discovered COVID-19 and is also known as B.1.1.7. It contains mutations in the spike protein. Beta was first documented in South Africa in May 2020 and appeared to be more infectious than the original virus. It is known as B.1.351 and has mutations in the spike protein. Delta has been dominant in Europe and the United States. It also caused a rise of virus cases in Asia as well as in India, where it was identified in October 2020. Data, gathered by the Centers for Disease Control and Prevention, show that Delta is much more transmissible than the original virus and can infect and be spread by fully vaccinated people [3]. People infected with Delta

have an increased amount of the virus in their respiratory system, so they may expel more virus into the air and cause the disease to spread faster. Delta is also known as B.1.617.2 and has the L452R spike protein mutation. This mutation involves a swap of the amino acid leucine for the amino acid arginine in the receptor-binding domain. As of late November 2021, the news media mentioned that the Omicron variant (B.1.1.529) of COVID-19 was first discovered in Botswana and then in South Africa. It seems to be very contagious and spreads quickly. Researchers determined that this variant has a high number of mutations. So far, according to the global health agency, about 30 of them have been identified in the spike protein. This is the part of the virus that binds to human cells which allow it to enter our bodies. As of December 2021, the Omicron variant has already appeared in Europe, Canada, Israel, Hong Kong, the United States, and other locations. NOTE: Variants arise in areas with low vaccination rates. Moderna, Pfizer, and J&J say they will update their vaccines to adapt for Omicron if it is resistant to their current vaccines. As of January 2022, Pfizer and Moderna are preparing a vaccine for the Omicron variant.

10.2 The Immune System

The immune system is very important because it protects the human body from germs, harmful substances, etc. that could make individuals sick. It includes cells, proteins, and various organs. Several examples are mentioned. Bone marrow produces white blood cells which target invading viruses. Skeletal muscles, especially the large muscles of the butt and thighs, release immuno-protective compounds during exercise. When the immune system causes part of our body to become red, swollen, hot, and painful (inflamed), it uses secreted proteins called cytokines to fight disease, fix injuries, and to get rid of germs or invaders [4]. Neutrophils (white blood cells) are also found in these areas of inflammation. The human body has an innate immune system and an adaptive immune system. When pathogens try to enter our bodies, the innate immune system is ready. The surface area of the skin provides a physical barrier. Also, mucous membranes secrete many kinds of enzymes to protect us like lysozyme, a component of saliva, sweat, and tears. The digestive system helps too because the stomach contains hydrochloric acid that kills bacteria and more. The innate immune system provides a general defense against viruses, etc. and mainly fights using immune cells like the natural killer cells and phagocytes. Phagocytes engulf and devour (eat) foreign particles. The process is called phagocytosis. See Fig. 10.2 [5]. (A macrophage is a large phagocytic cell.) It should be mentioned that for the innate immune response, macrophages quickly arrive at the infection site. They try to combat the microbes and collect information about them. Then they transmit the information to helper T cells which transmit signals (e.g., proteins such as cytokines) to killer T cells. The helper T cells also transmit information to B cells which finally produce antibodies.

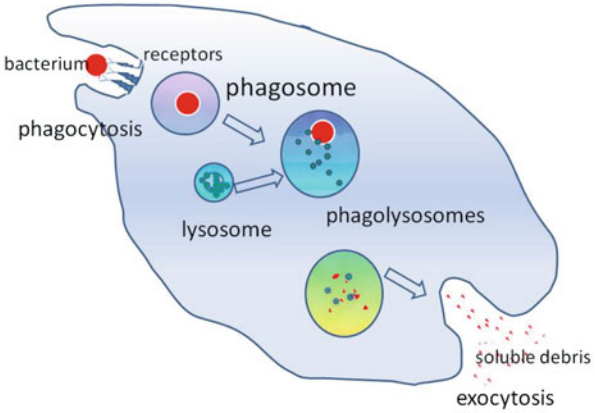

Fig. 10.2 A simple diagram of the phagocytosis process is displayed

The adaptive immune system uses lymphocytes known as B cells which produce antibodies. The antibodies fight certain germs that the body has previously encountered. They are special proteins produced in response to foreign substances called antigens. The antibody combines with a specific antigen and deactivates it. This type of immune system also involves T cells (thymus-derived lymphocytes, white blood cells). T cells can destroy foreign tissue directly. The adaptive immune system has the potential to compensate the weak points of the original immune response. If the immune response system works well, then a virus could be suppressed and controlled. Figure 10.3 shows the T-lymphocyte activation pathway [6].

Notice the major histocompatibility complex (MHC) mentioned in Fig. 10.3. It refers to a set of closely linked polymorphic genes that code for cell surface proteins that are essential for the adaptive immune system. These cell surface proteins are called MHC molecules.

10.3 Testing Methods for COVID-19

COVID-19 testing involves collecting and analyzing samples to determine if individuals currently have or previously had the disease. The two main testing methods are to detect the presence of the virus or of antibodies produced as a response to the infection. Tests that look for the virus by detecting the presence of its RNA (ribonucleic acid) are called molecular tests. As of 2021, a common form of this test (also referred to as a nucleic acid test) was the reverse transcription-polymerase chain reaction (RT-PCR) test [7]. To start, a sample (that might contain some virus RNA) is extracted from a nose or throat swab. Reverse transcription converts RNA into DNA. The polymerase chain reaction replicates a segment of the transcribed DNA numerous times to create enough of it for analysis. Short, virus-

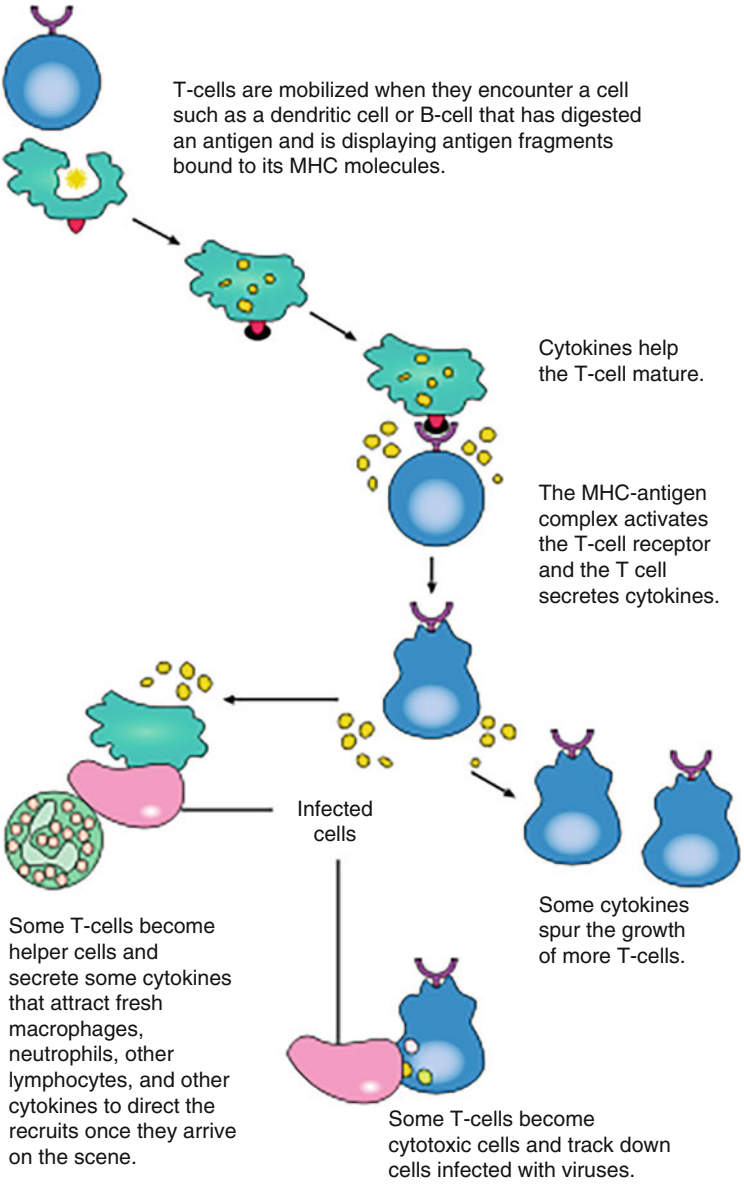

Fig. 10.3 This diagram shows the T-lymphocyte activation pathway. Some T cells direct and regulate immune responses and others directly attack infected cells

specific oligonucleotide probes with a fluorophore on one end bind to the copies. An enzyme cleaves the probe, which causes fluorescence and confirms infection. This type of test gives accurate results early in the infection of an individual but typically

Fig. 10.4 Above is an example of nucleic acid testing using an Abbott Laboratories ID NOW device

takes a few hours to complete. Figure 10.4 shows an example of nucleic acid testing using an Abbott Laboratories ID NOW device [8]. In more recent work, a small graphene transistor (developed by Dacheng Wei and colleagues at Fudan University) accurately detects COVID-19 virus RNA with speed and high sensitivity. The graphene transistor is covered with Y-shaped DNA fragments that bind to two genes encoded in the RNA genome of SARS-CoV-2. Viral RNA that binds to the DNA probes changes the current that flows through the transistor. This allows the researchers to measure the viral load in the sample [9]. Another molecular test involves CRISPR gene editing technology. CRISPR (clustered regularly interspaced short palindromic repeats) technology has primarily been used as a tool in gene editing. It identifies DNA sequences inside of cells and alters them. This technology has been modified to detect specific genes like those in COVID-19. CRISPR-based COVID-19 diagnostic systems have advantages such as a high detection speed, high sensitivity and precision, portability, and no need for specialized laboratory equipment [10].

Tests that look for parts of the virus (like fragments of viral proteins) are called antigen tests. In the case of a coronavirus, the antigens are often proteins from the surface spikes. Samples (mostly collected on swabs) are exposed to paper strips containing antibodies designed to bind to coronavirus antigens. Antigens bind to the strips and provide a visual readout for a positive result. These tests tend to be faster and cheaper than most nucleic acid tests. Various companies in the United States and other countries have developed antigen tests. However, Abbott's BinaxNOW COVID-19 Ag Card is the first SARS-CoV-2 antigen test to win an emergency use authorization from the US Food and Drug Administration, for a test that does not require a separate instrument to analyze its results. This authorization took place in

August 2020 [11]. The test has a lateral flow assay that shows a positive result as a pair of colored lines on a test strip. The process is fast and resembles a pregnancy test. Now antigen tests are available to self-administer at home. One of these tests is the BinaxNOW COVID-19 Self-Test for Antigens [12].

The breath test is another way to detect COVID-19. This type of testing, developed by Singapore-based Breathonix, is an alternative method to test for COVID-19. Infections with this virus cause metabolic changes that alter the ratios of volatile organic compounds (VOCs) in exhaled breath. Drivers crossing into Singapore at the Tuas Checkpoint need to roll down their windows and exhale into a large, disposable, cigar-sized mouthpiece connected to a mass spectrometer. In less than 60 s, their breath sample is analyzed to determine whether they have COVID-19 [13, 14]. Mass spec machines are expensive and too big to be used in many settings where rapid testing is needed. However, Singapore's Breathonix has gotten around this problem by putting the mass spectrometer on-site and using the Tuas Checkpoint to make the investment worthwhile. Other companies like Israel's Scentech Medical and TeraGroup and Owlstone Medical in the UK have started Breathalyzer-like tests to detect COVID-19.

Our bodies produce antibodies in response to viruses. Individuals, who have had COVID-19 in the past, have antibodies for that virus. These antibodies help neutralize the infections. Many types of antibody tests are available. They are used to detect antibodies in a person's blood, serum, or plasma sample. Most antibody tests mix a person's sample with viral proteins or protein fragments. The individual's antibodies bind to them. The antibody-protein complex can be detected with an antibody that produces a color or fluorescent result.

10.4 Antiviral Drug Treatments for COVID-19

People suffering with COVID-19 could be treated with antiviral drugs. During the pandemic, the antiviral medication remdesivir was authorized for emergency use to treat COVID-19. It helps fight the virus and was developed by Gilead Sciences. A group (led by researchers at the Chinese Academy of Sciences, Zhejiang University, and Tsinghua University) showed that the drug works by binding the viral polymerase to prevent it from copying RNA. This action shuts down the virus production [15, 16]. Remdesivir acts as a prodrug for the nucleotide adenosine. After it diffuses into cells, enzymes convert it to the monophosphate before it disrupts production of new strands of the virus's RNA. Remdesivir is metabolically activated to a nucleoside triphosphate metabolite, which is incorporated into the SARS-CoV-2 RNA viral chains. This prevents replication of the virus [17]. Figure 10.5 shows the conversion of remdesivir to the monophosphate and finally to a nucleoside triphosphate metabolite [18]. As of October 2021, it was the only antiviral drug approved by the Food and Drug Administration. However, it is an injectable drug that is mainly used for hospitalized adult patients.

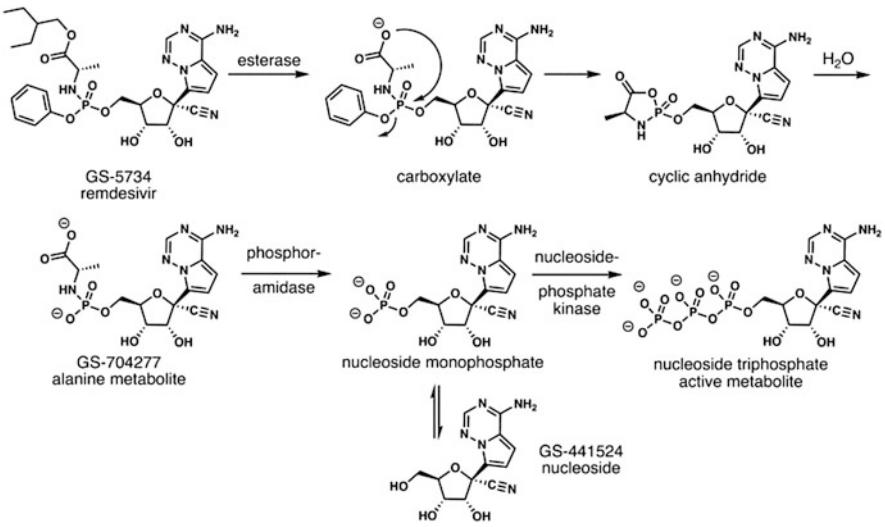

Fig. 10.5 Above is a diagram showing the conversion of remdesivir to the monophosphate

Two antiviral pills for COVID-19 include molnupiravir and PF-07321332. The pill form is advantageous because it is easier to distribute to patients, easier to take, and less of a burden on hospitals. Merck & Company and its partner Ridgeback Biotherapeutics are seeking authorization from the US Food and Drug Administration for emergency use of molnupiravir. They also hope to get approval from other regulatory agencies in the world. This oral antiviral drug reduces the risk of death and hospitalization by 50% for people with mild to moderate cases of COVID-19. The companies reported that it is equally effective at treating other variants of the disease including the Delta strain [19]. The pills are meant for people sick with COVID-19 but are not in the hospital. Also, they may be helpful to individuals who can't have the vaccine. The medicine should be taken as soon as a person has symptoms of the disease. The treatment requires 40 pills over a 5-day period (8 pills each day). These antiviral pills are designed to block the virus from replicating. Simply stated, molnupiravir tricks the virus into using the drug for replicating the virus's genetic material. The drug inserts errors (mutations) into the genetic code so that the virus can't replicate [20, 21]. In addition, Pfizer's pill known as PF-07321332 is another option for stopping the COVID-19 infection early enough to prevent hospitalization. The pill is expected to be effective at the early stages of the disease. It is a protease (enzyme) inhibitor that has successfully shut down the replication machinery of the virus SARS-CoV-2. Also, other antiviral pills are being developed by Atea Pharmaceuticals, Roche, etc.

10.5 Antibody Treatments for COVID-19

An antibody is a Y-shaped protein used by the immune system to identify and neutralize antigens (foreign items like pathogenic bacteria and viruses). It is also known as an immunoglobulin. Antibodies contained in convalescent plasma are used to treat some hospitalized COVID-19 patients who are in the early stages of their illness or have weakened immune systems. Convalescent plasma therapy uses blood donated by people who have recovered from COVID-19 and have antibodies to the virus. This treatment only involves the plasma and antibodies of the donated blood and needs to be compatible with an individual's blood type. It is administered intravenously and has the goals of lessening the severity and/or the length of the disease.

Eli Lilly and Company's monoclonal antibody (bamlanivimab) was granted authorization for emergency use by the US Food and Drug Administration (FDA) for treatment of COVID-19 on November 9, 2020 [22, 23]. It binds to the spike protein to help prevent the virus from entering human cells [24–26]. In April 2021, the FDA revoked the authorized emergency use of bamlanivimab because some virus variants were resistant to it. However, it is still authorized for use when combined with Lilly's second antibody, etesevimab. NOTE: Simply stated, a monoclonal antibody is made by cloning a unique white blood cell. It is generally made in a laboratory and given to patients directly with an infusion. This type of antibody is designed to target a specific virus or bacteria and bind to it to prevent it from infecting human cells.

Regeneron Pharmaceuticals manufactured an antibody cocktail containing two monoclonal antibodies that target the SARS-CoV-2 spike protein. The antibodies bind two distinct and nonoverlapping sites. This antibody cocktail is called REGEN-COV and contains casirivimab and imdevimab. Figure 10.6 is a simple display of the antibody cocktail bound to the receptor-binding domain of a SARS-CoV-2 spike protein [27]. Former President Donald Trump received this treatment, which got authorized for emergency use in the US by the Food and Drug Administration on November 21, 2020. It can stop the virus from infecting cells almost immediately but can't take the place of vaccines because the antibodies have short life spans [28]. Regeneron partnered with Roche to improve global access to the drug. Just like other antibody therapies, this one is given as an infusion in a hospital setting.

Vir Biotechnology, working with GlaxoSmithKline, successfully developed a monoclonal antibody therapy for treating COVID-19. Their antibody (sotrovimab) was granted an emergency use authorization by the US Food and Drug Administration on May 26, 2021. Sotrovimab is used for treating mild to moderate COVID-19 in people at high risk of progressing to a severe case of the disease. In a phase 3 clinical trial, the drug reduced the risk of hospitalization or death in high-risk adults by 85% when compared to the placebo. Previously in 2003, Vir looked for antibodies from a person who had recovered from an infection with severe acute respiratory syndrome coronavirus (SARS-CoV). The company found an antibody that neutralized both SARS-CoV and the novel coronavirus SARS-CoV-2. This

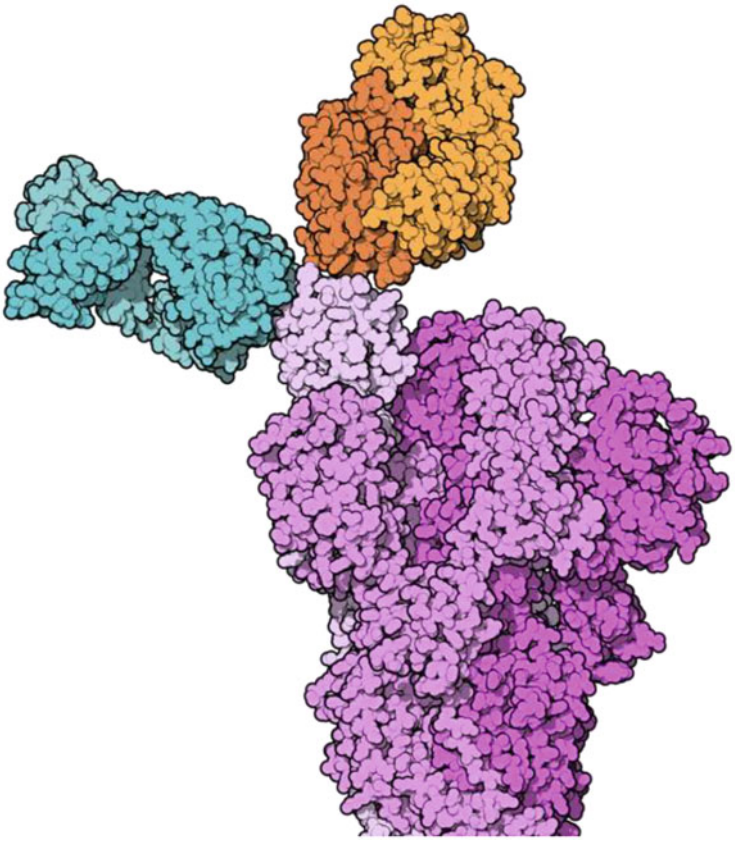

Fig. 10.6 Above is a display of the antibody cocktail's components casirivimab (blue) and imdevimab (orange) bound to the receptor-binding domain (pale pink) of a SARS-CoV-2 spike protein (medium/dark pink)

antibody binds to a part of the spike protein that is similar in both coronaviruses. Recent lab studies showed that sotrovimab is effective against variants of COVID-19 including those discovered in the UK, South Africa, Brazil, and India (where the Delta variant started). This broad neutralization capability is especially helpful to individuals who are not able to receive or tolerate the vaccines for COVID-19 [29, 30].

10.6 Vaccines for COVID-19

A vaccine (in simple terms) is a substance used to stimulate the production of antibodies to provide immunity from a specific disease. It is either prepared from

an agent causing the disease, its products, or a synthetic substitute (which acts as an antigen without introducing the disease). When scientists create vaccines, they need to consider various factors. A few examples include determining the individuals who need to be vaccinated, how the immune system responds to the virus, and the best approach to create the vaccine. Different types of vaccines exist [31]. Some are mentioned. Inactivated vaccines use the dead germ that causes a disease. They do not provide as much protection as live vaccines, so booster shots may be necessary. Live-attenuated vaccines use a weakened form of the germ that causes a disease, so they produce a longer lasting immune response. The Pfizer-BioNTech and Moderna COVID-19 vaccines are messenger RNA vaccines (mRNA vaccines). Messenger RNA vaccines use mRNA created in a laboratory to train our cells to make proteins to trigger an immune response inside of our bodies. The immune response produces antibodies to protect us from the virus (in this case, COVID-19). Subunit, recombinant, polysaccharide, and conjugate vaccines use a specific piece of the germ (like its protein) to give a strong immune response that targets key parts of the germ. Toxoid vaccines use a toxin made by the germ that causes a disease. They provide an immune response to the toxin instead of the whole germ. Viral vector vaccines use a modified version of a different virus as a vector to deliver protection. Adenovirus (which causes the common cold) is a viral vector used in Johnson & Johnson's (J&J's) COVID-19 vaccine.

To combat the COVID-19 pandemic, countries throughout the world developed their own vaccines. Take, for example, Russia's vaccine called Sputnik V or Gam-COVID-Vac [32]. Sputnik V was developed by the Gamaleya Research Institute, which is part of Russia's Ministry of Health [33]. It is a viral vector vaccine like Johnson & Johnson (J&J). However, it is unique in that it uses two different types of cold virus (or adenovirus) for the first and second shots. Sputnik V is the world's first registered (August 11, 2020) combination vector vaccine for the prevention of COVID-19. For this chapter, our focus is on the three prominent vaccines used in the United States: Pfizer, Moderna, and Johnson & Johnson (J&J).

10.6.1 Pfizer-BioNTech's COVID-19 Vaccine

Pfizer-BioNTech is the first COVID-19 vaccine licensed by the US government. The US Food and Drug Administration gave it full approval on August 23, 2021 [34, 35]. It is sold as Comirnaty and was approved for individuals 16 and older at about the same time. This approval supports the use of messenger RNA (mRNA) technology that Pfizer and BioNTech and their competitor Moderna used. The technology helped the companies rapidly develop highly effective vaccines against COVID-19. At first, Pfizer (an American company) and BioNTech (a German company) became partners to develop a flu vaccine. However, they decided to use the mRNA technology to combat COVID-19 instead. After about 8 months, the phase 3 data suggested their vaccine was more than 90% effective at preventing the disease. As a

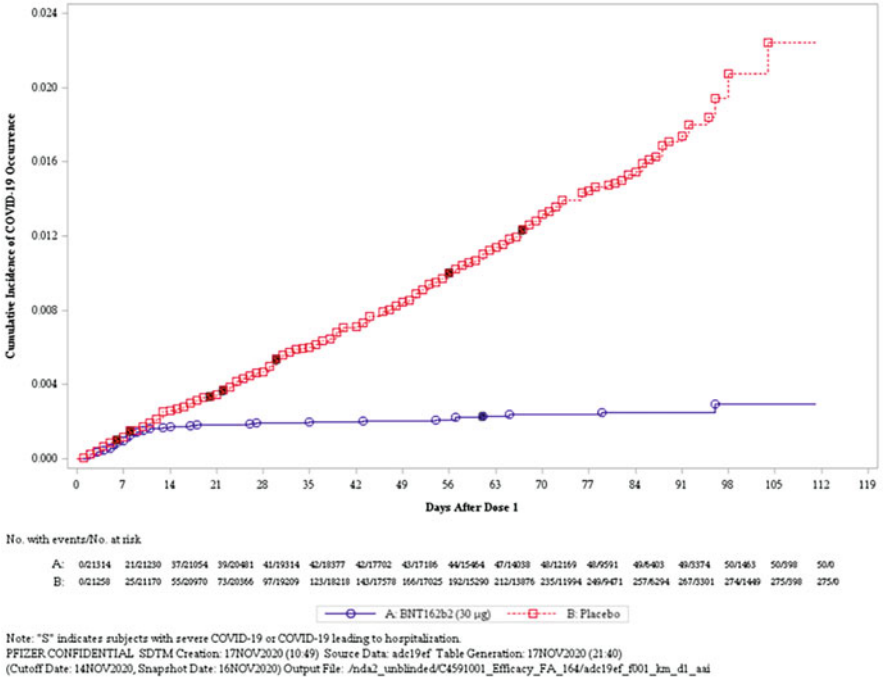

Fig. 10.7 Above is a graph of BNT162b2 (Pfizer-BioNTech) COVID-19 vaccine efficacy data. The vertical column represents the Cumulative Incidence of COVID-19 Occurrence (starting at 0.000 and ending at 0.024). The horizontal axis represents Days after Dose 1 (starting at 0 and ending at 119). The red squares represent the placebo, the blue circles indicate the vaccine with a dose of 30 μg, and the letter S (displayed as filled red squares) stands for individuals with severe COVID-19 or COVID-19 leading to hospitalization.

result, the US Food and Drug Administration issued an emergency use authorization for the vaccine in December of 2020 [36].

Figure 10.7 is a graph displaying BNT162b2 (Pfizer-BioNTech) COVID-19 vaccine efficacy data [37]. The red squares represent the placebo, and the blue circles indicate the vaccine with a dose of 30 μg. The letter "S" stands for individuals with severe COVID-19 or COVID-19 leading to hospitalization

During the month of November 2021, Pfizer's vaccine was granted emergency use authorization for children 5–11 years old. This is in addition to its similar status for children aged 12–15 years old. Note that individuals 12 and older receive the same dose as an adult. The vaccines are given by intramuscular injection. The younger children receive two doses, each of which is one-third of the amount prescribed for an adult shot. Their vaccines are administered by using a needle, smaller than the one used for older individuals. Pfizer is currently (as of November 2021) working on a vaccine for children of 6 months to 5 years old. In addition, booster shots are available (from Pfizer, Moderna, and J&J) to individuals 18 years of age or older, after 6 months of having their second shot for Pfizer and Moderna.

As for J&J, a second shot is considered its booster. Boosters can match your previous type of shots or be one of the other choices. Booster shots are highly recommended to restore individuals' levels of neutralizing antibodies. This is because a decline of vaccine effectiveness has been observed over a period of months. Also, it should be mentioned that vaccinated individuals with three shots have experienced break through cases of COVID-19. However, these people tend to have more mild forms of this disease.

The Pfizer-BioNTech vaccine contains the following components: mRNA, four lipids (two of which are cholesterol and a form of polyethylene glycol known as ALC-0159), potassium chloride, sodium chloride, dibasic sodium phosphate dihydrate, monobasic potassium phosphate, sucrose, and water for injection [38].

A simple description is provided for the preparation of the Pfizer-BioNTech vaccine, which mainly takes place at three Pfizer facilities in the United States [39, 40]. It starts in Chesterfield, Missouri, where vials of DNA are removed from cold storage. The vials contain small rings of DNA called plasmids. Each plasmid has a coronavirus gene (the genetic instructions for the human cell to build coronavirus proteins and trigger an immune response to the virus). Scientists modify a batch of *E. coli* bacteria to take the plasmids into their cells and multiply. Then they add chemicals to break open the bacteria and release the plasmids, which are tested for purity. Enzymes are used to cut the circular plasmids into straight segments. In Andover, Massachusetts, the DNA templates are transcribed into strands of mRNA, the active ingredient of the vaccine. The finished vaccine will carry the mRNA into human cells which will read the coronavirus gene and begin producing coronavirus proteins. In another process, oily lipids are prepared to protect the mRNA and help it enter human cells. The addition of the lipids to the mRNA and finishing the vaccine take place in Kalamazoo, Michigan. During the encapsulation process, the mRNA strands are enclosed in tiny balls of fat known as lipid nanoparticles. This allows them to travel from the syringe into the bloodstream and then into cells before they dissolve. Finally, the completed vaccine is tested, packaged in freezers at very low temperatures, and shipped to various locations for distribution and use.

10.6.2 Moderna's COVID-19 Vaccine

Moderna is an American pharmaceutical and biotechnology company based in Cambridge, Massachusetts. It uses messenger RNA (mRNA) for its vaccine technologies. The Moderna COVID-19 vaccine (mRNA-1273) is sold under the brand name of Spikevax and was developed by the company Moderna, the US National Institute of Allergy and Infectious Diseases (NIAID), and the Biomedical Advanced Research and Development Authority (BARDA). The vaccine was 94.5% effective at preventing the disease according to an early analysis of a phase 3 trial [41]. Moderna requires two shots, 4 weeks apart. Each injection includes liquid nanoparticles filled with mRNA strands. These strands encode genetic instructions for making the SARS-CoV-2 spike protein that the virus uses to infect human cells. After receiving

the vaccine, our cells (for a short time) make the spike protein to give our immune system time to make antibodies that protect us from catching the infection.

As previously mentioned, Moderna and Pfizer both use messenger RNA technologies for their vaccines and have many similarities. Their common side effects include headaches, muscle pain, a sore arm, fever, chills, and nausea [42]. One major difference is the vaccine's stability. Pfizer's vaccine needs to be transported and stored at −70 °C. On the other hand, Moderna's vaccine requires just −20 °C for transportation and long-term storage of up to 6 months. In addition, Moderna plans to build a messenger RNA facility both in Africa and Canada [43].

10.6.3 Johnson & Johnson's (J&J's) COVID-19 Vaccine

The Johnson and Johnson's COVID-19 vaccine has been developed by Janssen Vaccines in Leiden, Netherlands, and its Belgian parent company, Janssen Pharmaceuticals, a subsidiary of the American Company Johnson & Johnson. J&J's shot is made with adenoviral vector vaccine technology, while those from Pfizer and BioNTech and one from Moderna are messenger RNA (mRNA) vaccines [44]. There are differences for the two types of vaccines. The messenger RNA vaccines require two shots and need to be shipped and stored in freezers. On the other hand, the J&J vaccine is administered as a single shot and can be kept in a refrigerator for up to 3 months [45, 46]. On October 15, 2021, the US Food and Drug Administration approved a booster dose of J&J for all Americas 18 years old and older who received a single dose.

As stated earlier, the J&J shot is a viral vector vaccine. It uses a weakened common cold virus to deliver a single coronavirus gene into human cells. That gene encodes instructions for making the SARS-CoV-2 spike protein (an antigen) to trigger our immune systems. In simple terms, one can say that viral vector vaccines use a modified version of a different virus as a vector to deliver protection. Adenovirus (which causes the common cold) is a viral vector used in Johnson & Johnson's (J&J's) COVID-19 vaccine.

10.7 Conclusions

This chapter starts by introducing COVID-19 and its variants which continue to increase in number. Then it gives brief descriptions of the human immune system and COVID-19 testing methods for antigens and antibodies. The testing process involves collecting and analyzing samples to determine if individuals currently have or previously had the disease. Information is also provided about COVID-19 treatments with antiviral drugs like remdesivir and antiviral pills. Antibody treatments such as convalescent plasma and antibody cocktails, etc. are available too. Finally, there is a discussion about vaccines including Pfizer, Moderna, and

Johnson & Johnson. They provide the best protection from COVID-19 and its variants. Pfizer-BioNTech and Moderna are messenger RNA vaccines, and J&J is a viral vector vaccine which uses a modified version of a different virus as a vector to deliver protection. In this case, adenovirus (which causes the common cold) is used as the vector.

References

1. Eckert, A., & Higgins, D. (2020). *File: SARS-CoV-2 without background.png*. License: This image is in the public domain. File: SARS-CoV-2 without background.png - Wikimedia Commons.
2. Howes, L. (2021). What you need to know about SARS-CoV-2 variants. *Chemical & Engineering News*, 18–19.
3. Mahase, E. (2021). COVID-19: How many variants are there, and what we know about them? *BMJ, 374*, n1971. https://doi.org/10.1136/bmj.n1971
4. Zhang, J. M., & An, J. (2007). Cytokines, inflammation, and pain. *International Anesthesiology Clinics, 45*(2), 27–37. https://doi.org/10.1097/AIA.0b013e318034194e
5. Colm, G. (2009). *File: Phagocytosis 2.png*. License: Creative Commons Attribution-Share Alike 3.0 File: Phagocytosis2.png - Wikimedia Commons.
6. Rehua. (2012). *File: T cell activation.svg*. License: This work is in the public domain. File: T cell activation.svg - Wikimedia Commons.
7. Wang, H., Li, G., Zhao, J., Li, Y., & Ai, Y. (2021). An overview of nucleic acid testing for the novel coronavirus SARS-CoV-2. *Frontiers in Medicine, 7*, 571709. https://doi.org/10.3389/fmed.2020.571709
8. U.S. Secretary of Defense. (2021). *File: ID Now Testing (51038387158).jpg*. License: Creative Commons Attribution 2.0. File:ID Now testing (51038387158).jpg - Wikimedia Commons.
9. Peplow, M. (2021). Transistor detects SARS-CoV-2 in less than a minute. *Chemical & Engineering News, 99*, 6.
10. Rahimi, H., Salehiabar, M., Barsbay, M., Ghaffarlou, M., Kavetskyy, T., Sharafi, A., Davaran, S., Chauhan, S. C., Danafar, H., Kaboli, S., Nosrati, H., Yallapu, M. M., & Conde, J. (2021). CRISPR systems for COVID-19 diagnosis. *ACS Sensors, 6*(4), 1430–1445. https://doi.org/10.1021/acssensors.0c02312
11. Peplow, M. (2020). 15 min, $5 COVID-19 test rolls out. *Chemical & Engineering News, 98*, 4.
12. CDC. (2021). Evaluation of Abbott BinaxNOW Rapid Antigen Test for SARS-CoV-2 Infection at Two Community-Based Testing Sites — Pima County, Arizona, November 3–17, 2020. *MMWR, 70*, 100. Retrieved from cdc.gov
13. Arnold, C. (2021). Sniffing out COVID-19. *Chemical & Engineering News, 99*, 21–24.
14. Ruszkiewicz, D., Sanders, D., et al. (2020). Diagnosis of COVID-19 by analysis of breath with gas chromatography-ion mobility spectrometry – A feasibility study. *EClinical Medicine, 29*, 100609. https://doi.org/10.1016/j.eclinm.2020.100609
15. Yin, W., Mao, C., Luan, X., Shen, D. D., Shen, Q., Su, H., Wang, X., Zhou, F., Zhao, W., Gao, M., Chang, S., Xie, Y. C., Tian, G., Jiang, H. W., Tao, S. C., Shen, J., Jiang, Y., Jiang, H., Xu, Y., Zhang, S., Xu, H. E. (2020). Structural basis for inhibition of the RNA-dependent RNA polymerase from SARS-CoV-2 by remdesivir. *Science (New York, N.Y.), 368*(6498), 1499–1504. https://doi.org/10.1126/science.abc1560
16. Howes, L. (2020). How remdesivir blocks SARS-CoV-2. *Chemical & Engineering News, 98*, 10.
17. Deb, S., Reeves, A. A., Hopefl, R., & Bejusca, R. (2021). ADME and pharmacokinetic properties of remdesivir: Its drug interaction potential. *Pharmaceuticals (Basel, Switzerland), 14*(7), 655. https://doi.org/10.3390/ph14070655

18. Boghog. (2020). *File: Remdesivir activation.svg*. License: Creative Commons Attribution-Share Alike 4.0 International. File:Remdesivir activation.svg - Wikimedia Commons.
19. Satyanarayana, M. (2021). Two COVID-19 antiviral pills advance to late-stage trials. *Chemical & Engineering News, 99*, 11.
20. Kabinger, F., Stiller, C., Schmitzová, J., et al. (2021). Mechanism of molnupiravir-induced SARS-CoV-2 mutagenesis. *Nature Structural & Molecular Biology, 28*, 740–746. https://doi.org/10.1038/s41594-021-00651-0
21. Dolgin, E. (2021). The race for antiviral drugs to beat COVID—and the next pandemic. *Nature, 592*, 340–343.
22. Cross, R. (2020). FDA authorizes COVID-19 antibody therapy. *Chemical & Engineering News*, 15.
23. Cross, R. (2020). Rapid antibody development came of age. *Chemical & Engineering News*, 39.
24. Taylor, P. C., Adams, A. C., Hufford, M. M., et al. (2021). Neutralizing monoclonal antibodies for treatment of COVID-19. *Nature Reviews. Immunology, 21*, 382–393. https://doi.org/10.1038/s41577-021-00542-x
25. Renn, A., Fu, Y., Hu, X., Hall, M. D., & Simeonov, A. (2020). Fruitful neutralizing antibody pipeline brings hope to defeat SARS-Cov-2. *Trends in Pharmacological Sciences, 41*, 815–829.
26. Shanmugaraj, B., Siriwattananon, K., Wangkanont, K., & Phoolcharoen, W. (2020). Perspectives on monoclonal antibody therapy as potential therapeutic intervention for coronavirus disease-19 (COVID-19). *Asian Pacific Journal of Allergy and Immunology, 38*, 10–18.
27. Fvasconcellos. (2020). *File: REGN-COV2 binding SARS-CoV-2 spike protein.png*. License: This work is in the public domain. File:REGN-COV2 binding SARS-CoV-2 spike protein.png - Wikimedia Commons.
28. Weinreich, D., Sivapalasingam, S., et al. (2021). REGN-CoV2, a neutralizing antibody cocktail, in outpatients with COVID-19. *NEJM, 384*, 238.
29. Gupta, A., Gonzalez-Rojas, Y., et al. (2021). Early COVID-19 treatment with SARS-CoV-2 neutralizing antibody sotrovimab. *The New England Journal of Medicine, 385*, 1941. https://doi.org/10.1056/NEJMoa2107934
30. Cross, R. (2021). Third COVID-19 antibody is authorized. *Chemical & Engineering News, 99*, 11.
31. HHS. (n.d.). *Vaccine types*. Author. Retrieved from HHS.gov
32. Kramer, A. (2021). Russia's vaccine is safe and effective, published study shows. *The New York Times*. Retrieved from nytimes.com
33. Cross, R. (2021). AstraZeneca, Gamaleya, Novavax, and J & J post positive vaccine results. *Chemical & Engineering News, 99*, 4–5.
34. Satyanarayana, M. (2021). FDA approves the Pfizer-BioNTech COVID-19 vaccine. *Chemical & Engineering News, 99*, 10.
35. Roychoudhury, S., Koury, K., Bouguermouh, S., Kalina, W. V., Cooper, D., Frenck, R. W., Jr., Hammitt, L. L., & C4591001 Clinical Trial Group. (2021). Safety and efficacy of the BNT162b2 mRNA Covid-19 vaccine through 6 months. *The New England Journal of Medicine, 385*(19), 1761–1773.
36. Cross, R. (2020). Pfizer COVID-19 vaccine rolls out across the U.S. *Chemical & Engineering News, 98*, 4–5.
37. U.S. Food and Drug Administration and Pfizer Inc. (2020). *File: BNT162b2 vaccine efficacy data.png*. License: This work is in the public domain. File:BNT162b2 vaccine efficacy data.png - Wikimedia Commons.
38. Health Canada. (2020). *Pfizer-BioNTech COVID-19 vaccine: Health Canada recommendations for people with serious allergies*. Author.
39. Cott, E., deBruyn, E., & Corum, J. (2021). How Pfizer makes its COVID-19 vaccine. *The New York Times*. Retrieved from nytimes.com

40. Weise, E., & Weintraub, K. (2021). A COVID-19 vaccine life cycle: From DNA to doses. *USA Today*. How a COVID vaccine is made: The step-by-step journey of a Pfizer dose. Retrieved from usatoday.com
41. Cross, R. (2020). Moderna says COVID-19 vaccine is 94.5% effective in preliminary analysis. *Chemical & Engineering News, 98*, 4–5.
42. Cross, R. (2021). Moderna's COVID-19 vaccine to rollout across the US. *Chemical & Engineering News, 99*, 10.
43. Mullin, R. (2021). Moderna announces plans to make vaccines in Africa. *Chemical & Engineering News, 99*, 13.
44. Livingston, E. H., Malani, P. N., & Creech, C. B. (2021). The Johnson & Johnson vaccine for COVID-19. *Journal of the American Medical Association, 325*(15), 1575. https://doi.org/10.1001/jama.2021.2927
45. Cross, R. (2021). US authorizes J & J vaccine. *Chemical & Engineering News, 99*, 5.
46. CDC. (2021). Comparative effectiveness of Moderna, Pfizer-BioNTech, and Janssen (Johnson & Johnson) vaccines in preventing COVID-19 hospitalizations among adults without immunocompromising conditions — United States, March–August 2021. *MMWR, 70*, 1337. Retrieved from cdc.gov

Part IV
The Future

Chapter 11
Controlling COVID-19 and Preparing for Future Pandemics

Dana Barry and Hideyuki Kanematsu

Abstract This chapter starts by discussing the status of COVID-19 and ways to improve the situation. Then it presents a general plan (prepared by the World Health Organization) for controlling a pandemic. Next, four methods to prepare for future pandemics are introduced. One involves the use of sharks' antibody-like proteins as effective therapeutics against coronaviruses. A second way is called the One Health plan that recognizes the interconnections and health interdependencies among humans, animals, and shared environments where we live and interact. Another one is the use of serological testing, checking blood serum to detect antibodies that are formed in response to an infection from a pathogen. Finally, metagenomic sequencing is described. This approach reads the genomic material in a sample and identifies the organisms present.

11.1 Introduction

The World Health Organization (WHO) declared COVID-19 to be a global pandemic in March 2020. Despite advances in antiviral drugs, vaccinations, clinical management of COVID-19 patients, etc., this public health crisis still exists. To prepare for the next pandemic, we need to learn and benefit from the mistakes made in the handling of the current COVID-19 crisis (which has caused dreadful human, economic, etc. problems). Sadly, initial warnings and the presence of the virus were ignored and/or not taken seriously. This lag in time allowed COVID-19 to spread worldwide and to mutate into other variants. Presently (January 2022),

D. Barry (✉)
Department of Electrical & Computer Engineering, Clarkson University, Potsdam, NY, USA

State University of New York at Canton, Canton, NY, USA
e-mail: dmbarry@clarkson.edu

H. Kanematsu
National Institute of Technology, Suzuka College, Shiroko-cho, Suzuka, Mie, Japan
e-mail: kanemats@mse.suzuka-ct.ac.jp

D. Barry, H. Kanematsu (eds.), *Studies to Combat COVID-19 using Science and Engineering*, https://doi.org/10.1007/978-981-19-1356-3_11

the number of patients with the delta and omicron variants is increasing globally and overwhelming hospitals and healthcare facilities. While the COVID-19 virus remains active (especially if individuals refuse to get vaccinated), it will continue to create new variants (some of which will disappear soon or others that may be very contagious and deadly). To combat such a deadly disease, global solidarity is needed [1–8]. This means that all states, countries, etc. must adhere to a uniform set of rules and protocols (as much as possible) that represent the health and safety of all according to the scientific data and the input of medical experts. The public should not reject these protocols because of misinformation, their political views, and other nonscience-related reasons. Therefore, we should get the vaccines and booster shots (from Pfizer, Moderna, and J&J) that are available and effective against COVID-19. It would be great if a vaccine could be developed to protect us from all forms of the COVID-19 virus. Vaccines, antiviral drugs, etc. must also be available to people in poor and developing countries, etc. to control a global pandemic. In addition, to achieve our proposed goals, much money and numerous types of global collaborations are needed. These collaborations should be between government agencies, industries, engineers, research scientists, medical experts and facilities, clinicians, chemical supply companies, and others.

11.2 General Plan to Control a Pandemic

The coronavirus may disappear, or appear each year like the flu, or periodically recur, etc. In any case, the next unknown disease may already be here. Each year, the World Health Organization sets up a committee of experts to update its list of the most threatening infectious diseases that lack effective treatments or vaccines. One might wonder if there is a plan to identify such a pathogen early and to organize scientists, healthcare facilities, politicians, the public, etc. to fight it. Yes. There is a plan. For example, after the SARS (severe acute respiratory syndrome) pandemic, WHO prepared steps to control a pandemic [9–20]. They are summarized in the following paragraph.

11.2.1 General Steps to Control a Pandemic

Be prepared for a new pandemic. When it arrives, report early cases (of the disease) and alert the world about it. Provide leadership and promote international collaborations with scientists, public health experts, etc. to possibly control and eliminate the disease. Provide the public with safety guidelines. Have an adequate supply of medicine, equipment, and hospitals/healthcare facilities for expected surges of infected patients. Educate healthcare workers and protect them with protective personal equipment (PPE). When necessary, enforce screening and travel

limitations. Also, have a program for testing, contact tracing, and isolation for infected individuals.

It should be mentioned that memories of a prior disease recede with time. Also, our safety plans against pandemic diseases tend to be underfunded and difficult to carry out. However, we need to be prepared for future diseases.

11.3 Using Sharks' Proteins to Combat Future Coronaviruses

New research suggests that sharks' proteins may be able to protect us from the coronavirus. Sharks have antibody-like proteins that can stop the virus (SARS-CoV-2) that causes COVID-19, according to a news release from the University of Wisconsin-Madison, which collaborated on the study [21–32]. Professor Aaron LeBeau (of the University of Wisconsin-Madison) is one of the lead researchers for this project. He mentioned that the study involves male, nurse sharks because they are easy to work with and it is easy to obtain their blood samples. The nurse sharks tend to be slow and have a sedentary nature as compared to aggressive sharks. They are typically inshore, bottom-dwellers with a flattened body and a broad, rounded head. Figure 11.1 shows a nurse shark [33]. The nurse shark's antibody-like proteins are known as VNARs (variable new antigen receptors). They are very tiny and a natural part of the shark's immune system. This study highlights the use of VNARs as effective therapeutics against coronaviruses. The work identifies a series of VNARs from a VNAR library display screened against the SARS-CoV-2

Fig. 11.1 This figure shows a nurse shark

receptor binding domain (RBD). It was found that VNARs neutralize pseudotype and authentic live SARS-CoV-2 virus, as well as or better than full-length immunoglobulins and other single-domain antibodies. (Neutralizing antibodies, Nab, block virus entry into the host cell.) Structural and biochemical data (using crystallographic analysis, etc.) suggest that VNARs would be effective therapeutic agents against emerging SARS-CoV-2 mutants including the delta variant and others. At this point in time (January 2022), it is too early to test the shark's so-called antibodies on humans.

11.4 One Health: A Plan to Prepare for Future Pandemics

One Health is a way to prevent and prepare for future pandemics [34]. One Health is a concept that recognizes the interconnections and health interdependencies among humans, animals, and the shared environments where we live and interact. In some cases (in shared environments), it may be possible for viruses to be transmitted from animals to humans or vice versa. It is estimated (in December 2021) that about 75% of the emerging infectious diseases in humans have originated from animals. The One Health approach refers to the health of all living organisms in a global ecosystem that would put all of us at risk for future pandemics if it is rapidly changed.

Since many of our viruses come from animals, it is important to find out why. This process where viruses jump from animals to people is called zoonotic spillover [35]. Scientists are trying to figure out how SARS-CoV2, the virus that causes COVID-19, spilled over from bats into humans. A virus must overcome many hurdles to leap from one species to another one. It needs to be able to attach to receptors on the surface of a new host cell and learn how to replicate in that cell without alerting the host's immune system. Certain factors must line up for this zoonotic spillover to be successful. We are talking about interactions relating to ecology, viral evolution, and human immunity. One problem that scientists are considering is people living in wilderness areas with lots of biodiversity. These individuals are close to animals carrying potentially dangerous viruses. This is a big requirement for zoonotic spillover. Biologist Zhengli Shi, at the Wuhan Institute of Virology, and her team reported in 2018 that people living close to caves containing bats with different SARS coronaviruses have antibodies to such viruses. Keep in mind that bats were the source of viruses causing Ebola, rabies, etc.

The World Health Assembly (the decision-making body of the WHO) proposed establishing a pandemic treaty. An international treaty on pandemics would mandate and support WHO member states to build national, local, and global pandemic capability and resilience by providing improved prediction, preparedness, response, and prevention.

11.5 Prepare for Future Pandemics Using Serological Testing

Scientists want to check blood samples from all over the world for antibodies to determine if a population has robust immunity to a pathogen ahead of time. A much smaller but somewhat similar project is being carried out by Dr. Michael Mina (an epidemiologist at the Harvard T.H. Chan School of Public Health) and his team. He has about half a million vials of plasma from human blood arriving from all over the country. The plasma is stored in freezers. These samples were collected from the plasma donation company Octapharma in 2020. They are starting to undergo serological testing with a focus on the new coronavirus. (This work is being funded by a grant from Open Philanthropy.) Serological testing studies blood serum to detect antibodies that are formed in response to an infection from a pathogen. This test looks back on what you have caught. It is not really interested in an active viral infection. Dr. Mina and his group hope to use this data to show how the virus entered the USA and how immunity to COVID has grown and changed.

Dr. Mina and his collaborators have a bigger goal and plan. They want to have a very large surveillance system that can check blood samples from all over the world for antibodies to hundreds of viruses at once [36]. This way when the next pandemic arrives, scientists will have detailed information about the number of people infected by the virus and how their bodies responded. This ambitious project is called the Global Immunological Observatory. Of course, it would require funds and agreements with hospitals, blood banks, patients, donors, etc.

11.6 Prepare for Future Pandemics Using Metagenomic Sequencing

Dr. Jessica Manning, a public health researcher with the National Institute of Allergy and Infectious Diseases, is part of the global effort to look for emerging diseases. For her work at a lab in Cambodia, she uses metagenomic sequencing to identify unknown pathogens [37, 38]. Traditional methods for genomic diagnosis look for the genetic sequence of a single pathogen, one that you are looking for. On the other hand, metagenomic sequencing reads the genomic material in a sample and identifies the organisms present. Identifying these unknowns is a complicated process because common sequencing machines chop up DNA and RNA molecules into lots of short segments which need to be properly arranged. To better understand the obtained data, Dr. Manning's group uses IDseq. This is a free online open-source software package that reverse engineers use to put the short segments together to form various genomes and compare them to known genomes in public databases. (Note: A genome is the complete set of genes or genetic material in a cell or organism.) IDseq runs on servers in the cloud, so researchers in developing countries can do an analysis remotely for free. Dr. Manning also uses metagenomic analysis

on her patients' blood samples to identify what is wrong with them. Her work has funding from the Gates Foundation.

11.7 Conclusions

This chapter starts by discussing the status of COVID-19 and ways to improve the situation. Then it presents a general plan (prepared by the World Health Organization) for controlling a pandemic. Next, four methods to prepare for future pandemics are introduced. One involves the use of sharks' antibody-like proteins as effective therapeutics against coronaviruses. A second way is called the One Health plan that recognizes the interconnections and health interdependencies among humans, animals, and shared environments where we live and interact. Another one is the use of serological testing, checking blood serum to detect antibodies that are formed in response to an infection from a pathogen. Finally, metagenomic sequencing is described. This approach reads the genomic material in a sample and identifies the organisms present.

References

1. Nature Medicine Editorial. (2021). Preparing for the next pandemic. *Nature Medicine, 27*, 357. https://doi.org/10.1038/s41591-021-01291-z
2. Disparte, D. (2021). *Preparing for the next pandemic: Early lessons from COVID-19*. Brookings report. Retrieved from brookings.edu
3. Osterholm, M. T. (2005). Preparing for a pandemic. *The New England Journal of Medicine, 352*, 1839.
4. Johnson, N. P., & Mueller, J. (2002). Updating the accounts: Global mortality of the 1918-1920 Spanish influenza pandemic. *Bulletin of the History of Medicine, 76*, 105–115.
5. Stohr, K. (2005). Avian influenza and pandemics: Research needs and opportunities. *The New England Journal of Medicine, 352*, 405–407.
6. Sandman, P. M., & Lanard, J. (2005). *Pandemic influenza risk communication: The teachable moment*. Peter Sandman. Retrieved April 14, 2005, from http://www.psandman.com/col/pandemic.htm
7. Kobasa, D., Takada, A., Shinya, K., et al. (2004). Enhanced virulence of influenza A viruses with haemagglutinin of the 1918 pandemic virus. *Nature, 431*, 703–707.
8. Peiris, J. S., Yu, W. C., Leung, C. W., et al. (2004). Re-emergence of fatal human influenza A subtype H5N1 disease. *Lancet, 363*, 617–619.
9. Iserson, K. V. (2020). The next pandemic: Prepare for "Disease X". *The Western Journal of Emergency Medicine, 21*(4), 756–758. https://doi.org/10.5811/westjem.2020.5.48215
10. Heymann, D. L., & Rodier, G. (2004). SARS: Lessons from a new disease. In *Learning from SARS: Preparing for the next disease outbreak* (pp. 234–245). The National Academies Press. Retrieved May 8, 2020, from www.ncbi.nlm.nih.gov/books/NBK92462/pdf/Bookshelf_NBK92462.pdf
11. Alfani, G., & Murphy, T. E. (2017). Plague and lethal epidemics in the pre-industrial world. *The Journal of Economic History, 77*(1), 314–343.

12. WHO. (n.d.). *Prioritizing diseases for research and development in emergency contexts*. Author. Retrieved April 8, 2020, from www.who.int/activities/prioritizing-diseases-for-research-and-development-in-emergency-contexts
13. US Centers for Disease Control and Prevention. (n.d.). *National pandemic influenza plans*. CDC. Retrieved May 9, 2020, from www.cdc.gov/flu/pandemic-resources/planning-preparedness/national-strategy-planning.html
14. US Department of Health and Human Services. (2017). *Pandemic influenza plan*. CDC. Retrieved May 9, 2020, from www.cdc.gov/flu/pandemic-resources/pdf/pan-flu-report-2017v2.pdf
15. US Department of Homeland Security. (2019). *National response framework* (4th ed.). FEMA. Retrieved May 9, 2020, from www.fema.gov/media-library-data/1582825590194-2f000855d442fc3c9f18547d1468990d/NRF_FINALApproved_508_2011028v1040.pdf
16. Assistant Secretary for Preparedness and Response. *National health security strategy and implementation plan: 2015–2018*. Author. Retrieved May 9, 2018, from www.phe.gov/Preparedness/planning/authority/nhss/Documents/nhss-ip.pdf
17. Desmond-Hellmann, S. (2020). Preparing for the next pandemic. *Wall Street Journal*. Retrieved April 4, 2020, from www.wsj.com/articles/preparing-for-the-next-pandemic-11585936915?mod=itp_wsj&mod=&mod=djemITP_h
18. Kelland, K. (2016). The World Health Organization's critical challenge: Healing itself. *Reuters*. Retrieved May 7, 2020, from www.reuters.com/investigates/special-report/health-who-future/
19. Kamradt-Scott, A. WHO's to blame? The World Health Organization and the 2014 Ebola outbreak in West Africa. *Third World Quarterly*. Retrieved May 7, 2020, from www.tandfonline.com/doi/full/10.1080/01436597.2015.1112232
20. Centers for Disease Control and Prevention. (n.d.). *II. Lessons learned. Supplement G: Communication and education. Public health guidance for community-level preparedness and response to Severe Acute Respiratory Syndrome (SARS)*. Version 2/3. Retrieved May 8, 2020, from https://www.cdc.gov/sars/guidance/g-education/lessons.html
21. Johnson, M. (2021). UW researcher finds an unusual possibility for treating people with COVID-19: Shark antibodies. *Milwaukee Journal Sentinel*. UW study finds hope against COVID in unlikely source: Shark antibodies. Retrieved from jsonline.com
22. Ubah, O. C., Lake, E. W., Gunaratne, G. S., et al. (2021). Mechanisms of SARS-CoV-2 neutralization by shark variable new antigen receptors elucidated through X-ray crystallography. *Nature Communications, 12*, 7325. https://doi.org/10.1038/s41467-021-27611-y
23. Yadav, P. D., et al. (2021). Neutralization of variant under investigation B.1.617 with sera of BBV152 vaccinees. *Clinical Infectious Diseases, 74*, 366. https://doi.org/10.1093/cid/ciab411
24. Greaney, A. J., et al. (2021). Comprehensive mapping of mutations in the SARS-CoV-2 receptor-binding domain that affect recognition by polyclonal human plasma antibodies. *Cell Host & Microbe, 29*, 463–476.e466.
25. Liu, Y., et al. (2021). Neutralizing activity of BNT162b2-elicited serum. *The New England Journal of Medicine, 384*, 1466–1468.
26. Wang, P., et al. (2021). Antibody resistance of SARS-CoV-2 variants B.1.351 and B.1.1.7. *Nature, 593*, 130–135.
27. Couzin-Frankel, J. (2021). Relief and worry for immune-suppressed people. *Science, 372*, 443–444.
28. Boyarsky, B. J., et al. (2021). Immunogenicity of a single dose of SARS-CoV-2 messenger RNA vaccine in solid organ transplant recipients. *JAMA, 325*, 1784–1786.
29. Huang, Y., et al. (2020). Neutralizing antibodies against SARS-CoV-2: Current understanding, challenge, and perspective. *Antibody Therapeutics, 3*, 285–299.
30. Greenberg, A. S., et al. (1995). A new antigen receptor gene family that undergoes rearrangement and extensive somatic diversification in sharks. *Nature, 374*, 168–173.
31. Stanfield, R. L., Dooley, H., Flajnik, M. F., & Wilson, I. A. (2004). Crystal structure of a shark single-domain antibody V region in complex with lysozyme. *Science, 305*, 1770–1773.

32. Stanfield, R. L., Dooley, H., Verdino, P., Flajnik, M. F., & Wilson, I. A. (2007). Maturation of shark single-domain (IgNAR) antibodies: Evidence for induced-fit binding. *Journal of Molecular Biology, 367*, 358–372.
33. Stevelaycock21. (2020). *File: Nurse shark turning.jpg*. License: Creative Commons Attribution-Share Alike 4.0 International. File: Nurse shark turning.jpg - Wikimedia Commons.
34. Daily Excelsior. (2021). One health: A crucial approach to preventing and preparing for future pandemics - Jammu Kashmir Latest News. Tourism. Breaking News J&K. *Daily Excelsior*. Retrieved from dailyexcelsior.com
35. Katsnelson, A. (2020). Making the leap. *Chemical & Engineering News*, 27–33.
36. Greenwood, V. (2021). Trying to track new viruses before an outbreak. *The New York Times*, D4.
37. Kalantar, K. L., Carvalho, T., de Bourcy, C., Dimitrov, B., Dingle, G., Egger, R., Han, J., Holmes, O. B., Juan, Y. F., King, R., Kislyuk, A., Lin, M. F., Mariano, M., Morse, T., Reynoso, L. V., Cruz, D. R., Sheu, J., Tang, J., Wang, J., Zhang, M. A., DeRisi, J. L. (2020). IDseq-An open-source cloud-based pipeline and analysis service for metagenomic pathogen detection and monitoring. *GigaScience, 9*(10), giaa111. https://doi.org/10.1093/gigascience/giaa111
38. Zeeberg, A. (2021). A mission to piece together the next pandemic. *The New York Times*, D5.

Chapter 12
Pandemic and Reform in Funeral Services

David R. Penepent

Abstract The pandemic revealed the weaknesses in the funeral profession when it comes to handling a mass fatality situation. This problem was discovered during a rescue effort by a small group of volunteers from the State University of New York at Canton. In addition, the bureaucracy and inefficiencies of emergency readiness, coupled with archaic and antiquated rules governing the practice of funeral directing, were contributing factors to the backlog of human remains in New York City in the initial stage of the pandemic. Lessons learned during the pandemic could prove valuable to the funeral profession and governmental officials to overt another crisis situation in the future, if changes take place within the next 10 years. The pandemic will soon become a part of the history. However, failing to implement significant changes within the funeral profession will soon yield another mass fatality crisis in American society.

In 2008, I hosted a continuing education event for funeral directors to address the issue of a pandemic with mass fatalities. The comments made by some funeral directors at the time added up to, "I'll deal with that issue if it ever occurs." The lack of professional foresight that led to the mentality, "*if* a pandemic occurs," resulted in a greater crisis for many funeral homes in the New York City metropolitan area *when* it actually did occur. Several public health officials warned professional funeral directors to prepare for a pandemic and be proactive with an emergency disaster plan because pandemics occur every 100 years. Since that time, very few funeral directors have such an emergency management plan in place. When the COVID-19 pandemic hit New York City, the lack of foresight for good emergency management planning became obvious. I will outline some of the issues encountered that led to the overwhelming surplus of human remains in hospitals, nursing homes, and county morgues and how the funeral industry became incapacitated from the onset. Some of the problems that occurred were a direct result of bureaucratic ineptness

D. R. Penepent (✉)
State University of New York at Canton, Canton, NY, USA
e-mail: penepentd@canton.edu

D. Barry, H. Kanematsu (eds.), *Studies to Combat COVID-19 using Science and Engineering*, https://doi.org/10.1007/978-981-19-1356-3_12

that complicated the process of handling mass fatalities. A positive public image was everything, so inefficiencies were masked. What was experienced in New York City during the first 8 months of the pandemic and the way the government handled the death care problem became proof that the bureaucracy only complicated the grieving experiences for the families who lost loved ones to COVID-19. Funeral industry reform should take place to prevent similar mass fatalities' blunders in the future.

To put this bureaucratic death care problem in perspective, in 2021, the State of New York, one of the most densely populated states in the country, had a population of 19,299,981 [1]. The bordering State of Pennsylvania had 6.5 million [2] which is fewer people, and yet, according to the Cremation Association of North America, Pennsylvania had 191 crematories [3]. New York State, on the other hand, had only 48. The reason for the limited number of crematories in New York is a 1997 edict that prohibited funeral directors from establishing crematories in New York State. Prior to this statute, a funeral director was allowed to establish a crematory as part of their normal operations within their funeral homes. The anti-combination law, as it became known, allowed for crematories owned by funeral homes to remain in operation as long as the funeral director owned the business. When the funeral homes were sold or transferred, this grandfather clause expired, and the crematory had to be taken out of service. In 2019, an initiative by the Division of Cemeteries (the administrative power that regulates not-for-profit cemeteries and crematories in New York State) was put in place to evaluate and deactivate five crematories whose ownership had changed. If this deactivation initiative had been successful, the limited number of crematories in New York would have been greatly compromised, thus further exacerbating and impeding the ability to cremate large quantities of human remains during a pandemic. In addition, only five main crematories exist in the New York City metropolitan area. One of the most densely populated cities in the country does not have enough crematories to handle large quantities of human remains during a pandemic. This oversight, coupled with the Division of Cemeteries' inability to forecast how a mass fatality disaster would cripple the funeral director's ability to effectively serve families in a timely manner, is only one part of the complex issues involving lack of readiness for the pandemic or similar crises [4].

Based on conversations with metropolitan funeral directors, approximately 30% take their human remains to New Jersey and adjacent states for cremation. When the pandemic hit New York City, massive numbers of human remains began to accumulate, and the metropolitan crematories immediately became overwhelmed. In addition, New Jersey's abysmal 27 crematoriums [3] became filled up because that state had the second highest number of deaths in the nation from COVID-19 due to their proximity to New York City. Subsequently, the New Jersey crematories began to reject human remains from NYC funeral directors. This act, coupled with the limited number of crematories in the metropolitan area, created a backlog in many morgues throughout the city. Thus, the funeral directors began to experience a 6–8-week waiting period before being allowed to take human remains to routinely used crematories. Consequently, most funeral directors left human remains in

hospitals, nursing homes, or county morgues because their funeral homes were ill-equipped to store human remains for extended periods. Savvy funeral directors who were able to shift their paradigms sought other sources for crematories in Upstate New York and adjacent states.

To further complicate this issue, several upstate crematories had availability to receive large quantities of human remains because these facilities were not inundated with COVID-19 cases to the extent of those in New York City. In the early stage of the pandemic, the Division of Cemeteries required that the Cremation Authorization Form could not be altered or amended. Thus, a funeral director in New York State had 72 h from the date of death to file a death certificate. Initially, the funeral directors filed a death certificate with the name of the crematorium they had been using prior to the pandemic. Further, the authorization for cremation also bore the name of the routinely used crematory. The Division of Cemeteries insisted that all paperwork needed to be original and could not be amended with a simple phone call to the family requesting permission to change the crematory to be used for cremation. In late June 2020, the Division of Cemeteries changed their policy that allowed the funeral director to alter the paperwork as long as the family was notified of the change in crematory. The Division of Cemeteries insisted that amending the Cremation Authorization Form required an Executive Order by the Governor, when in fact this document was created and regulated by the Division of Cemeteries and could be changed internally. Executive Orders are usually made to amend state statutes. Despite several attempts to convince the Division Director that this issue was exacerbating the backlog of human remains in the city, he refused to act expeditiously. This issue was caught up in unproductive Zoom meetings, and in mid-June, the Governor's office advised the Division that an Executive Order was not needed to change the paperwork. Note: Bordering states such as Pennsylvania, Connecticut, and Vermont accept such amendments because their regulations are less rigid than those of New York.

Additionally, a change in crematories also required the burial transit permit and the death certificate to be amended with the registrar in the municipality in which the death occurred. Such a change to these legal documents costs an additional $40 per amendment, an added cost to the consumer. Some funeral directors refused to amend the death certificate because many families have limited financial means due to their inability to work, and the bureaucratic paperwork problem contributed to the backlog in the makeshift morgues throughout the city.

In the midst of 22,000 deaths by the beginning of May 2020 from the COVID-19 pandemic in New York City [5], funeral homes have been stretched to the limit with their capacity to help bereaved families bring closure to their loved ones' deaths. Several funeral homes refused to answer the phone. Others indicated to the bereaved that they were unable to assist them because of their current call volume. A few funeral homes even closed their operations because they did not have the ability to serve families in a timely way.

With cooperation from the State University of New York at Canton and some assistance from the New York State and Metropolitan Funeral Directors Associations, I spearheaded an operation to relieve some of the funeral directors with

their overabundance of human remains. By using mortuary science students from SUNY Canton and other volunteers to drive box trucks, *Operation Hands With A Heart* was implemented. At no cost to the funeral director, other than the crematory charge, these volunteers went to New York City firms and transported between 25 and 40 human remains at a time to crematories in Upstate New York, Pennsylvania, Connecticut, and Vermont. While this relief effort was designed for two or three box trucks, it could have been easily converted to a large-scale operation [4]. Convincing politicians to adopt this plan of operation on a macroscale was futile. Another problem that led to the backlog of human remains in the Metropolitan area had a great deal to do with state and local disaster plans that were not interconnected. Rather, even though each agency may have had a cohesion plan within their organization, they were disjointed when it came to solving the overall problem of efficiently handling mass fatalities in a timely manner. Even the Office of the Governor grossly underreported the magnitude of deaths occurring in NYC nursing homes.

On the Monday after Easter, I received an email from a family in Cortland, New York. The brother-in-law of a woman who died in a New York City nursing home begged me to help them locate and obtain his wife's sister. She died 6 weeks prior, and the family contacted 36 funeral homes that all refused to assist them with her final disposition. I called a colleague in Cortland and advised him that the family would be coming in to make funeral arrangements. When I arrived in the city on Wednesday, I went to a funeral home to remove 40 human remains for cremation. I asked the funeral director to make the removal from the nursing home, file the paperwork, and prepare her remains for cremation. It took over 4 h to find the woman's remains in the three refrigerated trucks stationed outside the nursing home. Once back at the funeral home, the remains were identified by the toe tag and placed in an alternative container for cremation. On Sunday evening, the last human remains placed on the *Operation Hands With A Heart* was that woman. Five hours later, her remains were taken off the removal truck and were the first to be cremated in a Central New York crematory. A few days later, the family finally had their loved one back.

This transition can be accomplished, yet the logistics of taking the developed concept and expanding it into a major operation is problematic. The key problem in the conversion of this distribution issue was financial resources. Some metropolitan funeral directors are charging below industry standards for cremation, and subsidizing a relief effort to alleviate their backlog of human remains is not financially justifiable. Thus, they would rather hold unembalmed human remains for an extended period, in less than optimal conditions, until their crematory of choice became available, which was one reason funeral homes stopped taking calls. The overwhelming number of calls became quickly taxing on funeral directors who became accustomed to handling fewer than 100 human remains per year. Even though this volume could create a potential health hazard in some funeral homes, the lack of annual or periodic inspections by the regulatory agency that governs the practice of funeral directing (i.e., the Bureau of Funeral Directing) only deals with issues of gross negligence. Coupled with their lack of police powers, their ability

to effectively regulate the industry at large is restricted due to budgetary limitations in New York State, even though the Bureau of Funeral Directing generates special revenue through renewal fees and fines. The special revenue is not retained within the agency. Routine and periodic inspection of funeral homes has not occurred since the mid-1990s due to budgetary restraints. The lack of annual inspections resulted in some funeral home practices in conduct (during the pandemic) to be questionable. Thus, some problems that occurred during the pandemic were handled in a reactionary manner.

When I began the *Hands With A Heart* endeavor, I used a technique that I learned while working in the morgue established at the crash site of American Eagle Flight 4184. The success of removing lots of human remains (in a mass fatality situation) rests in the tracking system. Human remains need to be tracked from the moment they leave the funeral home, to when they are received by the crematory, and finally when they return to the family. TR 050120_FH3/C03/015 is an example of the tracking number used to identify all human remains being sent to various crematories during *Operation Hands With A Heart*. The TR number indicates when the human remains were picked up from the funeral home; FH3 indicates the name of the funeral home; the C03 number identifies the crematory to which the human remains will be taken; and finally, the last three numbers in this tracking system identify the decedent's name to the manifest that accompanies each shipment of human remains. The tracking number is placed on the cremation container and all documents that accompany those remains to the crematory. Ultimately, the tracking number is placed on the temporary urn mailed, via the US Postal System, back to the funeral home. The funeral director could compare the tracking number on the temporary container to the tracking number on the original manifest [4].

Of the 740 human remains, *Operation Hands With A Heart* handled, not one set of cremated remains was misplaced. A funeral director called me 2 weeks after I removed several remains from their establishment, indicating to me that he never received one set of cremated remains. After reviewing the manifest, I called the funeral director and informed him that individual was never on the removal truck. After a thorough search of the funeral home, the deceased was discovered in a cooler in another building. When dealing with several human remains a day, identification and a number tracking system are key components to assuring the families they were getting their loved one back from the crematory. Verifying and identifying human remains were an essential part of our operation. Names were checked with the file. The tracking number became part of the file, and the manifest with the proper authorizations and permits was checked before they exited the funeral home. In view of all the expenses for this operation, I calculated that it cost this relief effort approximately $18 per human remains to transport them to crematories in adjacent states, as well as Upstate New York.

The issue of unclaimed human remains in this pandemic was caused and could have been averted if there had been an adequate number of crematories throughout New York State, especially in the New York City metropolitan area. The anti-combination laws that restrict professional funeral directors from owning a crematory in New York State only exacerbate the crisis to the point where the funeral

industry has become paralyzed from addressing this issue. Savvy funeral directors who live close to bordering states have established crematories in those states, thus driving financial revenue out of New York State. It is ironic that one of New York's largest marketing campaigns is "we want your business." Unfortunately, when it comes to funeral home/crematory operations, there appears to be a political stronghold on changing this law. The anti-combination law is funeral director and consumer unfriendly and should be repealed. Professional funeral directors should be given the opportunity to own and manage crematories in New York State [4].

New York State is unique in regulating cemeteries and crematories. The Division only regulates not-for-profit cemetery and crematory corporations formed under the Not-for Profit Corporation Law §1501. The problem with cemeteries that fall under the Division's jurisdiction is that most of them are run by a volunteer staff. As these aging volunteer pools shrink annually, and new volunteers are not stepping forward to assist with operating these cemeteries, municipalities like the Town of Oswegatchie (a town in Northern New York, near the Thousand Islands) are becoming the new owners of cemeteries that have been disbanded. The maintenance and upkeep of these cemeteries become a financial burden for the municipalities, and as a means of generating revenue, some towns have chosen to build crematories on the grounds of the cemetery. Considering that in the next 10 years, more people will be cremated as opposed to being buried, building a crematory appears to be a strategic solution to this financial problem. The Division regulates only not-for-profit cemeteries and all crematories in New York State. They do not regulate religious, private, municipal, or national cemeteries. I calculate that in the next 10 years, 55–65% of not-for-profit cemeteries in New York State will be maintained and managed by local municipalities.

Other archaic and antiquated laws governing the practice of funeral directing need to be revised and updated to reflect the current practice of funeral directing in New York State. Another such law that should be changed is restricting the ability for a funeral home to have multiple funeral homes located out of one location. This issue was brought to light when a storefront funeral home in Brooklyn received a great deal of nationwide negative press for storing unembalmed human remains in unrefrigerated box trucks in conditions less than optimal in their funeral homes. There is no law restricting the number of funeral homes that can practice out of one location. The funeral home in question had six funeral homes operating out of a storefront funeral home with very limited space. If each funeral home operator took on ten clients each week, within a very short time, the funeral home with limited capacity would immediately become overwhelmed. State laws currently do not have any laws prohibiting funeral homes from operating in accommodations not conducive to large quantities of human remains. Funeral homes that are "shingle holders" further exacerbated the problem on caring for the dead in a reasonable, respectful, and responsible manner.

Discount funeral homes that offer their services for below fair market pricing rely on volume to generate the amount of revenue to thrive. In a pandemic, such services are in great demand, and to make a profit, overhead costs need to be kept at a minimum to maximize profitability. The crematories that such budget funeral

homes use charge below $200 for a cremation. Unfortunately, during a pandemic, these crematories are the first to be filled. This creates the 6–8-week waiting period to receive a few available slots from each funeral director. Even when upstate or bordering state crematories have availability and immediate access, transportation costs for taking human remains to these crematories and the logistics and the increase in crematory charges limit such services from being able to effectively service their clientele at a discount rate. If there is an argument against such discount services, it can be made that during a pandemic, such services only complicate the problem and facilitate the backlog of human remains.

Some governmental officials were urging the governor to order crematoriums to operate 24/7 during the pandemic, which met immediate resistance because crematories cannot operate for long periods of time. Crematories need, what is known as, "cool down periods," in order for the retort to cool down and not create a fire hazard. Crematories with several retorts can rotate cool down periods. However, most crematories do not have trained personnel available to monitor the cremation process 24/7. In addition, one of the problems in the pandemic was that a large number of the casualties were overweight or morbidly obese individuals, which played a significant factor for a crematory operator. Large and obese remains need to be cremated at the beginning of the day when the retort is cool. Human remains are cremated in a temperature between 1400 and 1800 °F. The normal amount of time to cremate the said remains is between 1.5 and 2 h. The reason obese remains are cremated first is that they take the longest. A 400-pound body, for example, could take up to 4 h to cremate. Accelerating this process could lead to the adipose tissue catching fire and potentially burning down the crematory. The obesity problem in the United States has also been a contributing factor to the backlog of human remains at crematories.

Future legislation should be created for emergency situations like the present pandemic. The current regulations appear to be obstacles complicating the efficiency of the cremation process. Finally, funeral management planning for mass fatality situations should be more explicitly detailed and implemented nationwide. Funeral directors do one thing and one thing only: they take the death event and help people connect to their own grieving experience. Failing to plan for mass fatalities in the funeral industry only complicates the funeral director's ability to serve families efficiently. Every funeral home, no matter its current call volume, needs to have a plan in place to serve their community in pandemic or crisis situations.

Eventually, the pandemic will subside, as all pandemics do. Unfortunately, the next crisis in the funeral industry is looming in the next 8–10 years. Currently, there are approximately 1600 registered funeral homes in New York State, which is approximately 250 funeral homes fewer than in 2018. I predict that in 2030, there will be approximately 1100 funeral homes throughout New York State. The next death crisis with massive fatalities in New York State will happen in 2030 when the projected number of deaths in the United States will exceed 3.3 million. Lessons learned from the pandemic should stimulate government officials including the Bureau of Funeral Directing and the Division of Cemeteries to address this crisis with a plan to effectively address mass fatalities from an aging population.

Fewer funeral homes, an aging population of funeral directors, and a decrease in the number of people entering the funeral profession annually, coupled with an increase of more than one million more deaths in the United States in the next 10 years, will be the next mass fatality crisis in the death care industry. The problem with these minimal employment increases in funeral directors is that in the long term, the profession will reach a point where more funeral directors will be leaving the profession without a significant number of seasoned professionals able to replace them. Known as the *attrition cliff*, this employment crisis threatens the disruption in the practice of a profession and is brought on by ignoring increased social trends and a decreased workforce. In the funeral industry, the attrition cliff is a result of increased death rates, an aging population of funeral directors/owners, and a decrease in the number of people studying in mortuary science programs [6].

If the pandemic revealed anything to society, it should expose how ill-prepared the profession is to handle mass fatalities. Mortuary science only teaches this topic as a part of facilities management. However, a 1-h lecture fails to equip the next generation of funeral directors with the tools necessary to manage mass fatalities like a pandemic. The fact remains that some funeral directors died because of COVID-19, possibly because they failed to take necessary precautions to protect themselves from the virus. Being lulled in an invincible sense of false security is dangerous, especially in the funeral profession. My team of 13 volunteers was in what I called "the belly of the beast" during the second phase of the pandemic. Not one of the volunteers contracted COVID-19 because of the stringent protocol I put in place at the beginning of the mission. More education needs to be put in place for training funeral professionals on how to effectively handle a crisis, like a pandemic. While some actions from governmental agencies were positive, like deputizing mortuary science students to make removals during the pandemic, several of the blunders made during the pandemic could have been minimized with a cohesive plan that did not compartmentalize emergency relief efforts. Reform is needed in the laws that govern the practice of funeral directing, crematories, and cemeteries. Lessons learned from the pandemic and reforming the antiquated laws that govern the practice of funeral directing are the only ways to ensure that consumers can receive the dignity and respect necessary in the midst of crisis situations like pandemics.

References

1. World Population Review. (2021). *New York population 2021 (demographics, maps, graphs)*. Author. Retrieved from https://worldpopulationreview.com/states/new-york-population
2. World Population Review. (2021). *Pennsylvania population 2021 (demographics, maps, graphs)*. Author. Retrieved from https://worldpopulationreview.com/states/pennsylvania-population
3. Cremation Association of North America. (2021). *Industry statistical information*. Author. Retrieved June 14, 2021, from https://www.cremationassociation.org/page/IndustryStatistics
4. Penepent, D. (2020). Pandemic and reform in New York. *The Director, 92*(7), 34–37.

5. Elflein, J. (2021). *New York: Covid-19 deaths by day*. Statista. Retrieved December 15, 2021, from https://www.statista.com/statistics/1109713/new-york-state-covid-cumulative-deaths-us/
6. Penepent, D. (2015). The attrition cliff and the future of funeral directing. *The Director, 87*(2), 60–62.

Dr. David R. Penepent (Ph.D., CFSP) is the Program Director of Funeral Services Administration at State University of New York at Canton and co-owner of Johnson and Penepent Consulting. He served for 4 weeks in New York City, and *Operation Hands With A Heart* was responsible for transporting 740 human remains to various crematories in New York and bordering states. dpenepent@funeralbusinessconsulting.com.